NECROSOME ACTIVATION AND DEGRADATION IN MACROPHAGES

By

Norah Abdullah Alturki

A Thesis Submitted to
The Faculty of Graduate and Postdoctoral Studies

In Partial Fulfillment of the Requirements for the PhD degree in Microbiology and Immunology

Department of Biochemistry, Microbiology and Immunology

Faculty of Medicine

University of Ottawa

PREFACE

CONTRIBUTION OF COLLABORATORS

- Dr. Katey Rayner's laboratory (University of Ottawa Heart Institute) provided all the reagents and plates used for preparing and mounting the cells for the confocal microscopy, and images were captured using a ZEISS LSM 880 with Airyscan in their lab.
- Dr. Alexandre Blais's laboratory (University of Ottawa) performed and provided all the reagents and microarray slides used for gene expression profiling, and raw data were filtered and normalized using Expander 6.5.

APPROVALS

The experimental protocols used were approved by the University of Ottawa Animal Care Committee and include the protocols BMI1638 and BMI1639. A Biohazardous Materials Use Certificate was obtained from the University of Ottawa Office of Risk Management, Environmental Health and Safety.

ABSTRACT

Necroptosis is a recently discovered form of cell death that is distinct from apoptosis that promotes inflammation. Necroptosis is induced upon engagement of various classical death receptors such as tumor necrotic factor receptor (TNFR) and Fas ligand, and also by engagement of toll like receptors involved in recognition of various pathogen associated molecular patterns such as lipopolysaccharide (LPS) and polyinosinic: polycytidylic acid (poly I:C). Necroptosis is induced by the activation of receptor-interacting protein kinase-1 (RipK1) and receptor-interacting protein kinase-3 (RipK3) that leads to phosphorylation-driven trimerization and consequent translocation of the mixed lineage kinase domain-like (MLKL) protein to the cell membrane, resulting in cell rupture. The formation of this necrosome complex is highly regulated by phosphorylation and ubiquitination. The precise mechanisms through which members of the necrosome assemble sequentially in macrophages are not clear. Herein I have evaluated the mechanisms that promote the assembly and degradation of the necrosome in macrophages. In the first aim of my thesis I revealed that during early necrosome formation RipK3 destabilizes the complex by promoting degradation of interacting proteins. RipK3 promoted K48-ubiquitin dependent proteasomal degradation of various necrosome interacting proteins such as RipK1, CASPASE-8, and FADD. This degradation event occurred independently of other ubiquitin editing enzymes such as cIAP1/2, A20 and CYLD that are known to edit RipK1. I further show that this degradation of early necrosomal proteins is mediated by the E3-ubiquiting ligase Triad3a (RNF216). Knocking-down Triad3a prevented degradation of necrosome proteins, enhanced necroptosis and production of inflammatory cytokines. In the second section of my thesis, I evaluated the mechanisms responsible for necrosome signalling following engagement of type-I interferon receptor. I show that the downstream Janus kinase (JAKs) kinases (TYK2 and JAK1) are required for necroptosis in macrophages. My results indicate that IFNAR1 signalling promotes phosphorylation of RipK3 and MLKL, the two events that are required for necroptosis. Furthermore, I observed that type-I interferon signalling promotes the transcription of MLKL and the phosphorylation driven oligomerization of MLKL which is necessary for pore formation in cells. Finally, inhibition of the $p38^{MAPK}$ pathway abrogated the resistance of *Ifnar1*$^{-/-}$ macrophages. The results presented in this thesis reveal mechanisms that regulate necrosome signalling and will help identify potential therapeutic targets that could be exploited in chronic inflammatory conditions.

ACKNOWLEDGMENTS

First and foremost, I would like to thank Allah (SWT) who made this thesis possible and gave me the faith that I could do it and the strength and perseverance to finish this PhD thesis.

This thesis would never have been completed or have seen the light of day without the help and advice of my supervisor, Dr. Subash Sad. I still remember when we met for the first time in the elevator, in November 2013. That day you listened to me and accepted me as a PhD candidate, and I am very thankful to you that you allowed me to work and achieve my dream under your supervision. My profound appreciation to you for your patience, your advice, your wisdom and the friendship that you built with us in our lab. I will transfer what you taught me, and like you, I will always keep my door open. Thanks for guiding me during my PhD journey, thanks for believing in me, and thanks for developing my knowledge and skills and pushing me to challenge my limits and go beyond them. You helped me to grow with your advice, your constant meetings, your constructive critiques. Dr. Subash, thanks for the opportunity to work in your lab, with an amazing team, under your vision.

I would also like to extend my gratitude to my thesis advisory committee members, Dr. Daniel Figeys, Dr. Alexandre Blais, and Dr. Robert Korneluk. Thanks for valuable discussions, constructive criticism and useful recommendations during our annual meeting.

I owe my gratitude to all the members of the Sad lab, former and current, for their support and encouragement during my PhD. Thank you Dr. Bojan, Dr. Rajen, Erin, Dr. Julie, David, Dikchha, Emmanuelle, Naveen, Dr. Laila, Melisa, Palavi and Parva. Special thanks Ms. Kim Kwangsin for providing technical assistance during my studies. Thanks to Dr. Ardeshir Aryana, our idea maker, for his assistance and support during my PhD. I also thank Stephanie Hajjar for her emotional support and her encouragement words. I thank Ms. Mufida and her husband Mr. Mohammed for the unconditional love and endless support.

I also thank the Animal Care and Veterinary Service (ACVS) team who trained me in the essential, practical skills I needed to perform my animal experiments.

I thank Dr. Katey Rayner and Dr. Anne-Claire from the Ottawa Heart Institute for allowing me to perform immunofluorescence experiments.

My deepest gratitude to Dr. Lionel Filion (my beloved Canadian father) for his valuable advice, unlimited support, encouragement from when I was doing my master's degree to now. Your words are always in my mind and you are not comparable to anyone.

I would like to thank Ms. Fay Draper and everyone at the graduate office for the help, flexibility and continuous support during the difficult time I have been through. Thank you very much.

Special thanks to my soul mate Dr. Afaf Tawfiq for the unconditional love you gave, for relentless support, and for treating me as a daughter. I am very thankful that through my PhD experience I met you and know someone like you. I learned a lot from you. Thank you.

I would like to extend my gratitude to King Saud University for their financial support and scholarship. Thank you for your generosity all these years, and for funding my masters and doctoral studies in Canada. Also, I thank Saudi cultural bureau in Canada especially Ms. Saly Michael.

I thank my friends from my PhD journey, Abeer Zakariyah, Esraa Baitalmal and Roza, Albakri for been together all these years. I am blessed to have you as friends and I really appreciate your unlimited support and endless encouragement.

Special thanks to my lovely friend Dr. Hilary Phenix for taking the time to help revise this thesis; her presence and assistance have been irreplaceable.

Lastly, I owe my deepest gratitude to my family. To my ever-loving parents (Abdullah and Fatmah), you are the best parents in the world, and I owe my success to you. Thanks for the faith and for believing in me, that I would achieve my dreams. Thanks for the prayers over the years and the infinite love. Thanks for tolerating my absence over 10 years. I also thank my lovely siblings (Hadeel, Bader, Faisal, Shahad, Mohammed and Gadah), my sisters-in-law (Abrar and Jawaher) and my lovely nieces (Almaha, Shaima, Seba, Nourah and Latein). Thanks for taking care of my parents, listening to me complain, and keeping me motivated. Special thanks to my brother Faisal, who faced challenges with me and helped me to overcome them throughout my PhD studies.

Norah A. Alturki, 2019

TABLE OF CONTENTS

LIST OF ABBREVIATIONS

APAF-1	Apoptotic Protease Activating Factor 1
BAD	Bcl-2-associated death promoter
BAX	Bcl-2-associated X protein
BCL-2	B-Cell Lymphoma Protein-2
BCL-XL	B-cell lymphoma-extra large
BID BH3	(Bcl-2 homology 3) interacting-domain death agonist
BMDM	Bone Marrow Derived Macrophage
cFLIP1	Cellular FLICE (caspase-8/a–h)-like inhibitory protein
cIAP(1/2)	Cellular Inhibitor of Apoptosis 1 and 2
CYLD	Cylindromatosis
DAMP	Danger Associated Molecular Pattern
DD	Death Domain
DED	Death Effector Domain
DISC	Death-inducing signalling complex
ELISA	Enzyme-linked Immunosorbent Assay
ERK	Extracellular signal–regulated kinase
FADD	Fas-associated protein with death domain
FLIP	FLICE-Like Inhibitory Protein
GAS	Gamma Activated Site
HRP	The enzyme horseradish peroxidase
IFN	Interferon
IFNAR	Interferon α/β Receptor
IFNAR 1	Interferon α/β Receptor 1
IFN-I	Type-I Interferon
IkB	Inhibitor of kappa B
IKK	Inhibitor of Nuclear Factor Kappa-B Kinase
IL-10	Interleukin 10
IL-6	Interleukin 6
IRF	Interferon Regulatory Factor
IRFBS	IRF Binding Site
ISG	Interferon Stimulated Gene
ISGF3	Interferon Stimulated Gene Factor 3
ISRE	Interferon-Stimulated Response Element
JAK1	Janus Kinase 1
JNKs	c-Jun N-terminal kinases
LPS	Lipopolysaccharide
LUBAC	Linear ubiquitin chain assembly complex
MAPKs	Mitogen-activated protein kinases
M-CSF	Macrophage Colony Stimulating Factor
MFI	Mean fluorescence intensity
MLKL	Mixed Lineage Kinase domain-Like Protein
MTT	3-(4,5-dimethylthiazol-2-yl)-2,5-diphenyltetrazolium bromide
MyD88	Myeloid Differentiation Primary Response Gene 88
NEMO	NFκB Essential Modulator

NFκB	Nuclear Factor Kappa-light-chain-enhancer of Activated B Cells
NIK	NFκB Inducing Kinase
p38	MAPK p38 Mitogen-Activated Protein Kinase
p65	NFκB Subunit 65 of Nuclear factor kappa-light-chain-enhancer of activated B cells
PAMP	Pathogen Associated Molecular Pattern
PBS	Phosphate Buffered Saline
PCD	Programmed Cell Death
PIP	Phosphatidylinositol Phosphate
PM	Plasma Membrane
PolyI:C	Polyinosinic-polycytidylic Acid
PRR	Pattern Recognition Receptor
PS	Phosphatidylserine
R8	RPMI with 8% Fetal Bovine Serum
RCD	Regulated cell death
RHIM	Rip Homotypic Interaction Motif Domain
RIPK1/3	Receptor Interacting Protein Kinase 1 /3
RPM	Revolutions per minute, a measure of the frequency of rotation
RPMI	Roswell Park Memorial Institute Medium
SBE	STAT Binding Element
SIRS	Systemic Inflammatory Response Syndrome
SM	SMAC mimetic
SMAC	Secondary Mitochondrial Activator of Cell Death
ST	*Salmonella enterica* serovar Typhimurium
STAT	Signal Transducers and Activators of Transcription
TAB1	Transforming Growth Factor-Beta Activated Kinase 1 Binding protein 1
TAB2	Transforming Growth Factor-Beta Activated Kinase 1 Binding Protein 2
TAK1	Transforming Growth Factor-Beta-Activated Kinase 1
TBK1	Tank-Binding Kinase 1
TBS	Tris Buffered Saline
TBST	Tris Buffered Saline with Tween
TGF	Transforming Growth Factor
TLR	Toll Like Receptor
TNF	Tumor Necrosis Factor
TNFR	Tumor Necrosis Factor Receptor
TRADD	TNFR Associated Death Domain Protein
TRAF2	TNFR Associated Factor 2
TRAIL	TNF Related Apoptosis Inducing Ligand
TRAM	TRIF Related Adaptor Molecule
TRIF	TIR-domain Containing Adapter Inducing IFN-ß
TWEAK	TNF Like Weak Inducer of Apoptosis
TYK2	Tyrosine Kinase 2
xIAP	x-Linked Inhibitor of Apoptosis
zVAD	Benzyloxycarbonyl-Val-Ala-Asp-fluoromethylketone Pan-caspase Inhibitor
2BM	2 Beta Mercaptoethanol

LIST OF FIGURES

LIST OF TABLES

1.0 INTRODUCTION

Cell death plays a fundamental role in many biological and physiological processes ranging from embryogenesis to immunity. Every day the human body eliminates approximately one million cells every second, which is vital to maintain homeostasis (Ravichandran, 2011). In a multicellular organism, programmed cell death plays an essential role in development, disease progression and immunity. In the context of the immune system, programmed cell death eliminates T cells and B cells after massive clonal expansion in response to antigenic stimulation (Zhan, Carrington, Zhang, Heinzel, & Lew, 2017). Also, programmed cells death improves tolerance towards self-antigens by eliminating autoreactive cells during the education of immune cells in the thymus and bone marrow (Han, Zhong, & Zhang, 2011). Defects in programmed cell death are associated with immunodeficiencies, autoimmune diseases, neurodegeneration and cancer(Fuchs & Steller, 2011). Excessive programmed cell death contributes to a plethora of diseases, including neurodegenerative diseases, chronic inflammation, congenital neural anomalies and autoimmune diseases that may arise from overstimulation of T cells during chronic inflammation (Lockshin & Zakeri, 2007).

The field of programmed cell death has been advancing at a rapid rate, making it one of the most intensely studied research area in biology (Meier & Vousden, 2007). Multiple forms of programmed cell death have been revealed. Apoptosis and necroptosis are the two major mechanisms of cell death, each resulting in opposite outcome. Apoptotic death is a physiological, anti-inflammatory form of cell death that promotes immune response whereas necroptotic death induces a robust inflammatory response, a process referred to as necroinflammation (Heckmann, Tummers, & Green, 2019). Cytolysis such as necrosis is different than apoptosis and is generally mistaken for accidental non-programmed cell death. Necrosis involves a sudden loss of membrane

integrity that causes the release of cytoplasmic contents to the external milieu, leading to a massive immune response (Martin & Henry, 2013). The direct damage of cell membranes and the interference with the energy supply of the cells are two main mechanisms that distinguish necrosis from apoptosis (Elmore, 2007).

It is hypothesized that the development of necroptosis as an alternative cell death mechanism evolved to control infection with highly virulent and evasive pathogens. The mechanisms that lead to the activation of necroptosis are not totally clear, particularly in the immune cells. Better understanding of the regulation of necroptosis is therefore important to control this inflammatory form of cell death in various pathologies such as cancer, sepsis, rheumatoid arthritis, Alzheimer disease, multiple sclerosis and atherosclerosis (Ofengeim et al., 2015; Shan, Pan, Najafov, & Yuan, 2018). In this thesis, I will describe the work I performed to investigate the mechanisms regulating the formation of the core necroptotic complex (necrosome) and the necessity of type-I interferon signalling in necroptosis of murine macrophages.

1.1. The immune system

Immune system is a defense system that protects the host from pathogens and results in clearance of infection and harmful invaders. The science of vaccinology dates back to May 1796 when Edward Jenner inoculated a less virulent version of human disease vaccinia (cow) virus in his neighbor's son and after 6 weeks Jenner challenged him with live human smallpox and he found that the boy was protected against the virulent challenge. Thereafter the concept of vaccination was introduced (K. P. Murphy et al., 2008). In the late 19th century the findings by other scientists such as Robert Koch, who discovered that infectious diseases are caused by microorganisms, Louis Pasteur, who developed a rabies vaccine, and Elie Metchnikoff's, who

discovered phagocytic cells also known as “macrophages”, have led to deeper understanding of the immune system and have paved the way for immunological research (K. P. Murphy et al., 2008).

The immune system is an extraordinary protective mechanism within a host that effectively recognizes and defends against a staggering variety of microorganisms (Kotwal, 1997). The immune system in multicellular organisms is equipped with wide array of immune cells. Immune cells and their effector molecules recognize and destroying invading pathogens, thereby preventing pathogen spread (Buchmann, 2014). The mammalian immune system can be broadly classified into innate and adaptive systems. Innate immunity acts immediately as a first line of defense to a wide range of pathogens, initiated within minutes to hours of pathogen attack (Nicholson, 2016). Innate immunity relies on recognition of conserved structures on pathogens through a germ line-encoded receptor called pattern recognition receptors (PRRs) (Medzhitov, 2007; Mogensen, 2009). Mammalian immune cells express pattern recognition receptors (PRRs) such as toll-like receptors (TLRs), NOD-like receptors, RIG-I-like receptors and C-type lectin receptors which recognize pathogen-associated molecular patterns (PAMPs) and danger-associated molecular patterns (DAMPs) (Mogensen, 2009; Suresh & Mosser, 2013). Examples of PAMPs with particular relevance to bacterial pathogens include lipopolysaccharide (LPS), peptidoglycan and Lipoproteins. The engagement of LPS with a TLR4 receptor on a surface of innate immune cells such as macrophages, dendritic cells, monocytes or neutrophils initiates an antimicrobial response that leads to clearance of the bacterial infection. Such engagement of various PRRs by various types of pathogens can result in the activation of different mechanisms, such as phagocytosis, target cell lysis, pro-inflammatory cytokine production, chemokine release,

complement system activation, initiation of inflammation and induction of cell death (Medzhitov, 2007; Mogensen, 2009) ("Chapter 3 - Innate Immunity," 2014).

In contrast to the innate immune system, the adaptive immune response is known to develop at a slower rate relative to the innate immune system. As the numbers of immune cells of the adaptive immune system increase, the pathogen is eliminated comprehensively, and a state of specific memory against the pathogen is developed (Mogensen, 2009). Adaptive immunity is generated by specific clonal selection and expansion of pathogen-specific lymphocytes. B and T (CD4+ and CD8+) cells are the two major types of immune cells in the adaptive immune system. In contrast to the recognition receptors of the innate immune system, adaptive immune cells develop a highly specific antigen receptor via a process of somatic recombination of a large array of gene segments (Bonilla & Oettgen, 2010). The development of immunological memory is a unique feature of the adaptive immune system (Bonilla & Oettgen, 2010). Subsequent encounters with the same pathogen induces rapid activation of memory cells that mediate a robust response and prevent the spread of the pathogen early on (Bonilla & Oettgen, 2010).

1.1.1. Macrophages

Macrophages are mononuclear cells of the innate immune system that are distributed ubiquitously in different tissues. Their ability to phagocytose pathogens rapidly allows macrophages to recognize danger signals quickly, (Hirayama, Iida, & Nakase, 2017). Phagocytosis of pathogens activates and modulates intracellular signalling in macrophages, that results in the release both pro-inflammatory and antimicrobial mediators swiftly (Aderem, 2003).

Macrophages originate from the pluripotent hematopoietic stem cells (HSCs) in the bone marrow where they differentiate into monocytes that subsequently migrate to different tissues and

differentiate into tissue- resident macrophages (Hirayama et al., 2017; Williams, Giannarelli, Rahman, Randolph, & Kovacic, 2018). In addition, Takahashi et al. demonstrated that in addition to those that are derived from the HSCs, primitive macrophages can be derived from yolk sacs and are maintained in peripheral tissues by a self-renewal mechanism prior to the formation of HSCs or monocytes (K. Takahashi, Yamamura, & Naito, 1989). HSCs differentiate into common myeloid progenitors, which then can differentiate into all functional hematopoietic lineages including neutrophils, eosinophils, lymphocytes and monocytes (Dzierzak & Speck, 2008). Tissue-resident macrophages are continuously repopulated by blood-circulating monocytes in response to cytokines and chemokines in a process known as diapedesis (Ginhoux & Jung, 2014; Hirayama et al., 2017).

Monocytes can differentiate in various micro-environments which results in the heterogeneity of macrophages (Gordon, Pluddemann, & Martinez Estrada, 2014; Varol, Mildner, & Jung, 2015). Phenotypic heterogeneity of tissue macrophages is influenced by the anatomical location of macrophages and their cellular origins, i.e. self-replicating cells of the embryonic origin or monocyte-derived. Heterogeneity is also driven by tissue niche signalling, wherein macrophages may perform specialized functions (Epelman, Lavine, & Randolph, 2014). For example, splenic-red-pulp macrophages are unique in their ability to take up senescent red blood cells by utilizing the transcription factor SPI-C to drive the expression of genes involved in capturing circulating haemoglobin and iron uptake (Kohyama et al., 2009). Macrophages are rare in their remarkable diversity of function, ranging from tissue regeneration, iron recycling, surfactant homeostasis and immunity development, in comparison to other cell types.

Phagocytosis is a well characterized function of macrophages wherein macrophages may uptake large particles, microbes, dead cells or environmental debris (Aderem & Underhill, 1999).

Phagocytosis involves three main steps: (i) microbial recognition; (ii) phagosome formation; and (iii) phagolysosome maturation. Following microbial engagement with several receptors (for e.g. non-opsonic or opsonic receptors), a sequence of signalling events induces the phagocytosis process. Receptor-engagement leads to rearrangement of the cell membrane and actin cytoskeleton on the surface of a macrophage, thereby allowing the formation of pseudopods (Underhill & Goodridge, 2012) that surround and engulf the target into a newly formed vesicle known as a phagosome (Hirayama et al., 2017). The newly formed phagosome then begins to mature through a series of fusion and fission events with early and late endosomes. A mature phagosome eventually fuses with a lysosome, an intracellular hydrolase-rich organelle, forming a microbicidal vacuole known as the phagolysosome. Fusion with the lysosome results in the release of lysosomal degradative enzymes, including various cathepsins, proteases, lysozymes, and lipases that destroy a microorganism inside the phagolysosome without affecting macrophage integrity or homeostasis (Gordon & Martinez-Pomares, 2017; Uribe-Querol & Rosales, 2017; X. Zhang & Mosser, 2008).

1.2. Inflammation

Following activation of phagocytosis in macrophages, several signalling pathways are induced to activate transcription of essential genes that participate in the initiation and execution of the inflammatory response. As the front line cell type of the innate immune system, macrophages are involved in the initiation, maintenance and clearance of inflammation via the production of a variety of inflammatory mediators, including chemokines and cytokines (pro- or anti-inflammatory), in response to pathogens or sterile triggers (Medzhitov, 2008). Production of these inflammatory mediators is a highly regulated process in order to maintain homeostasis of the tissue and to avoid pathological conditions such as septic shock, rheumatoid arthritis, diabetes or

multiple sclerosis. Balance is the key in maintaining normal functioning of the host as insufficient inflammatory response or chronic, exaggerated inflammatory response can lead to tissue damage (Medzhitov, 2008; Sugimoto, Sousa, Pinho, Perretti, & Teixeira, 2016).

Cells of the innate and acquired immune system participate in the severity and duration of inflammation (Buckley, Gilroy, Serhan, Stockinger, & Tak, 2012; Medzhitov, 2008). Clinically, inflammation is characterized by the following cardinal signs: rubor (redness), calor (increased heat), tumor (swelling), dolor (pain), function laesa (loss of function) and fluor (secretion) around a site of injury. These signs occur due to increased blood flow, expression and migration of various plasma proteins, accumulation of fluid, and release of chemicals that trigger nerve endings (Kauppinen, Paterno, Blasiak, Salminen, & Kaarniranta, 2016). Activation of the inflammatory response results in the production and release of soluble effector molecules that prevent pathogens from spreading to uninfected neighboring cells. For example, release of platelet activating factor promotes the formation of blood clots, blocking blood vessels and capillaries and thereby eliminating spread of infection to the microenvironment (K. P. Murphy et al., 2008; White, 1999). Additional soluble mediators of inflammation, such as histamine, leukotrienes and prostaglandins, cause vasodilation via release of a vasoactive amines that increases permeability of blood vessels and increases infiltration of neutrophils and monocytes to the infected area (Ashley, Weil, & Nelson, 2012). Indeed, vasodilation results in the increase of blood flow that carries all cytokines and plasma proteins underlying swelling, redness and heat at the afflicted area.

Furthermore, in response to inflammation, endothelial cells of blood vessels express selectins, adhesion molecules that mediate the initial attachment of integrins and cytokines on leukocytes to the surface of endothelial cells. As soon as these binding events occur, circulating neutrophils and monocytes infiltrate into the inflamed tissue (Medzhitov, 2008). Once infiltrated,

neutrophils are activated, via direct pathogen contact or through the effect of cytokines secreted in the area, to release cytotoxic granules such as reactive oxygen species (ROS), reactive nitrogen species (RNS) and cathepsin to destroy pathogens. Infiltrating monocytes are also activated in response to the local stimuli, allowing their differentiation into macrophages or dendritic cells (Ashley et al., 2012; Medzhitov, 2008). Resolution of this acute inflammatory phase is usually followed by tissue repair, mediated by tissue-residing macrophages. These macrophages promote recruitment of monocytes, to remove the infected dead cells and initiate tissue remolding, and thereby terminate inflammation through expression of anti-inflammatory cytokines such as IL-10 (Medzhitov, 2008). In contrast, a failure to clear pathogens during this acute inflammatory response results in persistence of the infection and a chronic inflammatory state may develop (Medzhitov, 2008). Finally, various forms of programmed cell death, such as necroptosis, NETosis, pyroptosis and ferroptosis, exacerbate inflammation by releasing inflammatory mediator DAMPs, such as Interleukin 1 (IL-1), High mobility group box 1 (HMGB1), ATP, mitochondrial DNA and Heat shock proteins (HSPs) (Kolb, Oguin, Oberst, & Martinez, 2017; Pasparakis & Vandenabeele, 2015). Release of these DAMPs to the extracellular milieu leads to downstream signaling mechanisms that lead to tissue toxicity.

1.2.1. NFκB Signaling

Following the engagement of PRRs by exogenous PAMPs or endogenous danger-associated molecular patterns (DAMPs), several inflammatory signalling pathways are initiated (Tang, Kang, Coyne, Zeh, & Lotze, 2012) which results in intracellular signalling events such as protein ubiquitination, phosphorylation, activation of interferon regulatory factors (IRFs) and activation of nuclear factor kappa β transcription factor (NFκB) (Lawrence, 2009; T. Liu, Zhang,

Joo, & Sun, 2017). These events promote transcription of a large array of pro-and anti-inflammatory genes that promote or inhibit inflammatory response. NFκB is a transcriptional protein complex that responds to diverse stimuli and can be activated by engagement of the toll-like receptors (TLRs) or cytokine-receptors (Lawrence, 2009; T. Liu et al., 2017). Translocation of NFκB to the nucleus promotes the transcription of genes that mediate inflammatory response and that promote cell survival. Mammalian NFκB is composed of several proteins including RelA (p65), RelB, c-Rel, and the precursor proteins p105 (NF-κB1) and p100 (NF-κB2), which undergo processing to form p50 and p52 respectively. NFκB can be activated by canonical (classical) or non-canonical (alternative) pathways. Each of these pathways involves different IκB kinase (IKK) subunits. The IKK family encompasses two kinase subunits, IKKα and IKKβ, and a regulatory subunit, IKKγ, also known as NEMO. Activation of the canonical pathways is regulated by IKKβ, whereas the alternative pathways are regulated by IKKα (Lawrence, 2009). In the absence of activation, NFκB is inert and found as an inactive dimer in the cytoplasm due to association with inhibitors (IkBs).

1.2.2. Canonical NFκB signaling

Canonical activation of NFκB occurs in response to diverse stimuli including ligands that bind to cytokine receptors (e.g. TNFR1 , IL-1R, IFNAR1), PRRs (e.g. TLR4) and T- or B-cell receptors (T. Liu et al., 2017; Oeckinghaus, Hayden, & Ghosh, 2011; Pires, Silva, Ferreira, & Abdelhay, 2018). When TNFα binds to its receptor, for example, a number of signalling proteins are recruited to the cytoplasmic domain of TNF-R1 such as TNFR-associated death domain protein (TRADD) which also recruits receptor interacting protein kinase 1 (RipK1), TNFR-associated factor 2 (TRAF2) and cellular inhibitors of apoptosis proteins 1 and 2 (cIAP1/2)

to form complex-I (Oeckinghaus et al., 2011). Ubiquitination is triggered through cIAP1/2, E3 ubiquitin ligases that mediate ubiquitination to the target proteins in complex-I. More specifically, cIAP1/2 conjugates a K63-linked polyubiquitination chain on RipK1, which then induces canonical activation of NFκB (Beug, Cheung, LaCasse, & Korneluk, 2012). In addition to this K63 ubiquitination modification, linear ubiquitin chain assembly complex (LUBAC) mediates M1 linear ubiquitination of RipK1 (Beug et al., 2012). The ubiquitination state of RipK1 results in recruitment of TGF-beta activated kinase 1 binding protein 2 (TAB2) and transforming growth factor-beta-activated kinase 1 (TAK1) to the complex-I and consequently activates the IKK complex. Upon activation, IKK phosphorylates the NF-κB inhibitor, IκBα, triggering ubiquitin-dependent degradation of the inhibitor by the proteasome, and therefore allowing p50/RelA to translocate to the nucleus and initiate transcription of NF-κB target genes **(Fig. 1A)** (Beug et al., 2012; Pires et al., 2018).

Engagement TLR4 by ligands also leads to the activation of the canonical NF-κB pathway. For example, once lipopolysaccharide (LPS) engages with TLR4, adaptor proteins, such as myeloid differentiation primary response gene (MyD88), toll-interleukin 1 receptor (TIR) domain-containing adaptor protein (TIRAP), TIR domain-containing adaptor-inducing interferon-β (TRIF) and TRIF-related adaptor molecule (TRAM), are recruited to bind to the Toll/interleukin-1 receptor (TIR) domain of TLR4 (Takeuchi & Akira, 2010). Upon binding of adaptor proteins to TLR4, interleukin 1 receptor associated kinases (IRAKs) are recruited and directly interact with and activate TRAF6, an E3 ubiquitin ligase. This new complex interacts with a complex consisting of TGF-β-activated kinase 1 (TAK1) and TAK1-binding protein (TAB1-2-,3). This complex is activated via removal of K63 polyubiquitin chains and phosphorylation of IκB kinase (IKKβ), The IKK complex, consisting of IKKα, IKKβ and NEMO, phosphorylates IκBa, the NFκB inhibitory

protein. Phosphorylation of IκB results in its degradation, thereby allowing p65/RelA to translocate into the nucleus and induce the transcription of target gens (Takeuchi & Akira, 2010).

1.2.3. Non-canonical NFκB activation

Non-canonical activation of NF-kB involves processing of p100 (NF-κB2). The activation of this pathway occurs through various cell surface receptor such as CD40, B cell activating factor receptor (BAFFR), CD27, CD30 and OX40 (also known as CD134 and TNFR2 (S.-C. Sun, 2011; S. C. Sun, 2017). In absence of activation, TRAF3 continuously mediates degradation of the NF-κB-inducing kinase (NIK), a MAP3 kinase member and central signalling component of the non-canonical pathway activating NF-κB. Non-canonical signalling, activated upon engagement of, for example, the CD40 receptor with its ligand, results in formation of a complex composed of cIAP1/2, TRAF-2,-3 and NIK. Thereafter, cIAP1/2 catalyzes K48 ubiquitination of TRAF2 and TRAF3, inducing degradation of these proteins and disrupting the complex (S. C. Sun, 2017). Proteasomal degradation of TRAF3 results in elevation of NIK levels in cells, and in turn the phosphorylation of p100, activation of IKKα and binding of IKKα to its substrate, p100 (Shih, Tsui, Caldwell, & Hoffmann, 2011; S.-C. Sun, 2011). Active IKKα promotes further phosphorylation of p100, which is a signal for p100 to be recognized by a ubiquitin ligase complex, resulting in partial degradation of p100 by the 26S proteasome into p52 **(Fig 1B)** (Shih et al., 2011). The RelB/p52 dimer then localizes to the nucleus to induce the expression of multiple target genes. Non-canonical signalling for NF-κB activation is crucial for many immunological transcriptional programs including development of lymphoid organs, and development and activation of adaptive immune cells.

A study by Jin et al. addressed the link between non-canonical signalling and the development of antiviral innate immunity. Jin and colleagues (2014) found that, in the context of vesicular stomatitis virus and Sendai virus infections, mice lacking the NIK-encoding gene (*Map3k14-knockout*) displayed a significant increase in type-I IFN level. In contrast, they found TRAFF3 mutant cells, which expressed stable levels of NIK, displayed reduced levels of type-I IFN. These findings demonstrate that the signalling involved in non-canonical NF-κB activation also suppresses type-I interferon production (J. Jin et al., 2014; S. C. Sun, 2017).

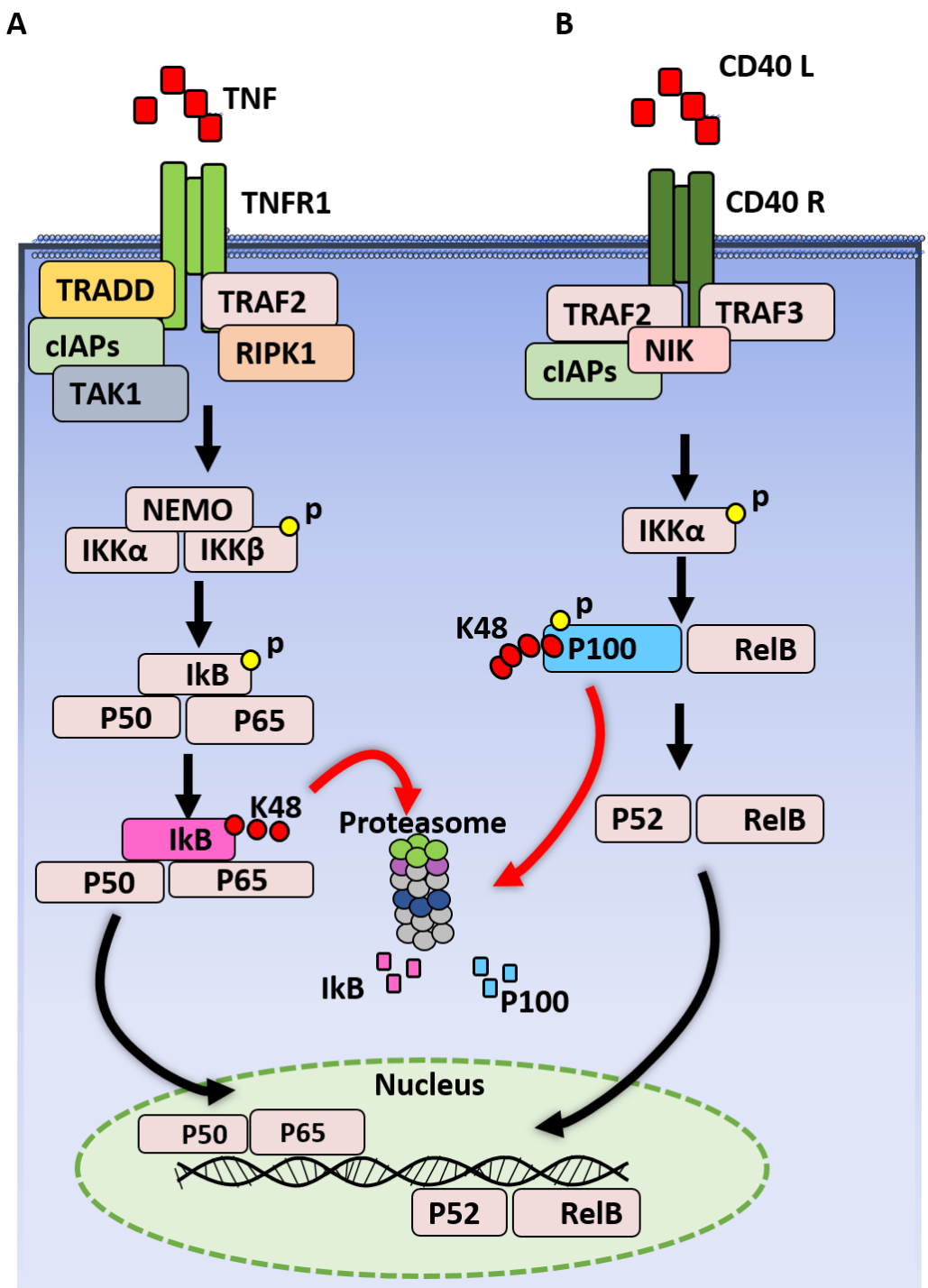
A
B
TNF
TNFR1
TRADD
TRAF2
cIAPs
RIPK1
TAK1
NEMO
IKKα
IKKβ
p
IkB
P50
P65
K48
Proteasome
IkB
P100
CD40 L
CD40 R
TRAF2
TRAF3
NIK
cIAPs
IKKα
K48
P100
RelB
P52
RelB
Nucleus
P50
P65
P52
RelB

Figure 1. The canonical and non-canonical pathways of NF-kB activation.

(A) The canonical pathway can be triggered by various stimuli (e.g. TNFα). Stimulation of TNFR leads to the recruitment of a number of proteins such as TRADD, FADD, RipK1 and TRAF2. RipK1, associated with TRAF2, induces phosphorylation and activation of IKKβ. IKKβ mediates phosphorylation of IkB, the inhibitor of NF-kB. This phosphorylation of IkB leads to IkB's polyubiquitination at K48 and degradation by the proteasome, allowing nuclear translocation of p50/RelA and subsequent DNA binding to specific sites. **(B)** The alternative (or non-canonical) pathway, in contrast, can be triggered by certain cytokines of the TNF family, for example CD40. NFκB-inducing kinase (NIK) activation leads to phosphorylation of IKKα, resulting in phosphorylation and degradation of p100, and thereby allowing formation of the p52 and RelB complex followed by nuclear translocation of this p52/RelB complex.

1.2.4. MAP kinases (MAPKs)

Mitogen-activated protein kinases (MAPKs) mediate a broad variety of cellular behaviors in response to extracellular stimuli. For example, MAPKs signalling plays an essential role in cell proliferation, differentiation, transformation and death (Zarubin & Han, 2005; W. Zhang & Liu, 2002). In mammals, there are three families of MAPKs: extracellular signal-related protein kinases (ERK1/2); C-Jun N-terminal kinase/stress-activated protein kinase (JNK/SAPK) and p38 kinase. MAPK signalling cascades are characterized by three sequentially acting kinases: (1) MAPK/ERK kinase (MEK kinase) (MEKK or MAPKKK); (2) MAPK kinase (MEK, MKK or MAPKK); and (3) MAPK. In response to extracellular stimuli, MAPKKK is activated by phosphorylation and in turn phosphorylates the second kinase, MAPK kinase, which in turn phosphorylates the third downstream MAPK kinase. These modifications occur at threonine and tyrosine residues within a conserved Thr-X-Tyr motif located in the activation loop of the kinase domains of these proteins (W. Zhang & Liu, 2002).

ERK1/2 is a well-characterized MAPK, first cloned and studied extensively in the early 1990s. ERK1/2 is expressed ubiquitously in most mammalian tissues, and at particularly high levels in the heart, brain and thymus. ERK1/2 is activated in response to insulin, nerve growth factor and epidermal growth factor (Shaul & Seger, 2007). These ligands induce dimerization of a cell surface receptor, such as receptor tyrosine kinase, causing receptor activation and autophosphorylation, and leading to the activation of ERK which in turn phosphorylates numerous substrates in the cytoplasm, nucleus or cell cytoskeleton (Cargnello & Roux, 2011). For example, ERK1/2 phosphorylates and activates a wide array of transcription factors, including Elk-1, c-FOS, c-Jun, P53, NF-kB/IkBα and Est1/2, and controls various cellular processes such as transcription, translation, differentiation, mitosis and apoptosis (W. Zhang & Liu, 2002). Generally, ERK

signalling promotes cell proliferation and survival. However, in certain microenvironments or cell types, ERK can promote pro-apoptotic functions(Lu & Xu, 2006; Strniskova, Barancik, & Ravingerova, 2002).

$P38^{MAPK}$ was first isolated as a 38 kDa protein that underwent rapid phosphorylation in response to the endotoxin lipopolysaccharide (Han, Lee, Tobias, & Ulevitch, 1993). Four members of p38 ^{MAPK} have since been identified: p38α; p38β; p38γ; and p38δ. Most cell lines and tissues express ubiquitous amounts of p38α and p38β, although the expression of p38γ and p38δ is restricted to particular tissue types (Zarubin & Han, 2005; W. Zhang & Liu, 2002). P38α is the predominant isoform expressed in cells in response to extracellular stimuli such as UV light, heat, osmotic shock, inflammatory cytokines and growth factors (Zarubin & Han, 2005). The direct upstream activators of p38 MAPK are MKK3, MKK4 and MKK6. The downstream substrates of p38 are MAPK-activated protein kinase 2 and 3 (MK2 and MK3). MK2 and MK3 are expressed in most cell types and predominantly localized in the nucleus. The activation of MK2 and MK3 influences many cellular processes, such as actin remolding, cell migration, cytokine production, transcriptional regulation and cell cycle control (Cargnello & Roux, 2011). For example, MK2 is known to increase the production of the pro-inflammatory cytokine TNFα, by promoting stability of TNFα mRNA and its translation. This is mediated by MK2's inhibitory phosphorylation of tristetraprolin (TTP), a protein involved in TNFα mRNA degradation (Cargnello & Roux, 2011).

$P38^{MAPK}$ is also reported to be necessary for inducing interferon signalling (Goh, Haque, & Williams, 1999). $P38^{MAPK}$ contributes to phosphorylation and activation of cytosolic phospholipase A2, a lipase enzyme required for the generation of interferon-stimulated gene factor 3 (ISGF3) (Goh, Haque, & Williams, 1999). Furthermore, $p38^{MAPK}$ is required for phosphorylation of STAT1 at serine-727 and thereby subsequent transcriptional activation by

STAT1 (Goh et al., 1999). Notably, another report demonstrates a contradictory finding, wherein p38 is dispensable for STAT1 phosphorylation at ser-701 and ser-727, instead suggests that p38 is required for gene transcription in response to type-I interferon but not type-II (Li et al., 2004). Specifically, in the absence of p38α, they found type-I IFN dependent activation of MK2 and MK3 was defective (Y. Li et al., 2004). There is consistency among various studies in the crosstalk between $p38^{MAPK}$ and IFN signalling which appears to impact immune responses.

1.2.5. Sterile Inflammation

Generally, inflammation is the result of a host immune system in response to a pathogen or irritant. However, the concept of sterile inflammation was coined to situations where inflammation was induced without any detectable infection. This type of inflammation occurs in response to ischemia-reperfusion injury, physical trauma, immunogenic antigens, autoimmune conditions, protein aggregates, cholesterol or urate crystals (G. Y. Chen & Nuñez, 2010). Sterile inflammation can be triggered through nonmicrobial signals such as DAMPs, silica dioxide, iron oxide, amyloid-β and cholesterol (Shen, Kreisel, & Goldstein, 2013). From the literature, sterile inflammation was linked to various pathologies such as systemic lupus erythematosus, tumor progression and cancer, Alzheimer's disease, multiple sclerosis, gout, and atherosclerosis. The identification of molecular mechanisms underlying sterile inflammation is important for the development of novel therapeutics against a plethora of chronic inflammatory diseases (Rock, Latz, Ontiveros, & Kono, 2010).

1.3.Type-I Interferon

Interferon was discovered in 1957 by Alick Isaacs and Jean Lindenmann as a substance that interfered with the replication of influenza virus (K. Chen, Liu, & Cao, 2017). IFNs are cytokines with three major functions. First, IFNs induce an intrinsic antimicrobial state that limits both replication and spread of pathogens in infected and surrounding cells. Second, IFNs function in the innate immune response to promote antigen presentation and activation of natural killer cells, while activating pro-inflammatory signalling and further cytokine production. Third, IFNs function in the adaptive immune response by promoting the proliferation of antigen specific T and B cells and thereby enhancing immunological memory (Ivashkiv & Donlin, 2013). Because of these unique properties, IFNs have been applied as treatment for cancers. IFNs are categorized into three major classes — type I, type II, or type III (Lin & Young, 2014). The type I IFN family (IFN-I) includes subtypes IFNα, IFNβ, IFN-ε, IFN-κ and IFN-ω. Type I IFNs signal by binding to a heterodimeric receptor, IFNAR, composed of IFNAR1 and IFNAR2. Type I IFNs are expressed by most cell types. The second class of IFN contains only one member — IFNγ — that signals through a specific IFNγ receptor (IFNGR) (Platanias, 2005). Lastly, type III IFNs are comprised of one of the three subtypes — IFNλ1, IFNλ2 or IFNλ3 — that bind to their corresponding receptor, IFNLR (Platanias, 2005).

One of the type-I IFNs, IFNβ, is expressed in response to infection and cytokines, such as TNFα. These signals promote expression of IFNβ through signalling that results in activation of interferon regulatory factors (IRFs) (Ivashkiv & Donlin, 2013). Following expression, IFNβ binds to IFNAR in an autocrine or paracrine manner (K. Chen et al., 2017). IFNAR is a heteromeric cell surface receptor composed of two transmembrane subunits IFNAR1 and IFNAR2, which are associated with tyrosine kinase 2 (Tyk2) and Janus kinase 1 (JAK1), respectively (K. Chen et al.,

2017). Upon engagement of IFNAR by IFNβ, TYK2 and JAK1 are activated which in turn phosphorylate tyrosine residues in the cytoplasmic domain of IFNAR. These phosphorylation modifications result in the creation of a docking site for signal transducers and activators of transcription (STAT-1,-2,-3), which in turn are phosphorylated by JAK1 (Lin & Young, 2014). Phosphorylation of STAT1 and STAT2 results in their heterodimerization, followed by recruitment of IRF9 to form a trimeric complex known as IFN-stimulated gene factor 3 (ISGF3) **(Fig. 2)** (K. Chen et al., 2017). Once formed, ISGF3 relocates to the nucleus and binds to IFN-stimulated response elements (ISREs) within the promotor regions of IFN-stimulated genes (ISGs), resulting in the transcription of a vast number of genes (Piehler, Thomas, Garcia, & Schreiber, 2012). Notably, it has been reported that during the late stages of infection or when IFN-I signaling is extinguished, an alternative non-phosphorylated ISGF3 is detectable, which promotes the expression of a unique set of genes **(Fig. 2)** (Cheon et al., 2013).

In the absence of viral infection, there is nonetheless constitutive expression of IFNβ at low levels (W. Wang et al., 2017). This low level is critical for priming cells to promote rapid responses to stimuli (Michalska, Blaszczyk, Wesoly, & Bluyssen, 2018). Low constitutive levels of IFNβ serve additional biological roles: to induce robust responses of cells to IL-6 and IFNγ, a key cytokine that regulates adaptive immunity; to enhance activation of $CD8^+$ T cells; to maintain adequate basal expression levels of various ISGs such as STAT1, IRF9 and IRF1; and to maintain expression of key cell death proteins, such as MLKL (Sarhan et al., 2019). On the other hand, a defect in this priming of cells with low IFNβ compromises the expression of STATs and other regulatory proteins, enhances cell susceptibility to infection and deregulates hematopoietic stem cell homeostasis (Gough et al., 2012). Notably, constitutive, low production of IFNβ is mediated

by a non-canonical pathway independent of ISGF3 (H. M. Chen et al., 2009; Gough, Messina, Clarke, Johnstone, & Levy, 2012).

Type-I interferons are pleiotropic cytokines that are well-characterized for their ability to induce numerous anti-viral genes. In contrast, their roles in the response to bacterial infection are enigmatic (Kovarik, Castiglia, Ivin, & Ebner, 2016). Although bacterial infections induce strong IFN responses, the role of interferon depends on the bacterial species or strain (Boxx & Cheng, 2016). For example, *Chlamydia* is an intracellular bacterium that induces type I IFN production, a response that then restricts the bacterium's growth (Boxx & Cheng, 2016). In contrast, induction of type I IFN by *Listeria monocytogenes*, another intracellular bacterium, is reported to worsen *Listeria* infection (Boxx & Cheng, 2016; O'Connell et al., 2004). Furthermore, a study conducted in our lab reported that infection with *Salmonella enterica* serovar Typhimurium (ST) promotes the production of type I IFNβ, which, similar to *Listeria*, results in detrimental responses that exacerbate the bacterial infection, including the induction of macrophage necroptosis, suppression of innate immune cell recruitment, and promotion of a proinflammatory response (Robinson et al., 2012).

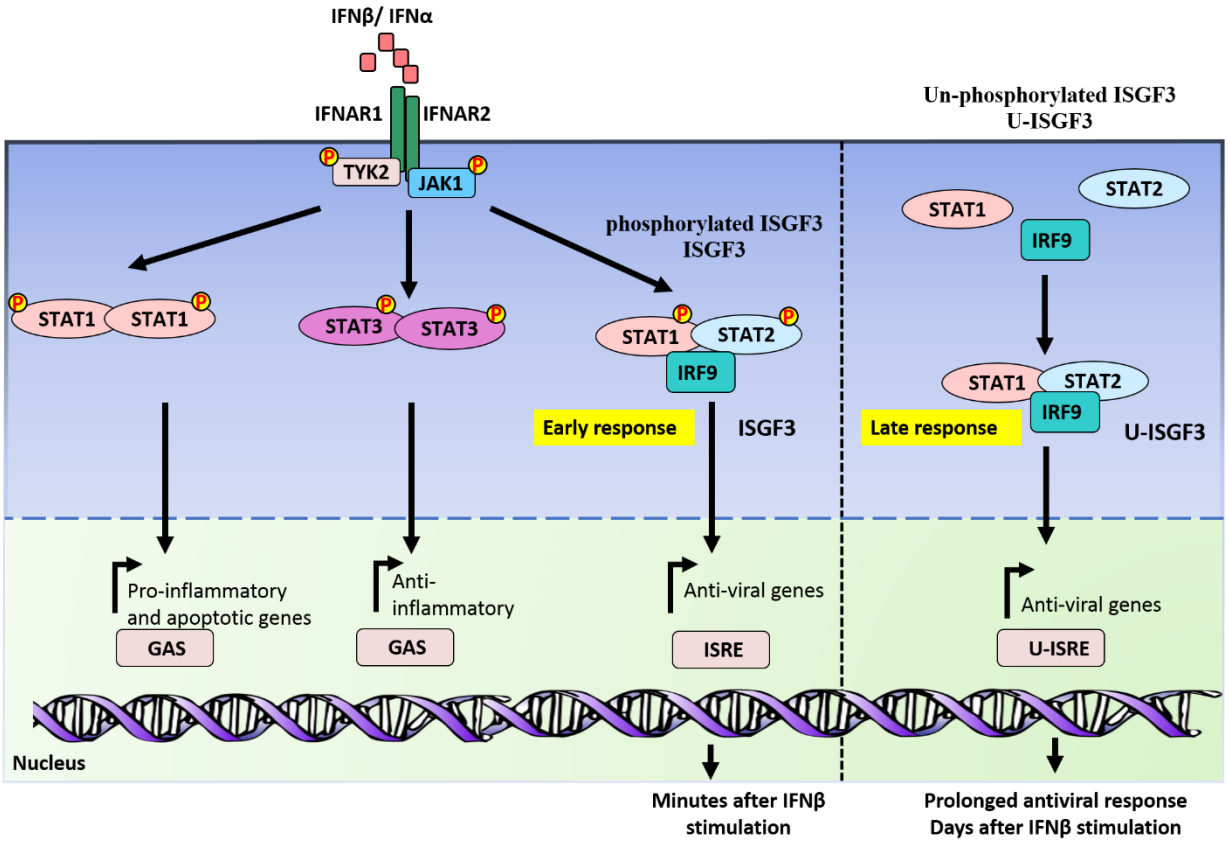
IFNβ/ IFNα
IFNAR1
IFNAR2
TYK2
JAK1
Un-phosphorylated ISGF3
U-ISGF3
phosphorylated ISGF3
ISGF3
STAT1
STAT1
STAT3
STAT3
STAT1
STAT2
IRF9
STAT2
STAT1
IRF9
STAT1
STAT2
IRF9
Early response
ISGF3
Late response
U-ISGF3
Pro-inflammatory
and apoptotic genes
GAS
Anti-
inflammatory
GAS
Anti-viral genes
ISRE
Anti-viral genes
U-ISRE
Nucleus
Minutes after IFNβ
stimulation
Prolonged antiviral response
Days after IFNβ stimulation

Figure 2. Type I interferon signalling pathway.

Engagement of IFN-Is to IFNAR1 (which is composed of IFNAR1 and IFNAR2 subunits) activates and phosphorylates Janus kinase 1 (JAK1) and tyrosine kinase 2 (TYK2). Phosphorylation of tyrosine kinases result in the recruitment and phosphorylation of signal transducer and activator of transcription (STAT) proteins. Phosphorylation of STAT1 can homodimerize, translocate into the nucleus and bind to a gamma activated site (GAS) to induce the expression of pro-inflammatory and apoptotic genes. The interferon-stimulated gene factor 3 (ISGF3) complex composed of STAT1, STAT2, IFN-regulatory factor 9 (IRF9), binds to IFN-stimulated response element (ISRE) to induce the expression of anti-viral and anti-bacterial genes. STAT3 homodimer binds to (GASs) to suppress pro-inflammatory gene expression. The formation of all of these complexes are IFN-dependent, although the assembly of ISGF3 is considered to be the dominant pathway through which IFN-I signaling operates. The un-phosphorylated ISGF3 (U-ISGF3) can be formed by IRF9 and STATs 1 and STAT2 without tyrosine phosphorylation. U-ISGF3 translocates to the nucleus and binds to the ISRE sites to promote the expression of antiviral genes under homeostatic conditions.

1.4.Ubiquitination

Ubiquitination plays an essential role in regulating tissue homeostasis through regulation of protein turnover within cells (Reed, 2002). Ubiquitination is involved in the regulation of NKκB and autophagy which impacts cell survival (Gomez-Diaz & Ikeda, 2018; Avram Hershko & Ciechanover, 1992). Ubiquitination is also involved in the regulation of both apoptosis and necroptosis. Ubiquitination is also central to additional fundamental cellular processes, including cell division and cell differentiation. Defects in ubiquitination are associated with the development of autoimmune and inflammatory diseases, such as arthritis, psoriasis and allergies (Nakamura, 2018; J. Wang & Maldonado, 2006).

Ubiquitination is a post-translation modification (PTM) wherein substrates are modified by their covalent conjugation with ubiquitin at lysine residues or the first methionine (M1) (Gomez-Diaz & Ikeda, 2018; Avram Hershko & Ciechanover, 1992). Ubiquitin is a relatively small, conserved protein composed of 76 amino acids, and is expressed in most cell types (Hershko & Ciechanover, 1998). Ubiquitination is regulated by a three-step cascade involving the ATP-dependent E1, E2 and E3 enzymes. The cascade is initiated when a single ubiquitin molecule becomes bound to E1 and activated by E1. This activated ubiquitin is then transferred to the E2, conjugating enzyme, which in turn transfers the ubiquitin to a target protein via the E3 ubiquitin ligase (Gomez-Diaz & Ikeda, 2018; A. Hershko & Ciechanover, 1998). Ubiquitination of a substrate can result in the addition of mono- or poly-ubiquitin chains and is reversible by deubiquitylating enzymes (DUBs) (Gomez-Diaz & Ikeda, 2018). A ubiquitinated substrate can be recognized by ubiquitin-binding domains of receptors (UBDs) or proteases (DUBs).

Notably, ubiquitin molecules themselves can undergo PTMs, including sumoylation, acetylation, phosphorylation and ubiquitination (Gomez-Diaz & Ikeda, 2018). The linking of

specific forms of ubiquitin to a substrate can determine the fate of substrate and thereby impact its biological function and cellular signalling. For example, a substrate's ubiquitin status can impact its stability, conformation and interactome.

The ubiquitin protein has seven lysine (K) residues, all of which can be ubiquitinated. Ubiquitination at lysine residue 48 (K48) is the predominant linkage type to signal substrate degradation by the proteasome (Swatek & Komander, 2016). In contrast, K63, the second most abundant linkage type, signals non-proteolytic functions such as kinase activation, signal transduction and DNA repair (Swatek & Komander, 2016). Other atypical linkages include K6, K11, K27, K29 and K33, each of which promote distinct functions. When ubiquitin is attached to the first methionine (M1), a linear ubiquitination chain may be generated.

Ubiquitination is integral to the regulation of cell death. For example, several ubiquitination events are involved in apoptotic cell death signalling induced by TNF family members (e.g. TNF, TRAIL, TEAK and FAS ligand), and this signalling can be modulated by both pro-degradation (K48) and non-degradation (K63, K11, Met1) ubiquitin chain modifications. Specifically, TNF family members stimulate recruitment of TRADD, TRAF2 and RipK1 to the TNFR receptor. TRAF2 then recruits the cellular inhibitor of apoptosis proteins, cIAP1/2, an E3 ligase that mediates K11 and K63 linkages of ubiquitin on RipK1. These linkages cause recruitment of a linear ubiquitin chain assembly complex (LUBAC) and the associated IKK complex (IKKα, IKKβ, and NEMO) and TAK1 complex (TAK1 and TAB2/3 (Seo et al., 2019)) **(Fig. 3)**. LUBAC is another E3 ligase that mediates linear ubiquitination of RipK1 and NEMO, leading to the recruitment of the IKK complex and thereby forming complex I. This ubiquitination event induces phosphorylation and activation of IKKβ that in turn activates the pro-survival NFκB pathway and induces expression of anti-apoptotic genes (Nakamura, 2018) **(Fig. 3)**. Notably, phosphorylation

of IKKβ causes IκBα phosphorylation, leading to IκBα K48 linked polyubiquitination and its proteasomal degradation **(Fig. 3)**.

Downregulation of the NFκB pathway is mediated through deubiquitination of K63 and M1 from RipK1 in complex I by the action of three DUBs: A20, a E3 deubiquitinase enzyme that induces RipK1 degradation by replacing K63 with K48 (Wertz et al., 2004); cylindromatosis (CYLD), which negatively regulates the NFκB pathway by deubiquitinating TRAF2, RipK1, NEMO and TAK1 (Seo et al., 2019); and OTULIN (OTU) family deubiquitinase, a DUB that hydrolyzes linear ubiquitin chains (M1) (Fiil et al., 2013) **(Fig. 3)**.

Ubiquitination plays a major role in promoting cell death, apoptosis and necroptosis. TNFα not only promotes cell survival but also can induce programmed cell death through formation of death complexes IIa or IIb. Apoptosis is induced when the expression of NFκB prosurvival genes, such as A20, c-FLIP and cIAP2, is suppressed. These NFκB-dependent prosurvival genes act as late checkpoints for TNF-induced survival or death (Seo et al., 2019). Suppression of their expression leads to the formation of complex IIa, consisting of TRADD, FADD, caspase-8 and RipK1, which induces RipK1-independent apoptosis (Annibaldi & Meier, 2018). K63 ubiqutination of RipK1 is an early checkpoint that suppresses the interaction between RipK1 and Caspase-8 (O'Donnell, Legarda-Addison, Skountzos, Yeh, & Ting, 2007). In contrast, suppression of early checkpoints, through inhibition of TAK1, p38, MK2, cIAPs and/or LUBAC, induces the formation of complex IIb, also known as the necrosome, composed of RipK1, FADD, caspa-8 and RipK3. Inhibition of caspase-8 activity and the formation of the necrosome mediates RipK1-RipK3 dependent necroptosis (Seo et al., 2019). Complex IIa and IIb formation relies on activity of DUBs **(Fig. 3)**.

1.4.1. RipK1 and RipK3 ubiquitination and necroptosis

Intriguingly, RipK1 ubiqutination can promote cell survival or induce necroptosis. Mass spectrometry analysis has revealed that RipK1 has several lysine residues that may undergo ubiqutination. Of these residues, K115 is reported to be required necrosome formation and the execution of necroptosis (Seo et al., 2019; H. Wang et al., 2017) This residue of RipK1 is reported to be ubiquitinated with a K63 linkage by Pellino-1, an E3 ligase. (H. Wang et al., 2017).

RipK3 is key to necroptosis and undergoes several regulatory post translational modifications including phosphorylation and ubiquitination. RipK3 has been reported to be ubiquitinated by cIAP1/2 following LPS stimulation in a TRIF-dependent manner (Seo et al., 2019). However, the biological significance of this modification remains unclear. Hsp70-interacting protein (CHIP) is an E3 ligase that ubiquitinates RipK3 and thereby mediates its lysosomal degradation in absence of immunological stimuli. CHIP knockout mice die within 2 months due to excess RipK3 levels that induce necroptosis unnecessarily (Seo et al., 2016). Additional E3 ligases have been reported to inhibit necroptosis by modifying the ubiquitin state to RipK3. Pellino protein ligase 1 (Pellino-1) is an E3 ligase that catalyzes K48 ubiquitination of kinase-active RipK3 (Choi et al., 2018). A20 also restricts RipK3 activity through K48 ubiquitination, at residue K5, which protects cells from necroptosis by preventing RipK1-RipK3 complex formation (Onizawa et al., 2015).

1.4.2. The role of deubiquitinating enzymes (DUBs) in cell death

Deubiquitinase enzymes (DUBs) function as checkpoints in the control of cell death. A20, also known as TNFα-induced protein 3 (TNFAIP3), has dual functions, having both deubiquitinase and E3 ligase activities. A20 can hydrolyze K63-linked ubiquitin chains as well as exert E3 ligase activity to mediate K48 ubiquitination. In the context of NF-κB signalling, A20 induces RipK1 degradation, resulting in suppression of the NF-κB pathway. A20 also deubiquitinates K63 of caspase-8, resulting in inhibition of caspase-8-dependent apoptosis (Z. Jin et al., 2009).

Cylindromatosis, CYLD, is another DUB that is involved in tumor suppression and inflammatory disease. A well-described function of CYLD is to deubiquitinate RipK1 to allow the transition from complex I to complex II, and thereby necrosome formation **(Fig. 3)**. CYLD plays an essential role in necroptotic cell death as it additionally deubiquitinates RipK1 within the necrosome, facilitating RipK1 kinase activation and necroptosis (Moquin, McQuade, & Chan, 2013).

Many pathways are regulated by TRIAD3a, also known as *RNF216*. TRIAD3a is a E3 ligase that catalyzes K48 ubiquitination linkages on proteins marking them for proteasomal degradation. Over-expression of TRIAD3a is reported to both reduce RipK1-mediated activation of NF-κB and promote apoptosis in response to TNFα (Chen, Li, Zhai, & Shu, 2002). These findings suggest that TRIAD3a negatively regulates TNF signalling. Furthermore, TRAID3a is reported to reduce protein levels of RipK1, TLR4, TLR9 and TRIF during TLR signalling, by promoting proteasomal degradation of these proteins (Chuang & Ulevitch, 2004; Fearns, Pan, Mathison, & Chuang, 2006).

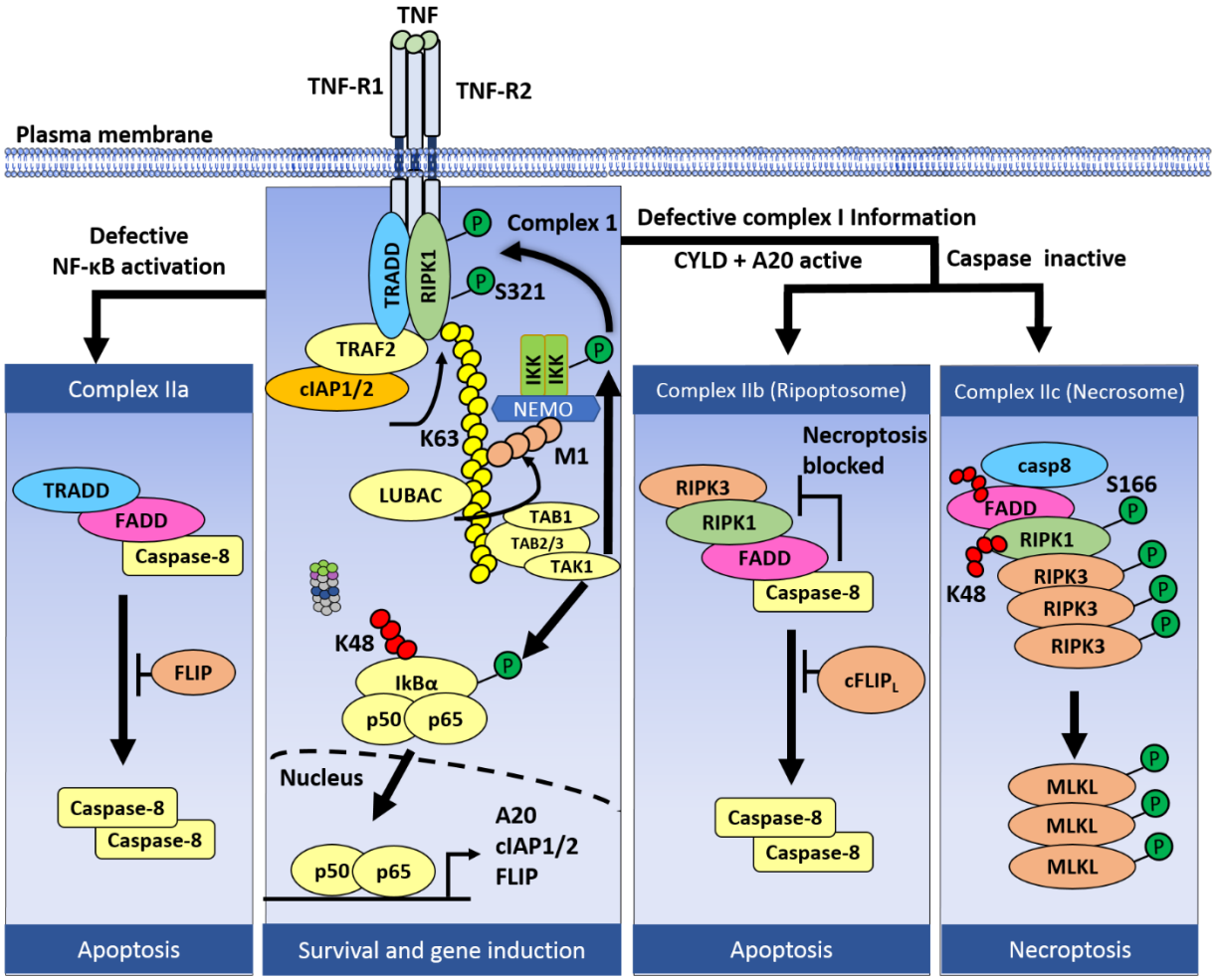
TNF
TNF-R1
TNF-R2
Plasma membrane
Defective
NF-κB activation
Complex 1
Defective complex I Information
CYLD + A20 active
Caspase inactive
TRADD
RIPK1
P
S321
TRAF2
cIAP1/2
IKK
IKK
NEMO
K63
M1
LUBAC
TAB1
TAB2/3
TAK1
K48
IkBα
p50
p65
Nucleus
A20
cIAP1/2
FLIP
Complex IIa
TRADD
FADD
Caspase-8
FLIP
Caspase-8
Caspase-8
Apoptosis
Survival and gene induction
Complex IIb (Ripoptosome)
Necroptosis
blocked
RIPK3
RIPK1
FADD
Caspase-8
cFLIP$_L$
Caspase-8
Caspase-8
Apoptosis
Complex IIc (Necrosome)
casp8
S166
FADD
RIPK1
K48
RIPK3
RIPK3
RIPK3
MLKL
MLKL
MLKL
Necroptosis

Figure 3. The role of ubiquitination in TNF-dependent programmed cell death.

TNF signalling proteins are regulated by phosphorylation and ubiquitination. Following ligation of TNFR1, signalling complexes are formed whose downstream function is governed by ubiquitination. Complex I, the first to form upon TNFR engagement is composed of Tumor necrosis factor receptor type 1-associated death domain protein (encoded by TRADD), TNF receptor-associated factor 2 (encoded by TRAF2), Receptor-interacting protein Kinase 1 (RipK1 protein) and cellular inhibitors of apoptosis 1 (cIAP1) and 2 (cIAP2). cIAP1 and cIAP2 mediate ubiquitination of RipK1 which results in the recruitment of the linear ubiquitin chain assembly complex (LUBAC), the inhibitor of NF-κB (IκB) kinase (IKK) complex — consisting of IKKα, IKKβ and the NF-κB essential modulator (NEMO) — and TAK1 and its adaptor proteins, TAK1-binding proteins-1 (TAB1), -2 (TAB2) and -3 (TAB3). Subsequently, the prosurvival transcription factor nuclear factor-κB (NF-κB) is activated. In contrast, if NF-κB signalling is inactivated, RipK1 is deubiquitinated by CYLD and dissociates from complex I to participate in the complex II. Complex II is composed of FAS-associated death domain protein (FADD), caspase-8, and either TRADD (forming complex IIa) or RipK1 (forming complex IIb or "Ripoptosome"). Complexes IIa or IIb typically induce apoptotic cell death. Finally, if caspases are inactivated, complex IIc forms, which is composed of RipK1, FADD, caspase-8 and RipK3. Complex IIc typically triggers necroptosis by RipK3-mediated phosphorylation of the mixed lineage kinase domain-like protein (MLKL). Adopted from Nat Rev Gastroenterol Hepatol 15, 738–752 (2018) (Schwabe & Luedde, 2018).

1.5. Programmed Cell Death (PCD)

While the adaptive immune system has potential to develop a large repertoire of lymphocytes capable of reacting to various pathogens or immunogenic foreign antigens, it also has the potential to generate lymphocytes that react to self-antigen. It is thought that programmed cell death (PCD) has evolved to eliminate such self-reactive lymphocytes. There are additional essential functions of PCD (Nagata & Tanaka, 2017). First, majority of the appropriately activated immune cells against foreign antigens must eventually be eliminated to create space for other lymphocytes and to avoid any potential toxicity. Second, host cells must be eliminated in order to avoid the spread of intracellular pathogens.

Carl Vogt first demonstrated cell death in 1842, in the notochord and adjacent cartilage of metamorphic toads (Clarke & Clarke, 1996). Much research and technological advances, particularly in the mid to late 1900's, have since founded the concept of programmed cell death (Clarke & Clarke, 1996). In the 1960s, techniques including electron microscopy, histology and histochemistry allowed discoveries of this cell death process, wherein cells undergo a sequence of controlled signalling events causing their own destruction (Lockshin & Zakeri, 2001). In 1990, the discovery of FAS ligand — a death factor — and its receptor, FAS, also advanced the field of PCD. Combined, studies conducted across many animal phyla, model organisms Caenorhabditis elegans, Drosophila melanogaster and mammals, have confirmed the conservation of many anti-apoptotic genes, including Bcl-2, P53 and FAS, establishing the evolutionary genetics of PCD (Horvitz, 1999).

In the present state of knowledge, many forms of programmed cell death have been characterized, that are distinguished by their impact on the host. These forms include necroptosis,

autophagy, pyroptosis, parthanatos, NETosis, mitochondrial permeability transition (MPT)-driven necrosis, and ferroptosis (Galluzzi et al., 2018; Y. Yang, Jiang, Zhang, & Fan, 2015). Among these forms, apoptosis, pyroptosis and necroptosis are the best characterized forms of cell death (Schwabe & Luedde, 2018). Deregulation of programmed cell death results in various pathologies. Thus, characterization of the mechanisms and signalling pathways involved in the regulation of pathological cell death is actively sought after for the development of therapeutic strategies against various diseases (Pettigrew & Cotter, 2009).

1.5.1. Apoptosis

Apoptosis is a non-immunogenic and well-characterized form of programmed cell death. The term apoptosis, assigned by John Kerr in 1972, is derived from the ancient Greek word for "falling of petals from a flower" or "falling of leaves from an autumn tree" (Lawen, 2003). Kerr and colleagues characterized several morphological features of apoptosis. These include plasma membrane blebbing, nuclear condensation or pyknosis, nuclear fragmentation and apoptotic body formation (known as budding) (Heckmann, Tummers, & Green, 2019; Kerr, Wyllie, & Currie, 1972). Apoptotic bodies express an "eat me" signal on cell surface, which promotes engulfment by neighboring phagocytic cells via a process known as efferocytosis (Kugelberg, 2016; Lawen, 2003). Apoptosis is considered to be a non-immunogenic form of cell death because apoptotic cells maintain an intact plasma membrane, thus preventing the release of intracellular contents into the microenvironment and hence limiting inflammation (Elmore, 2007). Apoptosis is associated with biochemical and physical changes in the cytoplasm, nucleus and plasma membrane (Lawen, 2003). These changes are driven primarily by two factors: caspases, which are cysteine aspartate specific proteases; and Bcl-2 protein. These factors can be activated by an intrinsic or extrinsic cell death mechanism (Heckmann et al., 2019; Taylor, Cullen, & Martin, 2008).

1.5.2. Intrinsic Apoptosis Pathway

Intrinsic apoptosis pathway responds to internal non-receptor-mediated stimuli, such as DNA damage, oxidative stress, toxins, hypoxia, hyperthermia or a viral infection (Elmore, 2007). The stimuli of intrinsic pathway result in the production of intracellular signals that may act differently in either a positive or negative signal (Elmore, 2007). Deprivation of hormones, growth factors, cytokines are examples of negative signals that lead to failure of suppression of regulated cell death, thereby resulting in apoptosis. (Elmore, 2007). In contrast, stimuli such as infection, expression of free radicals and other cell stress mechanisms activate apoptosis (Elmore, 2007). Activation of the intrinsic apoptosis pathway modulates the inner mitochondrial membrane and causes the mitochondrial permeability transition (MPT) pore to open, releasing pro-apoptotic proteins such as cytochrome c, secondary mitochondria-derived activator of caspases (SMAC), apoptosis-inducing factor (AIF), BAX (BCL-2-associated X protein), BAK (BCL-2-antagonist/killer-1) and the BH3 interacting domain death agonist (BID) (Elmore, 2007; Taylor et al., 2008). Once released from intermembrane space (IMS) of mitochondria, cytochrome c binds to apoptotic protease activating factor-1 (Apaf-1) in an ATP- or 2-deoxy ATP-dependent manner (Riedl & Salvesen, 2007). This binding induces formation of a heptameric structure known as the apoptosome complex, which in turn recruits procaspase-9 and induces its allosteric activation to caspase-9 (Parrish, Freel, & Kornbluth, 2013; Taylor et al., 2008; Zhang, Chen, Gueydan, & Han, 2018). Caspase-9 then cleaves other downstream caspases (caspase-3,-6 and -7) resulting in their activation (Parrish et al., 2013). Active caspase-3, -6, -7 cleave various substrates, for example PARP, nuclear protein NuMA and cytokines. Furthermore, these effector caspases activate both

a cytoplasmic endonuclease that is involved in DNA degradation and a protease that is involved in cytoskeletal protein degradation (Elmore, 2007; Parrish et al., 2013) **(Fig. 4)**.

1.5.3. Extrinsic Apoptosis Pathway

Extrinsic pathway responds to the binding of extracellular ligands to extracellular domains of transmembrane receptors (Riedl & Salvesen, 2007). For example, the extrinsic pathway can be induced by binding of ligands such as TNFα, Fas ligand (FasL) and TNF-related apoptosis-inducing ligand (TRAIL) to their respective cognate receptors: TNFR1; CD95 (FasR); TRAIL-R1; and TRAIL-R2 (Fulda & Debatin, 2006). Most receptors influencing the extrinsic pathway are members of TNF receptor gene superfamily, which have homology in their extracellular domains and cytoplasmic death domains (DD) (Elmore, 2007). The presence of death domain is essential for recruitment of other adaptor proteins and subsequent downstream signalling (Fulda & Debatin, 2006). The binding of FasL or TRAIL to its cognate receptor results in a conformational change in the receptor's death domain. This change results in recruitment of several adaptor molecules, including FAS-associated death domain (FADD) (Fulda & Debatin, 2006). Interactions between the death effector domains (DED) of FADD and either pro-caspase-8 or pro-caspase-10 then induce dimerization and activation of the pro-caspase (Elmore, 2007; Oberst et al., 2010). Together, these changes result in formation of a complex called the death inducing signalling complex (DISC) (Elmore, 2007; Lawen, 2003). Once formed, the catalytically active caspase-8 cleaves and activates the "executioner" caspases, from pro-caspase-3, pro-caspase-7 to capsase-3 and caspase-7, which in turn promote apoptosis as mentioned above (Heckmann et al., 2019).

Intriguingly, certain executioner caspases promote crosstalk between the intrinsic and extrinsic pathways. In context of TNF-mediated apoptosis, caspase-3 induces the activation of

caspases -8, -9 and -10, allowing crosstalk between intrinsic and extrinsic apoptosis pathways and strengthening the total apoptosis response (S. Yang, Thor, Edgerton, & Yang, 2006). Additionally, caspase-8 promotes crosstalk between the pathways by cleaving BID, resulting in activation of effector proteins BAX and BAK, and thereby causing release of cytochrome c to initiate intrinsic apoptosis (Green & Llambi, 2015; Heckmann et al., 2019).

Signalling of the extrinsic pathway is regulated by the endogenous inhibitor of apoptosis, cellular FLICE inhibitory protein (cFLIP). cFLIP has a long (cFLIPL) or short (cFLIPS) splice variant, which each share homology with caspase-8 and caspase-10 but lack a catalytic domain. The variants have preferential binding. For example, cFLIPL preferentially heterodimerizes with caspase-8 and inhibits apoptosis by inhibiting caspase-8 catalytic activity (Heckmann et al., 2019). Further regulation of the extrinsic pathway is conducted by XIAP (X-linked inhibitor of apoptosis protein), an E3 ubiquitin ligase and member of the IAP family. By polyubiquitination linkage, XIAP inhibits catalytic the activity of caspase-9 (at the initiation phase of apoptosis), and caspases -3 and -7 (at the execution phase) (Eckelman, Salvesen, & Scott, 2006) **(Fig. 4)**.

1.5.4. Pyroptosis

Pyroptosis is an inflammatory form of programmed cell death that occurs in infected cells or in cells that get stimulated by sterile triggers such as aggregated proteins, urate crystals, cholesterol crystals etc. Pyroptosis has evolved as a host defense mechanism against intracellular pathogens (Fink & Cookson, 2005). In the pyroptosis signalling pathway, first pro-caspase-1 is recruited and activated in a complex called the inflammasome, generating mature capsase-1. Caspase-1 then induces destruction of cytoskeleton proteins, degradation of cIAPs and pore formation in the plasma membrane, leading to cell swelling, water influx, and increased osmotic pressure that

ultimately results in osmotic lysis and the release of inflammatory molecules (Bergsbaken, Fink, & Cookson, 2009).

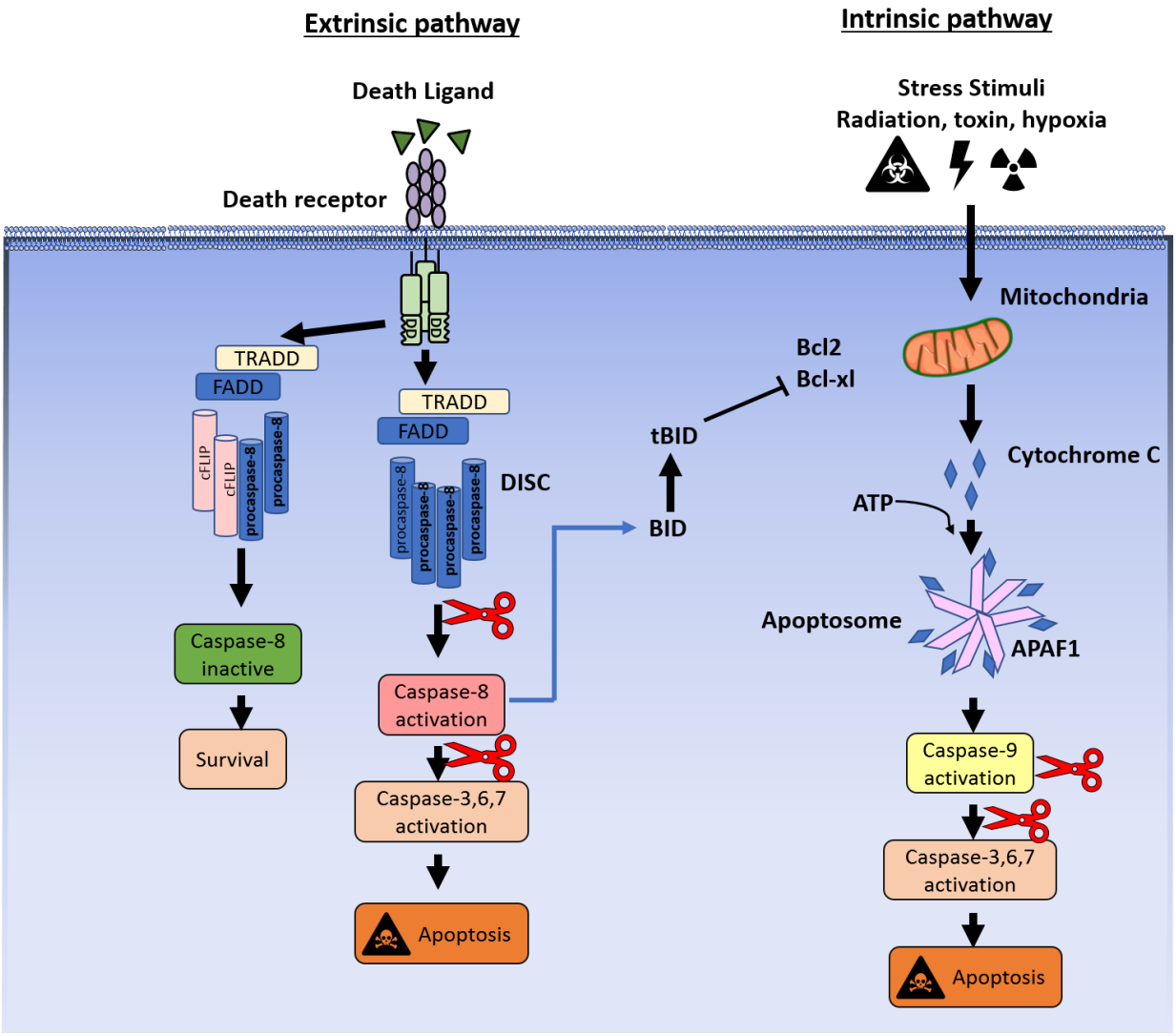
Extrinsic pathway
Intrinsic pathway
Death Ligand
Death receptor
Stress Stimuli
Radiation, toxin, hypoxia
Mitochondria
TRADD
FADD
cFLIP
procaspase-8
Caspase-8 inactive
Survival
DISC
Caspase-8 activation
Caspase-3,6,7 activation
Apoptosis
tBID
BID
Bcl2
Bcl-xl
Cytochrome C
ATP
Apoptosome
APAF1
Caspase-9 activation

Figure 4. The pathways of apoptosis.

Extrinsic apoptosis is triggered by multiple members of the TNFR superfamily proteins such as Fas and TNF-related apoptosis-inducing ligand (TRAIL). Once the ligand binds to its cognate receptor, TRADD and FADD adaptor proteins are recruited to the receptor through the interaction with their death domain (DD). Subsequently, FADD recruits procaspases-8 through interactions between their death effector domains (DEDs). These interactions result in the formation of the DISC complex. The homodimerization of procaspase-8 results in its activation which in turn activates executioner caspases, caspase-3, -6 or -7 and results in apoptosis. Heterodimerization of procaspase-8 with cFLIPL prevents procaspase-8 homodimerization and consequent inactivation that results in cell survival. Intrinsic apoptosis is triggered by various stress stimuli resulting in the release of the mitochondrial protein, cytochrome c which in turn binds APAF-1 (apoptotic protease activating factor-1) to form a complex called apoptosome that activates procaspase-9. Active Caspase-9 cleaves and activates executioner caspases that result in apoptosis. The extrinsic pathway bridges the intrinsic pathway via cleavage of BID by active caspase-8. Cleavage of BID results in the formation of truncated BID (tBid) that inhibits anti-apoptotic proteins and activates Bak and Bax which induce the release of cytochrome c to initiate intrinsic apoptosis.

1.5.5. Necrosis and Secondary Necrosis

Necrosis, or primary necrosis, originates from the Greek word for "dead body" (Vanlangenakker, Vanden Berghe, & Vandenabeele, 2012). Necrosis was previously considered as an unregulated, accidental mode of cell death. It is induced in response to uncontrolled exogenous stress conditions, trauma, depletion of ATP or physical damage. Morphologically, cells undergoing necrosis have specific features: oncosis (cell swelling); dilated organelles; DNA fragmentation; and plasma membrane rupture (Vanlangenakker et al., 2012). Cell membrane rupture results in the release of intracellular contents and DAMPs, causing inflammation in the tissue (Galluzzi et al., 2018).

In addition to this primary necrosis, studies have identified a form of secondary necrosis. In secondary necrosis, defective clearance of an apoptotic cell by resident macrophages results in necrosis, characterized by the loss of cell membrane integrity and cell autolysis (Sachet, Liang, & Oehler, 2017). Wyllie at al. (1980) described this autolysis step as "secondary necrosis", distinguishing it from accidental (primary) necrosis (Sachet et al., 2017; Wyllie, Kerr, & Currie, 1980). Secondary necrosis is reported to occur in pathological conditions wherein excessive apoptosis reduces the clearance capacity of macrophages (Garg, Romano, Rufo, & Agostinis, 2016; Nagarajan, Soundarapandian, Thorne, Li, & Li, 2019; Sachet et al., 2017). It is important to note, however, that there are studies with contrasting hypotheses about the cause of secondary necrosis. For example it is argued that secondary necrosis is the response to a failure in apoptosis signalling wherein phagocytosis cannot be initiated (T. Vanden Berghe et al., 2009). However, secondary necrosis has been reported in some patho-physiological conditions where apoptosis failed, and cells are shed into the extracellular milieu such as gut or the airways lumen where the

presence of phagocytic cells are very low. Also, mutations in phagocyte receptors increased the occurrence of secondary necrosis (Silva, 2010).

1.5.6. Necroptosis

Necroptosis is a highly inflammatory, regulated form of necrotic cell death (Oliveira, Amaral, & Rodrigues, 2018). In this process, cells have morphological features that more closely resemble cells having undergone the above-described unregulated necrosis (section 1.5.3) rather than apoptosis. Despite similarities in morphology, necroptosis is distinguished by its kinase-dependent regulation that occurs under caspase-compromised conditions (Dunai, Bauer, & Mihalik, 2011) with slower kinetics than primary necrosis (Kaczmarek, Vandenabeele, & Krysko, 2013).

Experimental observations of necroptosis have been delineated under conditions wherein Caspase activity is inhibited. In 1996, necroptosis was observed in pig kidney cells infected with a cowpox virus that expressed a cytokine response modifier A (CrmA) and a caspase-8 inhibitor (Tang, Kang, Berghe, Vandenabeele, & Kroemer, 2019). A second observation was in murine L929 fibrosarcoma cells, treated with TNF as well a broad-spectrum inhibitor of caspases, carbobenzoxy-valyl-alanyl-aspartyl-[O-methyl]-fluoromethylketone(Z-VAD-FMK) (Vercammen et al., 1998). Notably, the development of this pan-caspase inhibitor, Z-VAD-FMK, has had a major impact on the advancement of knowledge of necroptosis (Slee et al., 1996). The two above-mentioned observations demonstrated that caspases inhibit programmed necrosis, which helped in delineation of the signaling differences between necrosis and necroptosis. In 2000, Holler and colleagues characterized caspase-independent necroptosis signalling in T cells, in response to Fas, TRAIL and TNF, in the absence of active caspases (Holler et al., 2000). This study defined the

molecular basis of necroptosis signalling and demonstrated the requirement for both RipK1 kinase activity and FADD (Holler et al., 2000).

RipK1 is a key regulator of necroptosis. RipK1 has the following domains: an N-terminal kinase domain; an intermediate domain that mediates NF-κB and MAPK activation; a RIP homotypic interaction motif (RHIM) that enables RipK1-RipK3 interactions; and a C-terminal death domain (DD) required for RipK1 interactions with other proteins containing death receptors (Meng et al., 2018; Shan, Pan, Najafov, & Yuan, 2018). Degterev et al. (2005) established RipK1 as a pro-necroptotic protein by demonstrating that death-receptor-induced necroptosis could be blocked in cells treated with an inhibitor of RipK1 kinase activity, necrostatin-1 (A. Degterev et al., 2005).

1.5.7. The molecular basis of necroptosis and the necrosome complex

The molecular pathway leading to necrosome complex formation can be summarized as follows. First, following the ligation of the TNFR receptor various proteins are recruited to its cytosolic domain: TRAF2; FADD; cIAP1/2; TRADD; and RipK1. This recruitment results in the formation of complex I and activation of the NFκB pathway (described in section 1.4), promoting cell proliferation and differentiation. However, if the translation machinery is blocked, and caspases are inactive, the necrosome is formed, and not complex I. Necrosome assembly is regulated by both ubiquitination and phosphorylation. Specifically, a deubiquitinating enzyme, cylindromatosis (CYLD) or A20, removes M1 and K63 ubiquitin chains from RipK1 allowing dissociation from cytosolic complex I and interaction with FADD, RipK3 and caspase-8. This interaction between RipK1 with RipK3 (via their RHIM domains) induces RipK3 phosphorylation and triggers necroptosis (Mompean et al., 2018). This activation of RipK3 further results in

recruitment and phosphorylation of the pseudokinase mixed lineage kinase like (MLKL) protein **(Fig. 5)**, which mediates sodium influx via Ca^{2+} and Na^{+} ion channels. Increased osmotic pressure then causes plasma membrane rupture and the release of intracellular contents (Dhuriya & Sharma, 2018) **(Fig. 5).**

Many studies have emphasized the importance of RipK1 phosphorylation status on necrosome signalling. Within RipK1 protein, several serine residues have been shown to undergo autophosphorylation, and others to undergo phosphorylation by a yet unknown kinase (Degterev et al., 2008) or a defined kinase. Jacob and colleagues reported MK2 to phosphorylate RipK1 at S320/321 in response to TNF. They further identified that MK2 mediated phosphorylation of RipK1 at S320/321 inhibits the kinase activity of RipK1, thereby inhibiting RipK1 autophosphorylation at S166, and inhibiting the formation of the necrosome complex and TNF-mediated necroptosis (Jaco et al., 2017). IKKs have also been shown to inhibit RipK1 kinase activity and necroptosis by phosphorylating RipK1 at S25 (Yves Dondelinger et al., 2019).

On the other hand, it is unclear how RipK3 is phosphorylated; does the interaction of RipK3 with the other proteins like MLKL and RipK1 mediate autophosphorylation of RipK3 to induce necrosome signalling ?

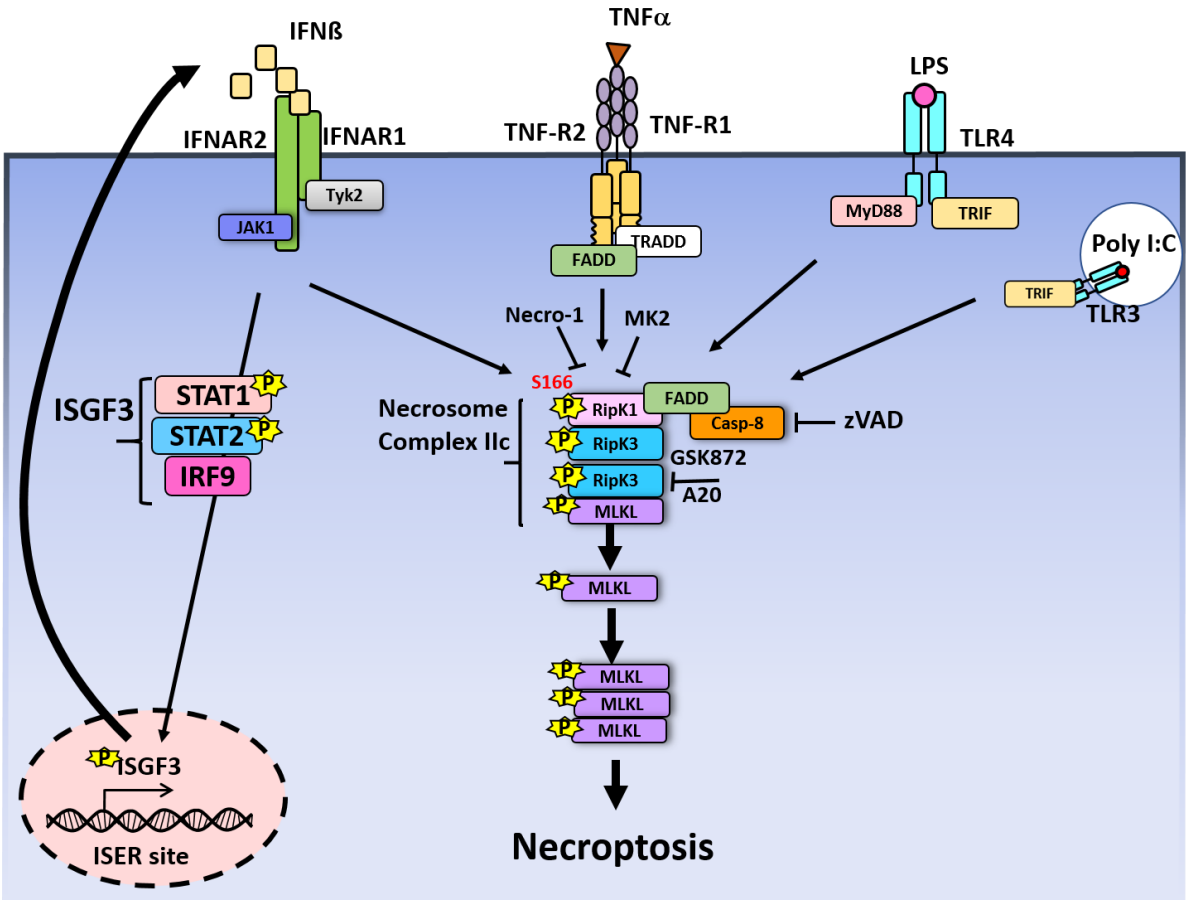
IFNß
IFNAR2
IFNAR1
Tyk2
JAK1
TNFα
TNF-R2
TNF-R1
TRADD
FADD
LPS
TLR4
MyD88
TRIF
Poly I:C
TRIF
TLR3
Necro-1
MK2
S166
ISGF3
STAT1
STAT2
IRF9
Necrosome
Complex IIc
RipK1
FADD
Casp-8
zVAD
RipK3
GSK872
RipK3
A20
MLKL
MLKL
MLKL
MLKL
MLKL
ISGF3
ISER site
Necroptosis

Figure 5. Triggers of necroptosis.

Necroptosis is triggered by various stimuli that lead to engagement of Toll-like receptors (TLRs), interferon receptor (IFNAR and IFNγR) and death receptors (TNFR and TRAILR). Engagement of these receptors with the cognate ligands leads to RipK1 S166 phosphorylation and when the caspase 8 activity is inhibited by zVAD, RipK1 interacts with RipK3 through its RHIM domain and results in phosphorylation of RipK3. Consequently, active RipK3 phosphorylates and activates the executor MLKL which results in necroptosis. Autocrine loop of de novo-transcribed IFNs/IFNAR1 signaling is essential to sustain RipK3 activity and necroptosis. GSK872: RipK3 kinase inhibitor. A20: deubiquitinate RipK3 in steady state. Nec-1 (necrostatin-1): RipK1 kinase inhibitor.

1.5.8. Execution of Necroptosis

Murphy et al. identified the pseudo kinase mixed lineage domain-like protein, MLKL, as an executioner of necroptosis (J. M. Murphy et al., 2013). Briefly, when RipK1 interacts with RipK3, inactive monomeric MLKL is recruited to the necrosome and activated by RipK3, which, in mice, phosphorylates MLKL within its activation loop, at serine 352 and threonine 349 (L. Sun et al., 2012). These phosphorylation events induce an open conformational structure of MLKL, exposing its four-helical bundle domain, and in turn promoting the oligomerization and translocation of MLKL from the cytosol to the plasma membrane (Cai et al., 2014; L. Sun et al., 2012). Thereafter, as proposed by Dondelinger et al., the MLKL oligomer binds to negatively charged phosphatidylinositol phosphates (PIPs) upon translocation, causing formation of a pore in the cellular membrane and resulting in membrane rupture (Y. Dondelinger et al., 2014). Furthermore, a recent report by Dovey et. al. found that the oligomerization and membrane localization of MLKL following phosphorylation by RipK3 required inositol phosphate (IP) kinases (inositol polyphosphate multikinase (IPMK) and inositol 1,3,4-trisphosphate 5/6-kinase (ITPK1) as essential mediators of necroptosis (Dovey et al., 2018). However, there are different hypotheses explaining how MLKL translocation induces cell death (reviewed in Huang et al., 2018). For example, MLKL may also induce ion-pore dysregulation (Na^+ and Ca_2^+ influx), thus expediting permeabilization of plasma membrane due to the increase in osmotic pressure (X. Huang et al., 2018). Alternatively, RipK3 may activate Ca_2^+-calmodulin-dependent protein kinase II (CaMKII), which may activate ion channels to induce an ion influx independent of MLKL (Huang et al., 2018). Yet another hypothesis is that MLKL induces necroptotic cell death by altering mitochondrial permeability, causing a depletion of cellular ATP and increase in reactive oxygen species (ROS) (Schenk & Fulda, 2015).

1.5.9. TLR signalling and necroptosis

Many signalling receptors are reported to initiate necroptosis in macrophages, including TNFR, toll-like receptors (TLR3, TLR4) and type I and II IFN receptors (James M. Murphy & Vince, 2015) . The engagement of TLR3 or TLR4/TLR2 by polyinosine–polycytidylic acid (poly(I:C)) and lipopolysaccharide (LPS), respectively, in caspase-inactive conditions, results in necroptosis through the interaction between adaptor protein TRIF and RipK3, via their RHIM domains (S. Wang, Zhang, Hu, & Yang, 2016). Pattern Recognition Receptor (PRR) engagement mediates necroptosis in innate immune cells and induces the release of co-stimulatory signals for adaptive immune cells. The engagement of PRRs also promotes a microbicidal and inflammatory response to eliminate pathogens and pathogen-infected cells that escape apoptosis (Amarante-Mendes et al., 2018).

Pathogens can manipulate or escape the immune response and inhibit apoptosis. For example, some DNA viruses inhibit apoptosis by promoting caspase inhibition, allowing viral persistance in the host. More specifically, cowpox virus encodes a cytokine response modifier A (CrmA) that inhibits caspase-8 to block apoptosis (Zhou et al., 1997). Such inhibition of caspase activity primes infected cells for necroptosis (Nailwal & Chan, 2019). Even so, some viruses express anti-necroptotic proteins (Nailwal & Chan, 2019). For example, vaccinia virus has been shown to express E3L, a protein that inhibits type-I IFN-induced necroptosis (Koehler et al., 2017). Similarly, Epstein–Barr virus (EBV) inhibits TNF-induced necroptosis by modulating ubiquitination of RipK1 and RipK3 (X. Liu et al., 2018). Understanding how viruses target necroptosis, and otherwise modulate the host's anti-viral immunity, is critical to the development of effective therapeutics for both viral infections and other diseases caused by similar dysregulation of the immune response (Nailwal & Chan, 2019).

1.5.10. Interferon signalling and necroptosis

A number of studies have demonstrated the pro-necroptotic role of type I IFN signalling. The role of type I IFNs in programmed cell death was first discovered in blind mole rat (BMR) cells which, intriguingly, exhibited remarkable cancer resistance (Gorbunova et al., 2012). The study revealed that this resistance, acquired by BMR fibroblasts, could be reversed by the release of IFNβ, which caused necrotic cell death (Gorbunova et al., 2012). In 2012, Robinson and colleagues found that *Salmonella enterica ssp. enterica ser. Typhimurium* (*S. Typhimurium*) induced necroptosis in a type I IFN-dependent manner (Robinson et al., 2012). In the same study, they demonstrated that IFNAR1-deficient mice had less pathology associated with poor necroptosis (Robinson et al., 2012). McComb et al. showed that type I IFNs mediate necroptosis through IFN-stimulated gene factor 3 (ISGF3), a transcriptional complex composed of STAT1, STAT2, and IRF9 (McComb et al., 2014). In this study, ISGF3 was also found to sustain RipK3 activity and promote necroptosis in macrophages (McComb et al., 2014). Moreover, MLKL, executioner of necroptosis, is one these interferon-stimulated genes (ISGs) (Knuth et al., 2019). The importance of IFN signalling and necroptosis was further supported by a recent study demonstrating that constitutive interferon signalling is essential to prime macrophages for necroptosis by maintaining a critical threshold of MLKL expression (Sarhan et al., 2019), and that elevated IFN signalling sensitizes macrophages to necroptotic cell death (Sarhan et al., 2019).

2.0 THESIS SUMMARY

2.1 Rationale

Macrophages are phagocytic cells that play a fundamental role in innate immunity against pathogens and involved in a wide array of pathologies. Activation of macrophages result in the production of ROS and proinflammatory cytokines which mediate the clearance of pathogens but also results in tissue inflammation and necroptotic cell death. Necroptosis in macrophages has been linked to a growing number of pathologies, such as inflammatory disease, atherosclerosis, pancreatitis, neurological disease and microbial infections (Linkermann et al., 2014). It could amplify the chronicity of inflammation because of the release of many inflammatory cytokines (e.g., IL-33, HGMB1) (Lanhout et al., 2014). Many *in vivo* studies have shown that deficiency in necroptosis signalling reduces inflammatory pathology. Therefore, it is critically important to understand the molecular basis that controls the formation of necrosomes and activation of necroptosis in order to develop a new and specific therapeutic target that could abolish necroptosis and prevent excessive inflammation. Moreover, the regulated induction of necroptosis may provide new avenues for cancer therapeutics (Gorbunova et al., 2012).

2.2 Hypothesis

Necrosome signalling leads to necroptosis, which is an undesirable form of cell death. Thus, there must be multiple mechanisms that regulate necrosome signalling. I hypothesize that RipK3 plays a dual role during necrosome signalling. While its kinase region induces necrosome activation, the RipK3 scaffold induces premature degradation of the necrosome. Furthermore, type-I interferon induces the maintenance of RipK3 and MLKL phosphorylation, and late necrosome formation leading to necroptosis of macrophages.

2.3 Aims

1. **To delineate the mechanisms that regulate the induction and maintenance of the necrosome.**

a. Examine the kinetics of necroptosis upon TLR4 activation.

b. Evaluate the impact of TLR4 stimulation on the expression of RipK1 and RipK3 during necroptosis will be evaluated.

c. Investigate the impact of TLR4 activation in the absence and presence of the pan-caspase inhibitor zVAD .

d. Evaluate the formation of the necrosome, and the time kinetics of cell death upon IFNβ- and TNFα- induced necroptosis.

e. Determine the time kinetics of RipK1 degradation.

f. Use specific knockout models to determine the specific roles of TRIF, RipK1 (K45A), and RipK3 in the regulation and maintenance of RipK1.

g. Explore the ubiquitination of key necroptotic proteins.

h. Utilize various chemical inhibitors and proteasome blockers to determine the mechanism of RipK1 degradation.

i. Explore the impact of different E3 ligases using sing small interference RNA knockdown approach.

j. Assess the relative release of the E3 ligase knockdown on inflammatory cytokine production during necrosome signaling.

2. **Delineation of the mechanisms responsible for necrosome signalling following engagement of type-I interferon receptor.**

a. Utilize IFNAR1 knockout mice to assess RipK1, RipK3, and MLKL activation.

b. Explore the role of IFNAR1 and its downstream kinase Tyk2 in activation of RipK3 and necroptosis.
c. Evaluate the gene expression profile of type-I interferon pathways in necroptosis.
d. Investigate the role of p38 MAPK kinase in IFN-I signalling.
e. Utilize various knockout mice and knockdown approaches to determine the role of specific genes in promoting necroptosis.

3.0 MATERIALS AND METHODS

3.1. Mice

All mice were housed and bred at the University of Ottawa Animal Facility in specific pathogen-free conditions. Mice were maintained in accordance with Canadian Council on Animal Care (CCAC) guidelines. Procedures and protocols were approved by the University of Ottawa Animal Care Committee and Ethics Board. Mice strains utilized for experiments, and their sources, are listed in Table 1. All mice utilized in experiments were age and sex matched. All mice used in experiments were between six and eight weeks of age and were on the C57BL/6 genetic background.

3.2.Generation of Bone Marrow Derived Macrophages

Mouse bone marrow was used as a source of cells to generate primary murine bone marrow derived macrophages (BMDMs). Briefly, mice were euthanized using CO_2 followed by coating with 70% ethanol. The fur surrounding the fore and hind legs was removed using sterile scissors and tweezers. Muscles and tissue were removed carefully, and clean bones were placed in cold RPMI + 8% FBS + 55μM β-mercaptoethanol (2ME) + 50 ng/mL gentamycin. Each bone was flushed with ice-cold R8+gentamycin using a small gauge needle and the harvested cells were passed through a 70-100 nm strainer into a 50 mL falcon tube. Ten to twenty μL aliquot was taken to count the number of cells and the remaining cells were pelleted at 1600 RPM for 8 minutes. Meanwhile, 50 mm non-tissue culture petri dishes were coated evenly with macrophage colony-stimulating factor (M-CSF) at a final concentration of 5 ng/mL. Following centrifugation, the cell pellet was resuspended in R8 with gentamycin and between $10x10^6$ to $17x10^6$ cells were added carefully to the coated petri dish. R8+ gentamycin was added to the cells to a final volume of 10

mL. Cells were incubated at 37°C for 6 days to allow differentiation of macrophages. Flow cytometry was used to confirm the purity of the bone marrow macrophages ($CD11b^{+}/F4/80^{+}$).

Table 1: Mouse strains utilized in experiments.

Mouse Strain	Source	Origin information
C57BL/6J	Jackson Laboratories	Stock #000664
cIap1$^{-/-}$ *cIap2*$^{-/-}$ *xIap*$^{-/-}$	A kind gift from Dr. Robert Korneluk. University of Ottawa.	Generated as described by (Harlin, Reffey, Duckett, Lindsten, & Thompson, 2001)
Cyld$^{-/-}$	A kind gift from Dr. Shao-Cong Sun. Pennsylvania State University, USA.	Generated as described by (W. W. Reiley et al., 2006)
Ifnar1$^{-/-}$	A kind gift from Dr. Kaja Murali-Krishna. Emory University, USA.	Mice were backcrossed to C57BL/6 for 14 generations as described by (Kolumam, Thomas, Thompson, Sprent, & Murali-Krishna, 2005)
Mk2-$^{-/-}$ *Mk3*$^{-/-}$ *DK*	A kind gift from Dr. Matthias Gaestel Hannover Medical School Germany.	Generated as described by (Kotlyarov et al., 1999), Double knockout (Ronkina et al., 2007)
Mlkl$^{-/-}$	A kind gift from Dr. Emad Alnemri. Thomas Jefferson University, Philadelphia, USA.	Generated as described by (J. M. Murphy et al., 2013)
Myd88$^{-/-}$	Jackson Laboratories	Stock #009088
Ripk1^{K45A}	A kind gift from Dr. Peter J. Gough. GlaxoSmithKline, Collegeville, USA.	Generated as described by (Berger et al., 2014)
Ripk3$^{-/-}$	A kind gift from Dr. Vishva Dixit. Genentech, USA.	Generated as described by (Newton, Sun, & Dixit, 2004)
Tnfr1$^{-/-}$	Jackson Laboratories	Stock #003242
Tnfr1,2$^{-/-}$	Jackson Laboratories	Stock #003243
Tnfr2$^{-/-}$	Jackson Laboratories	Stock #002620
Tnf-α$^{-/-}$	Jackson Laboratories	Stock #005540
Trif$^{-/-}$	Jackson Laboratories	Stock #005037
Ifit2$^{-/-}$	A kind gift from Dr. Ganes C Sen Lerner Research Institute, Cleveland, Ohio, USA	Generated as described by (Fensterl et al., 2012)
Gitr$^{-/-}$	A kind gift from Dr. Tania Watts University of Toronto, Canada	Generated as described by (Clouthier et al., 2015)

3.3. In vitro inhibitor assays

Bone marrow derived macrophages were treated with various inhibitors and agonists and the details of each treatment will be described in the text. A full list of inhibitors/agonists is provided in Table 2. In general, on day six of differentiation, the BMDMs were seeded in 96-well flat bottom tissue culture plates at $7x10^4$ cells/well and incubated overnight at 37°C to ensure the cell adherence to the plate before treatment. On day 7, BMDMs were treated with appropriate concentrations of inhibitors and left for 6 to 24 hours before measuring cell death or viability.

3.4. Cell viability assay

1- **MTT:** Cell viability was measured using a 3-[4,5-dimethylthiazol-2-yl]-2,5-diphenyltetrazolium bromide (MTT) assay. The MTT reagent was diluted with R8 media to a final concentration 0.5 mg/mL and added to cell cultures. After 2 hours of incubation at 37°C, 5 mM HCl in isopropyl alcohol was added to solubilize MTT crystals and absorbance was measured at a wavelength of 570 nm with a reference wavelength of 650 nm on a Molecular Devices FilterMax plate reader. Data was obtained and analyzed using SoftMax pro and Graphpad Prism V7 software. Depending on the experiment, optical density values were normalized to either untreated cells or to controls without zVAD.

2- **Cell Counting Kit-8 (CCK-8):** An aliquot of 10 µL of (CCK8) was added to each well and incubated at 37°C for 2–4 h. After incubation, absorbance at 450 nm was measured using Molecular Devices FilterMax plate reader. CCK-8 (cat# CK04-01) was obtained from Dojindo Molecular Technologies (Rockville, USA).

3- **Flow cytometry:** Zombie Yellow™ (BioLegend, San Diego, CA) was used to assess cell viability. Twenty-four hours after treating the cells in a 96-well plate with various reagents,

the seeded cells were washed twice with PBS buffer. Without detaching the cells, 50 µL of diluted Zombie Yellow™ solution (1:100 in PBS) was added to each well and then plates were incubated at room temperature, in the dark, for 15–30 minutes before washing with 100 µL FACS buffer (PBS, 1% BSA, 1 mM EDTA) once. Then, samples were fixed by using 1% paraformaldehyde and analyzed by Flow cytometry (LSR Fortessa and FACSDiva software (Becton Dickinson). The data was analyzed using FlowJo software.

4- **Alamar Blue**: Alamar blue solution was made by adding 25 mg of resaurin sodium salt (cat# R7017, sigma) dissolved in 250 mL distilled water and filter sterilized. An aliquot of 57 µM was added to each well and plates were incubated at 37°C and protected from light for 2-4 hours. Fluorescence intensity was measured using Molecular Devices FilterMax plate reader with excitation at 530 nm and emission at 595 nm. Data was obtained and analyzed using SoftMax pro and Graphpad Prism V7 software. Absorbance values were normalized to either untreated cells or to controls without zVAD.

Table 2. Inhibitors and agonists used for experiments.

Inhibitor/Agonist	Source	Notes	Final Concentrations
1,10-phenanthroline	LifeSensors (SI9649)	Deubiquitinase inhibitor	20 μM
Actinomycin-D	MP Biomedicals (0219452505)	Inhibitor of transcription	80 nM
Birinapant BP	Selleckchem (S7015)	cIAPs and xIAP inhibitor	10 μM
Cyclohexamide	Sigma-Aldrich (C4859)	Endosomal acidification inhibitor	1.7 μM
GSK843 and GSK'872	Aobious (AOB4898, AOB488)	Inhibitor of Rip3 kinase activity	3-5 μM
Hydroxychloroquine	Sigma-Aldrich (H0915)	Autophagy inhibitor	100 μM
Lactacystin	Sigma-Aldrich (Cat. # L6785)	Proteasome inhibitor	10 μg/mL
MG132	Sigma-Aldrich (C2211)	Proteasome inhibitor	10 μM
MG341 (Bortezomib)	Calbiochem (504314)	Proteasome inhibitor	10 μM
Necrostatin-1 (Nec-1)	Sigma-Aldrich (Cat. # 9037)	Inhibitor of Rip1 kinase activity	30 μM
P38 inhibitor (SB203580)	Cell Signalling (5633S)	P38 MAPK inhibitor	50 μM
P38 inhibitor (LY2228820)	Selleck Chemicals S1494	P38 MAPK inhibitor	5 μM
PR-619	LifeSensors (SI9619)	Deubiquitinase inhibitor	20 μM
Protease inhibitors	Roche Applied Science (04693132001)	EDTA-free Protease Inhibitor Cocktail	1 tablet
Recombinant mouse IFNβ	PBL (Cat. # 12400-1)	IFNAR ligand	100-1000 U/mL
Recombinant mouse TNFα	R&D Systems (Cat. # 410-MT)	TNFR ligand	50 μg/mL 1000U/mL
Ultra-pure LPS from E. coli 0111:B4	Sigma-Aldrich (Cat. # L3024)	TRL4 ligand	160 pg/mL-100 ng/mL
z-IETD-FMK	BioVision (064-20C)	Caspase-8 Inhibitor	50 μM
z-VAD-fmk	ApexBio (A1902)	Pan-caspase inhibitor	50-100 μM
JAK inhibitor	Calbiochem 420097	JAK kinase inhibitor	5-10 μM

3.5. Western blotting

Day 6 BMDMs were seeded in 24-well plates at 2.5-3 x10^5 cells/well in R8+gentamycin. The next day cells were treated with stimuli and inhibitors as indicated in the text. Supernatant was collected at various time intervals and saved at -80°C for cytokine analysis and macrophages were washed with ice-cold 1x PBS. PBS was aspirated, and cells were lysed in 1%SDS lysis buffer with 1% β-mercaptoethanol and boiled immediately at 95ºC for 5 minutes to minimize protein degradation. The lysed samples were stored at -20 °C for future use. Lysates were separated by 8% or 10% SDS-PAGE at 120 V for 75 minutes and transferred to activated PVDF membrane. The transfer was run at 100 V for 1 hour in an ice pack to avoid overheating. After transferring, the membrane was blocked in 5% skim milk or 5% bovine serum albumin in Tris Buffered Saline Solution (TBS-0.5M Tris, 1.5 NaCl pH 7.6) with 0.5% Tween-20 for 1 hour at room temperature on a rocker. Primary antibodies were then added and diluted in the same blocking buffer with 0.02% sodium azide and incubated overnight on a rocker at 4°C (see Table 3 for antibodies and corresponding dilutions). After incubation, the membrane was washed (5 minutes each) with TBS + 0.5% Tween-20 five times followed by adding a secondary conjugated antibody, diluted in the same blocking buffer for 30 minutes to 1 hour at room temperature on a rocker. After incubation, the membrane was washed five times at mentioned before. Finally, blots were visualized using either ECL reagents (Thermo Scientific #32106) or the highly sensitive West Femto ECL reagents (Thermo Scientific #34095) for proteins with very low expression. Protein expressions was visualized using photosensitive film (Sigma-Aldrich, Carestream Heath 785019). The densitometic analyses of expressed proteins was performed using Image-J 1.48 software (Maryland, USA).

3.6. Protein Dephosphorylation

Upon activation of a certain pathways, proteins like RipK1, RipK3, CYLD and A20 may be activated by phosphorylation. In order to examine their activation a phospho-specific antibody must be used. However, such antibodies are not commercially available. It has been reported that phosphorylated forms of these proteins migrate differently (more slowly) than corresponding non-phosphorylated protein. To confirm this observation, cells were treated as described in Western blotting section but lysed in RIPA-EDTA free buffer supplemented with a protease inhibitor (Roche Applied Science, 04693132001). Half of the lysates were treated with 500 units of lambda phosphatase (Santa Cruz Biotechnology, 200312) for 30 minutes at 30°C. Alternatively, lysates were treated with 50 units of calf intestinal phosphatase (CIP) (New England Biolabs, M0290) to dephosphorylate the total protein in 1× CutSmart NEB buffer for 50 minutes at 37°C. SDS lysis buffer was added to the treated samples which were boiled for 5 min at 95°C followed by Western blotting.

3.7. Immunoprecipitation

Cells were plated at $8x10^5$ cells/well in 6-well plates. BMDMs were treated as described in the text and lysed according to Dynabeads co-immunoprecipitation kit protocol (Invitrogena, 14321D) in the presence of protease inhibitor cocktail (Roche Applied Science 04693132001), phosphatase inhibitor cocktail (Sigma-Aldrich P5726) and deubiquitinase inhibitor (LifeSensors, SI9649 and SI9619). Specific antibodies targeting proteins of interest were used as follows: rabbit anti-RipK3 (2283, ProSci Inc., Poway, USA) and rabbit anti-K48 ubiquitin (Apu2, Millipore, USA). Bound proteins were eluted, neutralized with 1M Tris pH 9, denatured by boiling in 1%SDS lysis buffer for 5 minutes at 95°C and subsequently analyzed by western blotting

(standard protocols described above). The densitometric quantification of western blots was performed using ImageJ 1.48 software (Maryland, USA).

For immuno-precipitation with tandem ubiquitin-binding entities (TUBES) (LifeSensors, UM102), BMDMs were treated with a proteasome inhibitor MG132 (5 μg/ml) before stimulation with LPS/zVAD or TNF/zVAD. Cells were washed with ice-cold 1× PBS and lysed in buffer containing 50 mM Tris-HCL pH 7.5, 150 mM NaCl, 1 mM EDTA, 1% NP-40, 10% glycerol, protease inhibitor, phosphatase inhibitor, 20 μM deubiquitinase inhibitor PR-619 and 1× 1,10-phenanthroline (LifeSensors, SI9649 and SI9619). The lysates were sonicated for 10 seconds three times and then centrifuged at 14,000 × *g* for 30 minutes at 4°C to pellet cell debris. The clarified lysates were then incubated with equilibrated agarose-TUBEs for 16–24 hours at 4°C on a rocker platform. After incubation, beads were collected by low speed centrifugation 5000 × *g* for 5 minutes at 4°C. The unbound fractions were saved at -20°C and beads were washed three times with ice-cold TBS-T washing buffer containing 20 mM Tris-HCL pH 8, 150 mM NaCl and 0.1% Tween-20. The resin was re-suspended in 40 μL of 2× SDS lysis buffer and boiled for 5 minutes at 95°C then centrifuged at 13,000 × *g* for 5 minutes at room temperature. The eluent was analyzed by standard western blotting protocol (as described above).

Table 3. Primary and secondary antibodies used for western blot analysis.

Antibody	Source	Cat#	Dilution	Buffer	Expected band size
Mouse Anti-Rip1	BD	610459	1:1000	Milk	74 kDa
Rabbit Anti-Rip3	ProSci Inc.	2283	1:1000	Milk	57 kDa
Mouse Anti-actin	BD	612656	1:1000	Milk	42 kDa
Rabbit Anti-cIAP1/2	Cyclex	CY-P1041	1:1000	Milk	63-68 kDa
Mouse Anti-alpha-tubulin	Santa cruz	Sc-5286	1:1000	milk	55 kDa
Rat Anti-caspase8	Enzo	1G12	1:1000	Milk	55 kDa
Rat-Anti MLKL clone 3H1	Cedarlane	MABC604	1:1000	BSA	52, 150 kDa
Rabbit anti-pSTAT1 (Tyr701)	Cell Signalling	9167	1:1000	BSA	84, 91
Rabbit anti-pSTAT1 (Ser727)	Cell Signalling	9177	1:1000	BSA	91
Rabbit anti-STAT1	Cell Signalling	9172	1:1000	BSA	84, 91
Rabbit mAb CYLD (D1A10)	Cell Signalling	8462	1:1000 1:500	BSA	108
Rabbit mAb A20/TNFAIP (D13H3)	Cell Signalling	5630	1:1000	BSA	82
Rabbit anti-TRAF2 (C-20)	Santa cruz	sc-876	1:1000	Milk	50
Mouse anti-FADD monoclonal antibody (1F7)	Enzo	1F7ADI-AAM-212-E	1:1000	Milk	28 kDa
Rabbit polyclonal Anti-TRIF	Genetex	GTX13810	1:1000	Milk BSA	66 kDa
Rabbit anti NF-κB p65	Cell Signalling	8242	1:1000	BSA	65 kDa
Rabbit anti Phospho- p65	Cell Signalling	3033	1:1000	BSA	65 kDa
Rabbit anti-MK2	Cell Signalling	3042	1:1000	BSA	49 kDa
Rabbit anti-Phospho-MK2	Cell Signalling	3007	1:1000	BSA	49 kDa
Goat anti-Rabbit IgG (H+L) HRP	BioRAD	170-6515	1: 5000		
Goat anti-Rat IgG (H+L) HRP	Millipore	AP183	1: 5000		

3.8. RNA interference

The smart pool ON-TARGETplus siRNA against CYLD, A20, and TRIAD3A was purchased from Dharmacon (GE Healthcare, USA). BMDMs were transfected with siRNA using Lipofectamine® RNAiMAX Transfection Reagent (13778030, Invitrogen) according to the manufacturer's instructions. Briefly, BMDMs were plated at $2x10^5$ cells/well in 24-well plate 24 hours before transfection. An aliquot of 1.5 µL of Lipofectamine® RNAiMAX was mixed with 5 pmol of siRNA in 50 µL of Opti-MEM® Medium and incubated at room temperature for 10-20 minutes, to allow the formation of the complex, then added to the cells. After 24 hours, the transfected cells were treated as described in the text and tested in various experimental protocols. Sequences of the siRNAs are provided in Table 4.

Table 4. Si-RNA sequences utilized in experiments

Gene	Reference #	siRNA sequence
Cyld	L-055575-01-0005, ON-TARGETplus Mouse Cyld (74256) siRNA SMARTpool	A: ON-TARGETplus SMARTpool siRNA J-055575-09, Target Sequence: UGAAAUGACUGAGCGAUAA B: ON-TARGETplus SMARTpool siRNA J-055575-10, Target Sequence: AGAAACAGACUCCGACUAA C: ON-TARGETplus SMARTpool siRNA J-055575-11, Target Sequence: CUGCAUUGAUGAUACGAUA D: ON-TARGETplus SMARTpool siRNA J-055575-12, Target Sequence: GGACAGAGAUAGUCAAUCC
***Tnfaip3* (A20)**	L-058907-02-0005, ON-TARGETplus Mouse Tnfaip3 (A20) (21929) siRNA SMARTpool	A: ON-TARGETplus SMARTpool siRNA J-058907-09, Target Sequence: GCACCUAAGCCAACGAGUA B: ON-TARGETplus SMARTpool siRNA J-058907-11, Target Sequence: GCUGUGAAGAUACGAGAGA C: ON-TARGETplus SMARTpool siRNA J-058907-12, Target Sequence: AGAGACAUGCCUCGAACUA D: ON-TARGETplus SMARTpool siRNA J-058907-17, Target Sequence: GCUCAACUGGUGUCGUGAA
***Rnf216* (Triad3a)**	L-065113-02-0005 ON-TARGET plus Mouse Rnf216 siRNA SMART pool	A-ON-TARGETplus SMARTpool siRNA J065113-05 Target sequences: GCAGACAGCAGACGAUAUU B- ON-TARGETplus SMARTpool siRNA J065113-06 Target sequences: GAGCAGAAAGUCAUUAUAU C- ON-TARGETplus SMARTpool siRNA J065113-07 Target sequences: AGAGAAGACCGGCUUAUUA D- ON-TARGETplus SMARTpool siRNA J065113-08 Target sequences: ACAGAGCUCUUAUCAAAUC
Scramble Si-RNA	ON-Target plus Non-targeting pool	Catalog Item D-001810-10-20

3.9. Quantitative RT-PCR

Total RNA was isolated using TRIzol reagent (Life Technologies). Isolated RNA was reverse transcribed into cDNA in a 20-μL reaction volume using SuperScript III Reverse Transcriptase (Invitrogen,18080– 044) as follows: 1 μg of RNA template was added to 0.5 μL of oligo(dT) (50 μM), 0.5 μL of random primers (50–250 ng), 4 μL of 5× First Strand buffer, 1 μL of DTT (0.1 M), 1 μL of dNTP (10 mM), 1 μL of RNase OUT (40 units/μL), and 1 μL of SuperScript III (200 units/μL). After cDNA synthesis, 2 μL of cDNA was analyzed using the SYBR Green (Life Technologies) fast method performed on an Applied Biosystems 7500 quantitative RT-PCR system. The primers used in qRT-PCR are listed in Table 5.

Table 5. Primers used in Quantitative RT-PCR.

Gene	Primer	Sequence
Actin	Forward	5′-GATCAAGATCATTGCTCCTCCTG-3′
	Reverse	5′-AGGGTGTAAAACGCAGCTCA-3′
RipK1	Forward	5′-GGCCAACATTTCTTGGCATTGA-3`
	Reverse	5′-CTGCAGCACTGGGCTTTGAT-3`
Caspase-8	Forward	5′-TGCCCAGATTTCTCCCTACA-3`
	Reverse	5′-AAGCAGGCTCAAGTCATCTTCC-3`
Triad3a	Forward	5′-ACAGATGATCACCATGTTTGGTT-3′
	Reverse	5′-CATCCATTCCTTTCCCCGGT-3
XAF1	Forward	5`- TGTGCAGGAACTGCAAAAGA-3`
	Reverse	5`- TTGACTCTGGGATGGGCTCT-3`
MLKL	Forward	5`-CTGGCAGAGAACGAATCTTGG-3`
	Reverse	5`-TGCTCCCAGCAATAAGTTGA-3`
IRF9	Forward	5′-AGCAACTG CAACTCTGAGCTA-3′
	Reverse	5′-ACTCGGC CACCATA GATGAAG-3′
FADD	Forward	5`- CGCGTCGACGACTTCG-3`
	Reverse	5`- TTCTCCAATCTTTCCCCACATTAT-3`

3.10. Cytokine analysis

Enzyme linked immunosorbent assay was used to analyze the concentration of various cytokines upon necroptotic stimulation *in vitro* as mentioned in the text. Murine IL-10 (555252), TNFα (560478), IL-6 (555240), IL-1β (560232) and IL-12 (555256) was measured using kits from BD Bioscience (San Diego, CA). In brief, 96-well plates were coated with diluted capture antibody and incubated overnight at 4°C. On the next day, plates were washed three times with washing buffer PBST (1x PBS and 0.5% tween 20) followed by blocking with 10% FBS in PBS for 1 hour at room temperature. Plates were then washed three times with washing buffer and 50 µL of samples and standards (provided with kit) were added to the corresponding wells. Plates were incubated for 2 hours at room temperature followed by washing five times with washing buffer. A detection antibody with streptavidin-HRP was added for 1 hour at room temperature. Plates were washed seven times and 50 µL of substrate solution was added to each well. Plates were kept in the dark for up to 30 minutes, depending on the development of standards. Finally, the reaction was stopped by adding 25 µL of 96%H_2SO_4 in H_2O and absorbance was measured at 450–570 nm in a FilterMax F5 Multimode microplate reader (Molecular Devices). Data was analyzed using SoftMax Pro software and Graphpad Prism V7 software.

3.11. Confocal Microscopy

Day 7 bone marrow derived macrophages were seeded in 24-well plates overnight and treated with various inhibitors and agonists the next day as described in text. Cells were first washed with 1xPBS and then fixed using 4% paraformaldehyde for 30 minutes at room temperature and then overnight at 4°C. Cells were then washed with 1xPBS and permeabilized with 0.5% saponin (in 1x PBS) twice five minutes each, followed by blocking with (10% FBS + 0.05% saponin) for 20 minutes at room temperature. Primary antibodies against phospho MLKL (abcam rabbit (1/50))

and total MLKL (Millipore rat (1/50)) were added to fixed cells followed by a 1-hour incubation at room temperature. Cells were washed 3 times for 10 minutes each with 0.05 % saponin-FBS buffer, followed by addition of secondary antibodies: anti-rabbit 594 (Invitrogen) (2 μg/mL) and anti-rat 647 (Invitrogen) ((2 μg/mL) for 1 hour at room temperature. Nuclei were stained with DAPI (1:100) for 10 minutes. Finally, cells were washed 3 times for 10 minutes each with 1x PBS and mounting media from Dako (Florescence mounting medium) was added. Cells were visualized using ZEISS LSM 880 with Airyscan confocal fluorescent microscope.

3.12. Immunofluorescence

To confirm cell viability, Day 7 BMDMs were seeded at $7x10^4$ cells/well in a 96-well plate and treated as described in the text. After 24 hours incubation, media was replaced with 100 μL of staining solution for 30 minutes at 37°C. Staining solution mix includes Hoëchst (2.5μg/mL; Invitrogen 33342) and propidium iodide (PI) (1:10 dilution; BD Pharmingen, 550825) in RPMI lacking phenol red. A ZOE™ Fluorescent Cell Imager was used to acquire and analyze images.

3.13. Gene Expression Profiling

Wild-type and IFNAR1 knockout BMDMs (n=2) were generated and treated on Day 7 followed by RNA isolation using RNeasy kit (74104, QIAGEN). Total RNA was prepared from sixteen samples: two control samples including (no treatment, zVAD only) and six treated samples including (LPS, LPS/zVAD, LPS/zVAD/Necrostatin-1, IFN-β, IFN-β/zVAD and IFN-β/zVAD/Necrostatin-1). The purified RNA was quantified by optical density at 260 nm using a ND-1000 spectrophotometer from Nanodrop Technology. cDNA was synthesized , amplified with T7 RNA polymerase and labeled with Cyanine-3 (LowInput quickAmp Labeling Kit One-Color). For each sample, labeled cRNA was hybridized on SurePrint G3 Mouse GE 8x60K microarray (Design ID # 028005, Agilent Technologies, Santa Clara, CA, USA) at 65°C

for at least 16 hours followed by washing steps. Slides were dried and scanned with the Agilent DNA microarray scanner at 535 nm. Scanned images were extracted using Feature Extraction Version 10.1.1. Exported probe data was filtered using a script to retain probes with expression greater than background in at least 50% of arrays. The filtered probe set was imported to Expander 6 for further analysis including log scaling, quantile normalization, and merging of duplicate probes by selecting for those with highest median expression.

3.14. Statistical Analysis

All graphs show the average obtained from at least three independent experiments. Error bars show the standard error of the mean, and statistical significance between groups was determined by Student's t-test using Graphpad Prism 7 software package (La Jolla, California, USA).

4.0 RESULTS

4.1. Necrosome activation in macrophages

4.1.1. TLR4/TNFα stimulation and caspase inhibition are required for RipK1 and RipK3 phosphorylation in macrophages

To investigate the activation of necroptosis in bone marrow macrophages from WT mice, day 7 cells were treated with LPS/TNFα with or without pan-caspase inhibitor (zVAD) for up to 8 hours. Lysates were collected and examined for RipK1/3 phosphorylation by western blot (Fig. 6 A, B). The antibodies (anti-RipK1 and anti-RipK3) used for western blot were able to discriminate between the non-phosphorylated and phosphorylated forms. The phosphorylation of RipK1 was detected within 10 minutes of stimulation while RipK3 phosphorylation was detected at later time points. The phosphorylated bands can be observed as slightly slower migrating bands by western blotting. As a control, another set of cells was treated with zVAD only to eliminate the possibility that it has a role in RipK1/3 phosphorylation (Fig. 6C). zVAD treatment did not induce any phosphorylation of RipK1/3 and had no impact on RipK1 and RipK3 level. In addition, single stimulation with LPS- or TNFα- only induced RipK1 phosphorylation but not phosphorylation of RipK3 and had no impact on RipK1 protein level (Fig. 6A, B). To confirm the specificity of the phosphorylated bands, half of the lysate was treated with CIP (as described in the methods section) to dephosphorylate RipK1 and RipK3 proteins. The slower migrating RipK1 and RipK3 bands vanished upon treatment with calf intestinal alkaline phosphatase indicating that the upper bands were the phosphorylated forms of RipK1 and RipK3, respectively (Fig. 6D). Additionally, I examined the cell viability of BMDMs that were treated with same stimuli (LPS, LPS/zVAD, TNF, TNF/zVAD) for 24 hours. Cell viability was measured using 3-(4,5-dimethylthiazol-2-yl)-2,5-diphenyltetrazolium bromide

(MTT). Combined treatment of LPS/zVAD (Fig. 1E) or TNF/zVAD (Fig. 6F) resulted in massive cell death, that was rescued by using either addition of a RipK1 inhibitor (Nec-1) or a RipK3 inhibitor (GSK872), suggesting that the mechanism of cell death was necroptosis. The kinetics of death correlated with the phosphorylation of RipK3 (Fig. 6E, F).

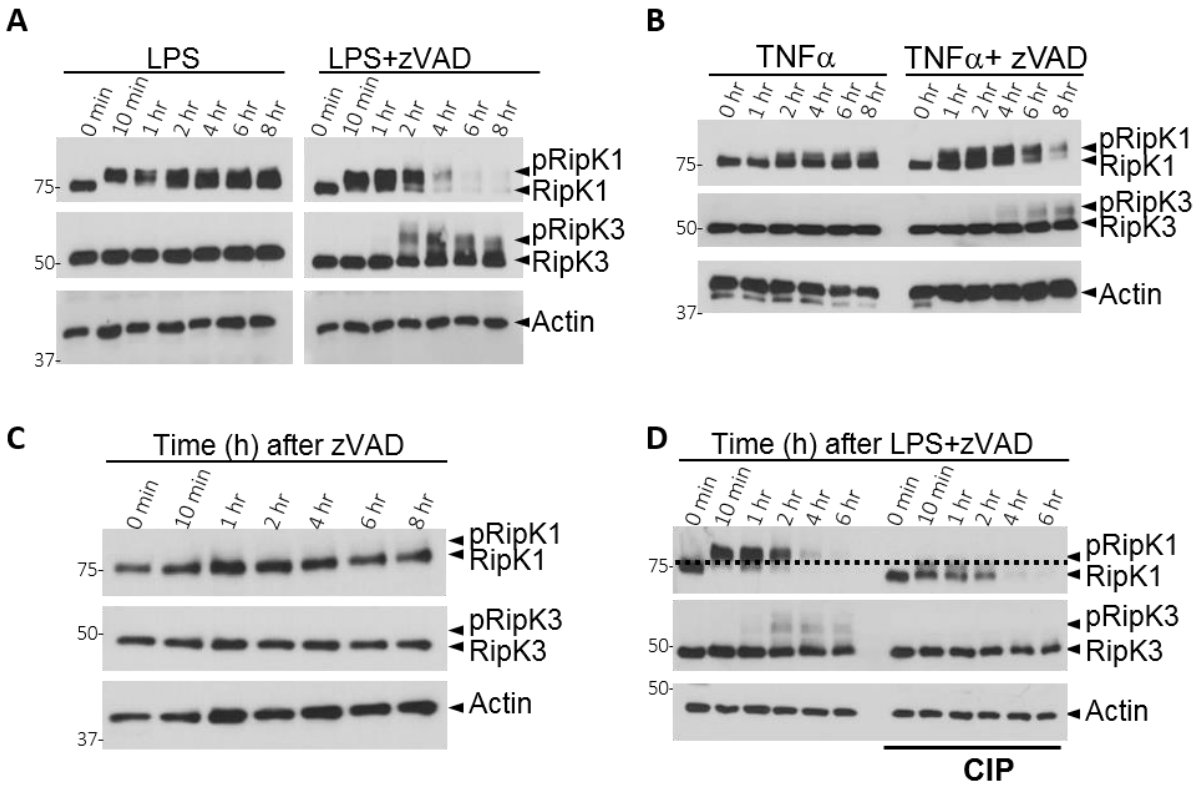
A
LPS
LPS+zVAD
0 min
10 min
1 hr
2 hr
4 hr
6 hr
8 hr
75-
50-
37-
pRipK1
RipK1
pRipK3
RipK3
Actin
B
TNFα
TNFα+ zVAD
0 hr
1 hr
2 hr
4 hr
6 hr
8 hr
C
Time (h) after zVAD
D
Time (h) after LPS+zVAD
CIP

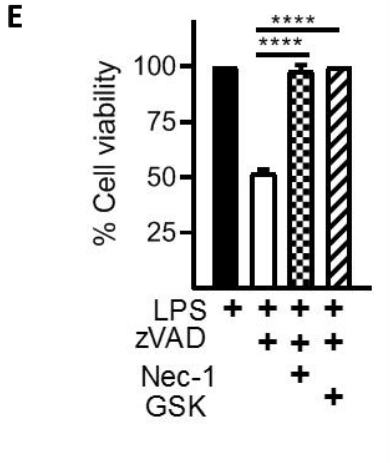
E
% Cell viability
100
75
50
25
****
LPS
zVAD
Nec-1
GSK

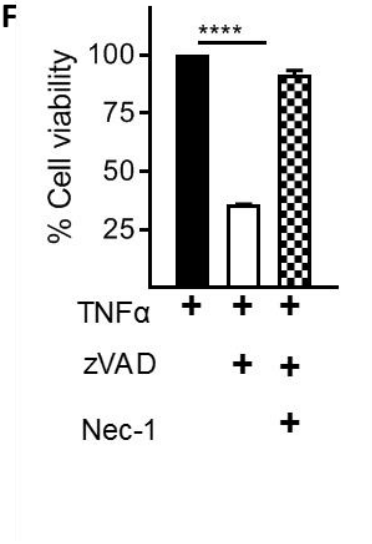
F
% Cell viability
100
75
50
25
****
TNFα
zVAD
Nec-1

Figure 6: Necrosome activation induces phosphorylation of RipK1 and RipK3 in WT BMDMs.

A, B. Day-7 wild-type bone marrow-derived macrophages were treated with LPS (100 ng/mL) or TNFα (50ng/mL) and zVAD (50 μM). Lysates were collected at various time intervals and the expression of proteins examined by western blotting. **C**. Cells were treated with zVAD (50 μM) only as indicated and the expression of proteins in cell lysates was examined by western blotting. **D.** Alkaline Phosphatase (CIP, 50 units) was added to some lysates as described in the Methods section and the impact on proteins analyzed by western blotting. **E+F**. Cell viability was measured by MTT assay at 24 h post stimulation of cells with different combinations of LPS (100mg/mL), TNFα (50ng/mL), zVAD (50 μM), Necrostatin-1 (30 μM) and GSK872 (5 μM). Graphs show the percentage of viable cells ±SEM relative to controls. Each experiment was performed in triplicate and repeated three times. **** $P < 0.0001$

4.1.2. Activation of necroptosis by LPS/zVAD leads to degradation of necrosome interacting proteins

Following treatment with LPS/zVAD or TNFα/zVAD, I noticed that the RipK1 expression level reduced progressively after 1-hour post-stimulation of WT cells (Fig. 6A, B). Since RipK1 is a critical cell signalling molecule that plays key role in inflammatory pathways, I evaluated the mechanism behind RipK1 reduction upon stimulation. Notably, there was no reduction in the levels of RipK3 level (Fig. 6A, B). To investigate whether the reduction of RipK1 protein level was due to reduced transcription of RipK1 gene or due a post-transcriptional mechanism, I measured RipK1 mRNA levels by qRT-PCR following LPS/zVAD treatment. The reduction of RipK1 expression was not due to reduced transcription: rather, it was increased during stimulation of cells (Fig. 7A). To further characterize the phenomenon of reduction of RipK1 expression during early necrosome signalling, I examined whether the degradation of RipK1 was impacted by the level of TLR4-ligand (LPS) used. BMDMs were treated with a low amount of LPS (1ng/mL) in the presence of zVAD. I found that RipK1 degradation was still observed at this low concentration of LPS (Fig. 7B). Densitometry of western blots indicate that the reduction of RipK1 expression after 2 hours of stimulation correlates with the phosphorylation of RipK3 (Fig. 7C). I investigated if components of the necrosome other than RipK1 are degraded following stimulation with LPS/zVAD. Western blotting showed that many other interacting proteins were degraded, including caspase-8, FADD, cIAP1,2, and TRAF2 (Fig. 7D). In contrast, expression and phosphorylation of proteins such RipK3, CYLD, and A20 increased during necrosome signalling (Fig. 7D). These results suggest that not all necrosomal proteins are degraded during early necrosome signalling. It has been reported that caspase-8- mediates cleavage of RipK1. I therefore evaluated whether caspase-8 inhibition prevented the degradation of RipK1 using a specific

caspase-8 inhibitor (zIETD) (Fig. 7E). Inhibition of caspase-8 failed to induce necroptosis in macrophages (Fig. 7G) and did not have any impact on the degradation of RipK1 (Fig. 7E). Combined treatment of cells with LPS+zVAD+zIETD did not rescue the degradation of RipK1 (Fig. 7F). This suggests that the loss of RipK1 expression during early necrosome signalling is not mediated by CASPASE-8. Additionally, CASPASE-8 itself was degraded during necrosome signalling.

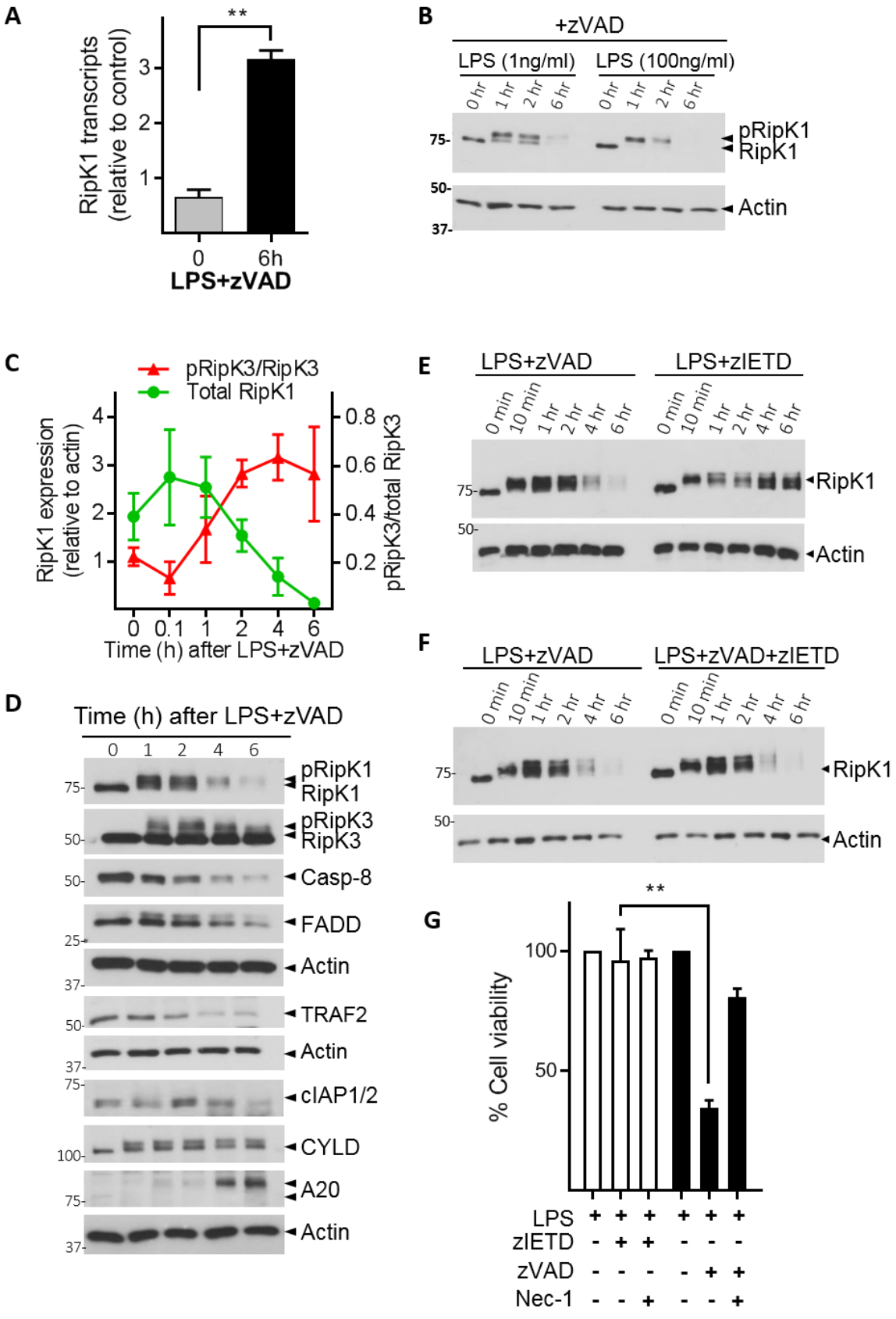
A
**
RipK1 transcripts (relative to control)
3
2
1
0
6h
LPS+zVAD
B
+zVAD
LPS (1ng/ml)
LPS (100ng/ml)
0 hr
1 hr
2 hr
6 hr
0 hr
1 hr
2 hr
6 hr
75-
50-
37-
pRipK1
RipK1
Actin
C
pRipK3/RipK3
Total RipK1
RipK1 expression (relative to actin)
pRIpK3/total RipK3
4
3
2
1
0.8
0.6
0.4
0.2
0 0.1 1 2 4 6
Time (h) after LPS+zVAD
D
Time (h) after LPS+zVAD
0 1 2 4 6
75-
50-
50-
25-
37-
50-
37-
75-
100-
75-
37-
pRipK1
RipK1
pRipK3
RipK3
Casp-8
FADD
Actin
TRAF2
Actin
cIAP1/2
CYLD
A20
Actin
E
LPS+zVAD
LPS+zIETD
0 min
10 min
1 hr
2 hr
4 hr
6 hr
0 min
10 min
1 hr
2 hr
4 hr
6 hr
75-
50-
RipK1
Actin
F
LPS+zVAD
LPS+zVAD+zIETD
0 min
10 min
1 hr
2 hr
4 hr
6 hr
0 min
10 min
1 hr
2 hr
4 hr
6 hr
75-
50-
RipK1
Actin
G
**
% Cell viability
100
50
LPS + + + + + +
zIETD - + + - - -
zVAD - - - - + +
Nec-1 - - + - - +

Figure 7: Necrosome signalling induces degradation of various necrosome-interacting proteins in WT BMDMs.

A. BMDMs were treated with LPS (100ng/mL) + zVAD (50 μM) for 6 hours and the expression of RipK1 mRNA was examined by quantitative RT-PCR. **B.** Macrophages were stimulated with zVAD (50μM) and 1ng/ml LPS or 100 ng/ml LPS. At various time intervals the expression of RipK1 was evaluated by performing western blotting of cell extracts. **C**. Densitometry analysis of total RipK1 vs. phosphorylated RipK3 was performed in cells treated with LPS + zVAD at various time intervals. **D.** Macrophages were treated with LPS + zVAD and the expression of various proteins was evaluated by western blotting of cell extracts collected at various time intervals. **E+F.** WT macrophages were treated with LPS+zVAD, LPS+ casp-8 inhibitor (zIETD), or LPS+zVAD+zIETD. Lysates were collected at various time intervals and the expression of RipK1 was evaluated by western blotting. **G.** WT macrophages were stimulated as indicated in the panel; LPS (100ng/ml), zVAD (50 μM), zIETD (50 μM) and Nec-1 (30 μM). Cell viability was evaluated at 24 hours by MTT assay. Graphs show the percentage of viable cells±SEM relative to cells treated with LPS in the absence of zVAD. Each experiment was repeated thrice with triplicate samples. (**P > 0.001).

4.1.3. Necrosomal degradation is driven by RipK3

To investigate whether the K45 of RipK1 plays a role in promoting RipK1 degradation during necroptosis, I treated WT and RipK1 kinase mutant (K45A) macrophages with LPS+zVAD at varying time intervals over the course of 6-hours. RipK1 (K45A) had a slight reduction in RipK3 phosphorylation (Fig. 8A) and significant resistance to necroptosis (Fig. 8B). However, the K45A mutation had no impact on RipK1 degradation (Fig. 8A). In contrast, the K45A mutation rescued RipK1 degradation upon TNFα+zVAD stimulation (Fig. 8C) which correlated with complete resistance to TNF-induced necroptosis (Fig. 8D). This result suggests that TNFα-induced degradation of RipK1 may be dependent on the RipK1 kinase function (Fig. 8C), and that the LPS induced degradation of RipK1 during necrosome signalling may involve an alternative mechanism. To explore the role of TLR4 interacting proteins that may cause RipK1 degradation, I treated WT, *Trif*$^{-/-}$ and *Myd88*$^{-/-}$ cells with LPS+zVAD. Interestingly, the degradation of RipK1, CASP-8, cIAP1+2 and FADD was rescued in *Trif*$^{-/-}$ but not in *Myd88*$^{-/-}$ cells, indicating that the degradation of in RipK1 is TRIF dependent (Fig. 9A). Additionally, *Trif*-deficient macrophages were significantly resistant to LPS-induced necroptosis (Fig. 9C). On the other hand, TNFα+zVAD-induced RipK1 degradation independently of TRIF (Fig. 9B) and TRIF-deficient macrophages were not protected from TNF-induced necroptosis (Fig. 9D). Overall, these results suggest that RipK1 degradation occurs by different mechanisms depending on whether necroptosis is induced by TNFα- or LPS. To explore the role of RipK3 in promoting RipK1 degradation, I treated WT and *Ripk3*$^{-/-}$ BMDMs with LPS+zVAD and collected cell extracts at various time intervals. In *Ripk3*-deficient macrophages phosphorylation of RipK1 was not impacted, and the degradation of RipK1, caspase-8, FADD and cIAP1,2 was completely rescued (Fig. 10A). *Ripk3*-deficient macrophages displayed complete resistance to LPS-induced necroptosis (Fig. 10B).The

same observation was made when I performed TNFα+zVAD treatment of cells (Fig 10C). *Ripk3*-deficient macrophages were completely resistant to TNF-induced necroptosis (Fig. 10D). These results suggest that RipK3, a key necrosome interacting protein, promotes both necrosome degradation and necroptosis. I investigated the role of the downstream substrate of RipK3, MLKL, in RipK1 degradation. I applied the same treatment (LPS+zVAD) on *Mlkl*-deficient macrophages. Although *Mlkl*$^{-/-}$ cells were resistant to necroptosis (Fig. 5B), they showed similar degradation of RipK1 compared to WT (Fig. 10E). This suggests that only RipK3 drives necrosome degradation (Fig. 10E). In addition, degradation still occurred in the absence of cell death as this was observed in *Mlkl*$^{-/-}$, *Ifnar1*$^{-/-}$, *Irf*-9$^{-/-}$ (Fig. 10F,G) and *Cyld*$^{-/-}$ cells (Fig. 10C). I also noticed that RipK3 phosphorylation was reduced in MLKL-deficient macrophages compared to WT control (Fig. 10E). These results suggest a possible feedback role for MLKL in RipK3 phosphorylation. However, MLKL does not contribute to necrosomal degradation following necroptotic stimulation.

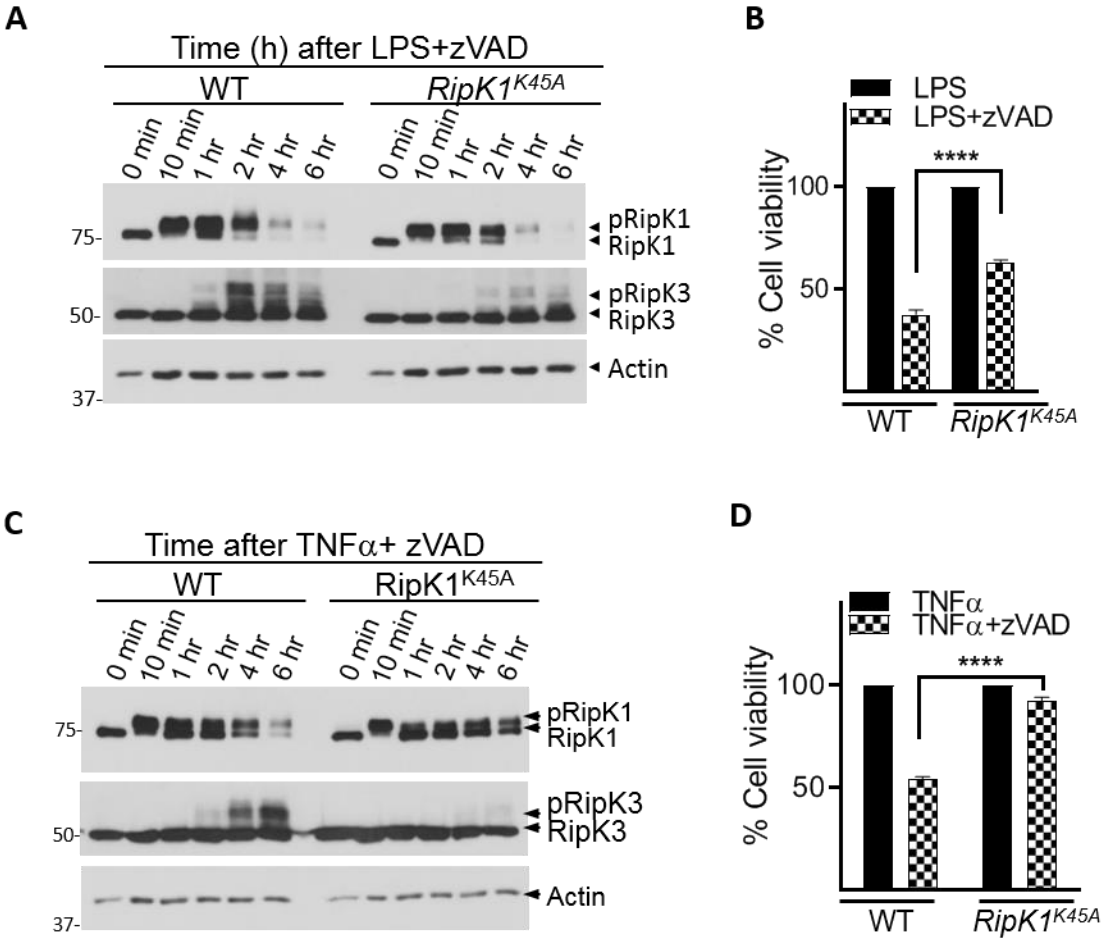
A
Time (h) after LPS+zVAD
WT
RipK1K45A
0 min
10 min
1 hr
2 hr
4 hr
6 hr
75-
50-
37-
pRipK1
RipK1
pRipK3
RipK3
Actin
B
LPS
LPS+zVAD
% Cell viability
100
50
****
WT
RipK1K45A
C
Time after TNFα+ zVAD
WT
RipK1K45A
0 min
10 min
1 hr
2 hr
4 hr
6 hr
75-
50-
37-
pRipK1
RipK1
pRipK3
RipK3
Actin
D
TNFα
TNFα+zVAD
% Cell viability
100
50
****
WT
RipK1K45A

Figure 8: TNFα-induced RipK1 degradation is dependent on RipK1 kinase function.

WT and RipK1 kinase mutant (K45A) BMDMs were generated and seeded on day 6 and treated with various stimulants and inhibitors on day 7. **A.** WT and RipK1^{K45A} mutant macrophages were treated with LPS (100ng/mL) + zVAD (50μM). Lysates were collected at different time intervals post-stimulation. Expression of RipK1 and RipK3 was evaluated by western blotting. **B.** Cell viability of WT and RipK1^{K45A} macrophages was evaluated by MTT assay at 24-hour post stimulation. **C+D.** WT and RipK1^{K45A} mutant macrophages were treated with TNFα (50ng/mL) + zVAD (50μM), and expression of RipK1 and RipK3 was evaluated by western blotting of cell extracts at various time intervals (C). **D.** Cell viability of WT and RipK1^{K45A} macrophages was evaluated by MTT assay at 24-hour post-treatment. Graphs show the percentage of viable cells ± SEM relative to controls. Each experiment was performed in triplicate and repeated three times. (***$P < 0.001$, ****$P < 0.0001$).

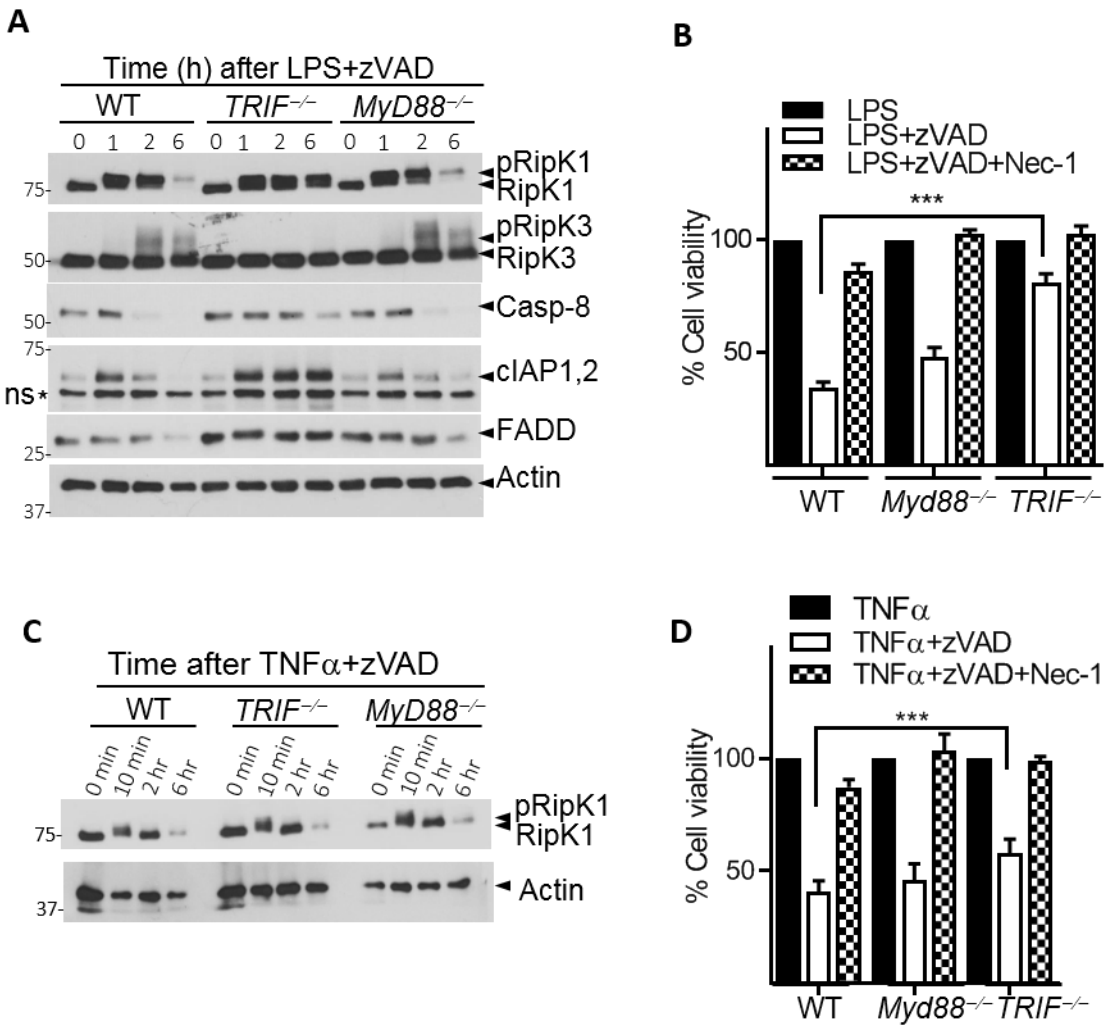
A
Time (h) after LPS+zVAD
WT
TRIF−/−
MyD88−/−
0 1 2 6 0 1 2 6 0 1 2 6
75-
pRipK1
RipK1
pRipK3
50-
RipK3
50-
Casp-8
75-
cIAP1,2
ns*
FADD
25-
Actin
37-
B
LPS
LPS+zVAD
LPS+zVAD+Nec-1
***
% Cell viability
100
50
WT
Myd88−/−
TRIF−/−
C
Time after TNFα+zVAD
WT
TRIF−/−
MyD88−/−
0 min
10 min
2 hr
6 hr
75-
pRipK1
RipK1
37-
Actin
D
TNFα
TNFα+zVAD
TNFα+zVAD+Nec-1
***
% Cell viability
100
50
WT
Myd88−/−
TRIF−/−

Figure 9: RipK1 degradation is TRIF-dependent in LPS-induced necroptosis.

BMDMs were generated from WT, *Trif*$^{-/-}$ and *Myd88*$^{-/-}$ and after 6 days of differentiation BMDMs were plated in 24-well and 96-well plates**. A.** WT, *Trif*$^{-/-}$, and *Myd88*$^{-/-}$ macrophages were treated with LPS (100ng/mL) + zVAD (50μM) and cell lysates were collected at various time intervals for western blotting. **B.** Cell viability was measured by MTT assay at 24 hours post stimulation of cells with LPS + zVAD**. C.** WT, *Trif*$^{-/-}$, and *Myd88*$^{-/-}$ macrophages were treated with TNFα (50ng/mL) + zVAD (50μM). Cell extracts were collected at various time intervals and protein expression examined by western blotting. **D.** Cell viability was measured by MTT assay at 24 hours post-stimulation of cells with TNFα+zVAD. Graphs show the percentage of viable cells ± SEM relative to controls. Each experiment was performed in triplicate and repeated three times. ***$P < 0.001$, ****$P < 0.0001$

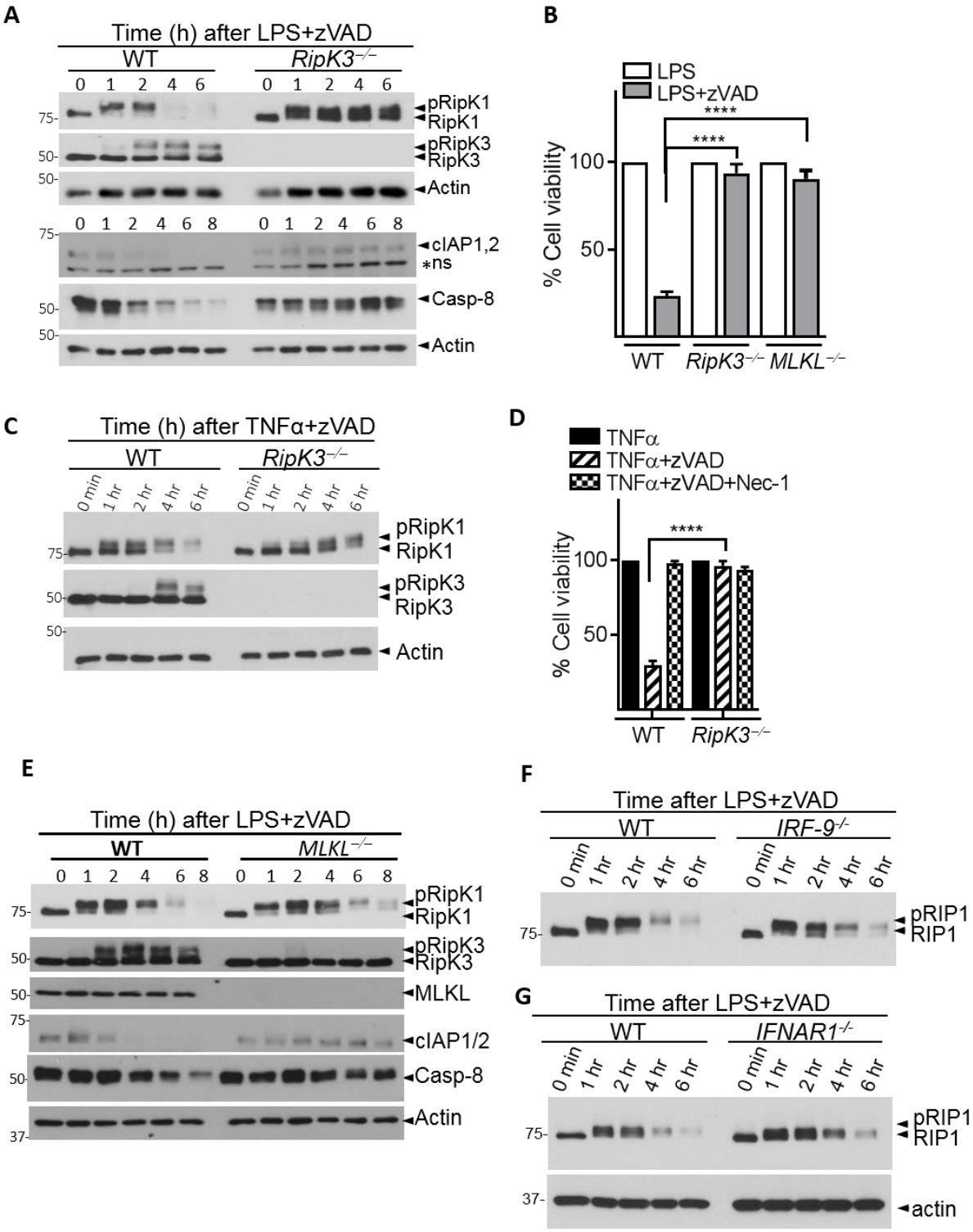
A
Time (h) after LPS+zVAD
WT
RipK3−/−
0 1 2 4 6
0 1 2 4 6
pRipK1
RipK1
pRipK3
RipK3
Actin
0 1 2 4 6 8
0 1 2 4 6 8
cIAP1,2
*ns
Casp-8
Actin
B
LPS
LPS+zVAD
****
****
% Cell viability
100
50
WT
RipK3−/−
MLKL−/−
C
Time (h) after TNFα+zVAD
WT
RipK3−/−
0 min
1 hr
2 hr
4 hr
6 hr
pRipK1
RipK1
pRipK3
RipK3
Actin
D
TNFα
TNFα+zVAD
TNFα+zVAD+Nec-1
****
% Cell viability
100
50
WT
RipK3−/−
E
Time (h) after LPS+zVAD
WT
MLKL−/−
0 1 2 4 6 8
0 1 2 4 6 8
pRipK1
RipK1
pRipK3
RipK3
MLKL
cIAP1/2
Casp-8
Actin
F
Time after LPS+zVAD
WT
IRF-9-/-
0 min
1 hr
2 hr
4 hr
6 hr
pRIP1
RIP1
G
Time after LPS+zVAD
WT
IFNAR1-/-
0 min
1 hr
2 hr
4 hr
6 hr
pRIP1
RIP1
actin

Figure 10: Activated RipK3 promotes the degradation of necrosomal proteins.

BMDMs were generated from WT, *Ripk3*$^{-/-}$ and *Mlkl*$^{-/-}$ cells. After 6 days of differentiation, macrophages were plated in 96-well and 24-well plates at 70x10^3 and 250x10^3 cells per well, respectively. **A+B.** WT, RipK3$^{-/-}$ and MLKL$^{-/-}$ macrophages were treated with LPS (100ng/mL) + zVAD (50µM) and Nec-1 (30µM). **A.** Cells were treated for various time intervals and lysates were collected for protein expression analysis by western blotting. **B**. Cell viability was measured by MTT assay at 24 hours post stimulation. **C.** WT and *Ripk3*$^{-/-}$ macrophages were treated with TNFα (50ng/mL) + zVAD (50µM) . Cell extracts were collected at various time intervals and the expression of various proteins evaluated by western blotting. **D.** WT and *Ripk3*$^{-/-}$ macrophages were treated with TNFα (50ng/mL) + zVAD (50µM) + Nec-1 (30 µM). Cell viability was measured by MTT assay at 24 hours post stimulation. **E.** WT and *Mlkl*$^{-/-}$ were treated with LPS (100ng/mL) + zVAD (50µM) for various time intervals and cell extracts were tested for protein expression by western blotting. **F+G.** BMDMs were generated from WT, *Irf-9*$^{-/-}$and *Ifnar1*$^{-/-}$ mice and plated in 24-well plates and treated with LPS (100ng/mL) + zVAD (50µM) for different time periods. Cell lysates were collected, and protein expression evaluated by western blotting. Graphs show the percentage of viability with ± SEM relative to controls. Each experiment was performed in triplicate and repeated three times. $***P < 0.001$, $****P < 0.0001$

4.1.4. Necrosomal degradation is driven by early RipK1-RipK3 association.

Having observed that the degradation of RipK1 was rescued in *Ripk3*-deficient macrophages and that the degradation of RipK1 coincided with the timing of RipK3-phosphorylation, I investigated whether blockade of RipK1-RipK3 interaction using Necrostatin-1 (Nec-1) would rescue RipK1-degradation. Nec-1 binds to the kinase domain of RipK1 near to the activation loop, resulting in an inactive conformation. I induced necrosome signalling by treating BMDMs with LPS+zVAD in the presence and absence of Nec-1 and evaluated the impact on RipK1 expression by western blotting. Interestingly, Nec-1 did not have any impact on RipK1 phosphorylation, while the phosphorylation of RipK3 was abrogated (Fig. 11A). Furthermore, the degradation of RipK1 was completely abrogated by Nec-1 treatment (Fig. 11A). I also used Necrostatin-1s (Nec-1S), which has been shown to be a better and more specific inhibitor of RipK1 kinase function and observed that Nec-1S completely blocked the degradation of RipK1, phosphorylation of RipK3 and cell death of BMDMs (Fig. 11B, C). Overall, results with Nec-1 reveal a strong correlation between RipK3 phosphorylation (but not RipK1 phosphorylation) and degradation of RipK1, implying that RipK1-RipK3 interaction during necrosome signalling may be required to drive the degradation of RipK1.

Since the K45 region of RipK1 promoted degradation of RipK1 following stimulation by TNFα+zVAD, I wished to evaluate the role of RipK1 phosphorylation further. Inhibition of $p38^{MAPK}$ kinase pathway during stimulation of cells with LPS+zVAD resulted in complete inhibition of RipK1 phosphorylation and had no impact on RipK1 degradation (Fig. 12A). Densitometric analysis was performed which showed that $p38^{MAPK}$ kinase promotes RipK1 phosphorylation (Fig. 12E). Although RipK3 phosphorylation was partially reduced in cells treated with $p38^{MAPK}$ inhibitor, there was no impact on cell death (Fig. 12B). Furthermore, the expression

of TNFα was significantly reduced in cells treated with the $p38^{MAPK}$ inhibitor (Fig. 12C). Collectively, these results indicate that the phosphorylation of RipK1 during TLR4 signalling is not necessary for its degradation. I was also able to test a new antibody that recognizes phospho-Serine 166 of RipK1 by western blotting. By comparing these results to those obtained for the same lysates with total RipK1 antibody, I found that only the non-phosphorylated RipK1 was degraded (Fig. 12D). I also explored the impact of RipK3 phosphorylation on RipK1 degradation. Cells were treated with LPS+zVAD with and without RipK3-kinase inhibitor (GSK843 or 872). RipK3 inhibition rescued cells from LPS-induced necroptosis. However, RipK1 and CASP-8 degradation were still observed (Fig. 13A). Interestingly, only cIAP1,2 degradation was prevented when I used GSK843/ GSK872 indicating that the loss of cIAP1,2 was dependent on the kinase activity of RipK3 . As a control, I confirmed the cell death using all inhibitors by MTT (Fig. 13B), CCK8 (Fig. 13C), Zombie yellow staining (Fig. 13D) for dead cells and PI/Hoechst staining (Fig. 13E). The addition of Nec-1 after 3 hours of LPS+zVAD stimulation was unable to reverse RipK1 degradation: RipK1 was only rescued after 1 hour (Fig. 14A). Cell death was also reversed after 1 hour, but not after 3 or 6 hours of LPS+zVAD treatment (Fig. 14C). In addition, I evaluated the formation of the necrosome in the presence of Nec-1 and GSK872 by performing immunoprecipitation using an anti-RipK3 antibody. I evaluated the necrosome by treating WT BMDMs with LPS+zVAD, +Nec-1 and GSK872 over 3 hours. In cells treated with LPS+zVAD we observed the association of RipK3 with RipK1, CASP-8, FADD and MLKL (Fig. 14 A). In contrast, addition of Nec-1 blocked the association of all these proteins with RipK1, implying that Nec-1 must block the necrosome formation early on. Interestingly, inhibition of the kinase activity of RipK3 with GSK872 resulted in only selective prevention of RipK3-MLKL association (Fig. 14B). Thus, using Nec-1 and GSK872 we could surmise that GSK872 blocks the late necrosome

which does not impact RipK1 degradation, whereas Nec-1 blocks the entire necrosome from early on, and this resulted in rescue of RipK1 degradation.

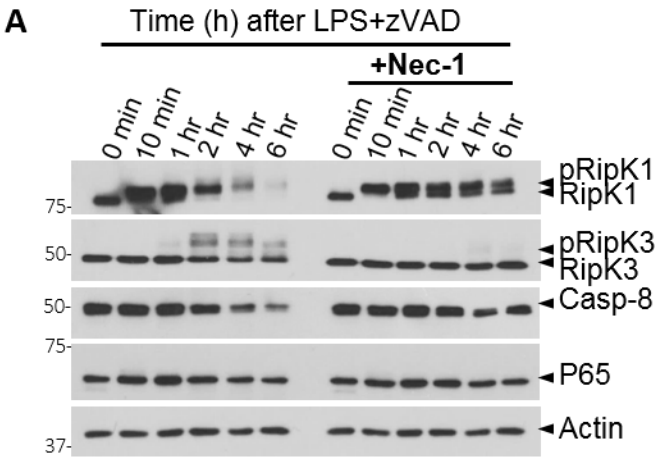
A
Time (h) after LPS+zVAD
+Nec-1
0 min
10 min
1 hr
2 hr
4 hr
6 hr
0 min
10 min
1 hr
2 hr
4 hr
6 hr
75-
50-
50-
75-
37-
pRipK1
RipK1
pRipK3
RipK3
Casp-8
P65
Actin

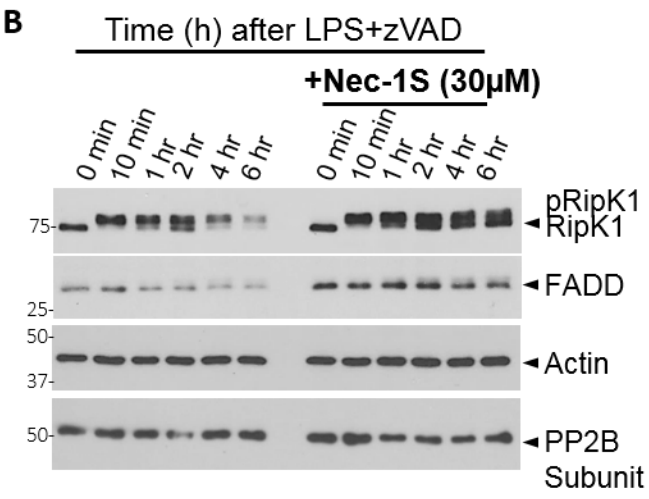
B
Time (h) after LPS+zVAD
+Nec-1S (30μM)
0 min
10 min
1 hr
2 hr
4 hr
6 hr
0 min
10 min
1 hr
2 hr
4 hr
6 hr
75-
25-
50-
37-
50-
pRipK1
RipK1
FADD
Actin
PP2B
Subunit

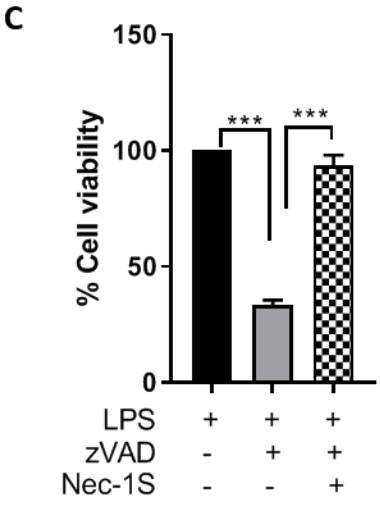
C
150
100
50
0
% Cell viability
***
***
LPS + + +
zVAD - + +
Nec-1S - - +

Figure 11: Blocking the RipK1-RipK3 interaction prevents RipK1 degradation.

WT BMDMs were generated and on day 6 of differentiation they were plated in 96-well and 24-well plates. **A.** Cells were treated with LPS (100ng/mL) + zVAD (50µM) with or without Nec-1 (30µM) for different time intervals. Cell extracts were collected, and protein expression was evaluated by western blotting**. B+C.** A specific RipK1 inhibitor (Nec-1S) 30µM was used with the same treatment as in **A** and protein expression was analyzed by western blot. **C.** Cell viability was measured by MTT after 24 hours post treatment. Graphs show the percentage of viability with ± SEM relative to controls. Each experiment was performed in triplicate and repeated three times. $***P < 0.001$.

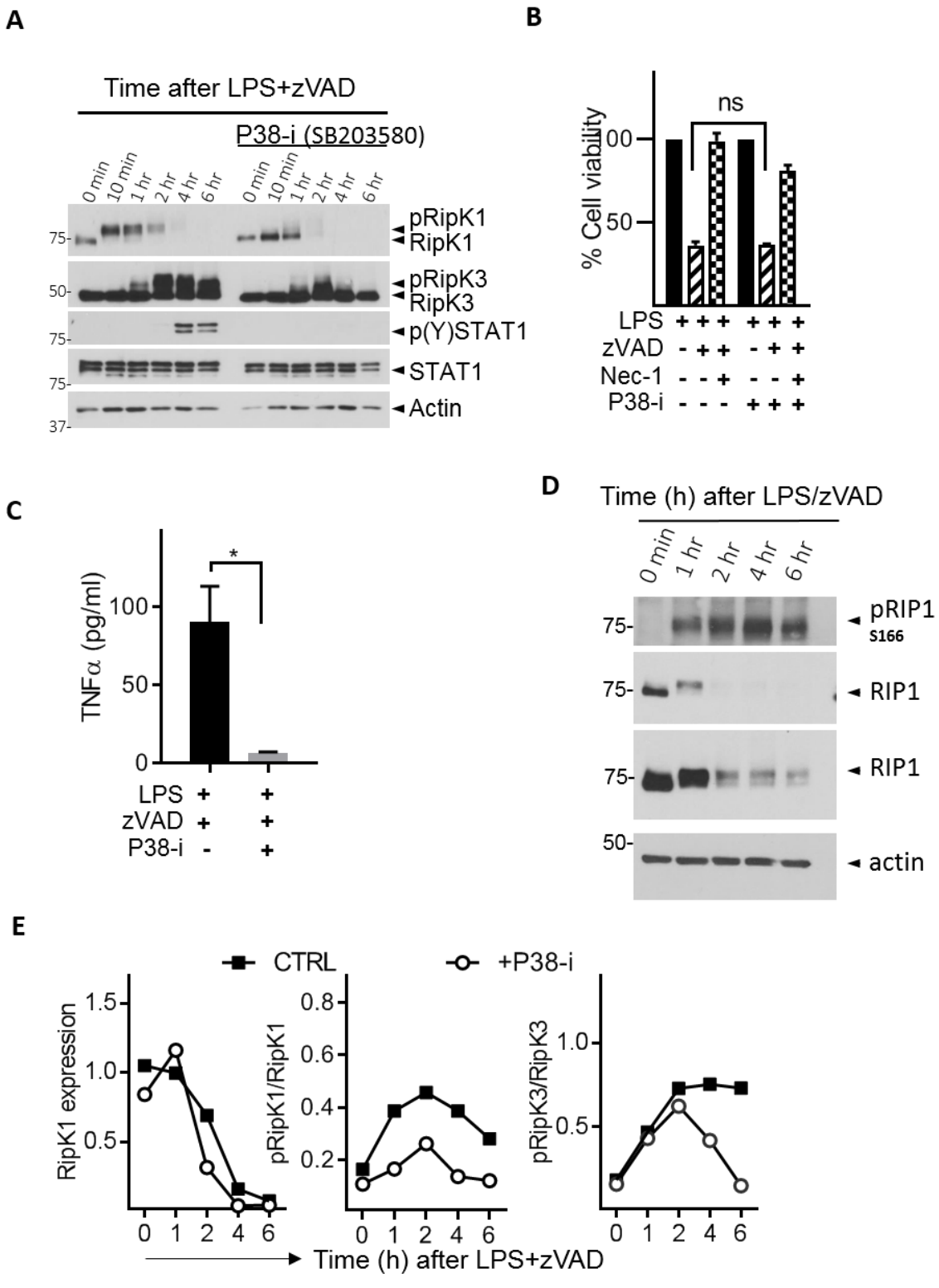
A
Time after LPS+zVAD
P38-i (SB203580)
0 min
10 min
1 hr
2 hr
4 hr
6 hr
pRipK1
RipK1
pRipK3
RipK3
p(Y)STAT1
STAT1
Actin
75-
50-
37-
B
% Cell viability
ns
100
50
LPS + + + + + +
zVAD - + + - + +
Nec-1 - - + - - +
P38-i - - - + + +
C
TNFα (pg/ml)
*
100
50
0
LPS + +
zVAD + +
P38-i - +
D
Time (h) after LPS/zVAD
0 min
1 hr
2 hr
4 hr
6 hr
pRIP1
S166
RIP1
RIP1
actin
75-
75-
75-
50-
E
CTRL
+P38-i
RipK1 expression
pRipK1/RipK1
pRipK3/RipK3
Time (h) after LPS+zVAD

Figure 12: Inhibition of RipK1 phosphorylation has no impact on RipK1 degradation.

WT BMDMs were generated and treated with LPS (100ng/mL) + zVAD (50μM) in the presence or absence of the $p38^{MAPK}$ inhibitor (SB203580) (50μM) for various time points. **A.** Lysates were collected and RipK1 expression was evaluated by western blotting. **B.** Viability of macrophages treated with LPS+zVAD with or without $p38^{MAPK}$ inhibitor (SB203580) (50 μM) was evaluated at 24 hours by MTT assay. **C.** Supernatants were collected from (A) at 6 hours post stimulation and analyzed by ELISA for TNFα cytokine expression. **D.** Cell lysates were collected from cells treated with LPS+zVAD and protein expression tested by western blotting for serine 166 RipK1-phosphorylation for various time intervals. **E.** Quantification of western blot data (A) was done for total RipK1, phospho RipK1 ratio and phospho RipK3 ratio. Quantified data represent a representative experiment (from three independent experiments). Graphs show the % of viability with ± SEM relative to controls. Each experiment was performed in triplicate and repeated three times. $*P < 0.01$.

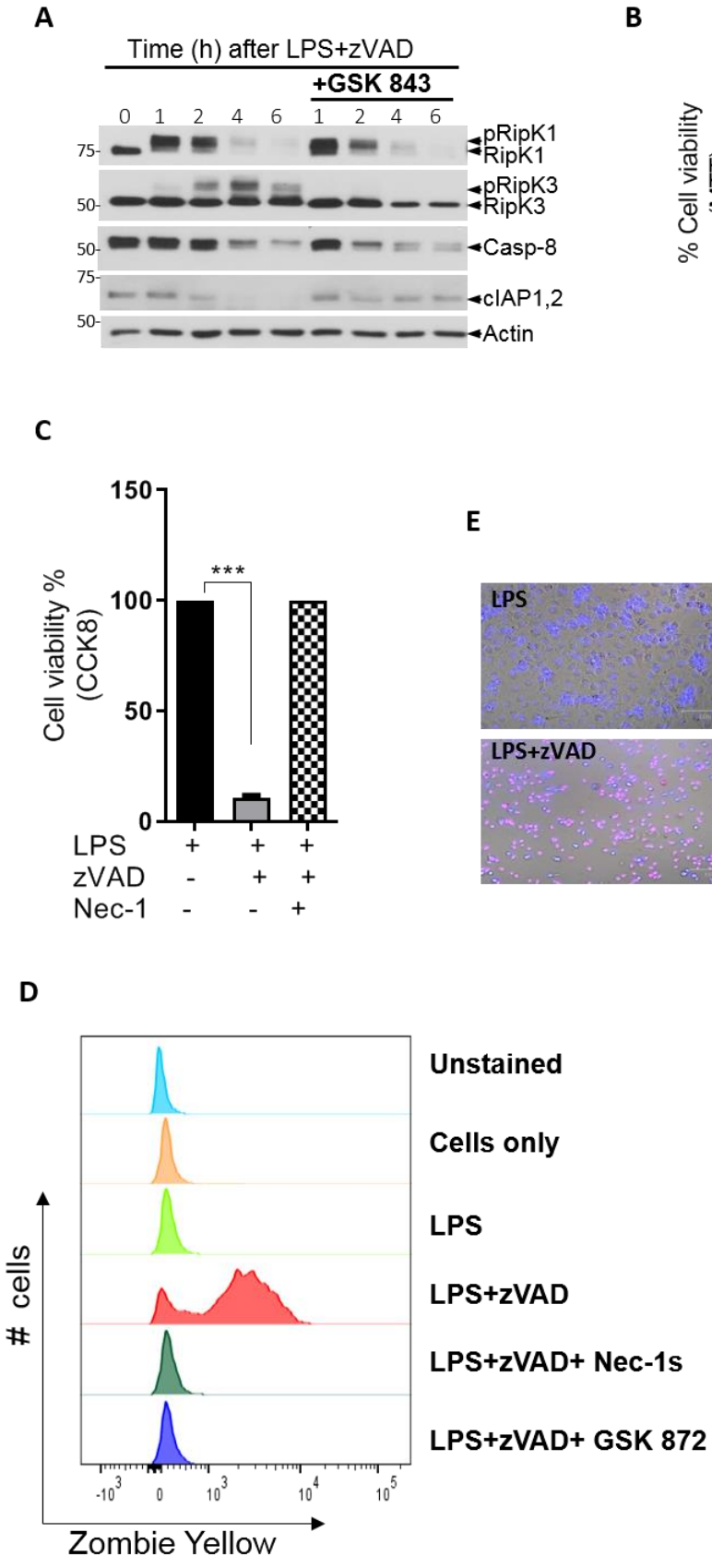
A
Time (h) after LPS+zVAD
+GSK 843
0 1 2 4 6 1 2 4 6
75-
pRipK1
RipK1
50-
pRipK3
RipK3
50-
Casp-8
75-
cIAP1,2
50-
Actin
B
% Cell viability (MTT)
100
75
50
25
****
****
LPS + + + +
zVAD - + + +
Nec1 - - + -
GSK - - - +
C
Cell viability % (CCK8)
150
100
50
0
***
LPS + + +
zVAD - + +
Nec-1 - - +
E
LPS
LPS+zVAD+Nec-1
LPS+zVAD
LPS+zVAD+GSK
D
cells
Zombie Yellow
Unstained
Cells only
LPS
LPS+zVAD
LPS+zVAD+ Nec-1s
LPS+zVAD+ GSK 872

Figure 13: Inhibition of RipK3 kinase activity does not impact RipK1 degradation in response to LPS+zVAD stimulation.

WT BMDMs were stimulated with LPS (100ng/mL) + zVAD (50μM) in the presence or absence of Nec-1 (30 μM) (**B, C, D**) or GSK843/872 (3 μM) (**A, B, E, D**). Cell lysates were collected at various time intervals and protein expression tested by western blotting **(A).** Cell viability of macrophages was examined by various methods: MTT **(B),** CCK8 **(C)** assay, Zombie yellow staining **(D)** at 24-hour post stimulation, or by immunofluorescence staining using Hoechst (blue: stained live and dead cells) and propidium iodide (PI) co-staining (red: stained dead cells) **(E)** at 6 hours post stimulation. Graphs show the % of viable cells ±SEM relative to controls without zVAD. Each experiment was performed in triplicate and repeated three times. ****$P < 0.0001$

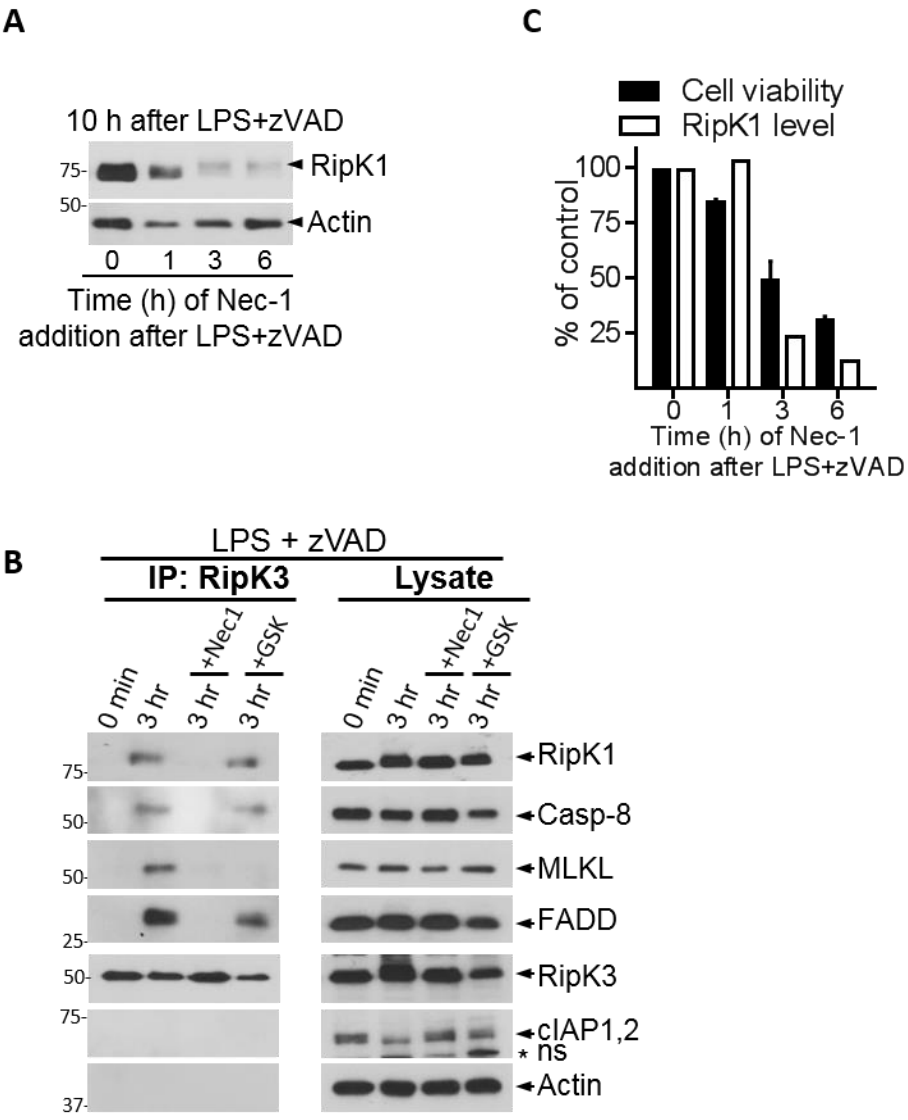
A
10 h after LPS+zVAD
75-
50-
RipK1
Actin
0 1 3 6
Time (h) of Nec-1
addition after LPS+zVAD
C
Cell viability
RipK1 level
% of control
100
75
50
25
0 1 3 6
Time (h) of Nec-1
addition after LPS+zVAD
B
LPS + zVAD
IP: RipK3
Lysate
0 min
3 hr
3 hr +Nec1
3 hr +GSK
RipK1
Casp-8
MLKL
FADD
RipK3
cIAP1,2
* ns
Actin

Figure 14: Early RipK1-RipK3 interaction drives the degradation of RipK1 and interacting proteins.

(A, C). BMDMs of WT were treated with LPS (100 ng/mL) + zVAD (50 µM). Nec-1 (30µM) was added immediately or at 1-,3-,6- hours post-stimulation with LPS+zVAD. After 10 hours of treatments, cells were lysed and protein expression evaluated by western blotting**. B.** RipK3 was immuno-precipitated in control cells (untreated) and in cells stimulated with LPS (100 ng/mL) + zVAD (50µM) for 3 h in the absence or presence of Nec-1 (30µM) or GSK872 (5µM). Expression of various proteins in the immuno-precipitates and whole cell lysates were evaluated by western blotting. **C.** Cell viability was determined at 24 hours by MTT and quantification of western blot was done for total RipK1.

4.1.5. Degradation of necrosome impairs cell death and cytokine expression

I next wanted to investigate the impact of early necrosome degradation on cytokine expression and susceptibility to cell death and. Thus, I treated WT BMDMs with LPS+zVAD in presence of Nec-1 or GSK872. While treatment with both inhibitors inhibited cell death (Fig. 15A), only Nec-1 treatment reduced degradation of the RipK1, CASP-8, cIAP1,2 and FADD (Fig. 15B). Based on these results, cell death could be uncoupled from necrosome degradation. I considered the possibility that the early degradation of the necrosome in cells treated with LPS+zVAD+GSK may result in a state of resistance against subsequent stimulations to induce necroptosis. I stimulated cells as described in Fig. 10A, and then removed the primary treatment by washing the cells twice and followed by a second stimulation that included LPS, LPS+zVAD and LPS+zVAD+GSK872. I noted that cells with depleted necrosomal proteins due to the primary treatment (LPS+zVAD+GSK) exhibited significant resistance to LPS-induced necroptosis (Fig. 15C). In contrast, other groups of cells that were treated with LPS, LPS+zVAD+Nec-1 and LPS+GSK872 which expressed high levels of necrosomal proteins were sensitive to necroptosis induction (Fig. 15C). These results suggest that early degradation of necrosome-interacting proteins creates a state of resistance in the cell to subsequent induction of necroptosis. Lastly, I evaluated the impact of early necrosome-degradation on cytokine expression in response to a secondary stimulation by LPS and noted that necrosome-degradation resulted in a significant reduction in the expression of TNF, IL-10 and IL-6 (Fig. 15D). Overall, these findings reveal that early necrosome-degradation may have a biological impact in cells.

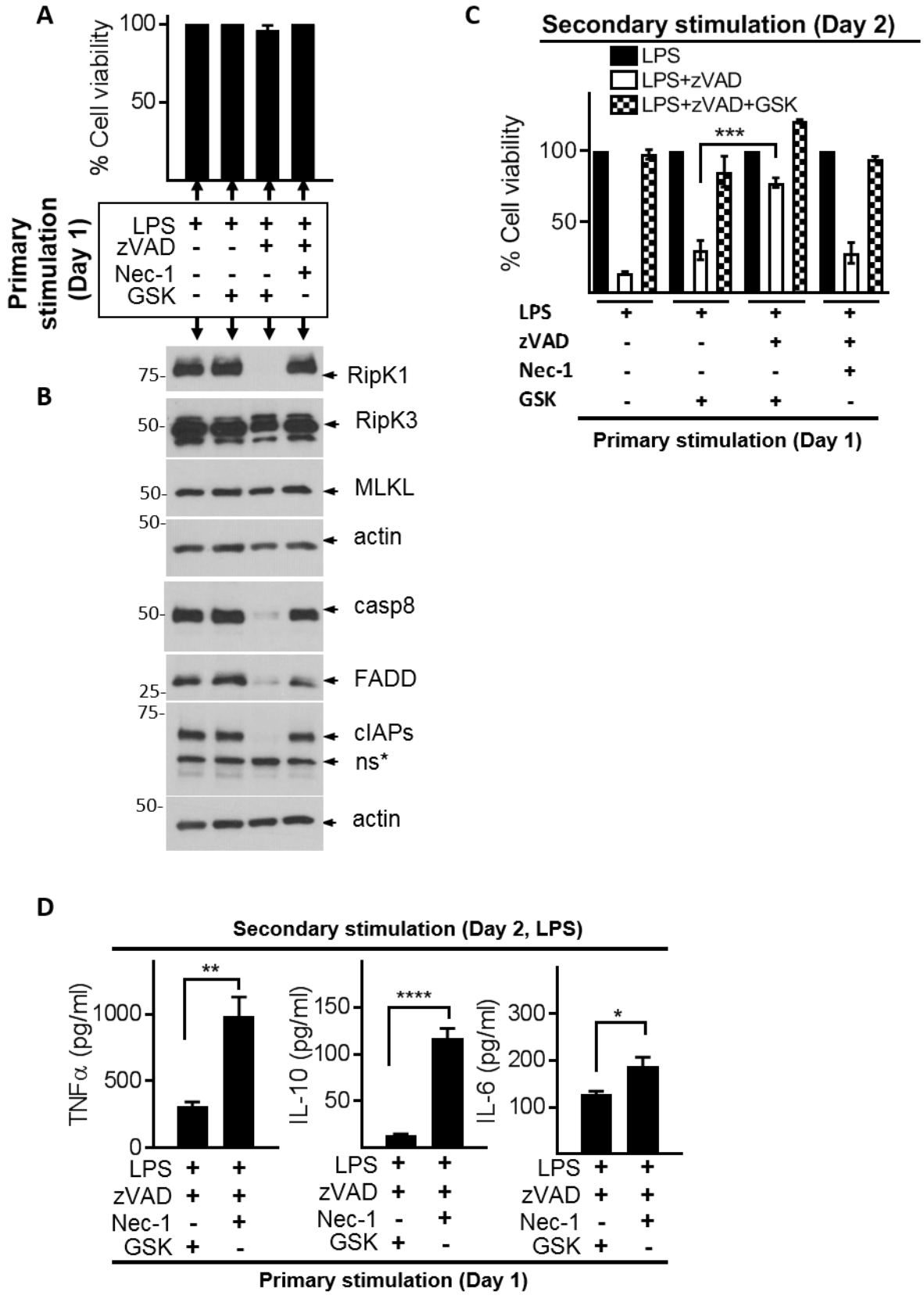
A
% Cell viability
100
50
Primary stimulation (Day 1)
LPS + + + +
zVAD - - + +
Nec-1 - - - +
GSK - + + -
B
75-
RipK1
50-
RipK3
50-
MLKL
50-
actin
50-
casp8
25-
FADD
75-
cIAPs
ns*
50-
actin
C
Secondary stimulation (Day 2)
LPS
LPS+zVAD
LPS+zVAD+GSK
***
% Cell viability
100
50
LPS + + + +
zVAD - - + +
Nec-1 - - - +
GSK - + + -
Primary stimulation (Day 1)
D
Secondary stimulation (Day 2, LPS)
TNFα (pg/ml)
1000
500
0
**
IL-10 (pg/ml)
150
100
50
****
IL-6 (pg/ml)
300
200
100
*
LPS + + + + + + + +
zVAD + + + + + + + +
Nec-1 - + - + - + - +
GSK + - + - + - + -
Primary stimulation (Day 1)

Figure 15: Early necrosome degradation enhanced resistances to cell death and reduced cytokine expression.

(A to D) WT BMDMs were plated in 96-well plates for cell death and on 24-well plates for western blotting and treated as described in panel. Primary treatments: LPS (100ng/mL), zVAD (50µM), Nec-1 (30µM) and GSK 872 (5µM). **A.** After 24 hours of stimulation, cell viability was measured by MTT. **B.** Western blotting was performed in cell extracts after 24 hours of stimulation. **C.** Primary treatments were removed by washing cells twice with media, followed by treatment with LPS (100ng/mL), zVAD (50µM) and GSK 872 (5µM). Cell viability was determined by MTT assay at 24hr post-secondary stimulation. **D.** Six hours post-secondary LPS stimulation supernatants were collected and cytokine expression was measured by ELISA. Graphs show the % of viable cells ± SEM relative to cells treated with LPS in the absence of zVAD. Each experiment was repeated three times with triplicate samples. $*P < 0.05$, $**P < 0.01$, $***P < 0.001$, $****P < 0.0001$

4.1.6. RipK1-RipK3 interaction promotes K48-ubiquitination during necrosome signalling

I investigated the mechanism that was responsible for early degradation of the necrosome. To investigate whether the degradation occurs through the proteasome, I tested whether a proteasome inhibitor (Lactacystin or MG132) could prevent the necrosome degradation. I performed a time course treatment with LPS+zVAD with or without Lactacystin. Inhibition of the proteasome resulted in substantial rescue of RipK1 levels, which correlated with an increase of RipK3 phosphorylation (Fig. 16A, D). Interestingly, CASP-8 and cIAP1,2 were partially rescued upon Lactacystin treatment (Fig. 16A, D). I also performed the same experiment using another selective proteasome inhibitor, MG341 (Bortezomib), and I observed similar results (Fig. 16B). I also tested whether the necrosome is degraded through lysosomal pathway. I blocked the transcription, autophagy and lysosomal function with specific inhibitors: actinomycin-D (Act-D), chloroquine (CHQ), and hydroxychloroquine (HCQ) respectively. Inhibition of these pathways did not rescue necrosome-degradation (Fig. 16C). These results suggest that RipK1 is degraded primarily by the proteasome.

Since proteasomal degradation of proteins involves ubiquitination of targeted proteins, I evaluated ubiquitination of RipK1 during necrosome signalling. I treated WT BMDMs with LPS and LPS+zVAD and performed immunoprecipitation using tandem ubiquitination binding entities (TUBE), followed by western blotting. Interestingly, RipK1 was massively ubiquitinated upon LPS+ZVAD stimulation, but not LPS alone (Fig. 17A). Similar results were obtained following TNFα+zVAD stimulation (Fig 17D). Since I had previously observed that the degradation of RipK1 was rescued in RipK3-deficient macrophages, I therefore examined the ubiquitination of RipK1 in *Ripk3*-deficient macrophages after LPS+zVAD stimulation. RipK1 ubiquitination was remarkably reduced in *Ripk3*$^{-/-}$ compared to WT BMDMs (Fig. 17B). To further characterize

ubiquitination, I examined K48-ubiqutination using a specific K48 antibody and performed immunoprecipitation in WT and *Ripk3*$^{-/-}$ BMDMs. RipK1 and CASP-8 were significantly ubiquitinated with K48 in WT macrophages following LPS+zVAD stimulation, which was highly reduced in *Ripk3*-deficient macrophages (Fig. 17C). I also examined K63 ubiquitination in parallel with K48 by performing time course treatment with LPS+zVAD, followed by immunoprecipitation with anti-K63 and anti-K48 antibodies. Interestingly, RipK1 was not ubiquitinated at K63 after 3-hours of treatment (Fig. 17E). These results suggest that the interaction of RipK1 with RipK3 in the early necrosome leads to K-48 ubiquitination of the necrosome which promotes the degradation of RipK1.

4.1.7. RipK1 degradation is not maintained by cIAP1,2 during necrosome signalling

Since IAPs are E3 ubiquitin ligases, I tested the involvement of cIAP1,2 in necrosome signalling and degradation. I treated WT and cIAP1- and cIAP2-deficient macrophages with LPS+zVAD for varying time intervals. I found that depletion of RipK1 level was not impacted by the loss of either cIAP1 or cIAP2 (Fig. 18A). Moreover, I evaluated the susceptibility of *cIAP1-,2*-deficent macrophages to necroptosis and I found that there was no significant difference in their susceptibility of necroptosis compared to WT cells (Fig. 18B). I also evaluated the impact of another IAP, xIAP and observed that xIAP did not have any impact on necroptosis or degradation of RipK1 (Fig. 18C, D). It is possible that other IAPs could compensate for the loss of a single IAP, I therefore depleted all IAPs to evaluate their role in necroptosis and RipK1 degradation. To achieve this, I treated macrophages with LPS+zVAD with or without SMAC mimetic Birinapant (BP). Birinapant is known to induce rapid auto-degradation of cIAP1,2 and inhibit xIAP activity. Depletion/inhibition of all IAPs had no impact on RipK1 degradation or necroptosis. In fact, cIAP1,2 itself is degraded during early necrosome signalling (Fig. 19A). Lastly, RipK1

degradation was also observed when I induced necroptosis following BP+zVAD stimulation (Fig. 19B, C). In contrast, treatment with BP alone did not impact RipK1 nor RipK3 phosphorylation (Fig. 19B). Taken together, these results indicate that IAPs do not have any impact on Ripk1 degradation or necrosome signalling.

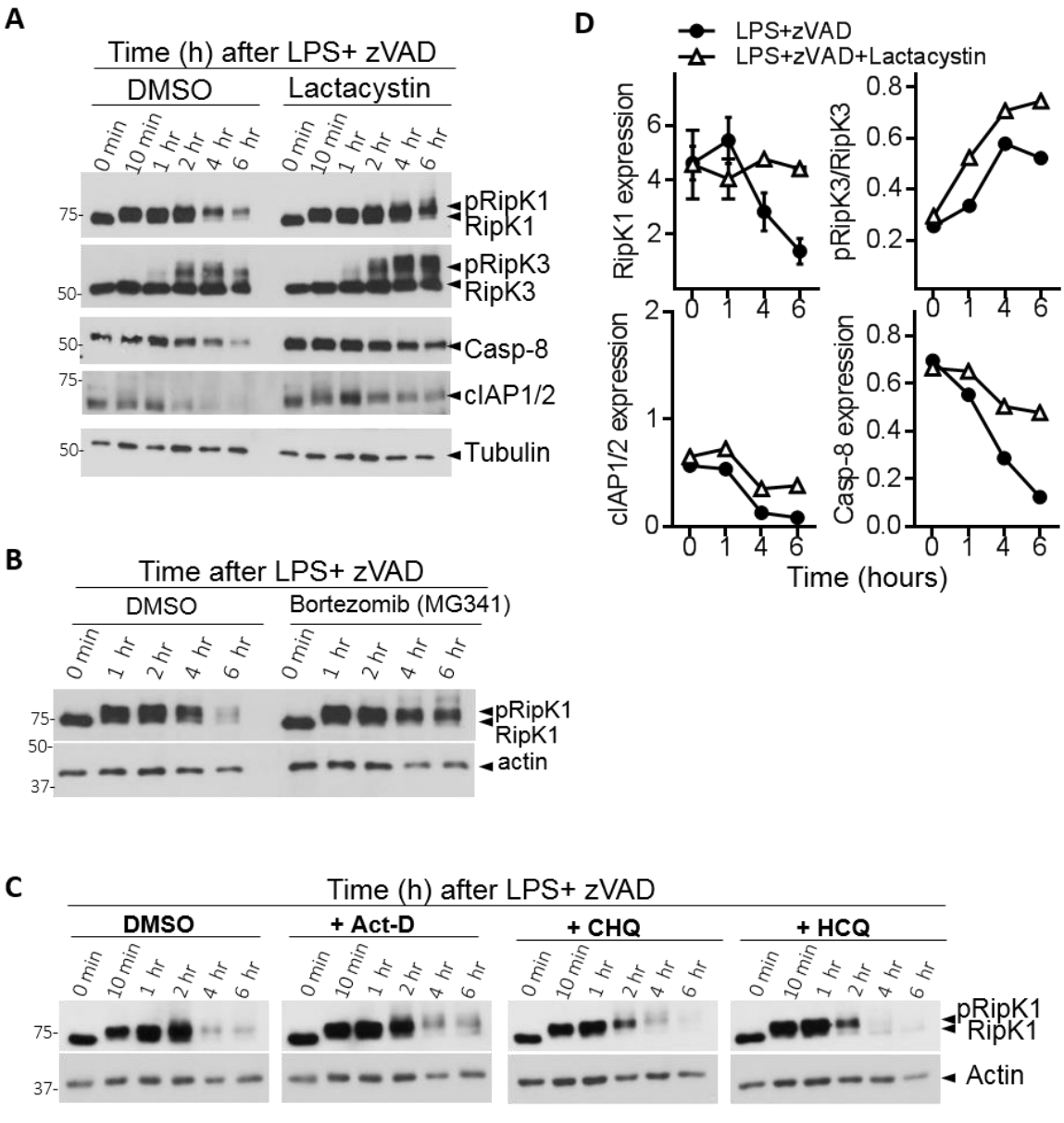
A
Time (h) after LPS+ zVAD
DMSO
Lactacystin
0 min
10 min
1 hr
2 hr
4 hr
6 hr
75-
50-
pRipK1
RipK1
pRipK3
RipK3
Casp-8
cIAP1/2
Tubulin
B
Time after LPS+ zVAD
DMSO
Bortezomib (MG341)
37-
actin
C
Time (h) after LPS+ zVAD
DMSO
+ Act-D
+ CHQ
+ HCQ
Actin
D
LPS+zVAD
LPS+zVAD+Lactacystin
RipK1 expression
pRipK3/RipK3
cIAP1/2 expression
Casp-8 expression
Time (hours)

Figure 16: The necrosome is degraded by proteasomal pathway in response to LPS-induced necroptosis.

A. WT BMDMs were treated with LPS (100ng/mL) + zVAD (50μM) in the presence or absence of Lactacystin (10μg/mL) for various time intervals. Cell extracts were collected, and the expression of various proteins evaluated by western blotting. **B.** BMDMs were treated with LPS (100ng/mL) + zVAD (50μM) in the presence or absence of selective proteasome inhibitor MG341 (Bortezomib) (10μM). Cell lysates were collected, and the expression of various proteins evaluated by western blotting. **C.** BMDMs were treated with LPS (100ng/mL) + zVAD (50μM) in the presence or absence of Actinomycin-D (Act-D) (80nM), Cycloheximide (CHX) (1.7μM) and Hydroxychloroquine (HCQ) (100μM). Cell extracts were collected at various time intervals and RipK1 expression was examined by western blotting. **D.** Quantification of western blot data in (A) was done for total RipK1, pRipK3, CASP-8, and cIAP1,2. Quantified data represent a representative experiment (from three independent experiments).

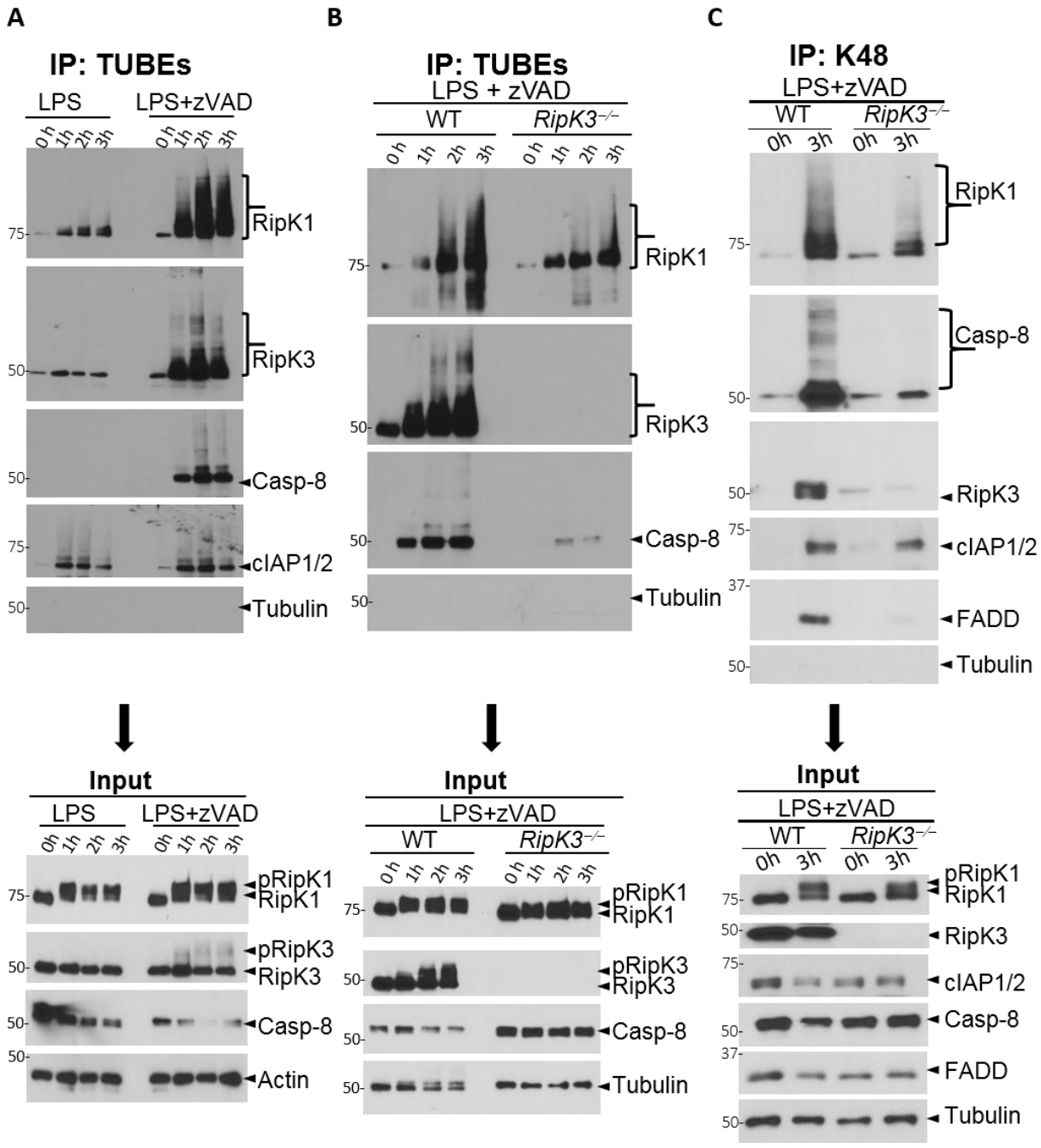
A
IP: TUBEs
LPS
LPS+zVAD
0h 1h 2h 3h 0h 1h 2h 3h
75-
RipK1
50-
RipK3
50-
Casp-8
75-
cIAP1/2
50-
Tubulin
B
IP: TUBEs
LPS + zVAD
WT
RipK3−/−
0h 1h 2h 3h 0h 1h 2h 3h
75-
RipK1
50-
RipK3
50-
Casp-8
50-
Tubulin
C
IP: K48
LPS+zVAD
WT
RipK3−/−
0h 3h 0h 3h
75-
RipK1
50-
Casp-8
50-
RipK3
75-
cIAP1/2
37-
FADD
50-
Tubulin
Input
LPS
LPS+zVAD
0h 1h 2h 3h 0h 1h 2h 3h
75-
pRipK1
RipK1
50-
pRipK3
RipK3
50-
Casp-8
50-
Actin
Input
LPS+zVAD
WT
RipK3−/−
0h 1h 2h 3h 0h 1h 2h 3h
75-
pRipK1
RipK1
50-
pRipK3
RipK3
50-
Casp-8
50-
Tubulin
Input
LPS+zVAD
WT
RipK3−/−
0h 3h 0h 3h
75-
pRipK1
RipK1
50-
RipK3
75-
cIAP1/2
50-
Casp-8
37-
FADD
50-
Tubulin

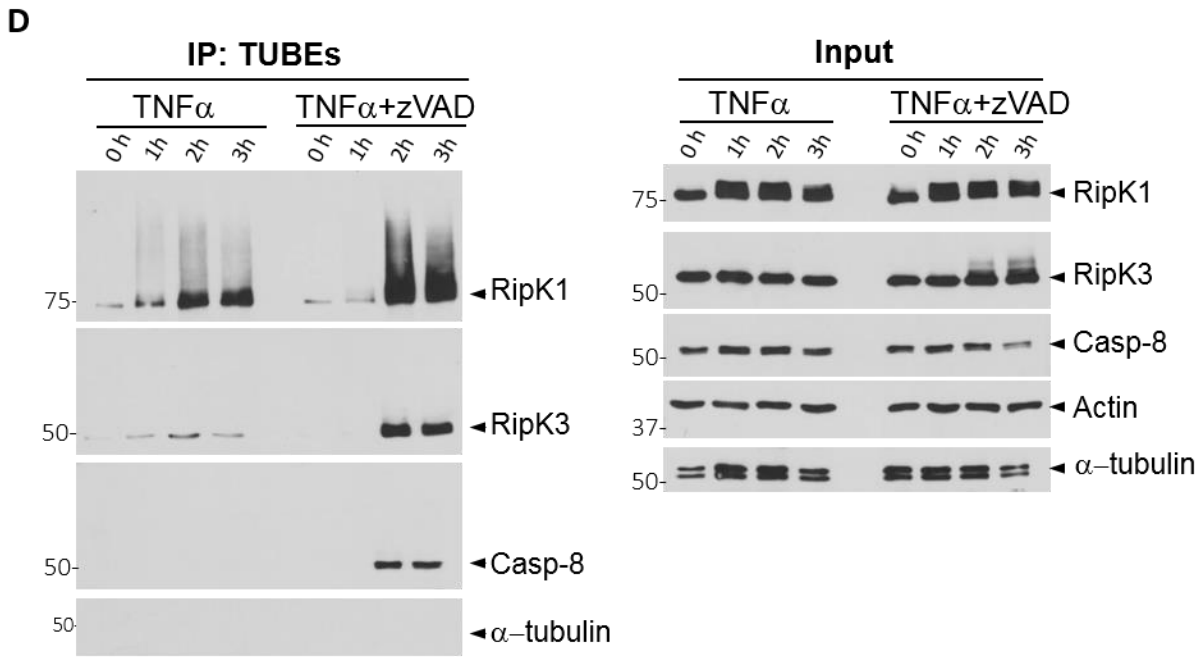
D
IP: TUBEs
TNFα
TNFα+zVAD
0 h
1h
2h
3h
75-
RipK1
50-
RipK3
50-
Casp-8
50-
α–tubulin
Input
75-
RipK1
50-
RipK3
50-
Casp-8
37-
Actin
50-
α–tubulin

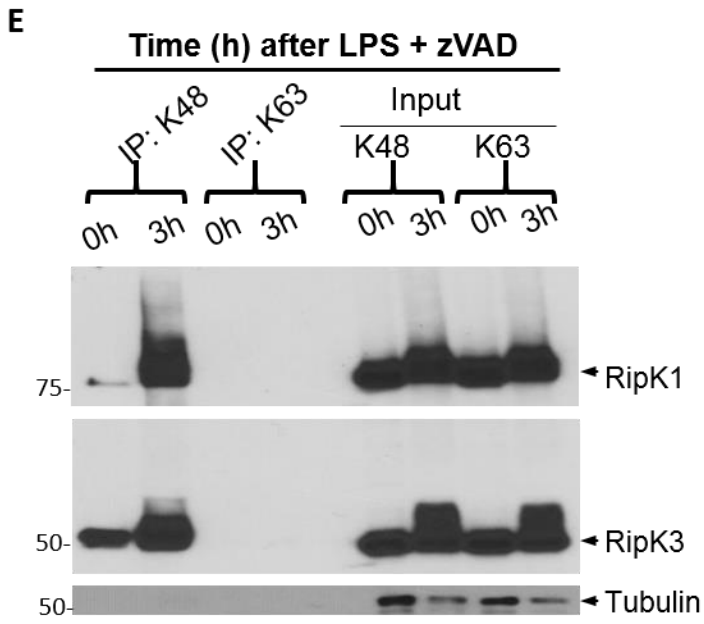
E
Time (h) after LPS + zVAD
IP: K48
IP: K63
Input
K48
K63
0h
3h
75-
RipK1
50-
RipK3
50-
Tubulin

Figure 17: Early RipK1-RipK3 interaction leads to K48-ubiquitination of RipK1.

(A+D) WT BMDMs were treated with proteasome inhibitor MG132 (10μM) with LPS (100ng/mL) or LPS + zVAD (50μM) **(A),** or with TNFα (1000U/mL) or TNFα + zVAD (50μM) **(D)** for varying time intervals. Cell lysates were collected and immuno-precipitated with TUBE for 16 hours at 4°C as described (in the methods 3.7. section). Eluent and input were evaluated by western blotting for ubiquitinated proteins. **B.** WT and RipK3$^{-/-}$ macrophages were treated as in (A) and examined by western blotting. **C**. WT and RipK3$^{-/-}$ macrophages were treated with proteasome inhibitor MG132 (10μM) prior to LPS (100ng/mL) + zVAD (50μM) for 3 hours. Cells were lysed and immuno-precipitation was performed using magnetic beads coupled with antibodies targeting K-48 for 16 hours at 4 °C. Immuno-precipitated eluent and the non-immunoprecipitated proteins were examined by western blotting. **E**. K48 and K63 immuno-precipitation was performed on WT BMDMs treated with LPS (100ng/mL) + zVAD (50μM) for 3 hours followed by incubating the lysate with the coupled beads for 16 hours at 4°C. Eluent and whole cell lysate were examined by western blotting.

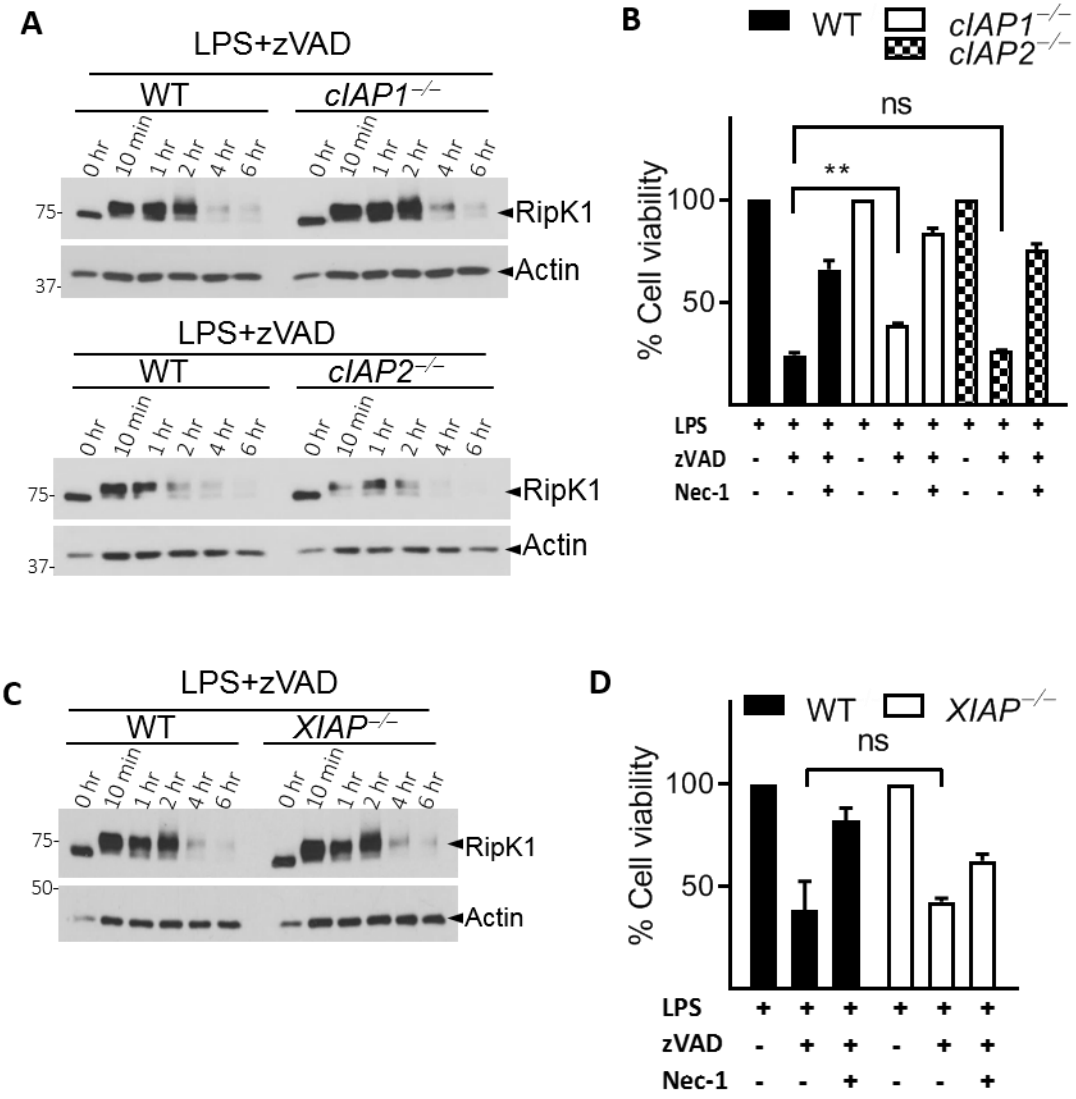
A
LPS+zVAD
WT
cIAP1−/−
0 hr
10 min
1 hr
2 hr
4 hr
6 hr
75-
RipK1
37-
Actin
LPS+zVAD
WT
cIAP2−/−
75-
RipK1
37-
Actin
B
WT
cIAP1−/−
cIAP2−/−
ns
**
% Cell viability
100
50
LPS
zVAD
Nec-1
C
LPS+zVAD
WT
XIAP−/−
75-
RipK1
50-
Actin
D
WT
XIAP−/−
ns
% Cell viability
100
50
LPS
zVAD
Nec-1

Figure 18: RipK1 degradation is not mediated by IAPs.

A-C. BMDMs from WT, *cIap1*$^{-/-}$, *cIap2*$^{-/-}$, and *xIap*$^{-/-}$ were generated and treated with LPS (100ng/mL) + zVAD (50μM) for varying time intervals. **A+C** cells were lysed and examined by western blotting for RipK1 expression. **B+D.** Macrophages from WT, *cIap1*$^{-/-}$, *cIap2*$^{-/-}$, and *xIap*$^{-/-}$ were treated with LPS (100ng/mL) + zVAD (50μM) with or without Nec-1 (30μM) for 24 hours before measuring cell viability by MTT assay. Graphs show the % of viable cells ± SEM relative to cells treated with LPS in the absence of zVAD. Each experiment was repeated three times with triplicate samples. (**$p < 0.01$).

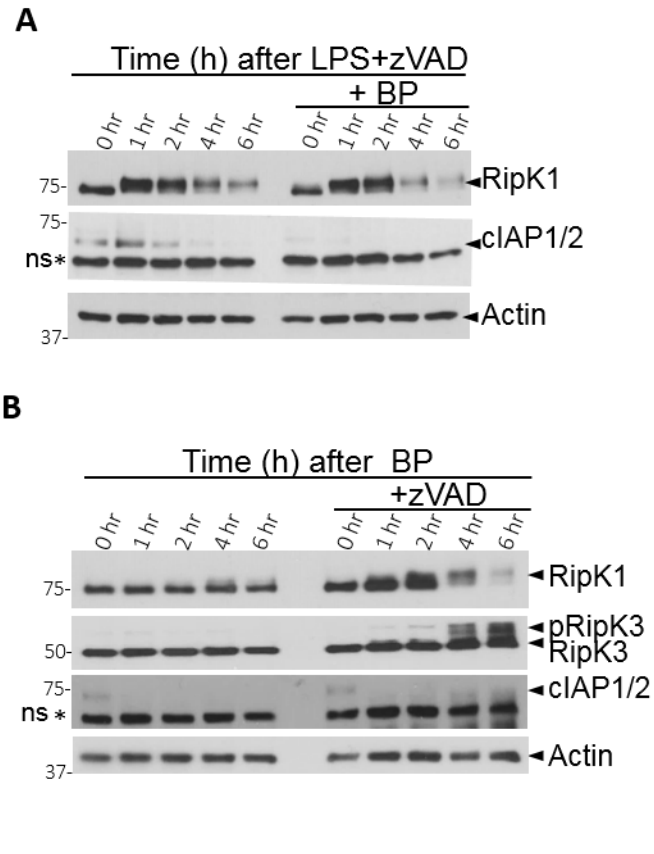
A
Time (h) after LPS+zVAD
+ BP
0 hr
1 hr
2 hr
4 hr
6 hr
0 hr
1 hr
2 hr
4 hr
6 hr
75-
RipK1
75-
ns*
cIAP1/2
Actin
37-
B
Time (h) after BP
+zVAD
0 hr
1 hr
2 hr
4 hr
6 hr
0 hr
1 hr
2 hr
4 hr
6 hr
75-
RipK1
pRipK3
50-
RipK3
75-
ns*
cIAP1/2
Actin
37-
C
****
% Cell viability
100
75
50
25
BP - + +
zVAD - + +
Nec-1 - - +

Figure 19: Depletion of IAPs by SMAC mimetic Birinapant does promote maintenance of RipK1.

A. WT BMDMs were stimulated with LPS (100ng/mL) + zVAD (50μM) in the presence or absence of Birinapant (10μM) for various time intervals. The expression of RipK1 and cIAP1/2 was measured by western blotting. **B.** Necroptosis was induced by stimulating macrophages with Birinapant (10μM) in the presence or absence of zVAD (50μM). Cell lysates were examined and analyzed by western blotting. **C.** Cells were treated with Birinapant (10μM), zVAD (50μM) and Nec-1 (30 μM) and cell viability was measured after 24 hours of treatment by MTT. Graphs show the % of viable cells ± SEM relative to untreated cells. Each experiment was repeated three times with triplicate samples. $****P < 0.0001$

4.1.8. RipK1 degradation during LPS-induced necroptosis occurs independently of A20 and CYLD

In other experimental models A20 and CYLD have been shown to modify RipK1 ubiquitination (Moquin et al., 2013). To test whether A20 and CYLD were involved in RipK1 degradation during LPS-induced necrosome signalling, I performed single and double knockdown of A20 and CYLD in WT BMDMs. Knockdown of these ubiquitin editing enzymes did not rescue RipK1 degradation (Fig. 20A, B). I examined the expression of RipK1 in *Cyld*-deficient macrophages, and treated WT and *Cyld*$^{-/-}$ BMDMs with LPS+zVAD for varying time intervals. RipK1 degradation was still observed in *Cyld*$^{-/-}$ BMDMs (Fig. 20C). However, RipK3 phosphorylation was significantly reduced in *Cyld*$^{-/-}$ BMDMs relative to WT cells (Fig. 20C). *Cyld*-deficient macrophages were significantly resistant to LPS-mediated necroptosis (Fig. 20D). Western blotting revealed that there was post translational modification of A20 and CYLD. Specifically, I found LPS+zVAD treatment promoted the expression and phosphorylation of CYLD and A20 (Fig. 21A). To quantify CYLD and A20 expression, I performed densitometric analysis and found that during necrosome signalling, expression of CYLD and A20 was upregulated (Fig. 21B). Finally, I evaluated the role of the M1 linear ubiquitination that is mediated by LUBAC complex. I was treating WT BMDMs with gliotoxin, a LUBAC inhibitor. This inhibition of linear ubiquitination had no impact on RipK1 degradation nor necroptosis (Fig. 21D, E).

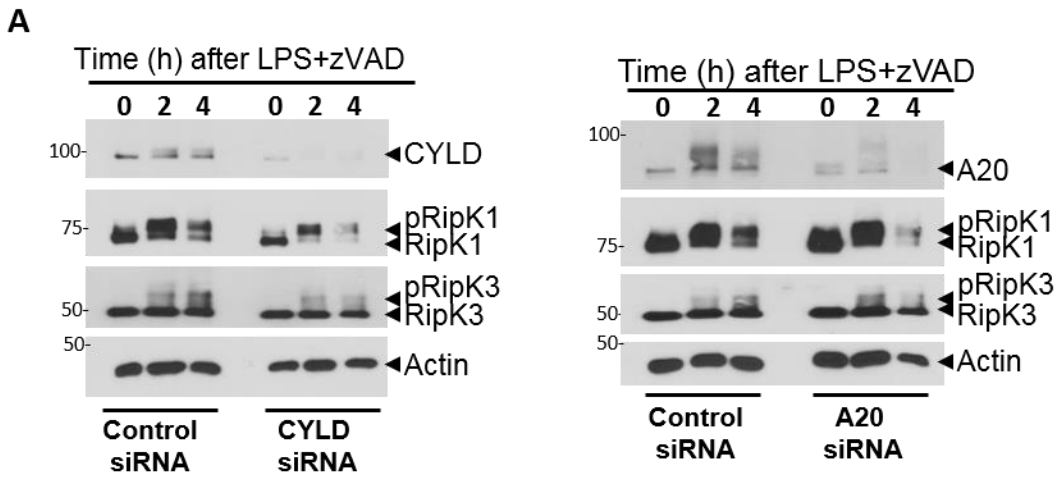
A
Time (h) after LPS+zVAD
0 2 4 0 2 4
100-
CYLD
75-
pRipK1
RipK1
pRipK3
50-
RipK3
50-
Actin
Control siRNA
CYLD siRNA
Time (h) after LPS+zVAD
0 2 4 0 2 4
100-
A20
75-
pRipK1
RipK1
pRipK3
50-
RipK3
50-
Actin
Control siRNA
A20 siRNA

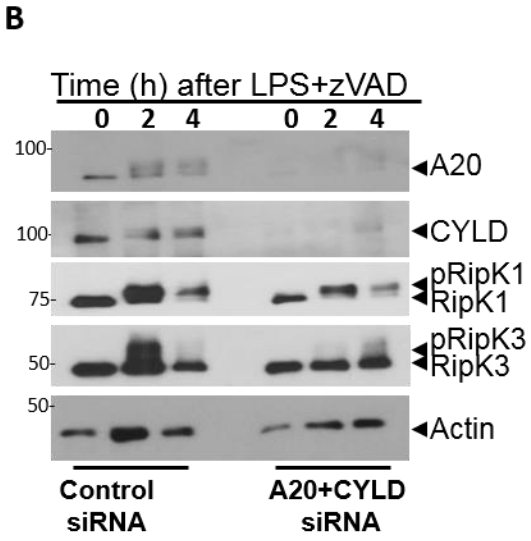
B
Time (h) after LPS+zVAD
0 2 4 0 2 4
100-
A20
100-
CYLD
75-
pRipK1
RipK1
50-
pRipK3
RipK3
50-
Actin
Control siRNA
A20+CYLD siRNA

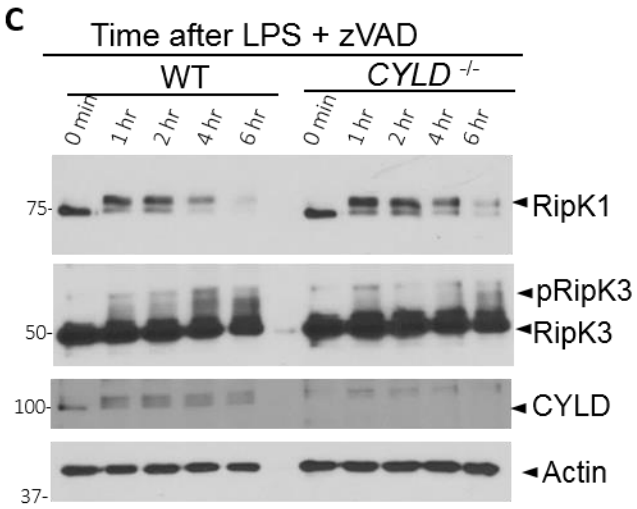
C
Time after LPS + zVAD
WT
CYLD -/-
0 min
1 hr
2 hr
4 hr
6 hr
75-
RipK1
pRipK3
50-
RipK3
100-
CYLD
37-
Actin

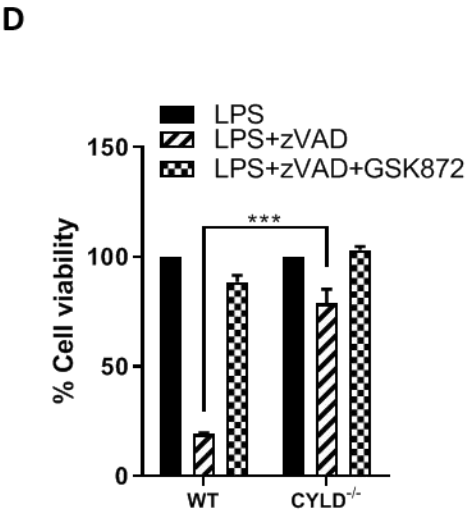
D
LPS
LPS+zVAD
LPS+zVAD+GSK872
150
100
50
0
% Cell viability
***
WT
CYLD-/-

Figure 20: RipK1 degradation during necrosome signalling is not mediated by A20 and CYLD.

A+B. BMDMs of WT mice were transfected with si-RNA against CYLD (15 pmol) or A20 (15 pmol) **(A)** or both **(B)** using RNAmaxi kit for 24 hours. The transfected cells were treated with LPS (100ng/mL) + zVAD (50μM) for various time intervals. After 4 hours cells were lysed and the expression of RipK1, RipK3 CYLD and A20 was evaluated by western blotting. **C.** BMDMs were generated from WT and *Cyld*$^{-/-}$ mice and treated with LPS (100ng/mL) + zVAD (50μM) for various time intervals. Cell lysates were evaluated by western blotting for RipK1, RipK3 and CYLD expression. **D.** Cell viability was measured by MTT assay after 24 hours of stimulation. Graphs show the percentage of viable cells ±SEM relative to controls. Each experiment was repeated three times. ***$P < 0.001$

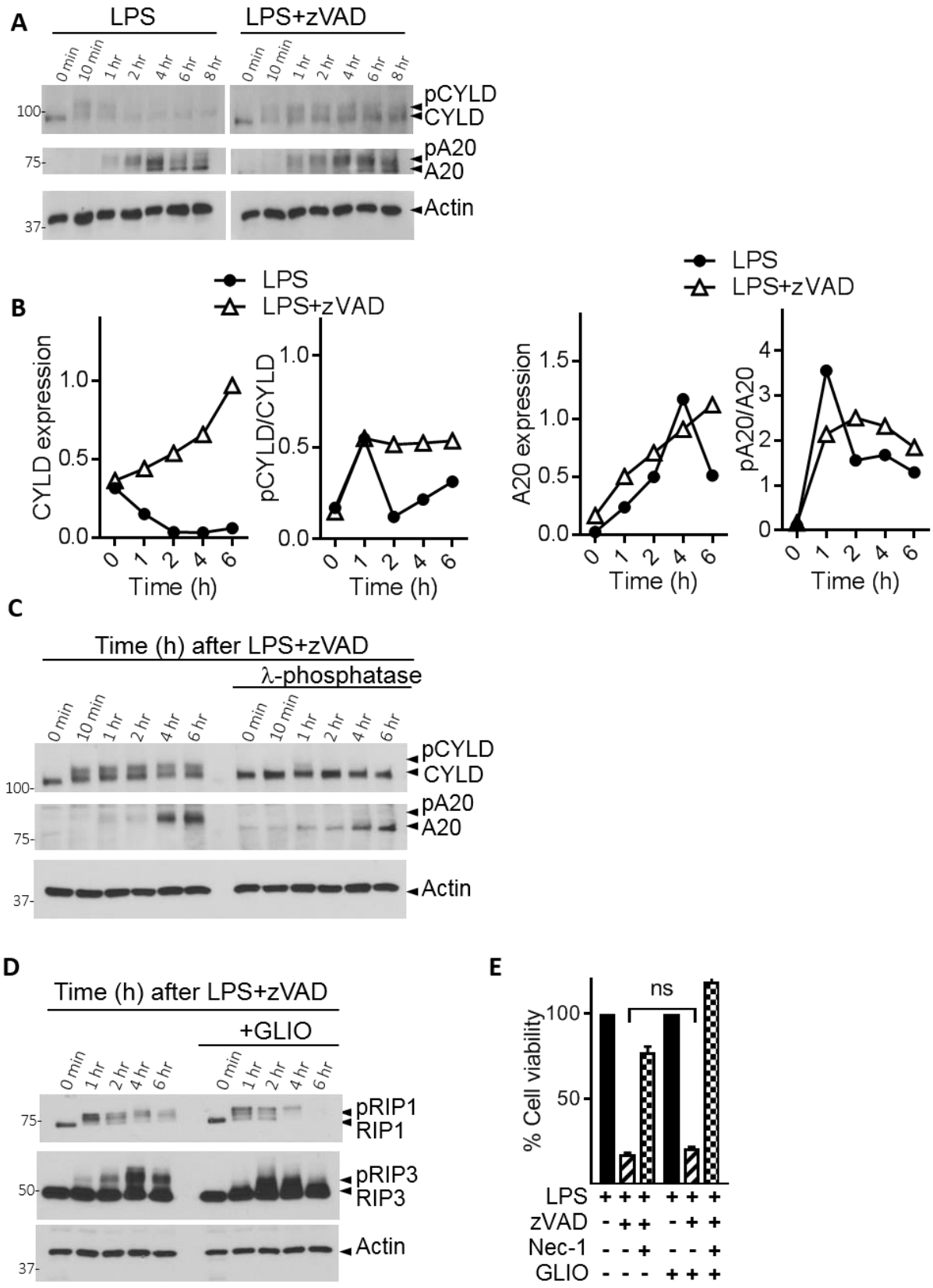
A
LPS
LPS+zVAD
0 min
10 min
1 hr
2 hr
4 hr
6 hr
8 hr
100-
75-
37-
pCYLD
CYLD
pA20
A20
Actin
B
LPS
LPS+zVAD
CYLD expression
pCYLD/CYLD
A20 expression
pA20/A20
Time (h)
C
Time (h) after LPS+zVAD
λ-phosphatase
D
Time (h) after LPS+zVAD
+GLIO
pRIP1
RIP1
pRIP3
RIP3
E
% Cell viability
ns
LPS
zVAD
Nec-1
GLIO

Figure 21: Expression and phosphorylation of CYLD and A20 are up-regulated during necroptosis.

A. BMDMs of WT mice were stimulated with LPS alone or LPS (100ng/mL) + zVAD (50μM) for various time intervals. Expression of CYLD and A20 was evaluated by western blotting followed by densitometric analysis (**B**). Quantified data represent a representative experiment (from three independent experiments). **C.** Cell lysates were treated as described in Methods with or without Lambda phosphatase (500 Units), and the impact on phosphorylation of A20 and CYLD was evaluated by western blotting. **D.** Macrophages were treated with LPS (100ng/mL) + zVAD (50μM) in presence or absence of Gliotoxin (5μM) for various time intervals. Cell extracts were evaluated by western blotting for RipK1 and RipK3 expression**. E.** Cell viability was analyzed after 24 hours for the treatments described in panel D. Graphs show the percentage of viable cells ± SEM relative to cells treated with LPS in the absence of zVAD. Each experiment was repeated in triplicate.

4.1.9. E3 ubiquitin ligase (Triad3a) promotes proteasomal degradation of the necrosome and enhances cell death and production of cytokines

RNF216 (*TRIAD3a*) is an E3 ubiquitin ligase that interacts with TLR, TRIF, and regulates TLR signalling. Because *Trif*-deficient macrophages are protected from degradation, I evaluated whether Triad3a drives the K48 ubiquitination and hence the degradation of the necrosome in macrophages. To achieve this, I performed knockdown of *RNF216* (*TRIAD3a*) in WT BMDMs. Because of the absence of a specific murine anti-Triad3a antibody, I measured the efficiency of knockdown by qRT-PCR (Fig. 22A), which I found to be around 75%. Thereafter, I treated cells with LPS+zVAD for varying time intervals. I found that TRIAD3a knockdown reduced the degradation of RipK1, CASP-8 and FADD. In contrast, cIAP1,2 were still degraded and thus unaffected by Triad3a-knockdown (Fig. 22B). Densitometric analysis revealed that *Triad3a*-knockdown improves the expression of RipK1, CASP-8 and cIAP1,2 (Fig. 22C). These results indicate that TRIAD3A promotes degradation of necrosomal proteins during necrosome signalling. Additionally, there was a noticeable increase in early cell death in cells that were treated with a siRNA against *TRIAD3a* (Fig. 22D). I also collected supernatant after 24 hours of stimulation to measure the impact of *TRIAD3a* knockdown on cytokine expression during necrosome signalling. Knockdown of *Triad3a* resulted in a significant increase in the expression of inflammatory cytokines IL-6, IL-12 and TNFα (Fig. 22E). Collectively, these results demonstrate the interaction of RipK1 and RipK3 leads to Triad3a dependent K48 ubiquitination of the necrosome that acts as a regulatory mechanism to limit cell death and inflammation.

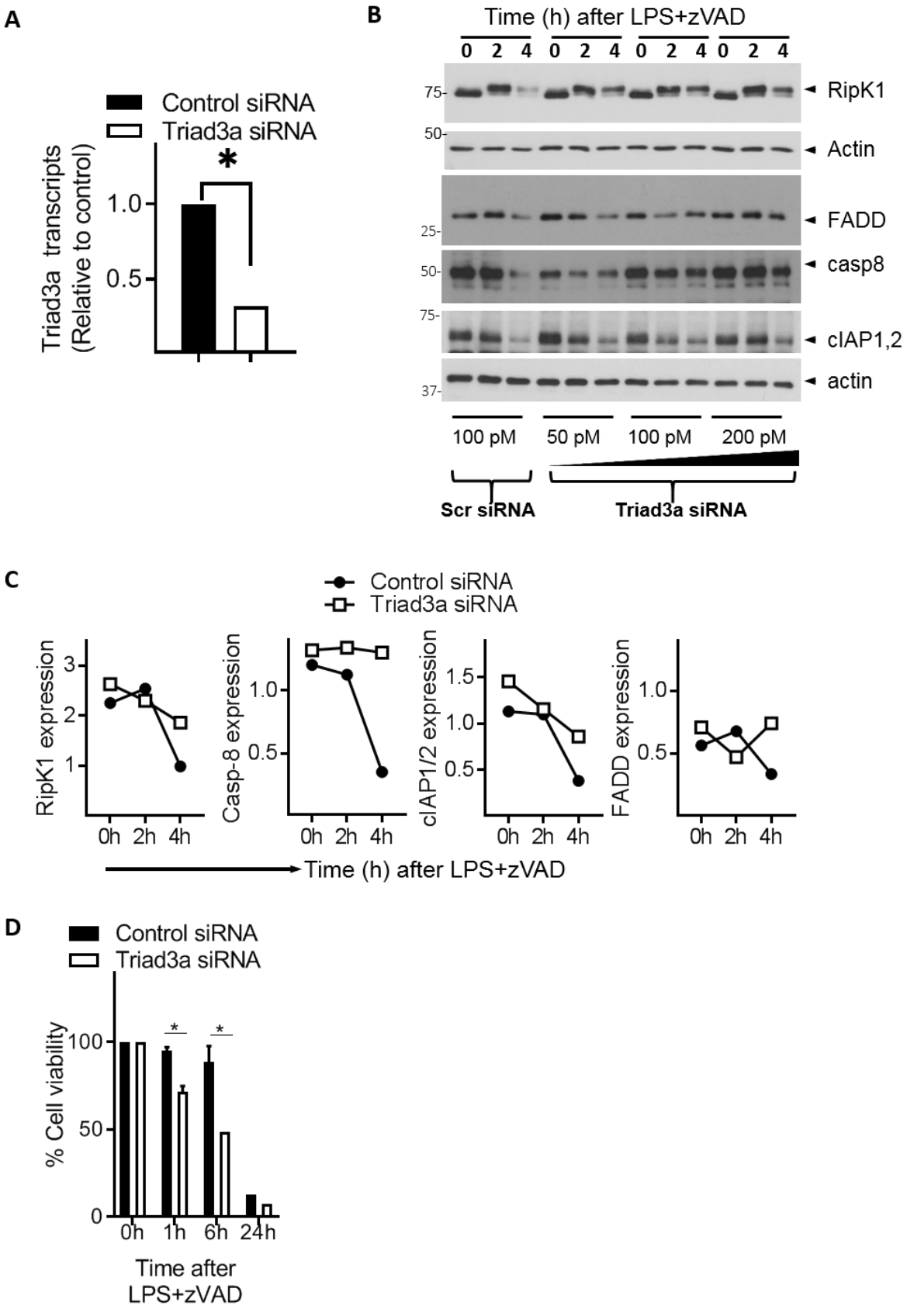
A
Control siRNA
Triad3a siRNA
Triad3a transcripts (Relative to control)
1.0
0.5
*
B
Time (h) after LPS+zVAD
0 2 4 0 2 4 0 2 4 0 2 4
75-
50-
25-
50-
75-
37-
RipK1
Actin
FADD
casp8
cIAP1,2
actin
100 pM
50 pM
100 pM
200 pM
Scr siRNA
Triad3a siRNA
C
Control siRNA
Triad3a siRNA
RipK1 expression
Casp-8 expression
cIAP1/2 expression
FADD expression
0h 2h 4h
Time (h) after LPS+zVAD
D
Control siRNA
Triad3a siRNA
% Cell viability
100
50
0
*
*
0h 1h 6h 24h
Time after LPS+zVAD

E

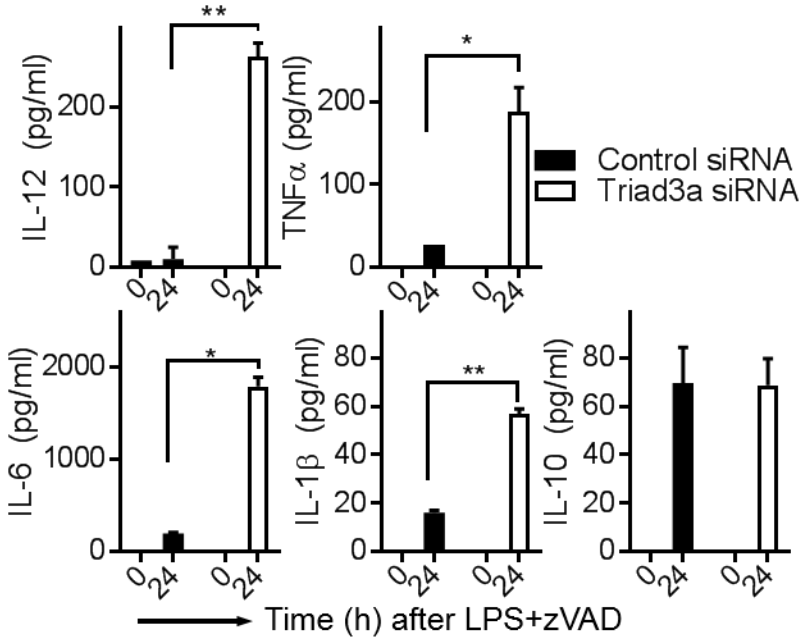
IL-12 (pg/ml)
TNFα (pg/ml)
IL-6 (pg/ml)
IL-1β (pg/ml)
IL-10 (pg/ml)
Control siRNA
Triad3a siRNA
Time (h) after LPS+zVAD

Figure 22: TRIAD3A mediates degradation of RipK1 and its partner proteins during necroptosis.

BMDMs of WT mice were transfected with siRNA against Triad3a (50, 100, or 200 pmol) for 24 hours. Control cells were transfected with scrambled siRNA (100 pmol). **A.** The knockdown efficiency of TRIAD3A was quantified by qRT-PCR. **B.** The transfected cells were treated with LPS (100ng/mL) + zVAD (50μM) for various time intervals and the expression of RipK1, Caspase-8, FADD, and cIAP1,2 were evaluated by western blotting. **C.** Densitometric analysis of representative western blots shown in panel B was performed. **D.** BMDMs were transfected with control or si-RNA against *Triad3a* for 24 hours and cells were washed the next day followed by treatment with LPS (1 ng/ml) + zVAD (50 μM). Cell viability was evaluated at various time intervals post stimulation by MTT assay. **E.** After 24 hours of transfection with scrambled or si-Triad3a, cells were washed and stimulated with LPS (100ng/ml) + zVAD (50μM). Supernatants were collected and cytokines were measured by ELISA. Graphs show the percentage of viable cells ±SEM relative to cells treated with LPS in the absence of zVAD. Each experiment was repeated three times with triplicate samples. *$P < 0.05$, **$P < 0.01$

4.2. Delineation of the mechanisms responsible for necrosome signalling following engagement of type-I interferon receptor (IFNAR)

4.2.1. IFNAR1 signalling promotes LPS-induced necroptosis in macrophages

The current state of knowledge of the regulatory pathways that cause necroptosis following LPS treatment is illustrated in figure 23A. Briefly, when LPS binds to the TLR4 receptor, several adaptor proteins are recruited, for example MYD88 and TRIF. TRIF recruits TRAF3, which in turn associates with TANK, TBK1 and IKKε to mediate downstream signalling. TBK1 and IKKε directly phosphorylate and activate interferon regulatory factor-3 (IRF3), which promotes the transcription of type-I interferons (IFN-I) (Fig. 23A). To explore the role of each adaptor protein involved in necroptosis, I measured their effect on necroptosis in macrophages using cells that were deficient in these pathways. Specifically, *Trif* and *Myd88*-deficient macrophages were generated and treated with LPS, LPS+zVAD and LPS+zVAD+Nec1 for 24 hours, followed by measuring cell viability by MTT assay (Fig. 23B). *Trif*-deficient macrophages were significantly resistant to LPS-induced necroptosis. By comparison, *Myd88*-deficient macrophages were highly susceptible to necroptosis induced by LPS+zVAD treatment (Fig. 23B). It has been shown that the translocation of IRF3 following TRIF activation induces the expression of IFN-β which is secreted and engages with the IFNAR (Fig. 23A). I therefore examined the role of IFNAR1 in necroptosis following TLR4 stimulation. IFNAR1-deficient macrophages were highly resistant to LPS-induced necroptosis relative to WT control (Fig. 23C). To further explore the participation of kinases downstream of the IFNAR1, I evaluated the role of TYK2 and JAK1 that bind to IFNAR1 and IFNAR2 respectively (de Weerd & Nguyen, 2012). TYK2-deficient macrophages were treated as described for *Ifnar1*-deficient cells and viability was evaluated by MTT after 24 hours of stimulation. TYK2-deficient macrophages were resistant to necroptosis induced by LPS+zVAD

treatment (Fig. 23D). After engagement of IFNAR1 by type-I interferon, a trimeric transcriptional complex called ISGF3 complex is formed which consists of IRF9, STAT1 and STAT2. ISGF3 translocates to the nucleus and transcribes numerous genes that harbour an ISRE in their promoter region. I examined the role of IRF9 in response to TLR4 stimulation. WT and IRF9-deficient macrophages were generated and treated with LPS and LPS+zVAD for 24 hours before measuring cell viability. Macrophages lacking IRF9 were resistant to LPS-induced necroptosis (Fig. 23E). These results demonstrate that IFNAR1 signalling is required for the induction of necroptosis in response to LPS stimulation in macrophages.

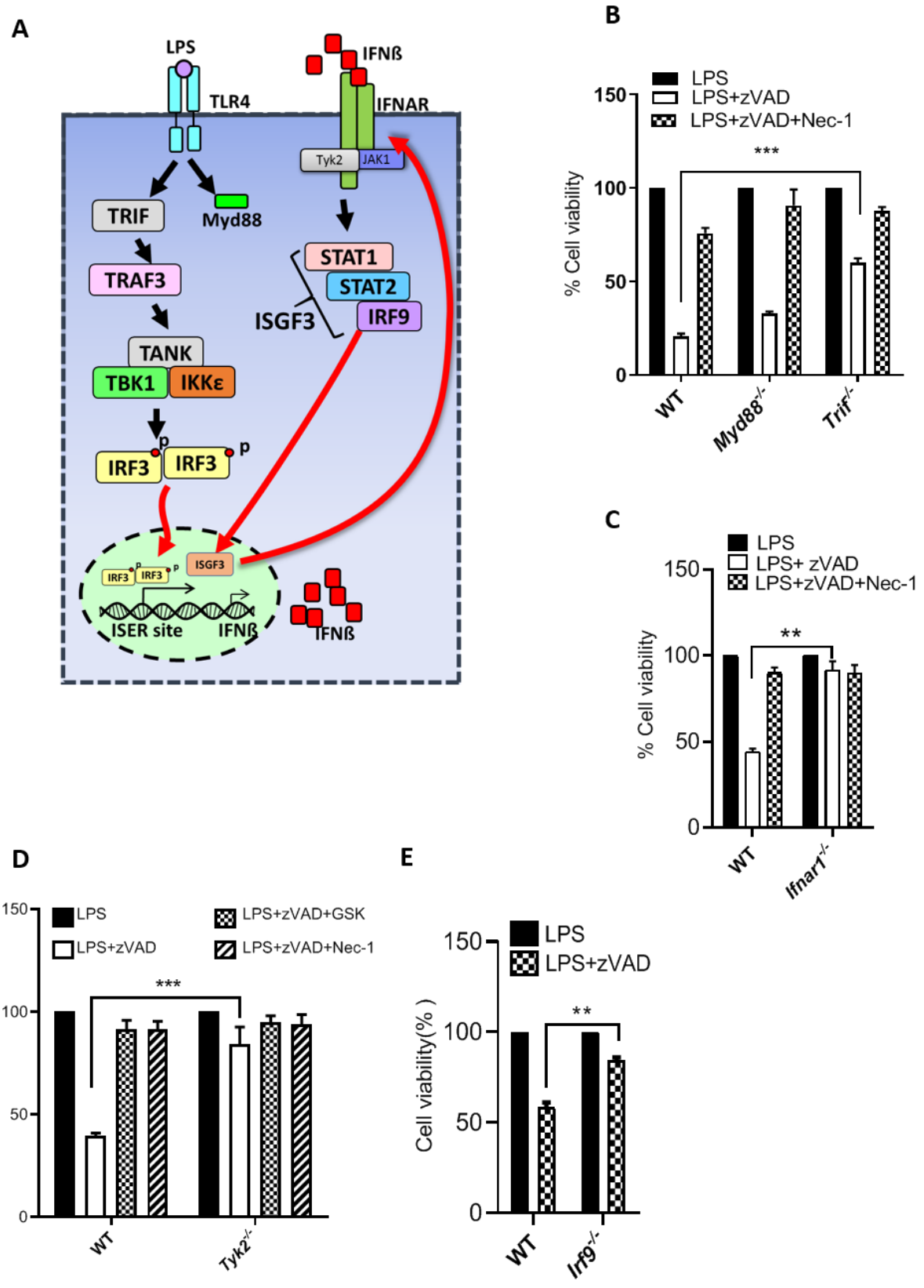
A
LPS
TLR4
IFNß
IFNAR
Tyk2
JAK1
TRIF
Myd88
TRAF3
STAT1
STAT2
ISGF3
IRF9
TANK
TBK1
IKKε
IRF3
IRF3
ISGF3
ISER site
IFNß
B
LPS
LPS+zVAD
LPS+zVAD+Nec-1
% Cell viability
***
WT
Myd88-/-
Trif-/-
C
LPS
LPS+ zVAD
LPS+zVAD+Nec-1
% Cell viability
**
WT
Ifnar1-/-
D
LPS
LPS+zVAD
LPS+zVAD+GSK
LPS+zVAD+Nec-1
% Cell viability
***
WT
Tyk2-/-
E
LPS
LPS+zVAD
Cell viability(%)
**
WT
Irf9-/-

Figure 23: IFNAR1 signalling is required for LPS-dependent necroptosis in macrophages.

A. Diagram illustrates the activation of TLR4 pathways after LPS treatment. WT, *Trif*$^{-/-}$, *Myd88*$^{-/-}$, *Ifinar1*$^{-/-}$, *Tyk2*$^{-/-}$ and *Irf9*$^{-/-}$ BMDMs were generated and treated on day 7 with LPS, LPS+zVAD, and LPS+zVAD+Nec1. Cell death was evaluated 24 hours later by MTT assay **(B-E)**. LPS was used at 100 ng/mL, zVAD at 50 μM, and Necrostatin-1 at 30 μM. Graphs show the percentage of viable cells ±SEM relative to cells treated with LPS in the absence of zVAD. Each experiment was performed in triplicate and repeated three times. (**P<0.001, ***P < 0.001, ****$P < 0.0001$).

I also evaluated the mechanisms responsible for IFN-I-induced necrosome signalling in macrophages. After treatment of cells with IFNβ+zVAD for 24 hours, cell viability was assessed by MTT. *Ifnar1*- and *Tyk2*-deficient macrophages were both resistant to IFN-induced necroptosis (Fig. 24B, C). In addition, I evaluated the effect of blocking JAK1 kinase activity using a specific JAK inhibitor. WT BMDMs were generated and treated with IFNβ, IFNβ+zVAD and IFNβ+zVAD+Nec1, each condition with and without JAK inhibitor for 24 hours., Viability was then determined by MTT assay. Blocking JAK1 pathway rescued macrophages from IFN-induced necroptosis (Fig. 24D). Western blot analysis revealed that the inhibition of JAK1 kinase abolished the phosphorylation of STAT1 at serine 727 (McComb et al., 2014) in response to IFNβ+zVAD treatment (Fig. 24E). Overall, these results indicate that TYK2 and JAK1 are required for IFN-induced necroptosis in macrophages. *Irf-9*-deficient macrophages were significantly resistant to IFNβ+zVAD induced necroptosis (Fig. 24F), which was similar to the result obtained in *Ifnar1*-deficient macrophages (Fig. 24B). Overall, these results (Figs. 23 and 24) demonstrate that the IFNAR1 and their downstream proteins promote necroptotic cell death in macrophages.

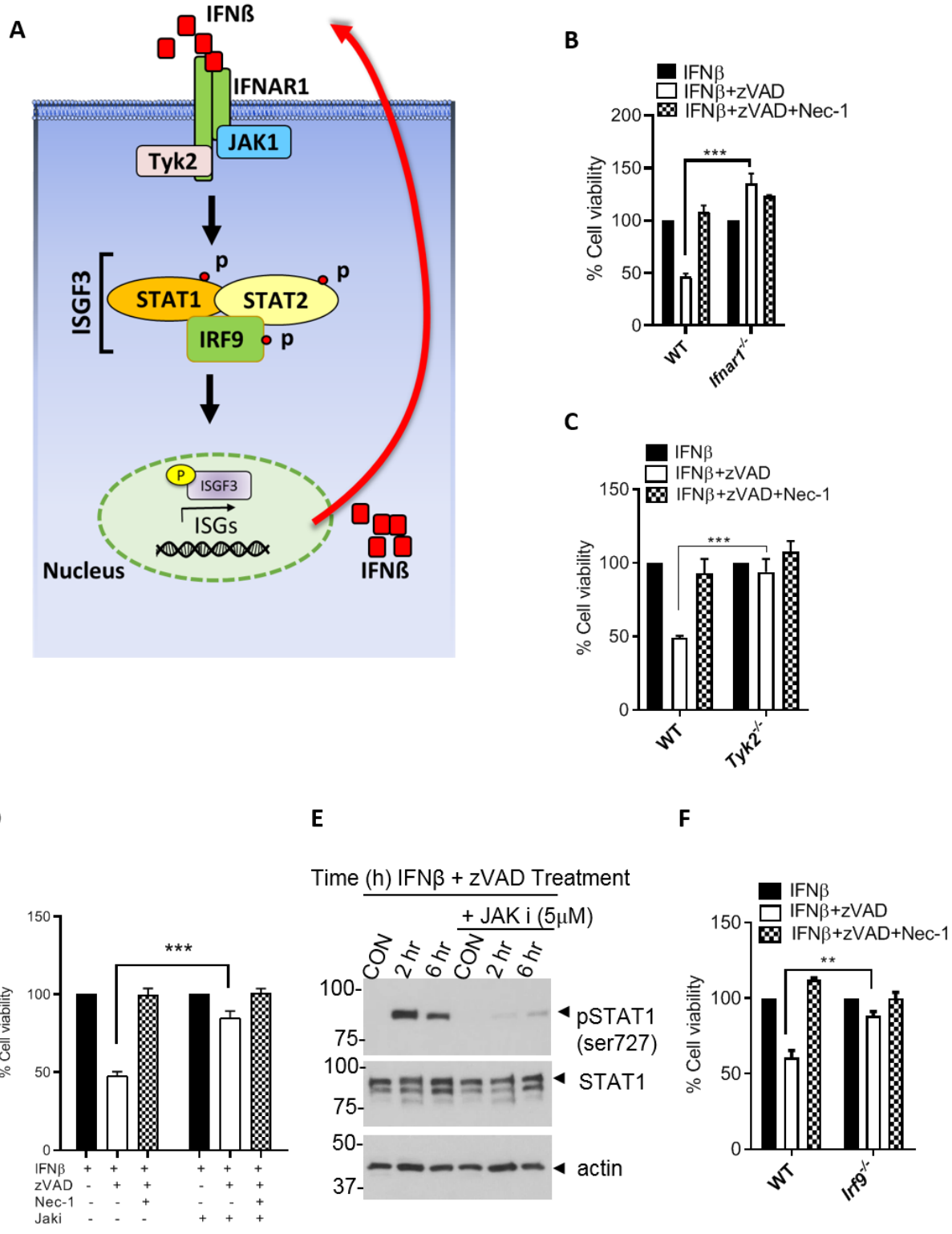
A
IFNß
IFNAR1
JAK1
Tyk2
ISGF3
p
STAT1
STAT2
IRF9
P
ISGF3
ISGs
Nucleus
IFNß
B
IFNβ
IFNβ+zVAD
IFNβ+zVAD+Nec-1
% Cell viability
***
WT
Ifnar1-/-
C
IFNβ
IFNβ+zVAD
IFNβ+zVAD+Nec-1
% Cell viability
***
WT
Tyk2-/-
D
% Cell viability
***
IFNβ
zVAD
Nec-1
Jaki
E
Time (h) IFNβ + zVAD Treatment
+ JAK i (5μM)
CON
2 hr
6 hr
CON
2 hr
6 hr
pSTAT1 (ser727)
STAT1
actin
F
IFNβ
IFNβ+zVAD
IFNβ+zVAD+Nec-1
% Cell viability
**
WT
Irf9-/-

Figure 24. TYK2 is required for necroptosis of macrophages.

A. Diagram illustrates IFN signalling following IFNβ treatment. WT, *Ifinar1*$^{-/-}$, *Tyk2*$^{-/-}$ and *Irf9*$^{-/-}$ macrophages were treated on day 7 with IFNβ, IFNβ +zVAD, and IFNβ +zVAD+Nec1 for 24 hours. Cell viability was measured by MTT assay **(B, C, D, F)**. IFNβ was used at a concentration of 1000 U/mL, zVAD at 50 μM, and Necrostatin-1 at 30 μM. **D.** JAK1 inhibitor was used at a concentration of 5 μM in cell death assay. **E.** WT BMDMs were treated with IFNβ (1000 U/mL) + zVAD (50 μM), with or without JAK inhibitor (10 μM) for various time intervals. Cell lysates were collected, and expression of various proteins tested by western blotting. Graphs show the percentage of viable cells ±SEM relative to cells treated with IFNβ in the absence of zVAD. Each experiment was performed in triplicate and repeated three times. (**P<0.001, ***P < 0.001, ****$P < 0.0001$).

Induction of necroptosis by IFNβ treatment required the addition of high concentration (50 μM) of the pan-caspase inhibitor zVAD (Fig. 25A). I evaluated the kinetics of cell death at 6-, 8-, 12-, and 24 hours post-stimulation of cells with IFNβ+zVAD and observed that detectable cell death was observed even at 6h post-stimulation (Fig. 25B). I then measured the activation of various proteins involved in necroptosis such as RipK1, RipK3 and MLKL. Cells were treated with IFNβ+zVAD and cell lysates were collected to evaluate the phosphorylation of RipK1 and RipK3 (Fig. 25C). IFN-induced necroptosis resulted in early phosphorylation of RipK1 at 1 hour but the phosphorylation of RipK3 was detected later at 6 and 8 hours. This response is unlike LPS-induced necroptosis, where the phosphorylation of RipK3 was detected at 2-4 hours. It is unclear how IFN-β signalling pathway recruits and induces the phosphorylation of RipK1. RipK3 phosphorylation leads to the phosphorylation and activation of the effector pseudokinase mixed lineage kinase domain-like protein (MLKL). I examined MLKL trimerization, wherein WT BMDMs were treated with IFNβ and IFNβ+zVAD for various time intervals (Fig. 25D). Western blotting showed that the oligomerization of MLKL occurred at 6 hours post-stimulation, combined with the reduction in the level of the monomeric form of MLKL (Fig. 25D). Densitometric analysis was performed and revealed the formation of the trimeric MLKL in IFN-induced necroptosis over time (Fig. 25E).

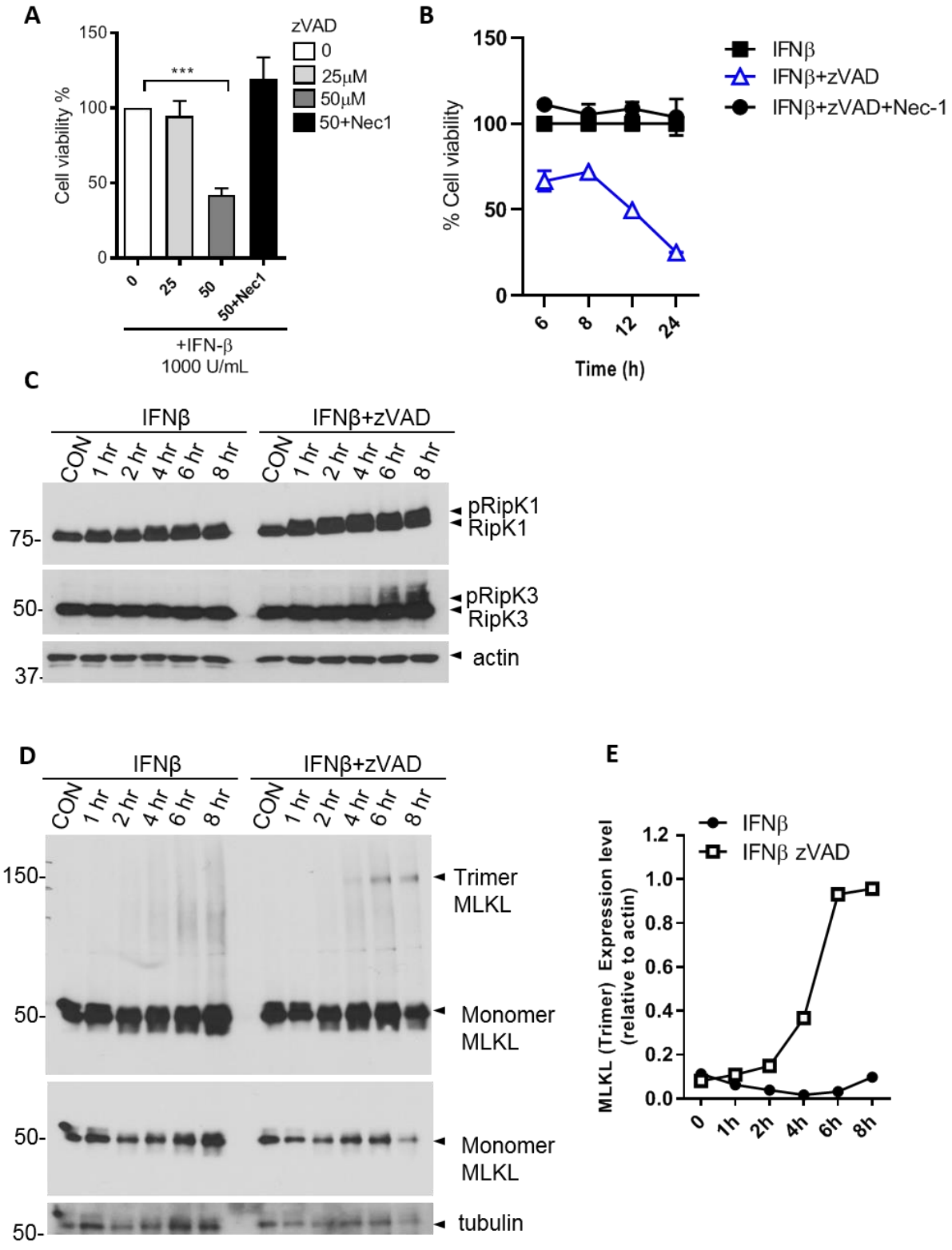
A
Cell viability %
150
100
50
0
***
zVAD
0
25μM
50μM
50+Nec1
0
25
50
50+Nec1
+IFN-β
1000 U/mL
B
% Cell viability
150
100
50
0
6
8
12
24
Time (h)
IFNβ
IFNβ+zVAD
IFNβ+zVAD+Nec-1
C
IFNβ
IFNβ+zVAD
CON
1 hr
2 hr
4 hr
6 hr
8 hr
75-
50-
37-
pRipK1
RipK1
pRipK3
RipK3
actin
D
IFNβ
IFNβ+zVAD
CON
1 hr
2 hr
4 hr
6 hr
8 hr
150-
50-
50-
50-
Trimer
MLKL
Monomer
MLKL
Monomer
MLKL
tubulin
E
MLKL (Trimer) Expression level
(relative to actin)
1.2
1.0
0.8
0.6
0.4
0.2
0.0
0
1h
2h
4h
6h
8h
IFNβ
IFNβ zVAD

Figure 25. IFN-β induces necrosome signalling in macrophages.

WT BMDMs were generated and treated on day 7 with IFNβ (1000 U/mL) + zVAD (25-50 μM) + Necrostatin-1 (30 μM). **A+B**, Cell viability was evaluated by MTT after 24 hours **(A)** and at 6-,8-,12-, and 24 hours **(B)**. **C+D**, Cells were treated with IFNβ (1000 U/mL) with and without zVAD (50 μM) for various time intervals. Cell lysates were collected, and activation of various proteins evaluated by western blotting. **E.** Densitometric analysis of the trimeric form of MLKL. Densitometric data represent a representative experiment (from three independent experiments). Graphs show the percentage of viable cells ±SEM relative to cells treated with IFNβ in the absence of zVAD. Each experiment was performed in triplicate and repeated three times. (***$P < 0.001$).

4.2.2. IFNAR1 signalling is essential for TNF-induced necroptosis in macrophages

TNFα is a critical cytokine that plays a role in cell signalling, systematic inflammation and cell death. In fibroblasts, TNFα, in the absence of caspase signalling has been shown to drive necroptosis (Vercammen et al., 1998). Having observed that necroptosis of macrophages is compromised in the absence of IFNAR1, I tested whether TNFα can induce necroptosis in BMDMs lacking the IFNAR1 and TYK2. WT, *Ifnar1*- and *Tyk2*-deficient macrophages were generated and treated with TNFα, TNFα+zVAD and TNFα+zVAD+Nec1 or GSK-872 for 24 hours. Cell viability was measured at 24 hours post-stimulation by MTT (Fig. 26A, B) and by Zombie Yellow™ staining (Fig. 26C). Both *Ifnar1*- and *Tyk2*-deficient macrophages displayed significant protection against necroptosis induced by TNFα+zVAD (Fig. 26A, B). This result indicates that IFNAR1 signalling is the predominant pathway required for necroptosis in macrophages.

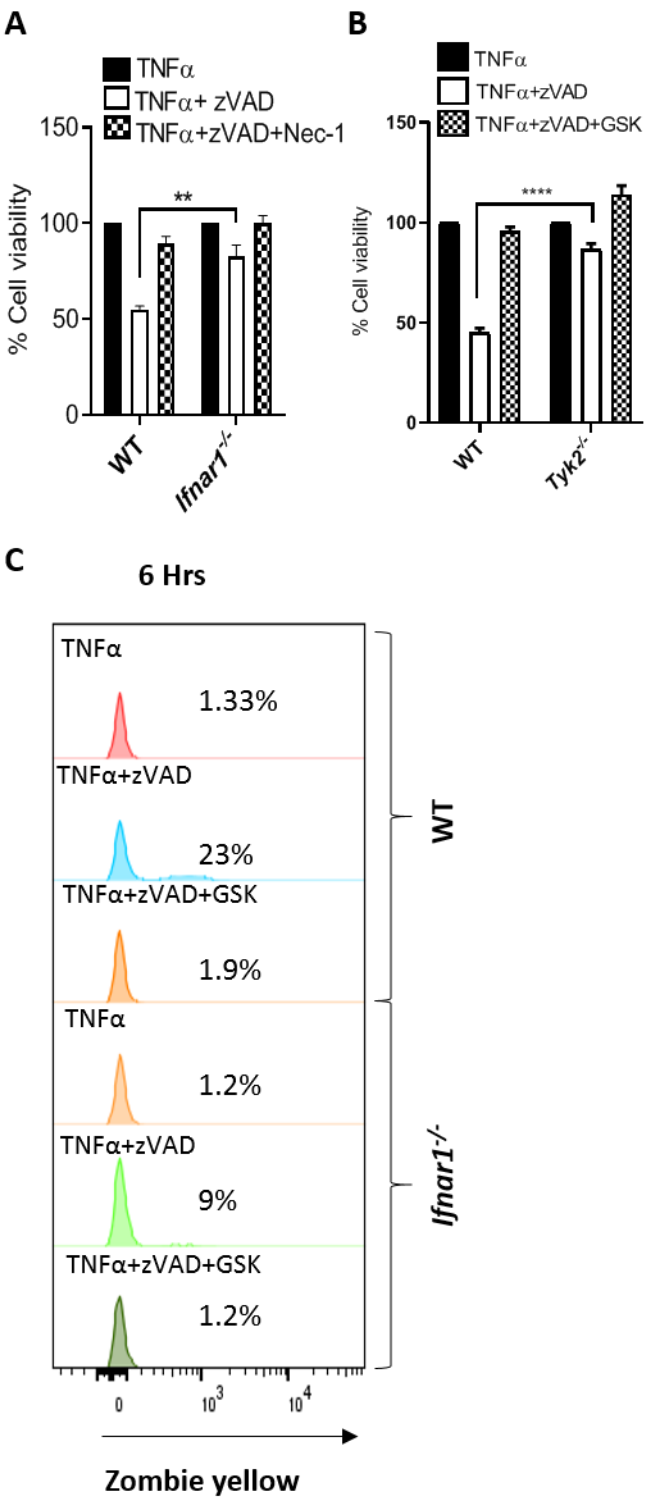
A
TNFα
TNFα+ zVAD
TNFα+zVAD+Nec-1
% Cell viability
150
100
50
0
**
WT
Ifnar1-/-
B
TNFα
TNFα+zVAD
TNFα+zVAD+GSK
% Cell viability
150
100
50
0
****
WT
Tyk2-/-
C
6 Hrs
TNFα
1.33%
TNFα+zVAD
23%
TNFα+zVAD+GSK
1.9%
TNFα
1.2%
TNFα+zVAD
9%
TNFα+zVAD+GSK
1.2%
WT
Ifnar1-/-
0
10^3
10^4
Zombie yellow

Figure 26. TNF-induced necroptosis is dependent on IFNAR1 signalling.

WT, *Ifnar1*$^{-/-}$ and *Tyk2*$^{-/-}$ macrophages were treated on day 7 with TNFα, TNFα +zVAD, and TNFα +zVAD+Nec1 or GSK872 for 24 hours before measuring cell viability by MTT assay **(A+B)**. TNFα was used at a concentration of 50 ng/mL, zVAD was used at 50 μM, Necrostatin-1 was used at 30 μM, and GSK872 was at a concentration of 5 μM. **C.** Cell viability was examined with Zombie Yellow™ staining 6 hours post stimulation. Graphs show the percentage of viable cells ±SEM relative to cells treated with TNFα in the absence of zVAD. Each experiment was performed in triplicate and repeated three times. (**P<0.001, ***P < 0.001, ****$P < 0.0001$).

4.2.3. IKKε and TBK1 restrict necroptosis in macrophages

Interferon regulatory factors IRF3 and IRF7 are transcription factors that promote expression of IFNβ. McComb and colleagues (2014) demonstrated that IRF3 and IRF7 promote necroptosis in macrophages. Downstream of TRIF, IKKε and TBK1 kinases promote activation of IRF3. In addition, it has been shown by Tenoever et al. (2007), that IKKε phosphorylates STAT1 on serine 708, enhancing the formation of STAT1-STAT2 heterodimers and possibly ISGF3 (tenOever et al., 2007). To investigate the role of IKKε in necroptosis, WT and *Ikkε*-deficient macrophage cells were generated and treated with LPS+zVAD, TNFα+zVAD, and IFNβ+zVAD for 24 hours followed by measuring cell viability by MTT assay (Fig. 27A-C). Interestingly, rather than being resistant, *Ikkε* -deficient macrophages revealed slightly more sensitivity to LPS, TNFα, and IFNβ-induced necroptosis compared to WT control (Fig. 27A-C). I also examined the cell viability of WT BMDMs that were treated with or without a TBK1 inhibitor (Fig. 27D). This inhibition of TBK1 resulted in a significant increase in the sensitivity of macrophages to LPS+zVAD treatment (Fig. 27D). Additionally, I examined the cell viability of *Ikkε* -deficient macrophages after TBK1 inhibition. After 24 hours, viability was assessed by MTT assay and it showed that inhibition of TBK1/IKKε induced significant increase of cell death by necroptosis (Fig. 27E). These results suggest that IKKε and TBK1 play an inhibitory role in necroptosis of macrophages.

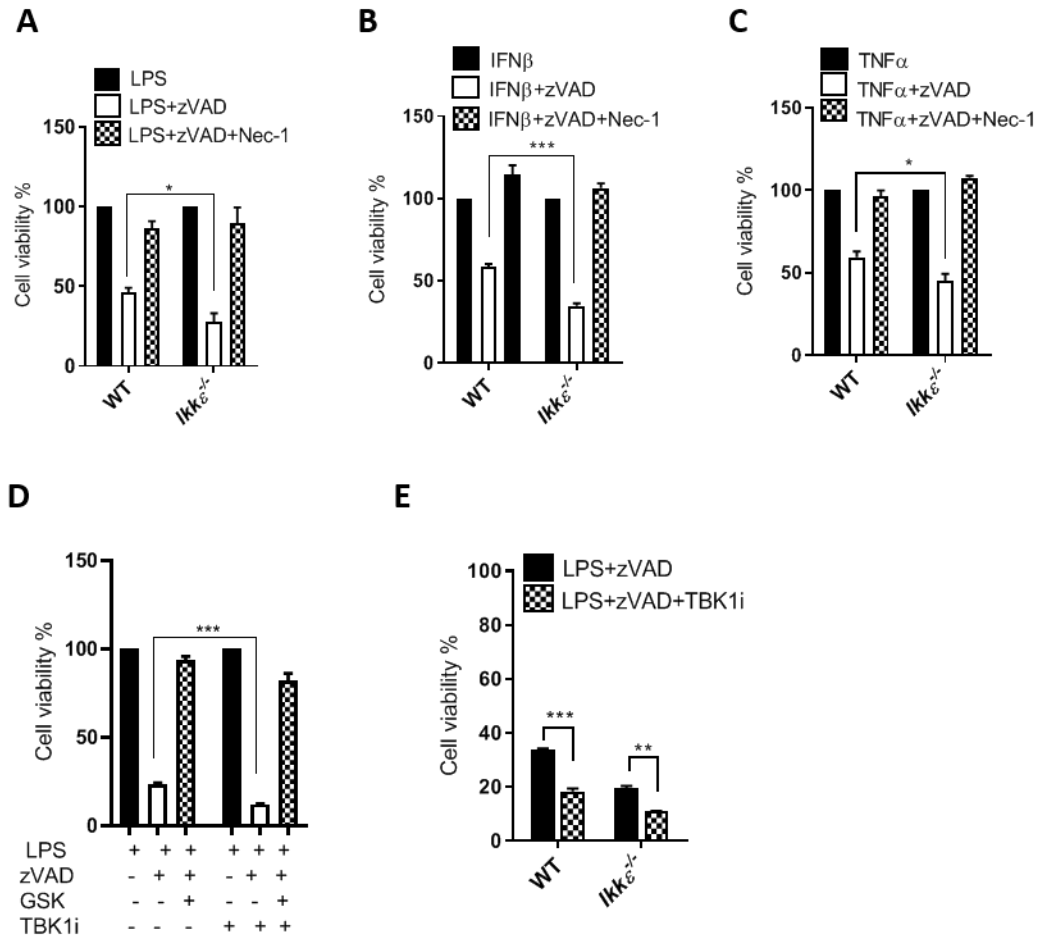
A
LPS
LPS+zVAD
LPS+zVAD+Nec-1
Cell viability %
150
100
50
0
*
WT
Ikkε-/-
B
IFNβ
IFNβ+zVAD
IFNβ+zVAD+Nec-1
Cell viability %
150
100
50
0
***
WT
Ikkε-/-
C
TNFα
TNFα+zVAD
TNFα+zVAD+Nec-1
Cell viability %
150
100
50
0
*
WT
Ikkε-/-
D
Cell viability %
150
100
50
0
***
LPS + + + + + +
zVAD - + + - + +
GSK - - + - - +
TBK1i - - - + + +
E
LPS+zVAD
LPS+zVAD+TBK1i
Cell viability %
100
80
60
40
20
0
***
**
WT
Ikkε-/-

Figure 27. IKKε and TBK1 restrict necroptosis in macrophages.

(A-C) WT and *Ikkε*$^{-/-}$ BMDMs were generated and treated on day 7 with LPS+zVAD, TNFα+zVAD or IFNβ+zVAD, with or without Necrostatin-1, for 24 hours before measuring cell viability by MTT assay. LPS concentration used in the experiments was 100 ng/mL, TNFα was used at 50 ng/mL, zVAD was at 50 μM, and Necrostatin-1 was 30 μM. **D.** WT cells were treated with LPS+zVAD+GSK with and without TBK1 inhibitor (TBK1i, 250 μM) for 24 hours followed by measuring cell viability by MTT assay. **E.** WT and *IKKε*$^{-/-}$BMDMs were treated with LPS+zVAD and LPS+zVAD+TBK1i for 24 hours before measuring cell viability by MTT assay. Graphs show the percentage of viable cells ±SEM relative to control. Each experiment was performed in triplicate and repeated three times. (*P<0.01, **P<0.001, ***P < 0.001, ****$P < 0.0001$).

4.2.4. TNFR2 signalling promotes LPS-induced necroptosis in macrophages

Engagement of TLR4 leads to the expression of many cytokines, and TNFα is one of them. To test whether TNFR1 or TNFR2 has a role in LPS-induced necroptosis of macrophages, *Tnfr1*- and *Tnfr2*-deficient macrophages were generated and treated with LPS+zVAD for 24 hours. Cell viability was measured by MTT assay (Fig. 28A). A significant rescue from LPS-induced necroptosis was observed in *Tnfr2*-deficient macrophages. This result suggests that TNFR2 promotes LPS-induced necroptosis (Fig. 28A). Since LPS stimulation also induces the expression of type-I interferon and my previous results indicate that IFNAR1 signalling promotes necroptosis, I evaluated whether IFNAR1-signalling promotes the expression of TNFR2. Therefore, I investigated whether TNFR2 expression is impaired in IFNAR knockout cells. WT, *Ifnar1*-, *Tnfr1*-, and *Tnfr2*- BMDMs were generated and the cell surface expression of the TNFR2 receptor was measured (Fig. 28B, C). My results indicate that IFNAR1-signalling does not have any impact on the expression of TNFR2 in macrophages (Fig. 28B). Furthermore, I did not observe any increase in the expression of TNFR2 after stimulation by LPS or LPS+zVAD. In agreement with these flow cytometry results, western blotting confirmed that the expression of TNFR2 was not impacted by cell stimulation or the expression of IFNAR1 (Fig. 28D). These results demonstrate that the resistance to necroptosis in IFNAR1-deficient macrophages is not due to a change in TNFR2 expression.

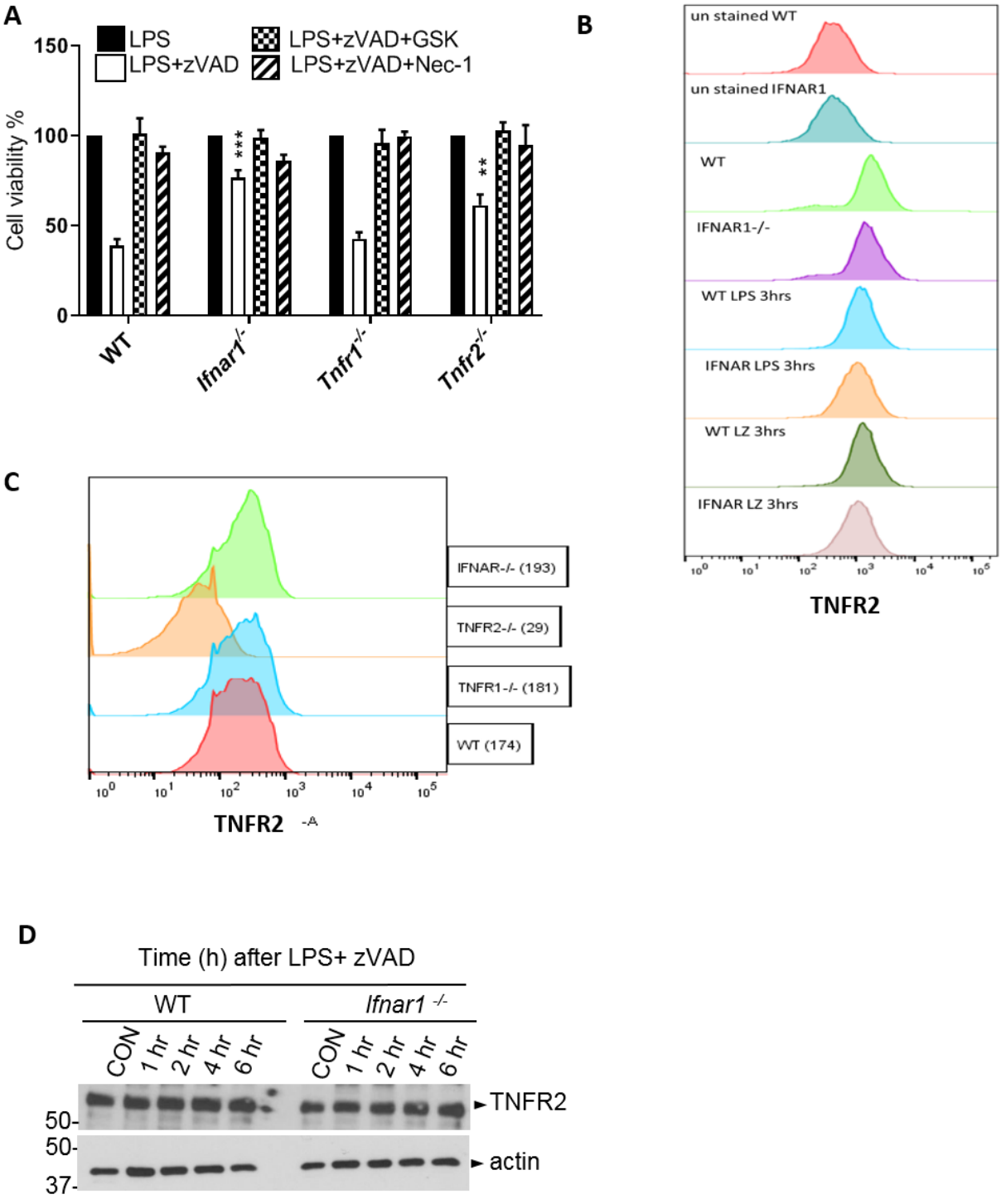
A
LPS
LPS+zVAD
LPS+zVAD+GSK
LPS+zVAD+Nec-1
Cell viability %
150
100
50
0
***
**
WT
Ifnar1-/-
Tnfr1-/-
Tnfr2-/-
B
un stained WT
un stained IFNAR1
WT
IFNAR1-/-
WT LPS 3hrs
IFNAR LPS 3hrs
WT LZ 3hrs
IFNAR LZ 3hrs
TNFR2
C
IFNAR-/- (193)
TNFR2-/- (29)
TNFR1-/- (181)
WT (174)
TNFR2 -A
D
Time (h) after LPS+ zVAD
WT
Ifnar1 -/-
CON
1 hr
2 hr
4 hr
6 hr
50-
50-
37-
TNFR2
actin

Figure 28. TNFR2 receptor signalling promotes necroptosis following TLR4 activation.

A. WT, *Ifnar1*$^{-/-}$, *Tnfr1*$^{-/-}$ and *Tnfr2*$^{-/-}$ BMDMs were generated and treated on day 7 with LPS, LPS+zVAD, LPS+zVAD+Nec1 and LPS+zVAD+GSK for 24 hours followed by measuring cell viability by MTT assay. **B.** WT and *Ifnar1*$^{-/-}$BMDMs were generated and treated as in (A), followed by staining with labelled anti-TNFR2antibody. **C.** Expression of TNFR2 was evaluated in WT, *Ifnar1*$^{-/-}$, *Tnfr1*$^{-/-}$ and *Tnfr2*$^{-/-}$ BMDMs by incubating cells with labelled anti-TNFR2 antibodies. Drug concentrations used: LPS, 100 ng/mL; zVAD, 50 μM; Necrostatin-1, 30 μM; and GSK872, 5 μM. D. WT and *Ifnar1*$^{-/-}$, BMDMs were treated with LPS+zVAD for various time intervals. Cell lysates were collected and the expression of TNFR2 evaluated by western blotting. Graphs show the percentage of viable cells ±SEM relative to cells treated with LPS in the absence of zVAD. Each experiment was performed in triplicate and repeated three times. (**P<0.001, ***P < 0.001).

4.2.5. IFNAR1 signalling promotes the phosphorylation of RipK3

It has been shown that *Ifnar1*-deficient macrophages have a significant survival advantage, regardless of the necroptotic signalling pathway initiated (Figs. 23D, 24B, and 25A) (McComb et al., 2014). I evaluated the phosphorylation of various signalling proteins that have been reported to be important in necroptotic pathway such as RipK1, RipK3, CASP-8. WT and *Ifnar1*-deficient macrophages were treated with LPS+zVAD and the expression of various proteins was evaluated by western blotting (Fig. 29A). I observed that the phosphorylation of RipK3 (upper band) was significantly compromised in *Ifnar1*-deficient cells in comparison to WT controls (Fig. 29A), suggesting that IFN-signalling is required to sustain RipK3 kinase activity. In contrast, there was no significant difference in the expression or total phosphorylation of RipK1 (Fig. 29A).

In addition, I noticed that while the expression of the deubiquitinase CYLD was similar in WT and *Ifnar1*-deficient macrophages, the expression of A20, which has both ubiquitin ligase and deubiquitinase activity was significantly enhanced in *Ifnar1*-deficient macrophages in comparison to WT controls (Fig. 29A). In addition to these changes, STAT1 expression and phosphorylation at tyrosine-701 and serine-727 were reduced in *Ifnar1*-deficient macrophages as expected (Fig 29A). In contrast, I noticed there was no impairment in the expression of FADD and CASP-8 expression in *Ifnar1*-deficient cells (Fig 29A). In the same batch of cells, we also measured cell viability following LPS+zVAD treatment and observed that *Ifnar1*-deficient macrophages were highly resistant to necroptosis (Fig. 29B).

It has been recently shown that $p38^{MAPK}$ signalling induces inhibitory phosphorylation on RipK1 (Jaco et al., 2017) and it is more likely that the phosphorylation of RipK1 that we observed in Fig. 29A measures the inhibitory phosphorylation or RipK1 since it was obliterated by inhibition of $p38^{MAPK}$ (Fig. 12). Thus, our results indicate that this inhibitory phosphorylation of RipK1 is

similar in WT and *Ifnar1*-deficient macrophages (Fig. 29A). Recently, an antibody against Ripk1 has become available which measures the phosphorylation at serine 166, and this phosphorylation of RipK1 correlates to necroptosis (Jaco et al., 2017). I evaluated serine-166 phosphorylation of RipK1 upon LPS+zVAD stimulation and observed that this phosphorylation was similar in WT and *Ifnar1*-deficient macrophages (Fig. 30A). To quantify RipK1 phosphorylation at serine-166 in WT and *Ifnar1*-deficient macrophages, densitometric analysis was performed. These results showed that the phosphorylation of RipK1 was not compromised in *Ifnar1*-deficient macrophages (Fig. 30B), indicating that IFN-signalling is not required for RipK1 phosphorylation.

I also measured the mRNA expression of IRF9, CASP-8 and RipK1 by performing qRT-PCR analysis of WT and *Ifnar1*-deficient cells. I treated WT and *Ifnar1*-deficient macrophages with LPS+zVAD and collected RNA at 6 hours post-stimulation I found that while the necroptotic stimulation induced IRF9 expression in WT cells, this was compromised in *Ifnar1*-deficient cells (Fig. 31A), CASP-8 transcript was also examined and was slightly reduced upon stimulation in *Ifnar1*-deficient macrophages relative to WT controls (Fig. 31B). Notably, this result differs from the corresponding protein expression I observed by western blotting (Fig. 29A), wherein a difference between WT and *Ifnar1*-deficient cells was not detected. Lastly, no significant differences were observed in RipK1 transcription following LPS+zVAD treatment between WT and *Ifnar1*-deficient macrophages (Fig. 31C).

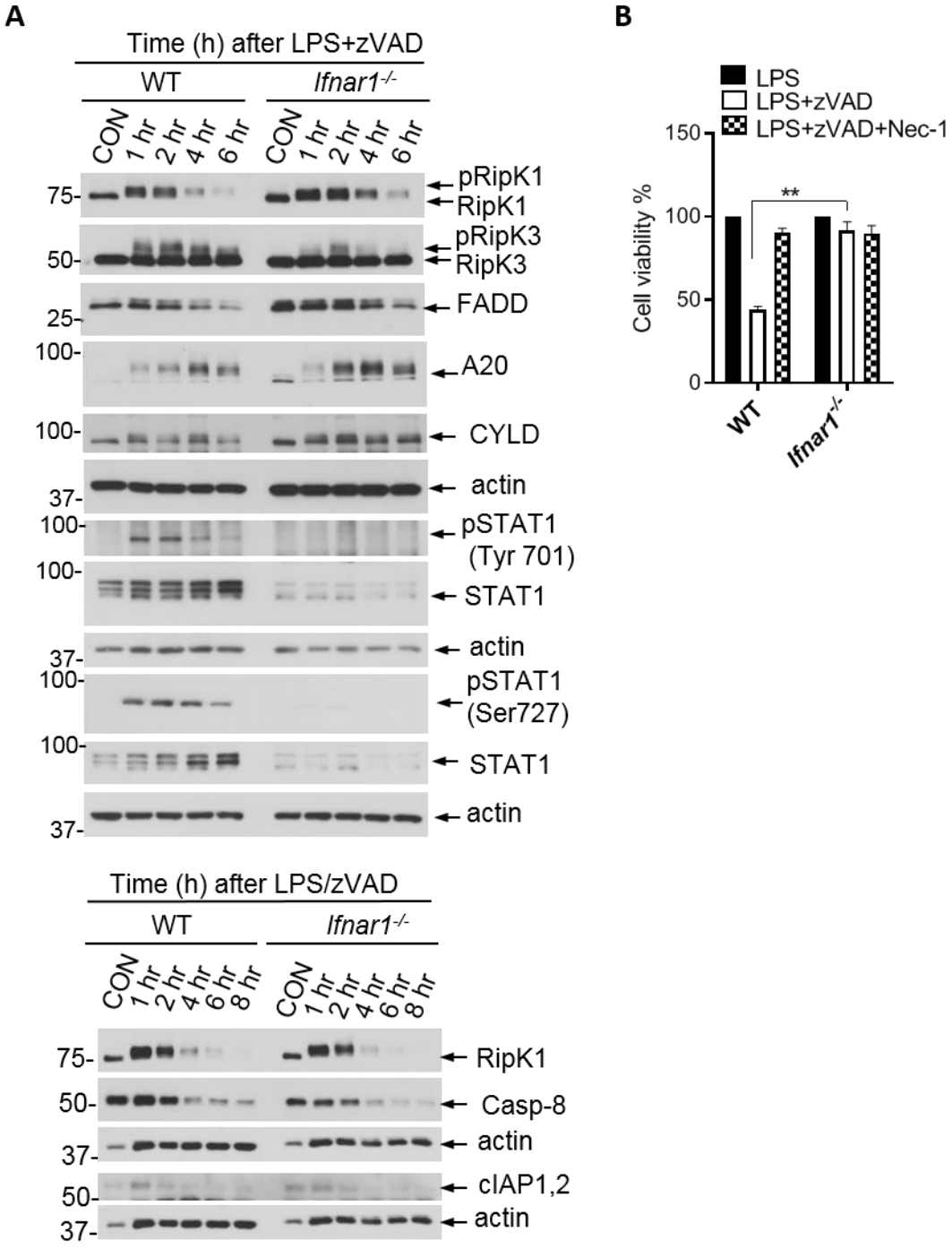
A
Time (h) after LPS+zVAD
WT
Ifnar1-/-
CON
1 hr
2 hr
4 hr
6 hr
pRipK1
RipK1
pRipK3
RipK3
FADD
A20
CYLD
actin
pSTAT1
(Tyr 701)
STAT1
pSTAT1
(Ser727)
Time (h) after LPS/zVAD
8 hr
RipK1
Casp-8
cIAP1,2
B
LPS
LPS+zVAD
LPS+zVAD+Nec-1
Cell viability %
**

Figure 29. IFNAR1 signalling promotes phosphorylation of RipK3.

A. WT and *Ifnar1*$^{-/-}$ BMDMs were generated and treated on day 7 with LPS+zVAD for various time intervals followed by western blotting for expression of various proteins. **B.** The same sets of cells were treated with LPS, LPS+zVAD, LPS+zVAD+Nec1 and LPS+zVAD+GSK for 24 hours followed by measuring cell viability by MTT assay. Concentrations used were as follows: LPS, 100 ng/mL; zVAD, 50 μM; and Necrostatin-1, 30 μM. Graphs show the percentage of viable cells ±SEM relative to cells treated with LPS in the absence of zVAD. Each experiment was performed in triplicate and repeated three times. (**P<0.001, ***P < 0.001).

A

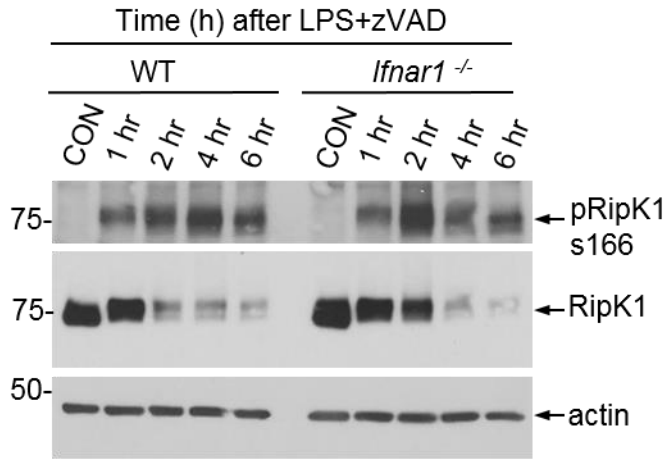
Time (h) after LPS+zVAD
WT
Ifnar1 -/-
CON
1 hr
2 hr
4 hr
6 hr
CON
1 hr
2 hr
4 hr
6 hr
75-
pRipK1
s166
75-
RipK1
50-
actin

B

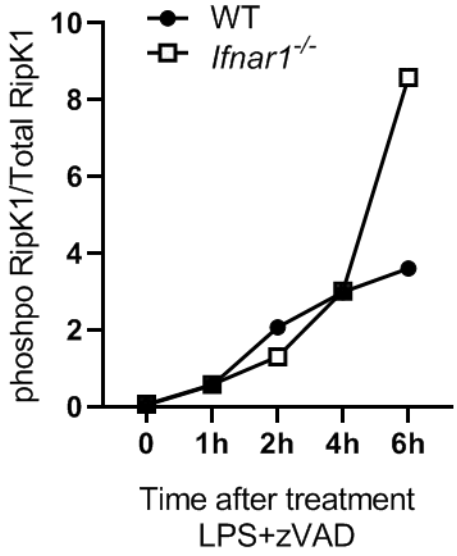
WT
Ifnar1-/-
phoshpo RipK1/Total RipK1
10
8
6
4
2
0
0
1h
2h
4h
6h
Time after treatment
LPS+zVAD

Figure 30. IFNAR1 signalling is not required for phosphorylation of RipK1 at Serine 166.

A.WT and *Ifnar1*$^{-/-}$BMDMs were generated and treated with LPS (100ng/mL) + zVAD (50μM) for various time intervals. Lysates were collected and the expression of total and phosphorylated RipK1 evaluated by western blotting. **B.** Quantification of western blot data (A) was done for total RipK1 and phospho-RipK1 (S166). Densitometric data represent a representative experiment (from three independent experiments).

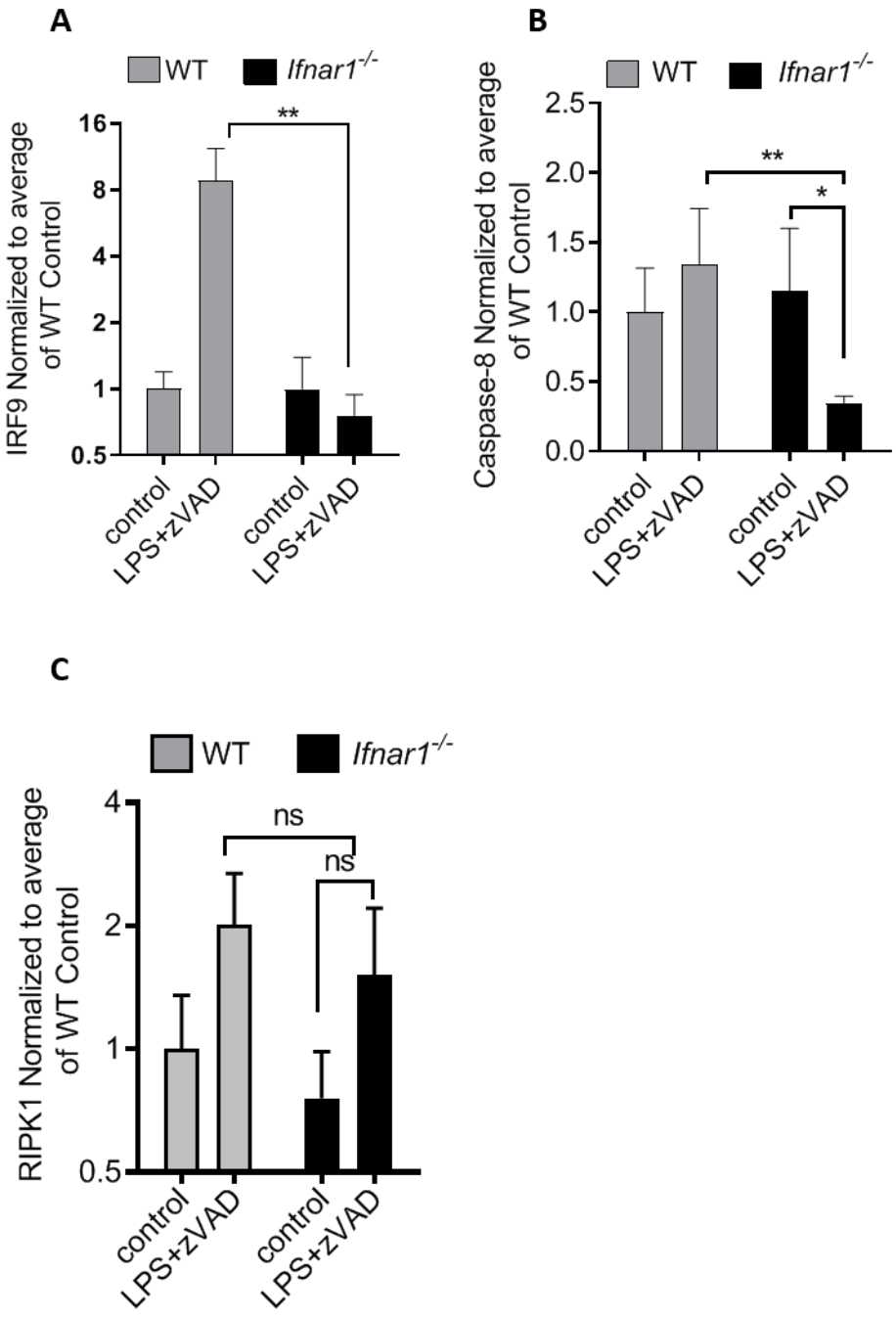
A
WT
Ifnar1-/-
IRF9 Normalized to average of WT Control
16
8
4
2
1
0.5
**
control
LPS+zVAD
control
LPS+zVAD
B
WT
Ifnar1-/-
Caspase-8 Normalized to average of WT Control
2.5
2.0
1.5
1.0
0.5
0.0
**
*
control
LPS+zVAD
control
LPS+zVAD
C
WT
Ifnar1-/-
RIPK1 Normalized to average of WT Control
4
2
1
0.5
ns
ns
control
LPS+zVAD
control
LPS+zVAD

Figure 31. IFNAR1-deficient macrophages have reduced transcription of IRF9 and Caspase-8.

A-C. WT and *Ifnar1*$^{-/-}$BMDMs (n=4) were treated with LPS (100 ng/mL) + zVAD (50 μM) for 6 hours and the expression of *Irf-9*, *Casp-8* and *Ripk1* mRNAs was examined by quantitative RT-PCR. Each experiment was performed in triplicate. (*P<0.01, **P<0.001).

4.2.6. Gene expression promoted by IFNAR1 signalling during necrosome activation of macrophages

IFN is a potent cytokine with a wide variety of functions affecting cellular physiology, particularly in immune system cells. The majority of these effects are mediated by the IFN-stimulated genes (ISGs), which are transcriptionally regulated by IFN signalling. Following IFNAR1 engagement, a trimeric transcriptional complex composed of STAT1, STAT2 and IRF9 is assembled. This complex, termed ISGF3 translocates to the nucleus to mediate transcription of numerous genes (de Weerd & Nguyen, 2012). The ISGF3 complex binds to interferon-sensitive response elements (ISREs) in transcriptional promoter regions and induces the transcription of many genes some of which may play a role in necroptosis. I performed DNA microarray analysis to reveal changes in the expression of various genes induced during necrosome activation of WT and *Ifnar1*-deficient macrophages. Day 7 bone marrow-derived macrophages were stimulated with LPS in presence of pan caspase inhibitor (zVAD) for 6 hours. After analyzing the fold changes in WT versus *Ifnar1*-deficient macrophages, I performed secondary analyses of several genes identified in the genome-wide analysis. As expected, numerous genes are modulated by IFNAR1-signalling, and it is quite likely that only a few may be important for necroptosis (Fig. 32, 33). I looked at the expression of various genes that have been known to influence cell death in general and observed that *Tnfsf10* (TRAIL) was potently reduced in *Ifnar1*-deficient macrophages. To test the functional significance of this finding in the context of necroptosis resistance, I treated WT and *Ifnar1*-deficient macrophages with recombinant mouse TRAIL along with LPS+zVAD. I found that exogenous addition of TRAIL did not induce necroptosis in *Ifnar1*-deficient macrophages (Fig. 34 A). This result suggests that the resistance of *Ifnar1*-deficient macrophages to necroptosis is not related to the reduced expression of TRAIL. *Ifit-2* is another gene that was

potently down-regulated in *Ifnar1*-deficient macrophages and has been implicated in cell death. To test the role of IFIT2, I tested the impact of *Ifit-1, Ifit-2* -deficiency on cell death by necroptosis. Cells were treated with various necroptotic stimuli to test whether the absence of IFIT-2 impacts TLR4-, TNF-, and IFN- induced necroptosis. Absence of IFIT-2 did not rescue cells from LPS-, TNF-, and IFN-induced necroptosis (Fig. 34B), suggesting that the reduced expression of IFIT-2 in *Ifnar1*-deficient cells is not responsible for the resistance of these cells to necroptosis. Since it was possible that there may be redundancy among various IFIT genes, I tested the impact of complete deficiency of the IFIT-locus and observed that this did not have any impact on necroptosis (Fig. 34B). I observed that in addition to TRAIL, another member of the TNF family, TNF Receptor Superfamily Member 18 (*Gitr*) was downregulated in IFNAR1-deficient macrophages particularly during necrosome signalling. To test the functional significance of this finding, I tested necroptosis of *Gitr*-deficient macrophages in response to various stimulations followed by measuring their viability by MTT assay. These *Gitr*-deficient macrophages were not rescued from necroptosis (Fig. 35), indicating that the reduced expression of GITR expression in *Ifnar1*$^{-/-}$ cells is not responsible for the resistance of *Ifnar1*$^{-/-}$ macrophages.

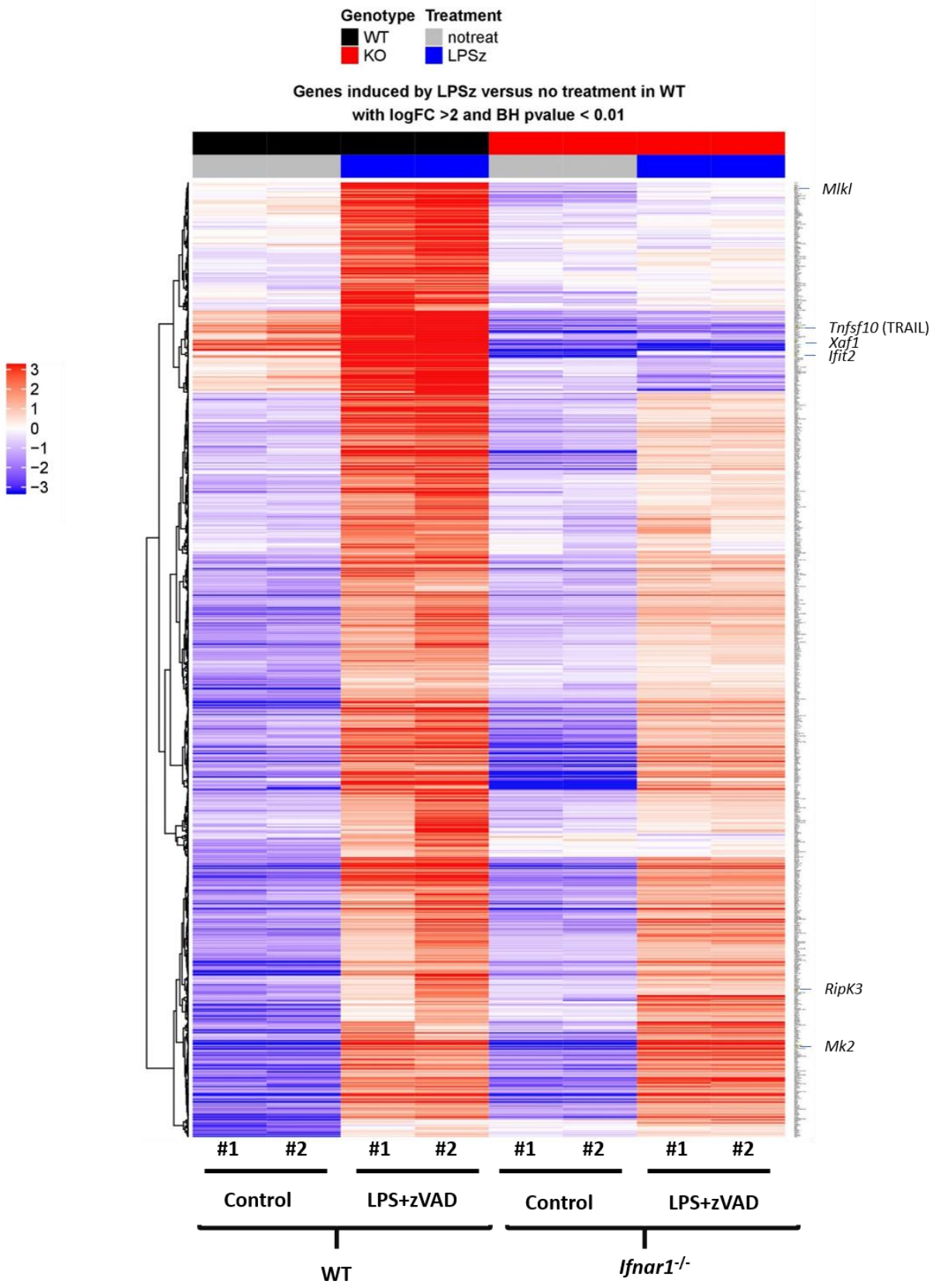
Genotype
WT
KO
Treatment
notreat
LPSz
Genes induced by LPSz versus no treatment in WT
with logFC >2 and BH pvalue < 0.01
3
2
1
0
−1
−2
−3
Mlkl
Tnfsf10 (TRAIL)
Xaf1
Ifit2
RipK3
Mk2
#1
#2
#1
#2
#1
#2
#1
#2
Control
LPS+zVAD
Control
LPS+zVAD
WT
Ifnar1-/-

Figure 32. Gene expression in WT and *Ifnar1*$^{-/-}$ cells during necrosome signalling.

Heatmap showing the median-centered log2 expression of genes following LPS+zVAD vs no treatment in *Ifnar1*$^{-/-}$ cells compared to WT. On Day 7, cells were treated with LPS (100 ng/mL) in presence of zVAD inhibitor (50 µM). Only genes with a log-2 fold-change cut-off of 3 (8-fold) and with a corrected p-value lower than 0.01 are represented. Genes of interest are labelled with their symbol and shown on the right of the figure.

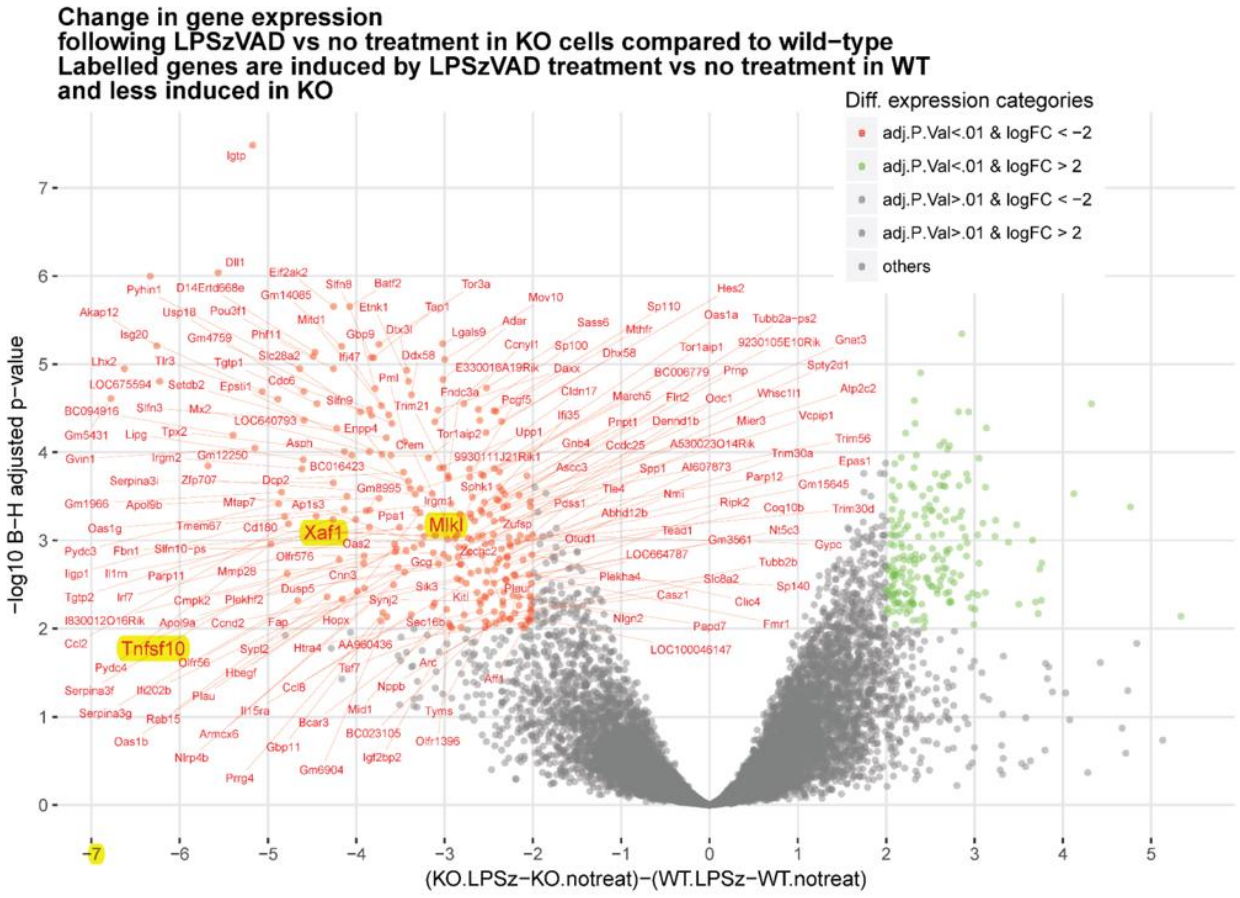
Change in gene expression
following LPSzVAD vs no treatment in KO cells compared to wild−type
Labelled genes are induced by LPSzVAD treatment vs no treatment in WT
and less induced in KO
Diff. expression categories
adj.P.Val<.01 & logFC < −2
adj.P.Val<.01 & logFC > 2
adj.P.Val>.01 & logFC < −2
adj.P.Val>.01 & logFC > 2
others
−log10 B−H adjusted p−value
(KO.LPSz−KO.notreat)−(WT.LPSz−WT.notreat)
Xaf1
Mlkl
Tnfsf10

Figure 33. Analysis of the change in gene expression during necrosome signalling of WT and *Ifnar1*$^{-/-}$ macrophages.

A volcano plot showing the change in gene expression following LPS (100 ng/mL) and zVAD (50 μM) treatment versus no treatment in *Ifnar1*$^{-/-}$ macrophages compared to WT. Spots are colored and labelled with their gene symbols if the difference in the log10 fold change between genotypes is greater than 4-fold and has a corrected p-value lower than 0.01.

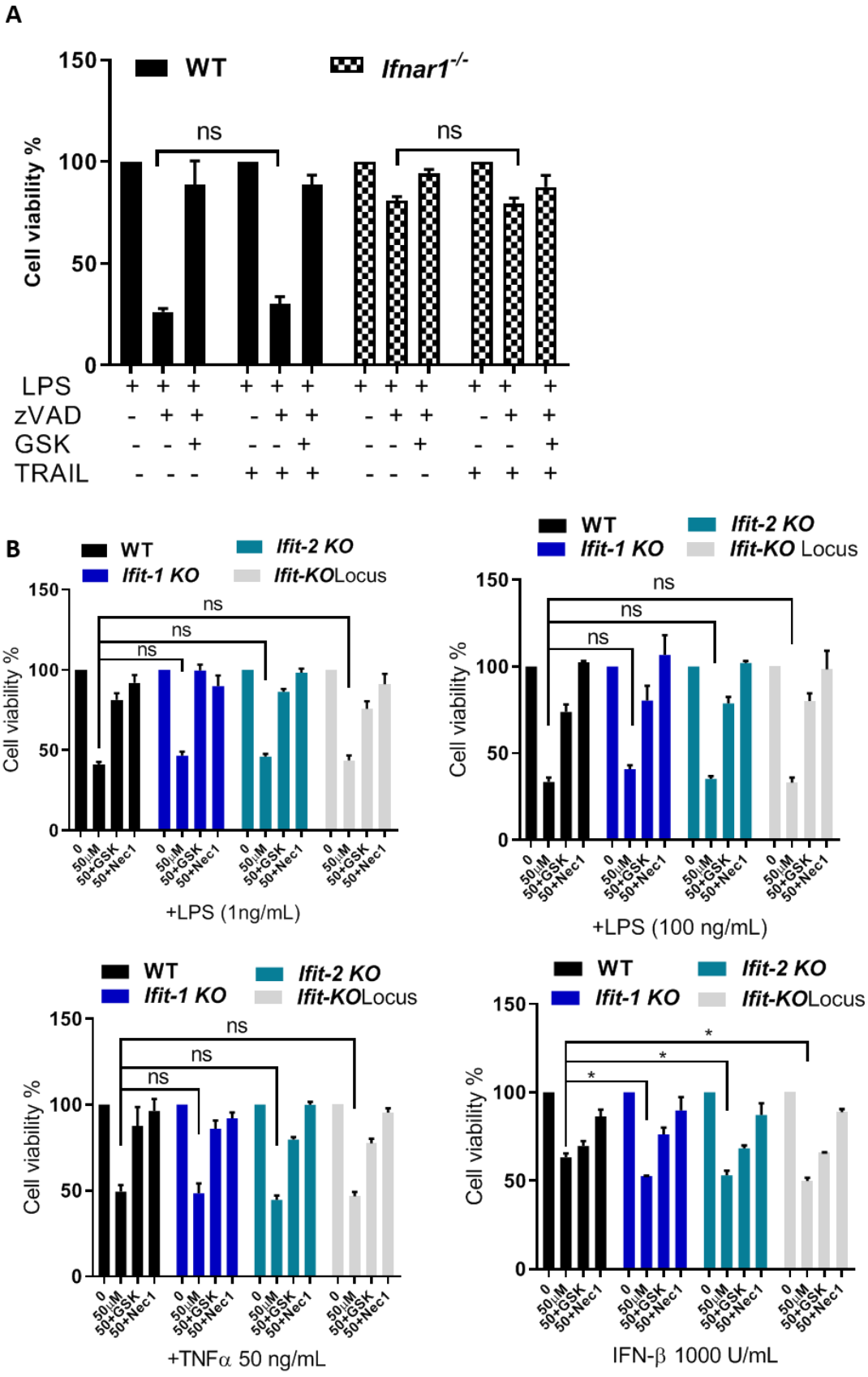
A
WT
Ifnar1-/-
Cell viability %
150
100
50
0
ns
ns
LPS + + + + + + + + + + + +
zVAD - + + - + + - + + - + +
GSK - - + - - + - - + - - +
TRAIL - - - + + + - - - + + +
B
WT
Ifit-1 KO
Ifit-2 KO
Ifit-KOLocus
ns
ns
ns
0
50μM
50+GSK
50+Nec1
+LPS (1ng/mL)
+LPS (100 ng/mL)
+TNFα 50 ng/mL
IFN-β 1000 U/mL
*
*
*

Figure 34. The absence of IFIT-2 had no impact on necroptosis.

WT, *Ifnar1*$^{-/-}$, *Ifit-1*$^{-/-}$ and *Ifit-2*$^{-/-}$ BMDMs were generated and treated on day 7. **A.** Cells were treated with LPS+zVAD with or without mouse recombinant TRAIL (1 µg/mL) and cell viability was measured by MTT assay. **B.** BMDMs were treated with LPS+zVAD, TNFα+zVAD or IFNβ+zVAD, with or without Necrostatin-1/GSK for 24 hours before measuring cell viability by MTT assay. The LPS concentration used in the experiments was 1or100 ng/mL as indicated in the panels, TNFα was used at 50 ng/mL, zVAD was used at 50 µM, Necrostatin-1 was used at 30 µM, and GSK872 was used at 5 µM. Graphs show the percentage of viable cells ±SEM relative to control. Each experiment was performed in triplicate and repeated three times. *P<0.05

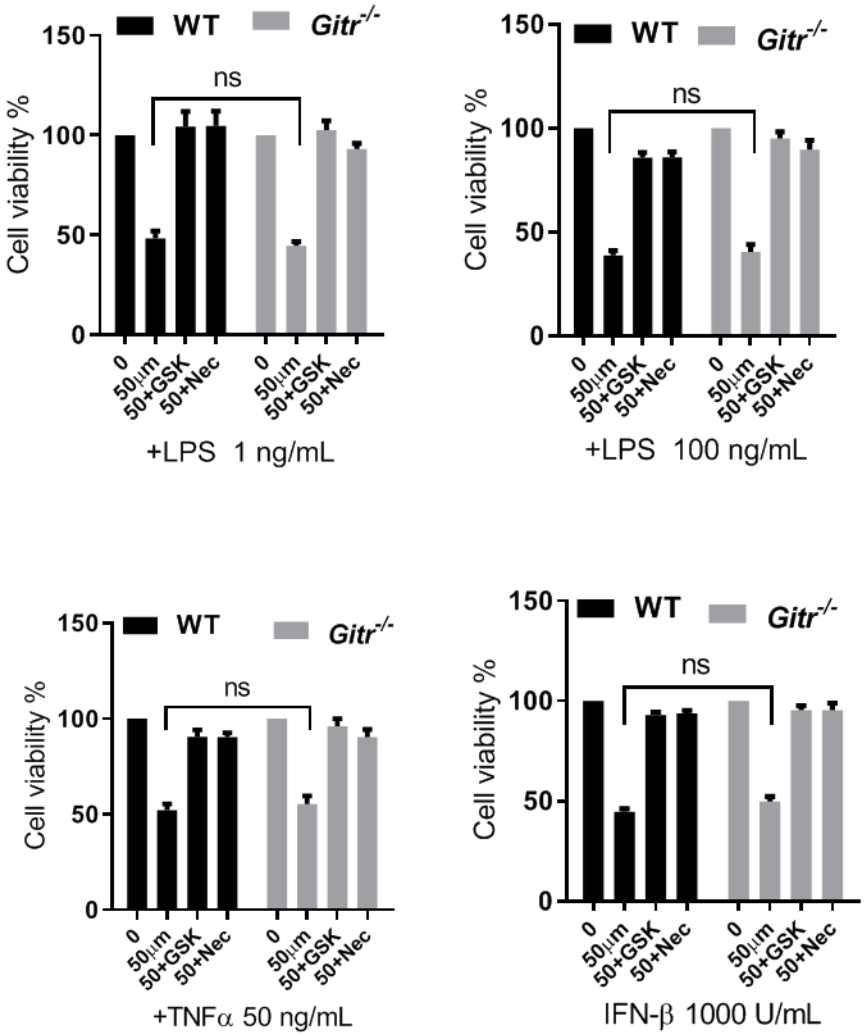
WT
Gitr-/-
ns
Cell viability %
150
100
50
0
0
50μm
50+GSK
50+Nec
+LPS 1 ng/mL
+LPS 100 ng/mL
+TNFα 50 ng/mL
IFN-β 1000 U/mL

Figure 35. The absence of GITR had no impact on necroptosis.

WT and *Gitr*$^{-/-}$ BMDMs were generated and treated on day 7. BMDMs were treated with LPS+zVAD, TNFα+zVAD or IFNβ+zVAD, with or without Necrostatin-1/GSK for 24 hours before measuring cell viability by MTT assay. The LPS concentration used in the experiments was 1or100 ng/mL as indicated in the panels, TNFα was used at 50 ng/mL, zVAD was used at 50 μM, Necrostatin-1 was used at 30 μM, and GSK872 was used at 5 μM. Graphs show the percentage of viable cells ±SEM relative to control. Each experiment was performed in triplicate and repeated three times.

It has been shown that TNF Alpha Induced Protein 3 (TNFAIP3, also called A20), negatively regulates type-I IFN production through inactivation of interferon regulatory factor 3 (IRF3) (Tatsuya Saitoh et al., 2005). In my experiments, I observed that the expression and phosphorylation of A20 in *Ifnar1*-deficient macrophages was increased in comparison to WT controls (Fig. 29A, 36B). Furthermore, it has been previously reported that A20 inhibits necroptosis in T cells (Onizawa et al., 2015). To determine if the increase in A20 expression in *Ifnar1*-deficient cells is responsible for their resistance to necroptosis, I performed si-RNA knockdown of A20 in WT and *Ifnar1*-deficient macrophages and measured the expression of A20 at 24h by western blotting of cell extracts (Fig. 36C). I measured the impact of A20 knock-down on necroptosis in WT and *Ifnar1*$^{-/-}$ cells and found that A20 knockdown did not enhance necroptosis of *Ifnar1*-deficient macrophages (Fig. 36D).

DNA microarray analysis also revealed other cell death related genes whose transcription was impacted by IFNAR1 deficiency such as XAF1 and MLKL. I measured mRNA expression of these genes following treatment with LPS and LPS+zVAD. These experiments revealed that XAF1 was significantly reduced in *Ifnar1*-deficient macrophages after stimulation (Fig. 37A). In contrast, WT cells upregulated XAF1 following particularly during necroptotic stimulation (Fig. 37A). The expression of XAF1 was severely impacted by the deficiency in IFN signalling since XAF1 expression is induced by the transcriptional complex, ISGF3 (W. Li et al., 2017). XAF1 is a pro-apoptotic gene. Because XAF1 knockout mice are not available due to embryonic lethality, I. Instead examined the cell death in *Xaf1*$^{+/-}$ macrophages. Macrophages were generated and treated with LPS+zVAD, TNFα+zVAD, and IFNβ+zVAD for 24 hours before measuring cell viability by MTT assay (Fig. 37B). Cell viability showed a slight rescue in *XAF1*$^{+/-}$ macrophages upon TNF- and IFN-induced necroptosis (Fig. 37B). On the other hand, no differences were observed after

LPS+zVAD stimulation. This result suggests that XAF1 might play a role in necroptosis of macrophages.

I also examined MLKL transcript by qRT-PCR in WT and IFNAR1-deficient macrophages after 6 hours of stimulation with LPS and LPS+zVAD. In agreement with the microarray data, the expression of MLKL was significantly reduced in *Ifnar1*-deficient macrophages compared to WT control (Fig. 37C). In contrast, MLKL expression was induced in WT macrophages upon LPS+zVAD (Fig. 37C). Since MLKL promotes necroptosis, this result suggests the reduced expression of MLKL in *Ifnar1*-deficient macrophages may be responsible for resistance against necroptosis.

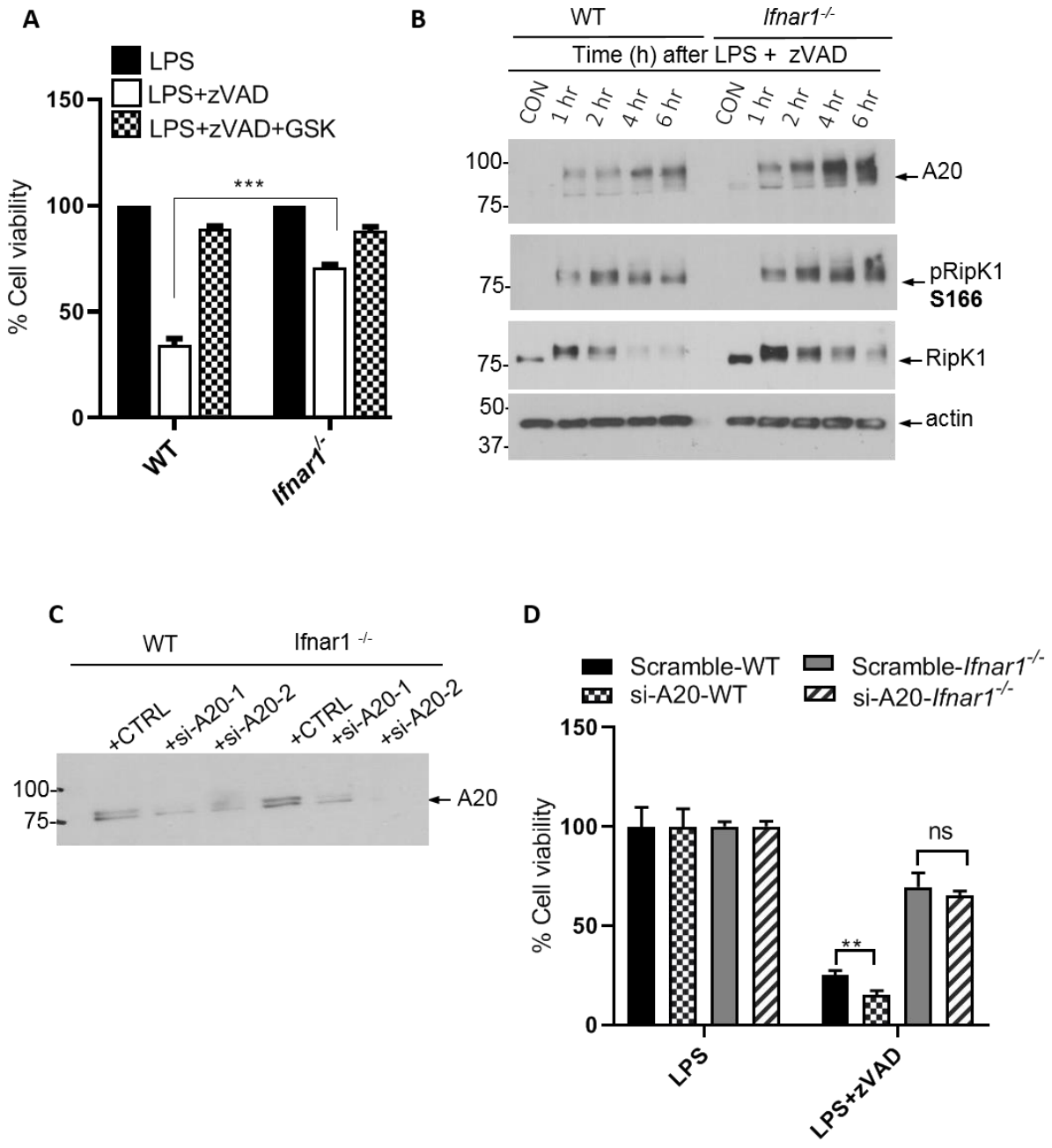
A
LPS
LPS+zVAD
LPS+zVAD+GSK
% Cell viability
150
100
50
0
***
WT
Ifnar1-/-
B
WT
Ifnar1-/-
Time (h) after LPS + zVAD
CON
1 hr
2 hr
4 hr
6 hr
100-
75-
A20
pRipK1
S166
RipK1
50-
37-
actin
C
WT
Ifnar1 -/-
+CTRL
+si-A20-1
+si-A20-2
100-
75-
A20
D
Scramble-WT
si-A20-WT
Scramble-Ifnar1-/-
si-A20-Ifnar1-/-
% Cell viability
150
100
50
0
**
ns
LPS
LPS+zVAD

Figure 36. A20 knockdown has no impact on resistance of *Ifnar1*-deficient macrophages to necroptosis.

A. WT and *Ifinar1*$^{-/-}$ BMDMs were treated with LPS, LPS+zVAD, and LPS+zVAD+GSK for 24 hours followed by measuring cell viability by MTT assay. **B.** The same sets of cells were treated with LPS+zVAD for various time intervals, and the expression of A20 expression was evaluated by western blotting of cell extracts. **C.** WT and *Ifinar1*$^{-/-}$ BMDMs were transfected with si-RNA against A20 (15 pmol) using RNAmaxi kit for 24 hours. The lysates of transfected cells were examined after 24 hours for A20 expression by western blotting. **D.** The transfected cells were treated with LPS, and LPS (100ng/mL) + zVAD (50μM) for 24 hours before measuring viability by Alamar blue. Graphs show the percentage of viable cells ±SEM relative to cells treated with LPS in the absence of zVAD. Each experiment was performed in triplicate and repeated three times. (**P<0.001, ***P < 0.001).

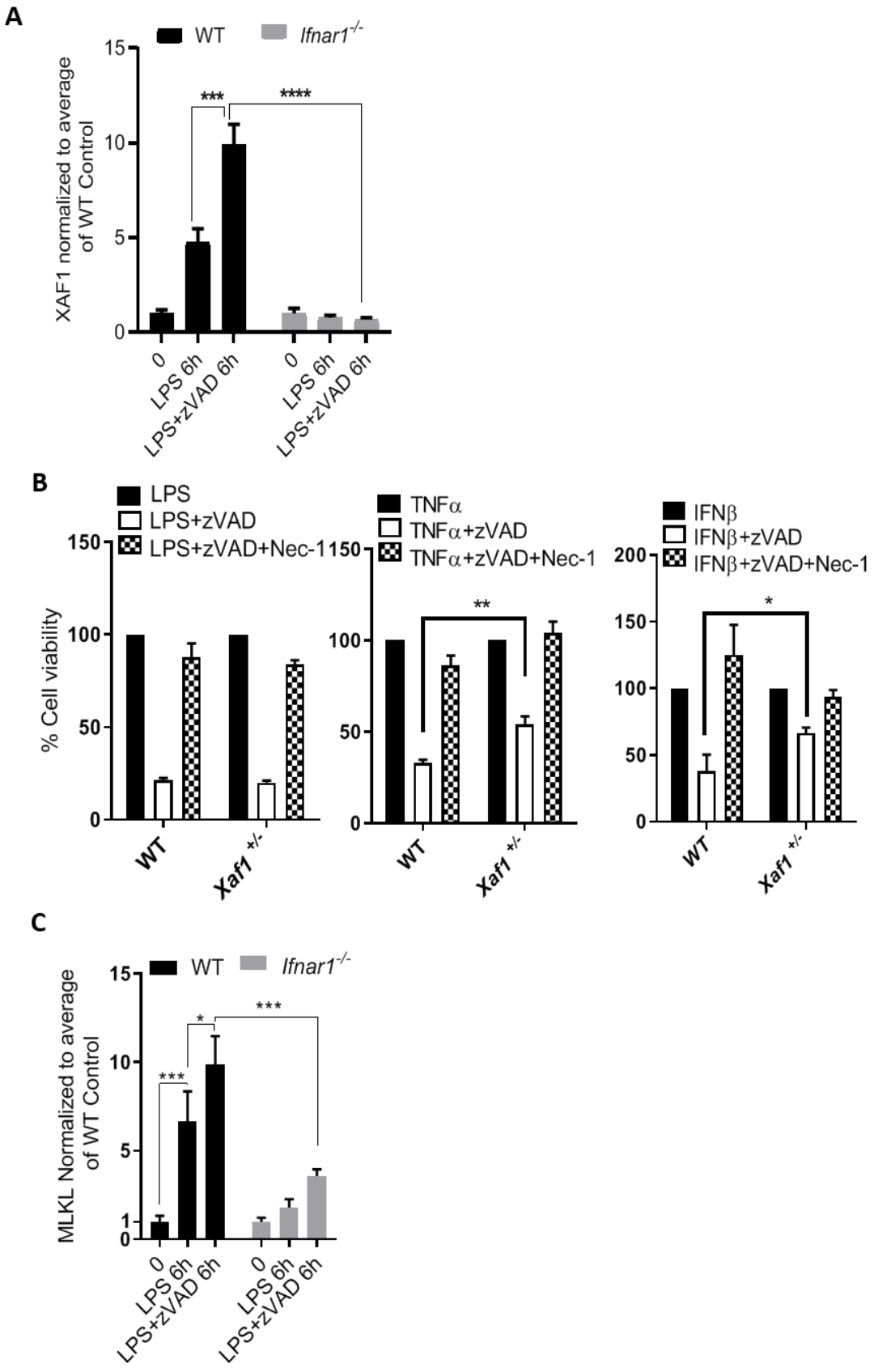
A
WT
Ifnar1-/-
XAF1 normalized to average of WT Control
15
10
5
0
***
****
0
LPS 6h
LPS+zVAD 6h
0
LPS 6h
LPS+zVAD 6h
B
LPS
LPS+zVAD
LPS+zVAD+Nec-1
% Cell viability
150
100
50
0
WT
Xaf1 +/-
TNFα
TNFα+zVAD
TNFα+zVAD+Nec-1
150
100
50
0
**
WT
Xaf1 +/-
IFNβ
IFNβ+zVAD
IFNβ+zVAD+Nec-1
200
150
100
50
0
*
WT
Xaf1 +/-
C
WT
Ifnar1-/-
MLKL Normalized to average of WT Control
15
10
5
1
0
***
*
***
0
LPS 6h
LPS+zVAD 6h
0
LPS 6h
LPS+zVAD 6h

Figure 37. Expression of XAF1 and MLKL is reduced in *Ifnar1*-deficient macrophages.

A-C. WT and *Ifinar1*$^{-/-}$ BMDMs (n=4) were treated with LPS, LPS (100 ng/mL) + zVAD (50 μM) for 6 hours and the expression of XAF1 and MLKL mRNAs was evaluated by qRT-PCR. Each experiment was performed in triplicate. (*P<0.01, **P<0.001, ***P<0.0001). **B.** WT and *Xaf1*$^{+/-}$ BMDMs were treated with LPS+zVAD, TNFα+zVAD or, IFNβ+zVAD, with or without Necrostatin-1 for 24 hours before measuring cell viability by MTT assay. LPS concentration used in the experiments was 100 ng/mL, TNFα was used at 50 ng/mL, zVAD was used at 50 μM, and Necrostatin-1 was used at 30 μM. Graphs show the percentage of viable cells ±SEM relative to control. Each experiment was performed in triplicate and repeated three times. (*P<0.01, **P<0.001, ***P < 0.001, ****P < 0.0001).

4.2.7. IFNAR1 signalling promotes phosphorylation of MLKL

To further investigate the role of MLKL in promoting necroptosis, I evaluated the activation of MLKL following necrosome signalling in WT and *Ifnar1*-deficient macrophages. Cells were treated with LPS+zVAD for various time intervals and the phosphorylation of MLKL was evaluated. Western blotting showed that the phosphorylation of MLKL was completely abolished in *Ifnar1*-deficient macrophages (Fig. 38A). To quantify MLKL phosphorylation at serine-345, densitometric analysis was performed and revealed that the phospho-MLKL level was reduced in *Ifnar1*-deficient macrophages (Fig. 38B). In addition, I quantified the monomeric form of MLKL and found that its basal expression level was also impacted in *Ifnar1*-deficient macrophages in comparison to WT control (Fig. 38B). This finding matches the decreased mRNA level of MLKL in *Ifnar1*-deficient macrophages (Fig. 37C). However, it is worth noting that the decrease in phosphorylation of MLKL is much more potent than the decrease in total MLKL observed in *Ifnar1*-deficient macrophages, suggesting that the reduced expression of MLKL by itself may not be responsible for resistance of these cells to necroptosis. As expected MLKL-deficient macrophages were completely resistant to LPS-induced necroptosis (Fig. 38C), implying that the reduced expression of MLKL in *Ifnar1*-deficient cells may be responsible for their reduced cell death, (Fig. 36A). Knowing that the phosphorylation of upstream kinase RipK3 was significantly compromised in *Ifnar1*-deficient macrophages, I tested the impact of MLKL-deficiency on phosphorylation of RipK3. The phosphorylation of RipK3 was compromised in MLKL-deficient macrophages (Fig. 38D, E) MLKL is a pseudokinase, which cannot phosphorylate proteins, hence this result is intriguing. I also examined the oligomerization of MLKL in *Ifnar1*-deficient macrophages. BMMs were generated and treated with LPS and LPS+zVAD for various time intervals (Fig. 39A and C). The trimerization of MLKL was only detected during necrosome

activation (Fig. 39C) whereas no MLKL trimers were formed upon stimulation with LPS only (Fig. 39A). Western blots were quantified, and the results indicated that fewer monomers and trimers of MLKL were present in *Ifnar1*-deficient macrophages compared to WT controls (Fig. 39 B and D). The specificity of oligomerization was examined in reducing and non-reducing conditions (Fig. 39E). Although the monomeric form was detected in both conditions, the trimeric form was only observed in a non-reducing condition where the disulphide bonds were not reduced by β-mercaptoethanol (Fig. 39E). Taken together, these results suggest that type-I IFN signalling is required for the phosphorylation and trimerization of MLKL.

Since trimeric MLKL relocates to the cell membrane to induce membrane rupture (Linkermann, Kunzendorf, & Krautwald, 2014), I evaluated the activation and localization of MLKL in WT and *Ifnar1*-deficient macrophages by immunofluorescence (IF) staining combined with confocal microscopy. Cells were treated with LPS and LPS+zVAD for 2 and 5 hours followed by staining with antibodies against total MLKL (cyan), phospho-MLKL (red) and TNFR1 (green) (as described in the method section 3.11). Nuclei were stained with DAPI (blue). This imaging showed that the phosphorylation of MLKL was undetectable in *Ifnar1*-deficient macrophages whereas in WT macrophages phospho-MLKL was observed as early as 2 hours post-stimulation. Moreover, the imaging experiments revealed that phospho-MLKL is membrane localized in WT cells at 2 and 5 hours. (Fig. 40). The translocation of phospho-MLKL was not detected during necrosome signalling in *Ifnar1*-deficient macrophages (Fig. 40). Collectively, these results indicate that type-I IFN signalling is needed to maintain the expression and activation of MLKL.

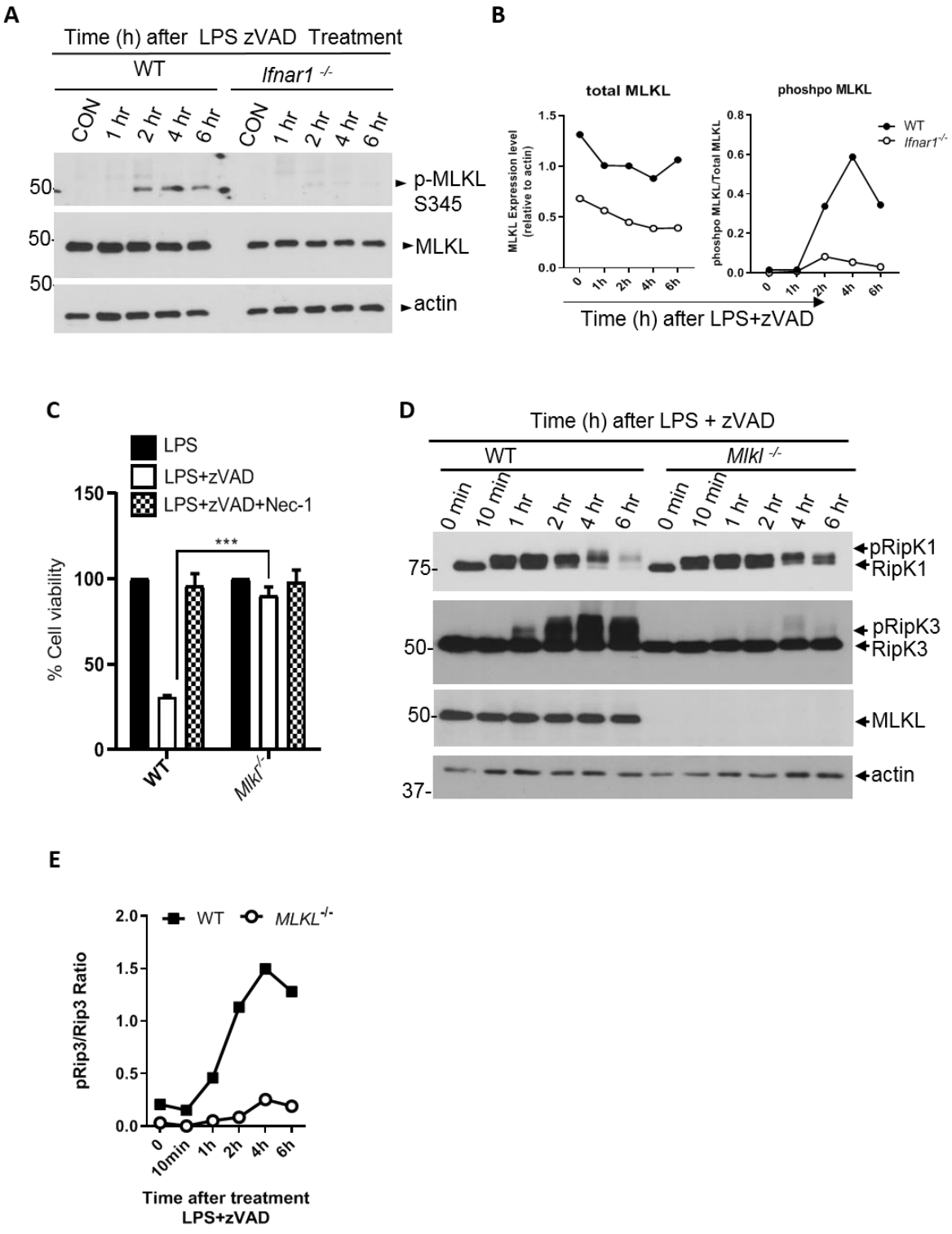
A
Time (h) after LPS zVAD Treatment
WT
Ifnar1 -/-
CON
1 hr
2 hr
4 hr
6 hr
CON
1 hr
2 hr
4 hr
6 hr
50
p-MLKL S345
50
MLKL
50
actin
B
total MLKL
phoshpo MLKL
MLKL Expression level (relative to actin)
phoshpo MLKL/Total MLKL
WT
Ifnar1-/-
0
1h
2h
4h
6h
Time (h) after LPS+zVAD
C
LPS
LPS+zVAD
LPS+zVAD+Nec-1
% Cell viability
150
100
50
0
***
WT
Mlkl-/-
D
Time (h) after LPS + zVAD
WT
Mlkl -/-
0 min
10 min
1 hr
2 hr
4 hr
6 hr
0 min
10 min
1 hr
2 hr
4 hr
6 hr
75-
pRipK1
RipK1
50-
pRipK3
RipK3
50-
MLKL
37-
actin
E
WT
MLKL-/-
pRip3/Rip3 Ratio
2.0
1.5
1.0
0.5
0.0
0
10min
1h
2h
4h
6h
Time after treatment
LPS+zVAD

Figure 38. IFNAR1 signalling promotes phosphorylation of MLKL.

A. WT and *Ifnar1*$^{-/-}$BMDMs were treated with LPS (100 ng/mL) + zVAD (50 μM) for various time intervals and the expression of various proteins was evaluated by western blotting. **B.** Quantification of western blot data from (A), was performed by densitometric analysis of monomeric MLKL and trimeric MLKL over time. **C.** WT and *Mlkl*$^{-/-}$BMDMs were treated with LPS (100 ng/mL) + zVAD (50 μM) with or without Necrostatin-1 (30 μM) for 24 hours and cell viability measured by MTT assay. **D.** WT and *Mlkl*$^{-/-}$BMDMs were treated as in (C) for various time intervals and the expression of various proteins evaluated by western blotting. **E.** Quantification of western blot data from (D), was performed by densitometric analysis of phospho-RipK3 versus total RipK3 over time. Densitometric data represent a representative experiment (from three independent experiments). Bar graphs show the percentage of viable cells ±SEM relative to control. Each experiment was performed in triplicate and repeated three times. (***$P < 0.001$).

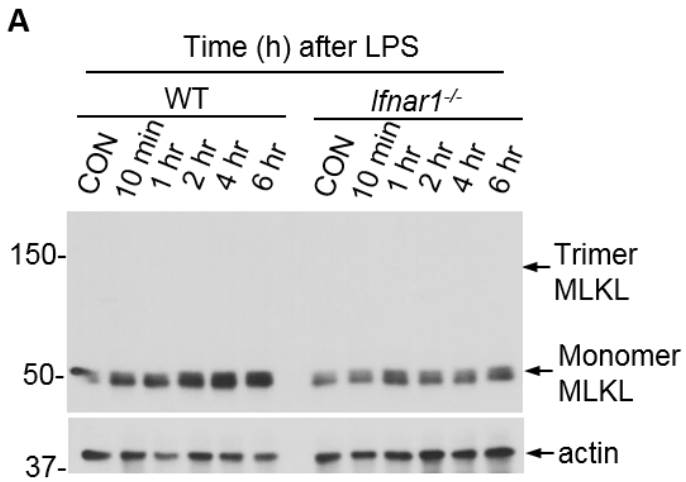
A
Time (h) after LPS
WT
Ifnar1-/-
CON
10 min
1 hr
2 hr
4 hr
6 hr
150-
50-
37-
Trimer MLKL
Monomer MLKL
actin

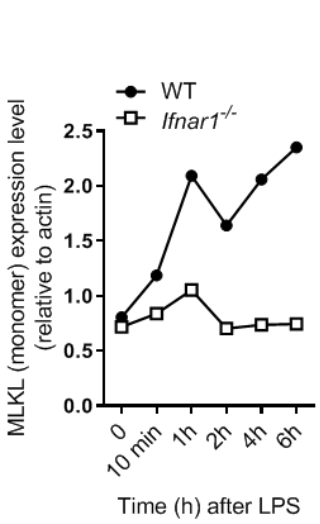
B
WT
Ifnar1-/-
MLKL (monomer) expression level (relative to actin)
2.5
2.0
1.5
1.0
0.5
0.0
0
10 min
1h
2h
4h
6h
Time (h) after LPS

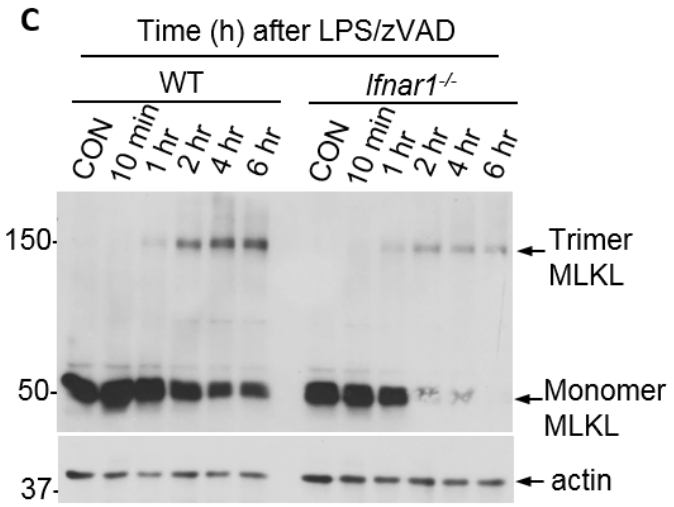
C
Time (h) after LPS/zVAD
WT
Ifnar1-/-
CON
10 min
1 hr
2 hr
4 hr
6 hr
150-
50-
37-
Trimer MLKL
Monomer MLKL
actin

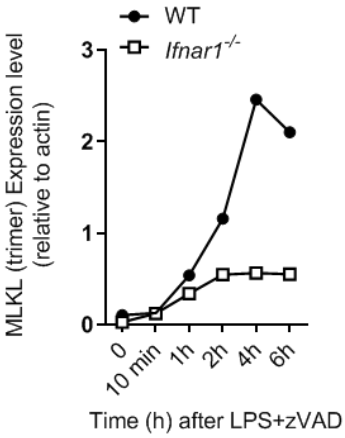
D
WT
Ifnar1-/-
MLKL (trimer) Expression level (relative to actin)
3
2
1
0
0
10 min
1h
2h
4h
6h
Time (h) after LPS+zVAD

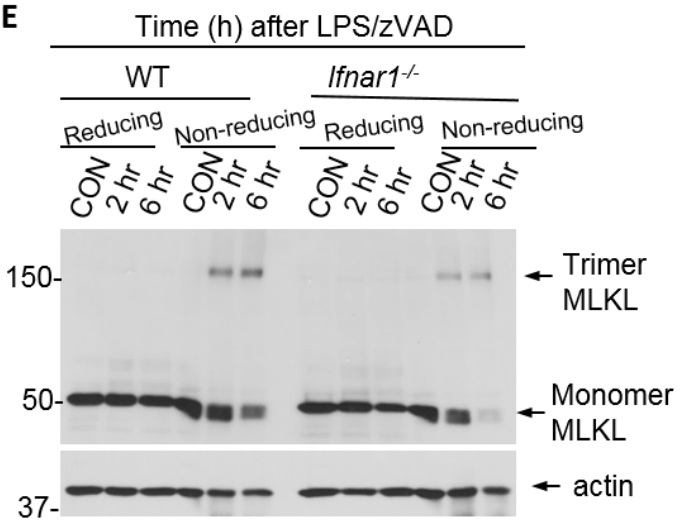
E
Time (h) after LPS/zVAD
WT
Ifnar1-/-
Reducing
Non-reducing
Reducing
Non-reducing
CON
2 hr
6 hr
150-
50-
37-
Trimer MLKL
Monomer MLKL
actin

Figure 39. IFNAR1 signalling promotes MLKL trimerization.

A+C. WT and *Ifnar1*$^{-/-}$BMDMs were treated with LPS for various time intervals up to 6 hours and the expression of MLKL and actin evaluated by western blotting of cell extracts. **B.** Quantification of western blot data from (A), was performed by densitometric analysis of monometric MLKL over time. **C.** WT and *Ifnar1*$^{-/-}$BMDMs were treated with LPS (100 ng/mL) + zVAD (50 μM) for various time intervals up to 6 hours and the expression of MLKL evaluated by western blotting of cell extracts. **D.** Quantification of western blot data from (C) was performed by densitometric analysis of trimeric MLKL over time. B+D Densitometric data represent a representative experiment (from three independent experiments). **E.** WT and *Ifnar1*$^{-/-}$ BMDMs were treated as in (C) and lysed in buffer with and without 1% β-mercaptoethanol followed by western blotting.

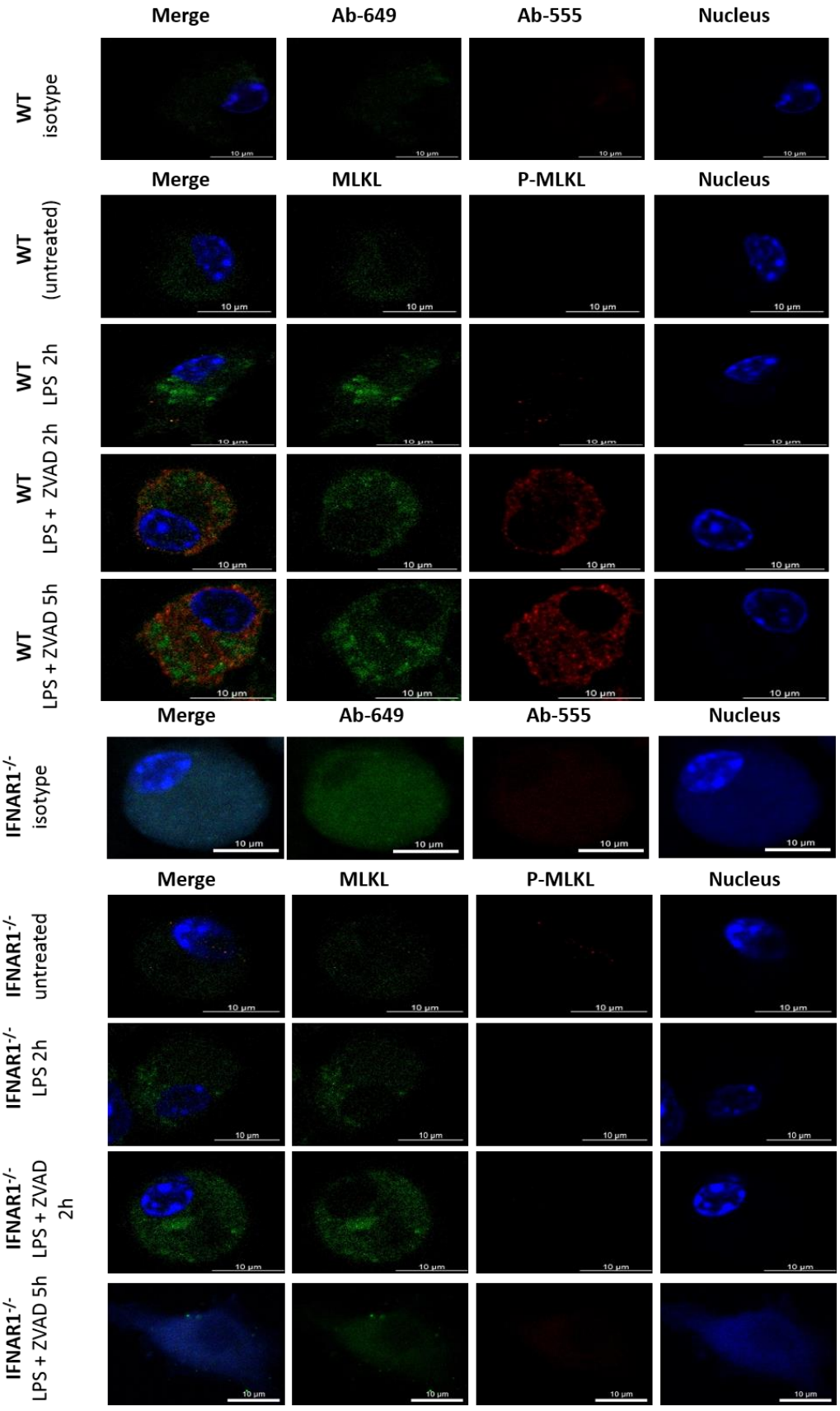
Merge
Ab-649
Ab-555
Nucleus
WT isotype
Merge
MLKL
P-MLKL
Nucleus
WT (untreated)
WT LPS 2h
WT LPS + ZVAD 2h
WT LPS + ZVAD 5h
Merge
Ab-649
Ab-555
Nucleus
IFNAR1-/- isotype
Merge
MLKL
P-MLKL
Nucleus
IFNAR1-/- untreated
IFNAR1-/- LPS 2h
IFNAR1-/- LPS + ZVAD 2h
IFNAR1-/- LPS + ZVAD 5h
10 µm

Figure 40. IFNAR1 signalling is needed to sustain MLKL expression and localization.

WT and *Ifnar1*$^{-/-}$BMDMs were plated on 24-well glass-bottom dishes and treated with LPS and LPS (100 ng/mL) +zVAD (50 µM) for 2 and 5 hours. Cells were examined by confocal microscopy after immunofluorescence staining with anti-phospho-MLKL (Red), anti-total MLKL (Green) and DAPI (blue) for the nucleus. The results represent 3 separate experiments. Bars are equal to 10 µm.

4.2.8. Type-I IFN signalling promotes the formation of necrosome

Since RipK3 phosphorylation was severely impacted in *Ifnar1*-deficient macrophages (Fig. 29A), I evaluated if the interaction of RipK3 with various proteins is compromised in IFNAR1-deficient macrophages. I generated WT and *Ifnar1*-deficient macrophages and treated them with LPS and LPS+zVAD for 3 hours. Lysates were immunoprecipitated using an anti-RipK3 antibody. Immunoprecipitates were then analyzed by western blotting against other known proteins involved in necrosome signalling such as RipK1, MLKL, CASP-8 and FADD and actin as a control. LPS treatment resulted in no interaction of RipK3 with necrosomal proteins while LPS+zVAD treatment showed that RipK3 was associated with RipK1, CASP-8, FADD and MLKL in WT cells (Fig. 41A). In contrast, *Ifnar1*-deficient macrophages showed reduced interaction between RipK3 and RipK1, and the interaction of RipK3 with MLKL, CASP-8 and FADD was potently reduced. I also examined the expression of necrosome signalling proteins in whole cell lysates (Fig. 41A). These results demonstrate that the reduced RipK3-MLKL interactions affect the formation of late necrosome in *Ifnar1*-deficient cells, which results in their resistance to necroptosis. In addition, I treated the cells with LPS, LPS+zVAD and LPS+zVAD+GSK for 6 hours followed by measuring their viability using Zombie Yellow™ staining. These results showed that *Ifnar1*-deficient macrophages were resistant to LPS-induced necroptosis (Fig. 41B).

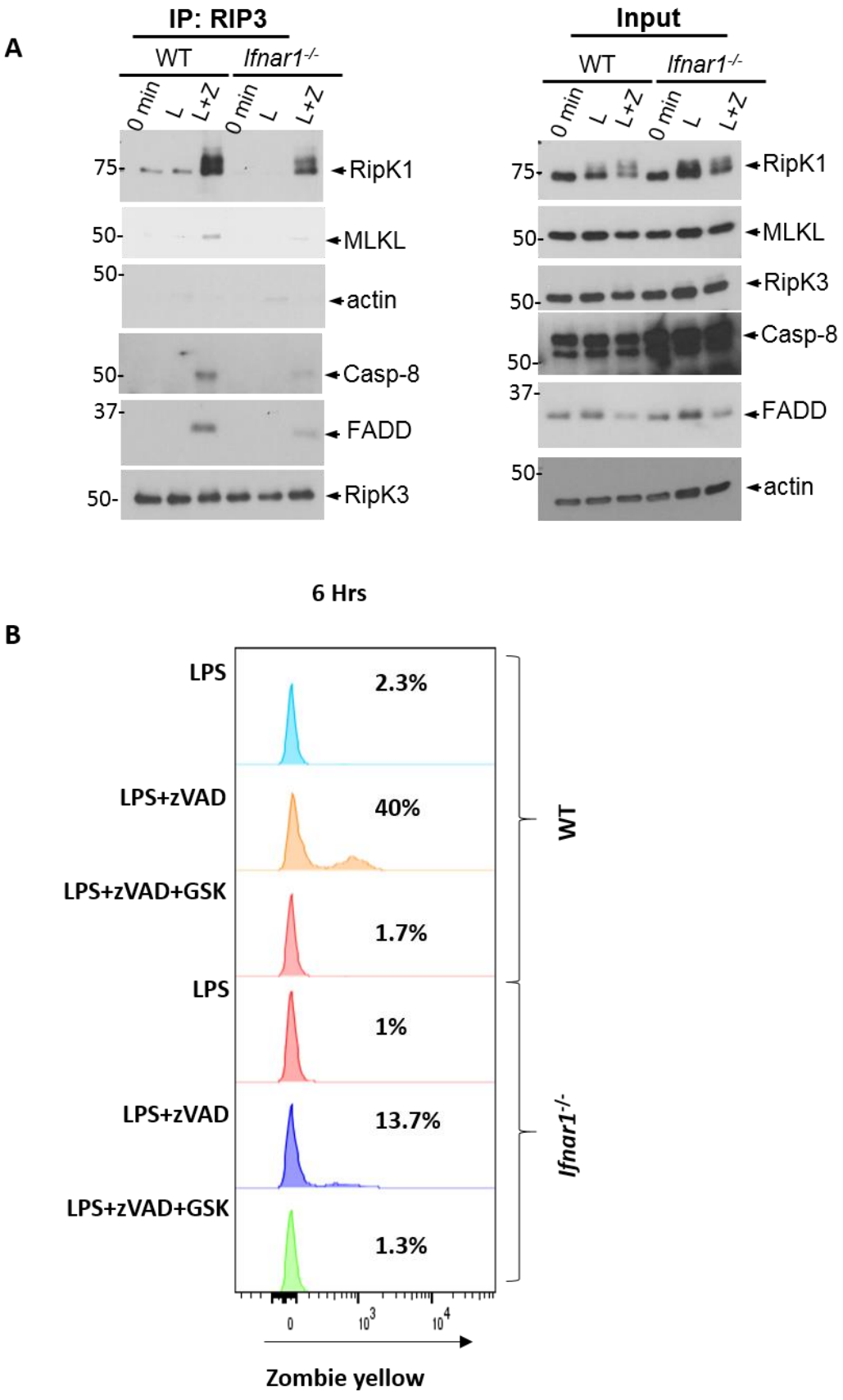
A
IP: RIP3
WT
Ifnar1-/-
0 min
L
L+Z
0 min
L
L+Z
75-
RipK1
50-
MLKL
50-
actin
50-
Casp-8
37-
FADD
50-
RipK3
Input
WT
Ifnar1-/-
0 min
L
L+Z
0 min
L
L+Z
75-
RipK1
50-
MLKL
50-
RipK3
50-
Casp-8
37-
FADD
50-
actin
6 Hrs
B
LPS
2.3%
LPS+zVAD
40%
LPS+zVAD+GSK
1.7%
LPS
1%
LPS+zVAD
13.7%
LPS+zVAD+GSK
1.3%
WT
Ifnar1-/-
0
10^3
10^4
Zombie yellow

Figure 41. IFNAR1 signalling promotes necrosome formation.

A. WT and *Ifnar1*$^{-/-}$BMDMs were generated and RipK3 was immunoprecipitated in control cells (0 min) or in cells treated with LPS or LPS+zVAD at 3 hours post-stimulation. Expression of various proteins in immune-precipitates and whole cell lysates were evaluated by western blotting. **B.** WT and *Ifnar1*$^{-/-}$BMDMs were treated as in (A) and cell viability was examined with Zombie Yellow staining 6 hours post stimulation.

4.2.9. Inhibition of the p38 ^{MAPK} pathway overcomes the resistance of *Ifnar1*$^{-/-}$ macrophages to LPS-induced necroptosis

Upon the engagement of the type-I IFN receptor various signalling pathways are activated such as the mitogen activated protein kinase cascade (MAPK) (Dedoni, Olianas, & Onali, 2014). Studies have shown that IFN-β activates p38^{MAPK} in a variety of cell lines. It has also been suggested that the p38 ^{MAPK} pathway regulates type-I IFN-dependent induction of proteins through post-translational modification (McGuire et al., 2017). To investigate the role of p38^{MAPK} in the resistance of *Ifnar1*-deficient macrophages to necroptosis, cells were treated with LPS+zVAD with and without p38^{MAPK} inhibitor for various time intervals. Western blotting showed that the p38^{MAPK} inhibitor blocked the phosphorylation of the downstream MAPK-activated protein kinase 2 (MK2). Total RipK1 phosphorylation was reduced in WT and *Ifnar1*-deficient macrophages after inhibition of p38^{MAPK} (Fig. 42A). Inhibition of p38^{MAPK} did not have any significant impact on RipK3 phosphorylation. While *Ifnar1*-deficient macrophages displayed reduced phosphorylation of MLKL, this was significantly enhanced by inhibition of the p38^{MAPK} pathway (Fig. 42A, B). Next, I investigated whether the increased phosphorylation of MLKL upon inhibition of the p38^{MAPK} pathway in *Ifnar1*-deficient macrophages abrogates their resistance to necroptosis. I treated the cells with LPS, LPS+zVAD, LPS+zVAD+GSK with and without p38^{MAPK} inhibitor for 24 hours before measuring the cell viability by MTT assay. I also evaluated the effect of p38^{MAPK} inhibitor combined with a low concentration of zVAD. Low zVAD (10μM) with LPS was examined previously and had no impact on cell viability. Combined treatment of LPS+zVAD with the p38^{MAPK} inhibitor resulted in significantly increased cell death in WT (Fig. 42C). Interestingly, inhibition of p38^{MAPK} significantly amplifies LPS-induced necroptosis in *Ifnar1*-deficient macrophages (Fig. 42C) even under conditions of low zVAD concentration (10μM). Cell death

was not observed with this low concentration of zVAD in the absence of $p38^{MAPK}$ inhibitor. This result indicates that $p38^{MAPK}$ signalling might contribute to the resistance of *Ifnar1*-deficient macrophages. Additionally, I evaluated the expression of TNFα during necrosome signalling of WT and *Ifnar1*-deficient macrophages. TNFα expression was measured by ELISA in the supernatants after 6 hours of stimulation (Fig. 42D). *Ifnar1*-deficient macrophages significantly expressed more TNFα than WT controls. Interestingly, the autocrine TNFα signalling does not induce necroptosis in *Ifnar1*-deficient macrophages. However, $p38^{MAPK}$ inhibition reduced TNFα secretion during LPS-induced necroptosis in both groups. These results suggest that in the absence of IFN signalling, $p38^{MAPK}$ might regulate some transcriptional factors to induce the expression of anti-necroptotic gene(s).

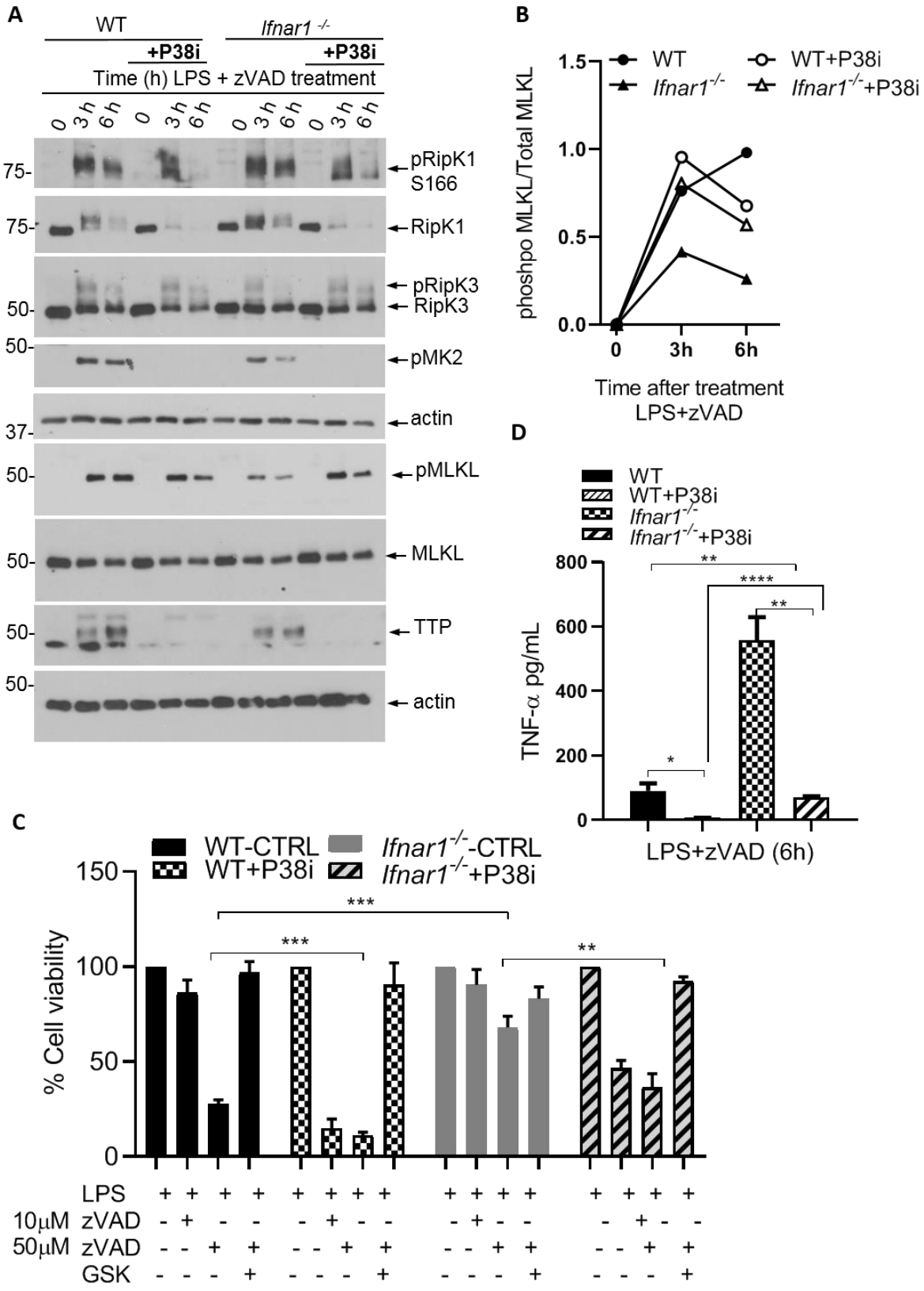
A
WT
Ifnar1 -/-
+P38i
+P38i
Time (h) LPS + zVAD treatment
0 3 h 6 h 0 3 h 6 h 0 3 h 6 h 0 3 h 6 h
75-
pRipK1 S166
75-
RipK1
pRipK3
50-
RipK3
50-
pMK2
37-
actin
50-
pMLKL
50-
MLKL
50-
TTP
50-
actin
B
WT
WT+P38i
Ifnar1-/-
Ifnar1-/-+P38i
phoshpo MLKL/Total MLKL
1.5
1.0
0.5
0.0
0
3h
6h
Time after treatment LPS+zVAD
D
WT
WT+P38i
Ifnar1-/-
Ifnar1-/-+P38i
TNF-α pg/mL
800
600
400
200
0
**
****
**
*
LPS+zVAD (6h)
C
WT-CTRL
WT+P38i
Ifnar1-/--CTRL
Ifnar1-/-+P38i
% Cell viability
150
100
50
0
***
***
**
LPS + + + + + + + + + + + + + + + +
10μM zVAD - + - - - + - - - + - - - + - -
50μM zVAD - - + + - - + + - - + + - - + +
GSK - - - + - - - + - - - + - - - +

Figure 42. Inhibition of p38^{MAPK} abrogates the resistance of *Ifnar1*$^{-/-}$ macrophages.

WT and *Ifnar1*$^{-/-}$ BMDMs were treated on day 7 with LPS (100 ng/mL) + zVAD (50 µM), with and without a P38 inhibitor (LY2228820,4 µM). **A.** Cells were treated for various time intervals and the expression of various proteins evaluated by western blotting of cell extracts. **B.** Quantification of western blot data from (A) was performed by densitometric analysis of phospho-MLKL in all 4 groups. Densitometric data represent a representative experiment (from three independent experiments). **C.** Cell viability was measured by MTT assay after 24 hours of stimulation. **D.** Supernatant was collected after 6 hours, and TNFα expression was measured by ELISA. Bar graphs show the percentage of viable cells ±SEM relative to cells treated with LPS in the absence of zVAD. Each experiment was repeated three times with triplicate samples. (*P<0.01, **P<0.001, ***P < 0.001, ****P < 0.0001).

5.0 DISCUSSION

The balance between cell survival and programmed cell death plays a critical role in embryogenesis and tissue homeostasis in multicellular organisms. Apoptosis is the best studied form of programmed cell death and is considered to be a silent form of non-inflammatory programmed cell death (Kolb et al., 2017). Necroptosis and pyroptosis, in contrast, are more recently discovered forms of non-apoptotic cell death (Douglas R. Green, 2019).

Necroptosis is an inflammatory form of programmed cell death (D. R. Green, Oberst, Dillon, Weinlich, & Salvesen, 2011). In many pathologies, necroptosis of macrophages contributes to the initiation of the immune response. Necroptosis thereby promotes the control of pathogens and elimination of injured or infected cells (Ahn & Prince, 2017). Despite the rapid pace at which new knowledge is generated in the field of necroptosis, many underlying molecular mechanisms remain unclear. For example, the molecular mechanisms of the activation and regulation of necroptosis in macrophages remains unclear.

Knowledge of necrosome signalling is also incomplete because it has been mainly derived from studies of non-immune cells, such as fibroblasts (Vanlangenakker et al., 2012). One would anticipate that necrosome signalling may differ between cell types which may have different consequences for the organism. For example, necroptotic death of macrophages has been shown to cause the release of damage-associated molecular patterns (DAMPs), in turn triggering inflammation, clearance of infection and recruitment of additional immune cells to the site of infection or injury. Innate immune cells such as dendritic cells, macrophages and neutrophils are considered more relevant in comparison to fibroblasts for the study of necroptosis in immunity. Macrophages, in particular, are considered the best cellular model to characterize programmed cell

death pathways because they are critical components of the innate immune system, and they are present in various anatomical compartments. Furthermore, macrophage-like cells play key role in various tissues such as the Kupffer cells in the liver and Microglia in the brain. Furthermore, macrophages are responsive to a wide variety of pathogen-associated molecular patterns (PAMPs), such as LPS, flagellin, and inflammatory cytokines.

Knowledge of necrosome signalling is additionally incomplete because it has been mainly derived from one type of stimulation. Typically, necroptosis is induced in MEFs by treatment with TNFα and the pan-caspase inhibitor, zVAD. One would anticipate that necrosome signalling may differ in response to different necroptotic stimuli. For example, it has been shown that type-I IFN signalling is required for necrosome activation in macrophages regardless of the necroptotic stimuli (TLR3,4, TNFα, IFNβ and BP) (McComb, Cessford, et al., 2014; Rijal et al., 2018). In addition, understanding how RipK1 and RipK3 are phosphorylated and assembled during necrosome signalling remains unclear (Declercq, Vanden Berghe, & Vandenabeele, 2009; Degterev et al., 2008).

Based on current understanding necroptosis proceeds and is controlled by three major checkpoints: ubiquitination (Hitomi et al., 2008), absences of caspases activity (He, Liang, Shao, & Wang, 2011) and phosphorylation of key necroptotic proteins (RipK1 and RipK3) (Cho et al., 2009).

In the context of TNFα and the pan-caspase inhibitor (zVAD) stimulation, the kinetics of necrosome signalling cascade involves activation of RipK1, interaction between RipK1 and RipK3 (J. Li et al., 2012), interaction of RipK3 with MLKL and phosphorylation of RipK3, followed by phosphorylation and trimerization of MLKL by RipK3 (Rodriguez et al., 2016; L. Sun et al., 2012; Zhao et al., 2012). MLKL is a kinase-dead protein because it lacks a phosphate-binding glycine-

rich p loop that is required for kinase function (L. Sun et al., 2012). Similar to RipK3, MLKL deficient macrophages are resistant to necroptosis. MLKL is considered to be the key necroptotic executioner protein as phosphorylation of MLKL results in its oligomerization (D. Huang et al., 2017) and subsequent translocation to the plasma membrane where MLKL interacts with phosphatidylinositol phosphates (PIPs) and cardiolipin. The homo-oligomer MLKL functions as a cation channel and disrupts the permeability of plasma membrane that leads to its rupture (Y. Dondelinger et al., 2014; H. Wang et al., 2014; Y. Zhang, Chen, Gueydan, & Han, 2017).

5.1. Necrosome degradation

Recent studies have discovered that necroptosis can be triggered by the activation of various receptors. However, the corresponding necrosomes have yet to be characterized in detail. To address this gap, the major aim of my thesis was to develop new knowledge about the mechanisms that regulate and maintain necrosomes following activation by various stimuli. The following sections will summarize my findings.

I first characterized components of the necrosome in macrophages treated with LPS in comparison to TNFα. I determined the dependency of necroptosis in each condition on pan-caspase activity (via co-treatment with the pan-caspase inhibitor, zVAD) as well as RipK1 activity (via co-treatment with the RipK1 inhibitor, Nec-1), and RipK3 activity (via co-treatment with the RipK3 inhibitor, GSK872). I observed that when pan-caspase activity is inhibited, LPS or TNFα treatment induces phosphorylation of RipK1 and RipK3 but reduces RipK1 expression (Fig. 6A, B). These same treatments cause an increase in cell death that can be abrogated by inhibiting the kinase function of RipK1 or RipK3 (Fig. 6E, F). Notably, these results were not observed in untreated

cells nor in cells treated with the pan-caspase inhibitor (zVAD) alone (Fig. 6C). Unless otherwise stated, all pro-necroptotic conditions I examine involved co-treatment with zVAD.

The mechanism by which the pan-caspase inhibitor zVAD influences necroptosis is unclear in the literature. While previous studies suggest that inhibition of caspase-8 activity is a requirement of necroptosis (Tom Vanden Berghe et al., 2004), other studies (McComb, Shutinoski, et al., 2014) are in disagreement. My experiments show that specific inhibition of caspase-8 fails to induce necroptosis. These results suggest that the induction of necroptosis by the pan-caspase inhibition may involve additional mechanisms that are promoted or suppressed by the pan-caspase inhibitor. It has been shown that cFLIPL, which is a caspase-8 homologue that lack catalytic activity, can interact with caspase-8 and act as an endogenous inhibitor of caspase-8 (X. Huang et al., 2018). However, a heteromer consisting of caspase-8 and cFLIP does retain some caspase-8 activity and it has been speculated that the activity of this heteromer is efficiently blocked by the pan-caspase inhibitor (Dickens et al., 2012; Hughes et al., 2009).

It has been previously reported that RipK1 deficient mice die within the first week of birth (Kelliher et al., 1998) as a result of uncontrolled activation of necrosis and apoptosis mediated by RipK3 and CASP-8 (Dillon et al., 2014; Roderick et al., 2014), suggesting that RipK1, RipK3 and CASP-8 regulate the over-activation of one other.

Although engagement of TLR-3 and -4 with ligands such as poly I:C or LPS respectively induces the phosphorylation of RipK1 and RipK3, the mechanism responsible remain unclear (Declercq, Vanden Berghe, & Vandenabeele, 2009; Degterev et al., 2008). To investigate these findings further, I characterized the role of two adaptor proteins: TRIF and MyD88.

Previously, He et al. (2011) reported that TRIF promotes the phosphorylation of RipK1 and necroptosis of macrophages upon TLR signalling. Similarly, others have found TRIF to be essential for TLR3,4-induced necroptosis (Kaiser et al., 2013; Saitoh et al., 2005). In agreement with these previous findings, I found that TRIF-deficient macrophages were significantly, but not completely, resistant to LPS-induced necroptosis (Fig. 9C), which was correlated to a significant attenuation of RipK3 phosphorylation (Fig. 9A).

TRIF is known to induce the activation of IRF3 and IRF7 in response to LPS which results in autocrine IFN production that is required for sustained activation of RipK3 and for necroptosis (McComb et al., 2014). My results revealed that the deficiency of TRIF also inhibited the degradation of RipK1 during TLR4- induced necrosome activation, suggesting that involvement of common signalling events during necrosome activation and degradation . In contrast, I observed that the induction and degradation of necrosome in response to TNFα-stimulation was not influenced by TRIF (Fig. 9B). These results suggest that the role of adaptors in necrosome signalling can vary with the nature of initial trigger.

I found the effects of TRIF versus MyD88 deficiency to be dramatically different. In contrast to TRIF, MyD88-deficiency had no impact on necroptosis (Fig. 9 C,D) or on the degradation of RipK1 (Fig. 9A, B) following either TNF- or LPS-induced necroptosis. Furthermore, MyD88-deficiency had no impact on phosphorylation of RipK3 following LPS-induced necroptosis. Thus, only TRIF is required for RipK3 activation in macrophages and is involved in RipK1-degradation in response to LPS-induced necrosome signalling.

Because previous studies have found that TRIF interacts with RipK3 (Kaiser et al., 2013; Saitoh et al., 2005) in the context of TLR-3,-4-induced necroptosis, I wanted to further investigate the involvement of RipK3 in RipK1 degradation. I found that RipK1 degradation was abrogated

in RipK3-null macrophages, independent of the type of pro-necroptotic treatment (Fig. 10), indicating that RipK3 promotes degradation of the necrosome. The role of RipK3 is complicated since inhibition of RipK3 kinase activity (GSK872/843) can prevent necroptosis (Kaiser et al., 2013; Mandal et al., 2014) (Fig. 13B, E, D), but has no impact on the degradation of RipK1, CASP8 and FADD proteins (Fig. 13A). The only protein degraded in this case was cIAP1,2 (Fig. 13A). These results suggest that the degradation of RipK1 is independent of the RipK3 kinase activity and of cIAP1,2 levels. These results indicate that the cell death (necrosome activation) and inhibition of cell death (degradation of necrosome proteins) can be uncoupled and this may be mediated by RipK3. I show that RipK3 promotes degradation of necrosome proteins whereas its kinase region promotes cell death.

To further examine the causes of degradation of RipK1 and other interacting protein during LPS-induced necroptosis, I evaluated the stability of RipK1 expression in cells deficient in MLKL, a downstream substrate of RipK3. Although *Mlkl*-deficient macrophages resembled RipK3 null macrophages in their complete resistance to necroptosis following LPS treatment (Fig. 10B), RipK1 was still degraded (Fig. 10E). These results indicate that the degradation of RipK1 and other interacting proteins occurs at an earlier step during necrosome signalling that does not involve MLKL. This result further indicates that the degradation of RipK1 and other interacting proteins can be uncoupled from cell death, as degradation proceeded normally even in cells that did not die (MLKL-deficient).

An unexpected result from these experiments was that RipK3 phosphorylation was abrogated in MLKL-deficient macrophages. Since MLKL lacks kinase function, this suggests that the RipK3-MLKL platform could provide a scaffold for RipK1-mediated phosphorylation of RipK3 or auto-phosphorylation of RipK3. It has been suggested that RipK3 is activated by interactions

with RHIM-containing proteins such as TRIF and the DNA-dependent activator of interferon (DAI) regulatory factor, neither or which have kinase activity (Moriwaki & Chan, 2017). Thus, it is most likely that a RipK3-MLKL platform would expose residues on RipK3 that facilitate RHIM-RHIM interactions between RipK3 and other proteins, or facilitate RipK3 dimerization and subsequent auto-phosphorylation (Cook et al., 2014; Wu et al., 2014). In this model, the rate of RipK3 activation and MLKL recruitment would determine the proportion of necroptotic death that occurs. To further test this model, I used RipK3 kinase inhibitors to block the formation of the late necrosome (RipK3-MLKL) (Fig. 14B) and found this resulted in resistance to necroptosis without having any impact on the degradation of various necrosome interacting proteins (Fig. 13 A-E).

Collectively, these data reveal a new mechanism of self-regulation built into necroptotic signalling, wherein RipK3 recruitment influences the competition between necrosomal degradation and necrosomal maturation. What remains missing from this model is the mechanism through which RipK3 is phosphorylated during necrosome signalling. Intriguingly, I have observed that inhibiting the activity of the Src kinase family fully inhibited necroptosis and RipK3 phosphorylation in response to both LPS- or TNF-induced necroptosis (data not shown).

Having determined that MLKL promotes necroptosis yet cannot explain the cause of RipK1 degradation, I considered the possibility that RipK1 auto-phosphorylation is required for its own degradation during necroptosis. I tested this idea by examining the effect of inhibiting RipK1 kinase activity with Necrostatin-1 (Nec-1) and a more stable variant of Nec-1, Nec-1S (N. Takahashi et al., 2012). Nec-1 has been demonstrated to bind to the RipK1 activation loop and stabilize RipK1 in an inactive confirmation, thus inhibiting the interaction between RipK1 and RipK3, and rescuing cells from necroptosis (He et al., 2011; Xie et al., 2013). Although I found that Nec-1 did not inhibit RipK1 phosphorylation, the degradation of RipK1 and other interacting

proteins was abolished (Fig. 11A, B). This suggests that RipK1 kinase activity or RipK1-RipK3 interaction is required for RipK1-degradation but not via RipK1 auto-phosphorylation. Furthermore, I examined RipK1 kinase mutant (K45A) cells, and found that although RipK1 phosphorylation was unaffected, RipK1 degradation was altered. Notably, this degradation differed according to the pro-necroptotic stimulus used: RipK1 degradation was prevented by K45A mutation of RipK1 in response to TNF (Fig. 8C) but not LPS (Fig. 8A) (Alturki et al., 2018).

To further understand the mechanisms responsible for phosphorylation of RipK1and their potential role in necrosome activation and degradation, I considered the potential role of other kinases. For example, Jaco et al., 2017 have shown that MK2, a kinase downstream of p38-^{MAPK}, induces an inhibitory phosphorylation on RipK1 at serine 321. To investigate whether p38-^{MAPK} influences RipK1 degradation, I examined the effect of pharmacological inhibition of p38-^{MAPK} activity. I found that inhibition of the p38^{MAPK} pathway completely abolished RipK1 phosphorylation, but RipK1 degradation was still detected (Fig. 12A). This result confirmed that RipK1 phosphorylation state does not impact the degradation of RipK1. Additionally, inhibiting the p38^{MAPK} pathway resulted in enhanced necroptosis of cells. This result agrees with the recent report of inhibitory phosphorylation (S321) of RipK1 mediated by MK2, the downstream kinase of the p38^{MAPK} pathway (Jaco et al., 2017).

RipK3 appears to have contrasting function of necrosome degradation and activation. On one hand, RipK3 kinase function is indispensable to the activation of necroptosis. On the other hand, the RipK3-RipK1 interaction results in the degradation of RipK1 and other necrosomal proteins. In my experiments, I found that the formation of an early necrosome platform initiates a decision between degradation via K48-ubiquitination or cell death via RipK3 kinase activity and MLKL recruitment (Fig. 14B).

Briefly, ubiquitination is a form of post-translational modification wherein a substrate is conjugated to ubiquitin molecules at specific residue and this process is mediated by the activity of three ATP dependent enzymes (E1, E2, and E3) (Deshaies & Joazeiro, 2009; A. Hershko & Ciechanover, 1998). First, the activation reaction involves the transfer of ubiquitin to E1 ligase in presence of ATP. (Seo et al., 2019)The activated ubiquitin is then transferred to ubiquitin conjugating enzyme E2. Lastly, E3 ligase transfers the ubiquitin from E2-ubiqutin complex to the lysine on a substrate protein (Berndsen & Wolberger, 2014; Deshaies & Joazeiro, 2009). Ubiquitin has an amino terminus and seven lysins residues (K6, K11, K27, K29, K33, K48, and K63) that can be ubiquitinated and each has a distinct function. K48 and K63 are the best characterized forms of polyubiquitination chains. K48-linked ubiquitination targets protein for proteasomal degradation whereas K63-linked ubiquitination promotes protein-protein interaction, leading to activation, protein trafficking and DNA damage repair (G. Wang et al., 2012).

Cell death pathways are highly regulated by ubiquitination, and the ubiquitination state of RipK1 influences many immune signalling pathways. For example, RipK1 ubiquitination at K63 controls cell survival via activation of NF-κB signalling (Ea, Deng, Xia, Pineda, & Chen, 2006), whereas RipK1 ubiquitination at K48 controls cell death via activation of apoptosis, necroptosis and pyroptosis pathways (Seo et al., 2019; Wertz et al., 2004). One of the aims of my thesis was to determine what proteolytic machinery is responsible for RipK1 degradation. By co-treating cells under conditions of LPS-induced RipK1 degradation with a 20S or 26S proteasomal inhibitor (lactacystin or MG321, respectively), the degradation of RipK1, CASP-8 and cIAP1,2 was significantly rescued (Fig. 16A, B), which in turn was associated with an increase in the level of phosphorylated RipK3 (Fig. 16A). In contrast, in a parallel experiment, lysosomal inhibition (hydroxychloroquine, HCQ) had no impact on RipK1 degradation. These experiments suggest

RipK1 degradation during LPS-induced necroptosis is driven mainly by the proteasome (Fig. 16C). I further investigated the ubiquitination status of RipK1 and found that cells were enriched with K48-ubiquitinated RipK1 - (Fig. 17C, D).

The E3 ligases cIAP1,2 have been reported to facilitate ubiquitination of RipK1, resulting in restriction of cell death pathway signalling via activation of MAPKs and NF-κB, whose signalling promotes prosurvival gene expression (M. J. Bertrand et al., 2008; Beug et al., 2012). Although cIAP1,2 are known for the addition of non-degradative K63-linked ubiquitin on RipK1 (M. J. M. Bertrand et al., 2011; Declercq et al., 2009), it has also been reported that cIAP1,2 can ubiquitinate RipK1 at K48 (M. J. M. Bertrand et al., 2011). To investigate the role of cIAP1,2 in RipK1 degradation I examined cells lacking cIAP1, cIAP2 or xIAP and found that IAPs had no effect on RipK1 degradation (Fig. 18A, C). I also used an alternative way of depleting cIAP1,2 and inactivating xIAP, via treatment with the SMAC mimetic Birinapant (BP). Treatment of cells with BP causes degradation of cIAP1/2 but had no impact on RipK1 degradation (Fig. 19A). These results indicate that RipK1 degradation during necroptosis occurs through a mechanism that does not involve IAPs. Notably, this conclusion was somewhat anticipated since my experiments suggest that cIAP1,2 and RipK1 are both degraded during LPS-induced necroptosis.

A family of deubiquitinases (DUBs), including A20 and CYLD, can influence the ubiquitin state of RipK1 and the progression towards necroptosis. For example, in response to TNFα, A20 has been shown to downregulate NF-κB signalling by removing the K63-ubiquitin chains from RipK1, resulting in RipK1 dissociation from the TNF-R-complex (Wertz et al., 2004). Additional studies have shown that A20 prevents the formation of the necrosome complex by deubiquitinating RipK3 at K63 which inhibits formation of the RipK1-RipK3 complex (Gurung, Man, & Kanneganti, 2015; Onizawa et al., 2015). Similarly, CYLD has been shown to deubiquitinate

RipK1 at K63, resulting in the dissociation of RipK1 from the TNFR at the plasma membrane , thereby facilitating interaction of RipK1 with other cytoplasmic proteins leading to the formation of cell death complexes (ripoptosome or necrosome) (Moquin et al., 2013; Najafov, Chen, & Yuan, 2017). To evaluate the roles of CYLD and A20 in RipK1 degradation during necroptosis, I performed knockdown of CYLD and A20, and evaluated the impact on RipK1 degradation. I found that these two DUBs did not contribute to the RipK1 degradation (Fig. 20A, B).

The experiments with *Cyld*-deficient cells nonetheless revealed that RipK3 activation is influenced by CYLD. Specifically, phosphorylation of RipK3 was impaired in *Cyld* -deficient cells (Fig. 20C). This observation is supported by a study wherein CYLD deficiency increased RipK1 ubiquitination, and impaired phosphorylation of both RipK1 and RipK3 (Moquin et al., 2013). Indeed, I have observed that during necrosome signalling, both CYLD and A20 expression levels and phosphorylation increase (Fig. 21A-C). These findings would agree with previous studies wherein CYLD was shown to undergo transient phosphorylation after stimulation with TNFα or LPS, negatively regulating its DUB activity (W. Reiley, Zhang, Wu, Granger, & Sun, 2005; S. C. Sun, 2010). Whether CYLD phosphorylation promotes necroptosis or not remains unknown.

To further identify potential regulators of RipK1 ubiquitination state and their role in RipK1 degradation, I considered the role of another E3 ligase, Triad3a. TRIAD3A (RNF216) has been shown to interact with the Toll/interleukin-1 receptor domain (TIR) of several TLRs (Chuang & Ulevitch, 2004), specifically TLR4, -9, -3 and -5 but not TLR2 (Chuang & Ulevitch, 2004). Triad3a restricts inflammatory responses by increasing K48-linked ubiquitination of these TLRs thus promoting their degradation and reducing their activation. Traid3a is further implicated in influencing signalling downstream of TLR and TNFR1, by promoting degradation of TIRAP, TRIF and RipK1 proteins (Fearns et al., 2006).

To examine the effect of TRIAD3A activity on necroptosis, I treated cells with *Triada3a*-targetted si-RNA. I found that reduction in TRIAD3A expression rendered macrophages hyperresponsive to LPS-induced necroptosis, resulting in increased cell death rate after one hour of stimulation (Fig. 22C). In addition, reduced Triad3a expression inhibited the RipK1 degradation as well as the degradation of other necrosomal proteins such as CASP-8, FADD and cIAP1,2 (Fig. 22B). Together, these results suggest that maintaining the necrosome stability exacerbates cell death. Unfortunately, due to the poor quality of anti-Triad3a antibodies, I was unable to investigate how Triad3a is recruited to the necrosome.

To further investigate the role of Triad3a in necroptosis, I considered the effect of Triad3a knockdown on cytokine production. Reduction in Triad3a expression augmented the production of pro-inflammatory cytokines TNF-α, IL-1β, IL-6 and IL-12 (Fig. 22E). These results reveal that Triad3a is a negative regulator of necrosome-degradation and cell death by necroptosis.

The identification of Triad3a as a negative regulator of necroptosis is highly relevant to human disease. In comparison to apoptosis, the cellular release of immunogenic signalling molecules (DMAPs) during necroptosis (Kaczmarek, Vandenabeele, & Krysko, 2013; Pasparakis & Vandenabeele, 2015) promotes inflammatory responses. Understanding the mechanisms of activation and inhibition of necroptosis opens opportunities to develop therapeutic strategies to stop inflammation in various conditions.

5.2. IFN-I signalling and necroptosis of macrophages

The importance of IFN-I signalling in initiating necroptosis of macropahges was highlighted in several published studies, and lead me to investigate, in the second aim of my thesis, the underlying mechanisms responsible for necrosome signalling following engagement of the type-I

interferon receptor. First, a study from our lab, Robinson et al. (2012) reported that type-I interferon-deficient macrophages resist *Salmonella enterica* serovar Typhimurium induced cell death. In the same study, it was reported that *Salmonella* Typhimurium infection resulted in capsase-8 inhibition and necroptosis via type-I interferon signalling that limited pathogen control (Robinson et al., 2012). In a second study by Hos et al. (2017), *Salmonella* Typhimurium was shown to promote necroptosis by type-1 IFN-dependent inhibition of antioxidative stress responses. A third study, also from our lab (McComb et al., 2014), demonstrated that type-I interferon signalling via the ISGF3 complex is indispensable for necroptosis of macrophages. This finding was confirmed by another research group (Legarda et al., 2016), who showed that type-I IFN signalling promote necroptosis of macrophages. Finally, in 2018, separate studies showed that type-I interferon signalling is critical in promoting necroptosis during *Acinetobacter baumannii* infection (Yang Li et al., 2018) and that tonic IFN-I signalling maintains a critical threshold of MLKL expression that is required to induce necroptosis of macrophages (Sarhan et al., 2019).

To further delineate the molecular mechanism of type-I IFN induced necroptosis, I examined the role of TRIF, IKKε, and IRF-9 that promote IFN-I production/signalling. In these experiments, I observed that TRIF-deficient cells were significantly, but not completely, resistant to LPS-induced necroptosis (Fig. 23B) and had undetectable levels of phosphorylated RipK3 (Fig 9A). Notably, this result agrees with a previous study (Hyvert & Imler, 2010), which showed that loss of TRIF impairs phosphorylation of IRF3 and subsequently compromised production of IFNβ in response to LPS stimulation.

MYD88 is a TLR4 adaptor protein that when deleted does not impart resistance to LPS-induced necroptosis (Fig. 23B). MyD88 is known to be involved in type-I IFN induction by interacting with IRF1, IRF5 and IRF7 (O'Neill & Bowie, 2007). These interactions lead to the

translocation of IRF3 to the nucleus which results in the expression of type-I interferon. Once expressed, IFNβ is known to bind to its receptor, IFNAR1, in an autocrine manner. Although MyD88 may promote type-I IFN production (O'Neill & Bowie, 2007), the role of TRIF appears to be more dominant in both IFNβ production (K. Honda, Yanai, Takaoka, & Taniguchi, 2005) and induction of cell death by necroptosis (Fig. 23C)

Collectively, my results, combined with previous studies, demonstrate that the type-I IFN-receptor and its "immediate-downstream" signalling proteins (TYK2, JAK1) induce necroptosis of macrophages. Engagement of the type-I interferon receptor is previously reported to result in the formation of the heterotrimeric complex called interferon stimulatory gene factor 3 (ISGF3). This complex is composed of two signal transducer and activator of transcription proteins (STAT1, STAT2) and interferon regulatory factor 9 (IRF9) (Kenya Honda, Takaoka, & Taniguchi, 2006). In my experiments, *Irf9*-deficient macrophages showed similar resistance to that observed in *Ifnar1*-deficient macrophages (Fig. 23E). IRF9 promotes recognition of the ISRE sites in the promotor regions of genes, and IRF9-DNA-binding allows ISGF3 to activate transcription of genes that harbor ISRE sites (Tsuno et al., 2009). The importance of IRF9 was further demonstrated in a study from our lab (McComb et al., 2014), which showed that *Irf9*-deficiency reduces RipK3 phosphorylation and necroptosis.

I also characterized type-I interferon signalling in response to IFNβ. One of my first findings was that *Ifnar1*-deficient macrophages were completely resistant to IFNβ-induced necroptosis, as expected (Fig. 24B). I additionally showed that *Tyk2* deficiency mimicked the resistance observed in *Ifnar1*-deficient macrophages (Fig. 24C). Tyrosine kinase 2 (TYK2) is kinase that belong to a Janus kinase family of non-receptor tyrosine kinases whose activation mediates immune signalling. TYK2 play a vital role in both innate and adaptive immunity (Minegishi et al., 2006).

After engagement of type-I IFN receptor and receptor dimerization JAK1 and TYK2 bind to IFNAR2 and IFNAR1 respectively. This binding increases the kinase activity through transphosphorylation. Both kinases phosphorylate tyrosine residues in the receptor subunits that serve as docking site for Src homology 2 (SH2) domain of signal transducer and activator of transcription (STAT) family. Upon association of STATs with the receptor, STATs are phosphorylated by JAK1 and TYK2 at their tyrosine residues which stimulates the formation of STAT heterodimers. In type-I IFN signalling the phosphorylation of STAT1 and STAT2 recruits IRF9 leading to the formation of ISGF3 (Blaszczyk et al., 2016). TYK2 scaffolds are required for surface expression of IFNAR1 (Ragimbeau et al., 2003). TYK2 kinase activity is also required for functional type-I interferon response (Prchal-Murphy et al., 2012). The necroptosis-resistance seen in *Tyk2*-deficient macrophages is due to the defect in the overall type-I IFN signalling which results in the impairment of the formation of ISGF3 that is required for necropsies (McComb et al., 2014).

I additionally examined the effect of blocking the tyrosine kinase (JAK1), which also resulted in the resistance of macrophages to IFN-β induced necroptosis (Fig. 24D). It is possible that this resistance is due to off-target effects, since the Jak1 inhibitor that I used may inhibit JAK1, JAK2, JAK3 and TYK2. To precisely examine the effect of Jak1 inhibition, a specific JAK1 inhibitor or knockdown of JAK1 expression would be required. Nonetheless, a recent study showed that blocking JAK1 with Ruxolitinib down regulates IRF7 and STAT1 levels (Sarhan et al., 2019), an effect known to impair the formation of ISGF3, which is required for necroptosis (McComb et al., 2014). In summary, it appears that the IFNAR1 receptor and its protein kinases (TYK2 and JAK1) are required to induce necroptosis of macrophages.

Although necrosome formation is well characterized for TNF-induced necroptosis in fibroblasts, it is unclear whether or not necrosome formation occurs following IFN signalling,

particularly in macrophages. This gap in knowledge was the basis of one of the aims of my thesis. Towards this aim, I showed that engagement of TLR4 with LPS, in presence of the pan caspase inhibitor (zVAD), results in the formation of a necrosome that results in RipK1,RipK3 and MLKL interaction, leading to necroptosis.

It remains an open question whether necrosome signalling following IFN-β treatment is different than that induced by LPS or TNF-α. My experiments suggest that type-I interferon signalling promotes necroptosis induced by LPS, IFNβ or TNFα which is indicative of a dominant role played by IFN-I pathway. My experiments appear to indicate that the kinetics of necrosome signalling may differ depending on the stimulus used. The phosphorylation of RipK3 was detectable at a much earlier time interval during LPS induced necrosome signalling in comparison to IFNβ induced necroptosis where pRipK3 was detectable much later. I have also observed that *Ifnar1*-deficient macrophages are completely resistant to necroptosis in response to IFNβ-, but not in response to LPS, which suggests that there may be other pathways of necroptosis induction during LPS signalling which may be IFNAR1-independent.

5.2.1 IKKε inhibits RipK1 activation

Based on previous literature, I hypothesized that the resistance of TRIF-deficient cells to necroptosis was dependent on the downstream mediators of IRF3-signalling such as IKKε and TANK-binding kinase 1 (TBK1). IKKε and TBK1 are non-canonical IκB kinases that function downstream of TRIF, as well as in multiple other signalling pathways. Their activation results in phosphorylation of IRF3, thereby inducing the expression of IFNβ (Ahmad, Zhang, Casanova, & Sancho-Shimizu, 2016; Fitzgerald et al., 2003). It was reported that IRF3-deficiency results in significant resistance of macrophages to necroptosis (McComb et al., 2014). By conducting

experiments to examine the contributions of IKKε and TBK1 to LPS-induced necroptosis, I found that necroptosis was enhanced in macrophages lacking IKKε (Fig. 27A-C). Similarly, inhibiting TBK1 also enhanced necroptosis in macrophages (Fig. 27D). These findings demonstrate that both IKKε and TBK1 inhibit necroptosis of macrophages. Indeed, two recently published studies (Lafont et al., 2018; Xu et al., 2018) have reported this result, and more specifically showed that IKKε and TBK1 promote inhibitory phosphorylation of RipK1 that limits its pro-death function. Lafont et al, showed this result in the context of TNF-stimulation, wherein pharmacological inhibition or genetic ablation of IKKε and TBK1 prevented RipK1 activation, phosphorylation and promoted TNF-induced necroptosis or apoptosis by inducing formation of the cell death complex II. Taken together, IKKε and TBK1 restricts necroptosis induced by multiple stimuli, however, their mechanism of inhibiting RipK1 in the context of TLR4 or IFN-I stimulation remains unclear.

5.2.2 TNFR2 expression is not modulated during necroptosis signalling in macrophages

A previous study reported that, similarly to LPS-induced necroptosis, TNF-induced necroptosis required type-I IFN signalling, however the mechanism underlying this requirement remained unclear (McComb et al., 2014). I first corroborated this finding in my experiments, wherein I showed that treatment of cells with TNF in the presence of the pan caspase inhibitor zVAD failed to induce necroptosis in IFNAR1- or TYK2-deficient macrophages, concluding that TNF-induced necroptosis is type-I interferon dependent (Fig. 26A, B). Thereafter, I sought to investigate the mechanism of this dependency. Recently, it was reported that the defect in TNF-mediated necroptosis in IFNAR1 knockout cells is due to poor expression of the TNF receptor-2 (Legarda et al., 2016). In this study the authors demonstrated that the expression of TNFR2 was induced upon LPS stimulation in an IFNα/β-dependent manner. These results led me to investigate the role of TNFR2 in necroptosis. In my experiments, I found that cells deficient in the TNFR2

receptor were significantly resistant to LPS-induced necroptosis while TRNFR1-deficient cells were susceptible (Fig. 23A). However, I found that TNFR2 expression was unaffected by the loss of IFNAR1 in macrophages (Fig. 28C). This is contradictory to the results reported by Legarda et al, 2016, I found that none of the treatments I performed on cells had any impact on TNFR2 expression (Fig. 28B). Even by western blot analysis I did not observe any impact of IFNAR1 signalling on TNFR2 expression levels in macrophages (Fig. 28D). Despite the inconsistency between my results and those of Legarda et al. (2016), their study had additional results that support the notion that the dependency of TNF-induced necroptosis on IFNAR1 activity is not due to the effect on TNFR2 expression. Specifically, they (Legarda et al., 2016) showed that restoring the expression of TNFR2 in *Ifnar1*-deficient cells was insufficient to reverse the resistance observed in *Ifnar1*-deficient cells.

5.2.3 The role of IFNAR1 signalling in necrosome formation

To further examine the role of the IFNAR1 signalling pathway in necroptosis, I evaluated necrosome formation in response to LPS (with zVAD) under various conditions. First, I observed that total phosphorylation of RipK1, which mainly appears to be the inhibitory phosphorylation of RipK1 as per (Fig. 29 A), was similar in WT and *Ifnar1*-deficient macrophages (Fig. 29 A). Thus, there isn't any increased inhibitory RipK1 phosphorylation observed in *Ifnar1*-deficient macrophages. In comparison to the total phosphorylation of RipK1, I also showed that type-I IFN signalling does not have any impact on the phosphorylation of RipK1 at serine 166) (Fig. 30A), and that the mRNA levels of RipK1 are unaffected by *Ifnar1*-deficiency (Fig. 31C). Phosphorylation of RipK1 at Serine 166 is considered to be the first signalling step that leads to necrosome signalling (Jaco et al., 2017), and my results indicate that this step is not compromised in *Ifnar1*-deficient cells. Thus, the resistance of *Ifnar1*-deficient cells must occur downstream of

RipK1 phosphorylation. I also observed that the phosphorylation of RipK3 was impaired and drastically reduced in *Ifnar1*-deficient macrophages (Fig. 29 A). The reduction in RipK3 phosphorylation therefore likely explains the phenotype of *Ifnar1*-deficient cells (Fig. 29B). Notably, these results indicate that IFN signalling is required to sustain RipK3 phosphorylation.

I also examined the expression of other proteins that have been reported to promote or inhibit necroptosis in fibroblasts. In these experiments, I showed that the deubiquitinases A20 and cylindromatosis (CYLD) had slightly increased levels in *Ifnar1*-deficient macrophages (Fig. 29A). CYLD is known to induce necroptosis by deubiquitinating K63-linked- and M1- linked chains from RipK1, thereby allowing RipK1 to interact with RipK3, and subsequently leading to necrosome formation. In addition, CYLD has been shown to negatively regulate IFN signalling by removing K63-linked chains from the retinoic acid-inducible gene I (RIG-I) and TBK1 proteins, thereby leading to inhibition of IFN production (Friedman et al., 2008).

The second protein, A20 (also known as TNFAIP3), is a known endogenous inhibitor of inflammation, and an important ubiquitin-editing enzyme. It has been shown that A20 is a potent inhibitor of the TRIF pathway. A20 has been shown to interact with TBK1 and IKKε, thereby suppressing the activation of IRF3, and hence inhibiting transcription of type-I IFN (T. Saitoh et al., 2005; Verstrepen et al., 2010; Y. Y. Wang, Li, Han, Zhai, & Shu, 2004). In humans, A20 activity is regulated by phosphorylation of serine 381 by IKKβ, which results in downregulation of NF-κB signalling. In my experiments, the absence of type-I IFN signalling leads to an increase in the levels of A20 during necrosome signalling, however, the precise function of A20 phosphorylation in the context of necroptosis requires further investigation (Fig. 29A). Lastly, knockdown of A20 in *Ifnar1*-deficient macrophages did not impact their resistance to necroptosis

(Fig. 36D). This suggests that the enhanced levels of A20 in *Ifnar1*-deficient macrophages are not responsible for poor cell death by necroptosis.

5.2.4 Gene expression profiling of IFNAR1-deficient cells during necrosome signalling.

By performing microarray analysis, I observed that numerous genes are downregulated in *Ifnar1*-deficient macrophages during necrosome signalling in macrophages (Fig. 32, 33). Among these genes, I selected several for which I performed additional screening and validation experiments. First, I found that the TNF-related apoptosis-inducing ligand, TRAIL, was downregulated in *Ifnar1*-deficient macrophages. TRAIL is a well-characterized cytokine that induces apoptosis in tumor cells by engaging DR4 (TRAIL-R1) and DR5 (TRAIL-R2) (Gonzalvez & Ashkenazi, 2010). TRAIL is also reported to induce necroptosis in Jurkat cells (Holler et al., 2000), murine prostate endocarcinoma cells (Kemp, Kim, Crist, & Griffith, 2003) HT29 colon and HepG2 liver cancer cells through RipK1-RipK3-PARP-1 activation (Jouan-Lanhouet et al., 2012; Voigt et al., 2014). To validate the impact of TRAIL on necroptosis, I supplemented *Ifnar1*-deficient macrophages with murine recombinant TRAIL and found that this does not result in induction of necroptosis (Fig. 34A). In addition, TRAIL supplementation did not enhance LPS-induced necroptosis in WT macrophages (Fig. 34A) and failed to abrogate the resistance of *Ifnar1*-deficient cells to necroptosis. Together these results suggest that although TRAIL expression is influenced by IFNAR1 signalling, this may not explain the resistance of *Ifnar1*-deficient cells to necroptosis.

Microarray analysis also revealed that IFIT-2 was considerably downregulated in *Ifnar1*-deficient macrophages. Interferon-induced proteins with tetratricopeptide repeats-2 (IFIT-2) is one

of many host protective antiviral genes encoded by interferon-stimulated genes (ISGs). IFIT-2 expression has be reported to be induced upon activation of ISGF3 and pattern recognition receptors (PRR) (Mears & Sweeney, 2018). Additionally, several studies have identified, in different cell lines, that IFIT-2 promotes apoptosis by activating caspase-3 (L. Chen et al., 2017; Stawowczyk, Van Scoy, Kumar, & Reich, 2011). To elucidate the role of IFIT-2 on necroptosis, I examined *Ifit-2*-deficient macrophages in response to various necroptotic stimulations. However, I found *Ifit-2*--deficient macrophages were not resistant to necroptosis. Furthermore, deletion of the entire IFIT-locus did not impact the susceptibility of macrophages to necroptosis (Fig. 34B). These findings suggest that IFIT locus is not responsible for the necroptosis-resistance observed in *Ifnar1* knockout cells.

Another relevant gene that I found to be downregulated in the absence of type-I interferon signalling was the glucocorticoid-induced tumor necrosis factor (GITR, TNFRSF18). GITR has been previously linked to limited clonal expansion by controlling apoptosis in activated T cells (Ronchetti, Nocentini, Riccardi, & Pandolfi, 2002), although the role of GITR in macrophages and necroptosis is unknown. To evaluate the contribution of GITR on necroptosis, I examined the viability of *Gitr*-deficient cells with various stimuli. No resistance was observed in GITR-knockout cells (Fig. 35) and therefore GITR downregulation does not appear to be related to the resistance of *Ifnar1*-deficient cells.

In addition to looking at the expression of pro-cell death genes, I also analyzed the expression of anti-cell death genes. In this regard, I observed that the expression of inhibitor of apoptosis proteins (cIAP1/2) was similar between WT and *Ifnar1*-deficient cells (Fig. 29A). Interestingly, I observed that the expression of XAF1 (XIAP-associated factor 1), a XIAP interacting protein that is known to antagonize XIAP function by suppressing its anti-caspase activity (Liston et al., 2001)

was potently impacted by *Ifnar1*-deficiency. Furthermore, XAF1 is a known transcriptional co-activator of interferon regulatory factor-1 (IRF-1) (Jeong et al., 2018), and IRF-1 is required for TNF-induced IFN-β production (Venkatesh et al., 2013; Yarilina, Park-Min, Antoniv, Hu, & Ivashkiv, 2008). Lastly, a previous study from our lab showed that IRF-1-deficient cells are protected against TNF-, LPS-induced necroptosis (McComb et al., 2014). Taken together, these studies indicated that *Xaf1* may be a relevant gene that promotes type-I interferon induced necroptosis of macrophages.

I performed qRT-PCR analysis to confirm the impact of IFNAR1-signalling on XAF1 expression. Deficiency of type-I IFN signalling resulted in a significant reduction of XAF1 expression (Fig. 37A). In addition, I found that the induction of necroptosis via TLR signalling significantly induced the expression of XAF1 in control cells. Although it would be ideal to evaluate the necroptosis susceptibility of XAF1-null macrophages, XAF1 deficiency is embryonically lethal and therefore I used mice that are heterozygous for XAF1 ($Xaf1^{+/-}$). I observed that $Xaf1^{+/-}$ macrophages were significantly resistant to TNF- and IFN-induced necroptosis but not to LPS stimulation (Fig. 37B), suggesting that indeed XAF1 may have stimulus-dependent role in necroptosis.

Given that the activation of MLKL is reported to be an obligatory terminal signalling step of necroptosis, I evaluated the expression level of MLKL in IFNAR1-knockout cells following LPS stimulation. It has been published recently that constitutive IFN signalling is crucial to maintain the threshold of MLKL needed for the rapid response of necroptosis (Sarhan et al., 2019). I observed that the impaired type-I IFN signalling resulted in a reduced expression of MLKL compared to WT controls (Fig. 37C). Furthermore, I observed that during LPS-induced necroptosis, IFN signalling promotes phosphorylation of MLKL at serine-345 (western blot and

Confocal Microscopy) (Fig. 38A, Fig. 40). Interestingly, *Ifnar1*-deficient macrophages showed poor formation of the MLKL trimers (Fig. 39C, D) and this might explain the 10-30% of cell death observed in *Ifnar1*-deficient macrophages. However, it has been recently reported that overexpression of MLKL in *Ifnar1*-deficient macrophages does not sensitize cells to necroptosis (Legarda et al., 2016; Sarhan et al., 2019). This indicates that there may be other mechanisms besides reduced MLKL expression that are responsible for poor necroptosis in *Ifnar1*-deficient macrophages. The activation of type-I IFN signalling leads to the induction of hundreds of IFN-stimulated genes (ISGs) and because of this finding, it is possible that other unknown protein(s) may contribute to MLKL phosphorylation. Additionally, it is possible that other unknown protein(s) play a role within the RipK3 scaffold to bring MLKL in a position required for its phosphorylation. To date, RipK3 activation was always thought to be upstream of MLKL, but I noticed in my experiments that RipK3 phosphorylation was severely impaired in *Mlkl*-deficient macrophages (Fig. 38 D, E), suggesting that there may be a feedback mechanism.

5.2.5 Inhibition of the p38^{MAPK} pathway abrogates the resistance of *Ifnar1*-deficient macrophages to necroptosis

Induction of type-I interferon signalling leads to the activation of various pathways, including the JAK-STAT and p38 Map kinase signalling cascades. It has been reported that p38^{MAPK} plays a critical role in the induction of IFN responses and is essential for gene transcription via binding to the GAS or ISRE elements that are present in the promoter region of genes (Platanias, 2003; Uddin et al., 2000). The process of phosphorylation of STAT(s), formation of the STAT complex(es) and binding of STAT(s) complex to the promoter region of interferon-stimulated response element (ISRE) are all unaffected by the P38^{MAPK} pathway (Y. Li et al., 2004; Uddin et

al., 1999). McGuire et al. (2017) showed that mitogen- and stress-activated kinases 1 and 2 (MSK1/2) negatively regulate IFNβ expression in macrophages through the dephosphorylation and inactivation of $p38^{MAPK}$. In addition, it has been reported that $p38^{MAPK}$ enhances IFNγ-induced gene expression in a STAT1 dependent manner (Ramsauer et al., 2002). Taken together, these studies suggested there may be a correlation between p38 activity and type-I interferon signalling. To characterize this possibility, I measured cell viability following LPS stimulation in cells where $p38^{MAPK}$ activity was blocked by a p38 inhibitor. Interestingly, inhibition of the p38 cascade significantly enhanced cell death of *Ifnar1*-deficient macrophages. This was the first result of many experiments where I could enhance necroptosis in *Ifnar1*-deficient macrophages (Fig. 42C). Cell death in *Ifnar1*-deficient macrophages induced by inhibition of the $p38^{MAPK}$ pathway was inhibitable by the RipK3 inhibitors, confirming the mode of cell death as necroptosis (Fig. 42C). After achieving this result, I evaluated the activation of phospho RipK3 and MLKL in the presence or absence of the p38 inhibitor. In these experiments, I observed that inhibition of the p38 pathway resulted in increased phosphorylation of RipK3 and MLKL in *Ifnar1*-deficient cells (Fig. 42A), which corroborates the cell viability data (Fig. 42C).

Induction of necroptosis is known to result in the secretion of inflammatory cytokines such as TNFα, IL-6, and IL-1β. Therefore, I measured the production of TNFα as a primary outcome of LPS stimulation. I found that *Ifnar1*- -deficient cells expressed significantly higher levels of TNFα compared to control cells (Fig. 42D). Inhibition of p38 signalling significantly impacted TNFα production in both WT and *Ifnar1*-deficient cells (Fig. 42D). The reduction of TNFα level is expected in this case since Tristetraprolin (TTP), the major regulator of TNFα, is active when $p38^{MAPK}$ activity is blocked. Further exploration into how inhibition of the p38 pathway induces necroptosis in *Ifnar1*-knockout cells is required to unveil the mechanism leading to necroptotic

cell death. Taken together, my results have increased the knowledge about the relationship between p38 signalling and type-I interferon signalling in the control of necroptosis in macrophages. Type-I IFN signalling promotes necroptosis and understanding the mechanisms of this phenomenon is crucial to understanding necroptosis, as well as the development of therapies for the treatment of inflammatory diseases.

6.0 CONCLUSION

The work presented in this doctoral thesis reveals some novel insights into the molecular mechanisms that regulate necrosome signalling during necroptosis of macrophages. I have revealed that activation of necrosome signalling results in the degradation of necrosome complex through the activity of Triad3a ligase. Specifically, I showed the specific recruitment of RipK3 to the initial necroptosis activating complex, which I identify as the 'early necrosome', which specifically causes the degradation of several key necrosome interacting proteins, including RipK1, CASP-8 and FADD. The degradation acts as an auto-regulatory mechanism for the necrosome and acts to delay necroptosis and decrease inflammatory cytokine production. Interestingly, that assembly of the necrosome without cell death via MLKL activation can lead to prolonged degradation of necrosomal signalling mediators, resulting in a cell with profound resistance to cell death and lower cytokines production. My results indicate that proteasomal degradation is driven by negative feedback by K48-ubiquitination which is dependent on the E3 ligase Triad3a. Furthermore, I showed that only RipK3 scaffold promotes necrosome degradation in macrophages. In this research project, I have showed for the first time that Triad3a inactivates necrosome signaling and profoundly cell death. Understating the autoregulatory mechanisms of necrosome formation is crucial and had a great impact on understanding this inflammatory form of death and present new molecules as a potential drug targets in various inflammatory diseases.

A previous work published by McComb et al., (2014) in Dr. Sad's lab, I next investigated the resistance the mechanisms responsible for necrosome signalling following engagement of type-I interferon receptor (IFNAR) of macrophages. I showed that IFNAR1 signalling is essential for LPS – and TNF-induced necroptosis in macrophages. Moreover, TNF-mediated necroptotic cell death is dependent on type-I IFN signalling and not the opposite. Importantly, my results indicate that type-I IFN signalling promotes the phosphorylation of RipK3 and the phosphorylation and trimerization of MLKL. My results also revealed that the inhibition of $p38^{MAPK}$ pathway enhanced phosphorylation of RipK3 and MLKL and overcomes the resistance of *Ifnar1*$^{-/-}$ macrophages to LPS-induced necroptosis. Further investigations are needed to reveal the interaction between p38 signalling and type-I interferon signalling in the control of necroptosis in macrophages. Type-I IFN signalling promotes necroptosis and understanding the mechanisms of this phenomenon is crucial to understanding necroptosis, as well as the development of therapies for the treatment of inflammatory diseases.

CONTRIBUTIONS OF COLLABORATORS

Collaborator	Affiliation(s)	Contribution
Dr. Subash Sad	University of Ottawa	Supervisor
Dr. Robert G. Korneluk	Children's Hospital of Eastern Ontario	Thesis Advisory Committee Member
Dr. Alexandre Blais	University of Ottawa	Thesis Advisory Committee Member
Dr. Daniel Figeys	University of Ottawa	Thesis Advisory Committee Member
Dr. Scott McComb	National Research Council	Manuscript revision
Dr. Katey Rayner	University of Ottawa Heart institute	Confocal microscopy
Dr. Anne-Claire Duchez	University of Ottawa Heart institute	Performed confocal microscopy and imaging
Ms. Kim Kwangsin	University of Ottawa	Former technician in the Sad lab. Responsible for maintaining mouse colony and in charge of media, reagent, inhibitor preparation.

REFERENCES

Aderem, A. (2003). Phagocytosis and the inflammatory response. *J Infect Dis, 187 Suppl 2*, S340-345. doi:10.1086/374747

Aderem, A., & Underhill, D. M. (1999). Mechanisms of phagocytosis in macrophages. *Annu Rev Immunol, 17*, 593-623. doi:10.1146/annurev.immunol.17.1.593

Ahmad, L., Zhang, S. Y., Casanova, J. L., & Sancho-Shimizu, V. (2016). Human TBK1: A Gatekeeper of Neuroinflammation. *Trends Mol Med, 22*(6), 511-527. doi:10.1016/j.molmed.2016.04.006

Ahn, D., & Prince, A. (2017). Participation of Necroptosis in the Host Response to Acute Bacterial Pneumonia. *Journal of innate immunity, 9*(3), 262-270. doi:10.1159/000455100

Alturki, N. A., McComb, S., Ariana, A., Rijal, D., Korneluk, R. G., Sun, S.-C., . . . Sad, S. (2018). Triad3a induces the degradation of early necrosome to limit RipK1-dependent cytokine production and necroptosis. *Cell Death & Disease, 9*(6), 592. doi:10.1038/s41419-018-0672-0

Amarante-Mendes, G. P., Adjemian, S., Branco, L. M., Zanetti, L. C., Weinlich, R., & Bortoluci, K. R. (2018). Pattern Recognition Receptors and the Host Cell Death Molecular Machinery. *Frontiers in immunology, 9*, 2379-2379. doi:10.3389/fimmu.2018.02379

Annibaldi, A., & Meier, P. (2018). Checkpoints in TNF-Induced Cell Death: Implications in Inflammation and Cancer. *Trends Mol Med, 24*(1), 49-65. doi:10.1016/j.molmed.2017.11.002

Ashley, N. T., Weil, Z. M., & Nelson, R. J. (2012). Inflammation: Mechanisms, Costs, and Natural Variation. *Annual Review of Ecology, Evolution, and Systematics, 43*(1), 385-406. doi:10.1146/annurev-ecolsys-040212-092530

Berger, S. B., Kasparcova, V., Hoffman, S., Swift, B., Dare, L., Schaeffer, M., . . . Gough, P. J. (2014). Cutting Edge: RIP1 kinase activity is dispensable for normal development but is a key regulator of inflammation in SHARPIN-deficient mice. *J Immunol, 192*(12), 5476-5480. doi:10.4049/jimmunol.1400499

Berghe, T. V., van Loo, G., Saelens, X., van Gurp, M., Brouckaert, G., Kalai, M., . . . Vandenabeele, P. (2004). Differential Signaling to Apoptotic and Necrotic Cell Death by Fas-associated Death Domain Protein FADD. *Journal of Biological Chemistry, 279*(9), 7925-7933. doi:10.1074/jbc.M307807200

Berghe, T. V., Vanlangenakker, N., Parthoens, E., Deckers, W., Devos, M., Festjens, N., . . . Vandenabeele, P. (2009). Necroptosis, necrosis and secondary necrosis converge on similar cellular disintegration features. *Cell Death Differ, 17*, 922. doi:10.1038/cdd.2009.184

https://www.nature.com/articles/cdd2009184#supplementary-information

Bergsbaken, T., Fink, S. L., & Cookson, B. T. (2009). Pyroptosis: host cell death and inflammation. *Nature reviews. Microbiology, 7*(2), 99-109. doi:10.1038/nrmicro2070

Berndsen, C. E., & Wolberger, C. (2014). New insights into ubiquitin E3 ligase mechanism. *Nature Structural &Amp; Molecular Biology, 21*, 301. doi:10.1038/nsmb.2780

Bertrand, M. J., Milutinovic, S., Dickson, K. M., Ho, W. C., Boudreault, A., Durkin, J., . . . Barker, P. A. (2008). cIAP1 and cIAP2 facilitate cancer cell survival by functioning as E3 ligases that promote RIP1 ubiquitination. *Mol Cell, 30*(6), 689-700. doi:10.1016/j.molcel.2008.05.014

Bertrand, M. J. M., Lippens, S., Staes, A., Gilbert, B., Roelandt, R., De Medts, J., . . . Vandenabeele, P. (2011). cIAP1/2 are direct E3 ligases conjugating diverse types of ubiquitin chains to receptor interacting

proteins kinases 1 to 4 (RIP1-4). *PloS one, 6*(9), e22356-e22356. doi:10.1371/journal.pone.0022356

Beug, S. T., Cheung, H. H., LaCasse, E. C., & Korneluk, R. G. (2012). Modulation of immune signalling by inhibitors of apoptosis. *Trends in Immunology, 33*(11), 535-545. doi:https://doi.org/10.1016/j.it.2012.06.004

Blaszczyk, K., Nowicka, H., Kostyrko, K., Antonczyk, A., Wesoly, J., & Bluyssen, H. A. R. (2016). The unique role of STAT2 in constitutive and IFN-induced transcription and antiviral responses. *Cytokine & growth factor reviews, 29*, 71-81. doi:https://doi.org/10.1016/j.cytogfr.2016.02.010

Bonilla, F. A., & Oettgen, H. C. (2010). Adaptive immunity. *J Allergy Clin Immunol, 125*(2 Suppl 2), S33-40. doi:10.1016/j.jaci.2009.09.017

Boxx, G. M., & Cheng, G. (2016). The Roles of Type I Interferon in Bacterial Infection. *Cell host & microbe, 19*(6), 760-769. doi:10.1016/j.chom.2016.05.016

Buchmann, K. (2014). Evolution of Innate Immunity: Clues from Invertebrates via Fish to Mammals. *Frontiers in immunology, 5*, 459-459. doi:10.3389/fimmu.2014.00459

Buckley, C. D., Gilroy, D. W., Serhan, C. N., Stockinger, B., & Tak, P. P. (2012). The resolution of inflammation. *Nature Reviews Immunology, 13*, 59. doi:10.1038/nri3362

Cai, Z., Jitkaew, S., Zhao, J., Chiang, H. C., Choksi, S., Liu, J., . . . Liu, Z. G. (2014). Plasma membrane translocation of trimerized MLKL protein is required for TNF-induced necroptosis. *Nat Cell Biol, 16*(1), 55-65. doi:10.1038/ncb2883

Cargnello, M., & Roux, P. P. (2011). Activation and function of the MAPKs and their substrates, the MAPK-activated protein kinases. *Microbiology and molecular biology reviews : MMBR, 75*(1), 50-83. doi:10.1128/MMBR.00031-10

. Chapter 3 - Innate Immunity. (2014). In T. W. Mak, M. E. Saunders, & B. D. Jett (Eds.), *Primer to the Immune Response (Second Edition)* (pp. 55-83). Boston: Academic Cell.

Chen, G. Y., & Nuñez, G. (2010). Sterile inflammation: sensing and reacting to damage. *Nat Rev Immunol, 10*(12), 826-837. doi:10.1038/nri2873

Chen, H. M., Tanaka, N., Mitani, Y., Oda, E., Nozawa, H., Chen, J. Z., . . . Takaoka, A. (2009). Critical role for constitutive type I interferon signaling in the prevention of cellular transformation. *Cancer Sci, 100*(3), 449-456. doi:10.1111/j.1349-7006.2008.01051.x

Chen, K., Liu, J., & Cao, X. (2017). Regulation of type I interferon signaling in immunity and inflammation: A comprehensive review. *Journal of Autoimmunity, 83*, 1-11. doi:https://doi.org/10.1016/j.jaut.2017.03.008

Chen, L., Liu, S., Xu, F., Kong, Y., Wan, L., Zhang, Y., & Zhang, Z. (2017). Inhibition of Proteasome Activity Induces Aggregation of IFIT2 in the Centrosome and Enhances IFIT2-Induced Cell Apoptosis. *Int J Biol Sci, 13*(3), 383-390. doi:10.7150/ijbs.17236

Cheon, H., Holvey-Bates, E. G., Schoggins, J. W., Forster, S., Hertzog, P., Imanaka, N., . . . Stark, G. R. (2013). IFNβ-dependent increases in STAT1, STAT2, and IRF9 mediate resistance to viruses and DNA damage. *The EMBO journal, 32*(20), 2751-2763. doi:10.1038/emboj.2013.203

Choi, S. W., Park, H. H., Kim, S., Chung, J. M., Noh, H. J., Kim, S. K., . . . Kim, Y. S. (2018). PELI1 Selectively Targets Kinase-Active RIP3 for Ubiquitylation-Dependent Proteasomal Degradation. *Mol Cell, 70*(5), 920-935.e927. doi:10.1016/j.molcel.2018.05.016

Chuang, T. H., & Ulevitch, R. J. (2004). Triad3A, an E3 ubiquitin-protein ligase regulating Toll-like receptors. *Nat Immunol, 5*(5), 495-502. doi:10.1038/ni1066

Clouthier, D. L., Zhou, A. C., Wortzman, M. E., Luft, O., Levy, G. A., & Watts, T. H. (2015). GITR intrinsically sustains early type 1 and late follicular helper CD4 T cell accumulation to control a chronic viral infection. *PLoS Pathog, 11*(1), e1004517. doi:10.1371/journal.ppat.1004517

Cook, W. D., Moujalled, D. M., Ralph, T. J., Lock, P., Young, S. N., Murphy, J. M., & Vaux, D. L. (2014). RIPK1- and RIPK3-induced cell death mode is determined by target availability. *Cell Death Differ, 21*(10), 1600-1612. doi:10.1038/cdd.2014.70

de Weerd, N. A., & Nguyen, T. (2012). The interferons and their receptors--distribution and regulation. *Immunol Cell Biol, 90*(5), 483-491. doi:10.1038/icb.2012.9

Declercq, W., Vanden Berghe, T., & Vandenabeele, P. (2009). RIP kinases at the crossroads of cell death and survival. *Cell, 138*(2), 229-232. doi:10.1016/j.cell.2009.07.006

Dedoni, S., Olianas, M. C., & Onali, P. (2014). Interferon-beta counter-regulates its own pro-apoptotic action by activating p38 MAPK signalling in human SH-SY5Y neuroblastoma cells. *Apoptosis, 19*(10), 1509-1526. doi:10.1007/s10495-014-1024-x

Degterev, A., Hitomi, J., Germscheid, M., Ch'en, I. L., Korkina, O., Teng, X., . . . Yuan, J. (2008). Identification of RIP1 kinase as a specific cellular target of necrostatins. *Nature chemical biology, 4*(5), 313-321. doi:10.1038/nchembio.83

Deshaies, R. J., & Joazeiro, C. A. (2009). RING domain E3 ubiquitin ligases. *Annu Rev Biochem, 78*, 399-434. doi:10.1146/annurev.biochem.78.101807.093809

Dhuriya, Y. K., & Sharma, D. (2018). Necroptosis: a regulated inflammatory mode of cell death. *Journal of Neuroinflammation, 15*(1), 199. doi:10.1186/s12974-018-1235-0

Dickens, L. S., Boyd, R. S., Jukes-Jones, R., Hughes, M. A., Robinson, G. L., Fairall, L., . . . Macfarlane, M. (2012). A death effector domain chain DISC model reveals a crucial role for caspase-8 chain assembly in mediating apoptotic cell death. *Mol Cell, 47*(2), 291-305. doi:10.1016/j.molcel.2012.05.004

Dillon, C. P., Weinlich, R., Rodriguez, D. A., Cripps, J. G., Quarato, G., Gurung, P., . . . Green, D. R. (2014). RIPK1 blocks early postnatal lethality mediated by caspase-8 and RIPK3. *Cell, 157*(5), 1189-1202. doi:10.1016/j.cell.2014.04.018

Dondelinger, Y., Declercq, W., Montessuit, S., Roelandt, R., Goncalves, A., Bruggeman, I., . . . Vandenabeele, P. (2014). MLKL compromises plasma membrane integrity by binding to phosphatidylinositol phosphates. *Cell Rep, 7*(4), 971-981. doi:10.1016/j.celrep.2014.04.026

Dondelinger, Y., Delanghe, T., Priem, D., Wynosky-Dolfi, M. A., Sorobetea, D., Rojas-Rivera, D., . . . Bertrand, M. J. M. (2019). Serine 25 phosphorylation inhibits RIPK1 kinase-dependent cell death in models of infection and inflammation. *Nat Commun, 10*(1), 1729. doi:10.1038/s41467-019-09690-0

Dovey, C. M., Diep, J., Clarke, B. P., Hale, A. T., McNamara, D. E., Guo, H., . . . Carette, J. E. (2018). MLKL Requires the Inositol Phosphate Code to Execute Necroptosis. *Mol Cell, 70*(5), 936-948.e937. doi:10.1016/j.molcel.2018.05.010

Dzierzak, E., & Speck, N. A. (2008). Of lineage and legacy: the development of mammalian hematopoietic stem cells. *Nat Immunol, 9*(2), 129-136. doi:10.1038/ni1560

Ea, C. K., Deng, L., Xia, Z. P., Pineda, G., & Chen, Z. J. (2006). Activation of IKK by TNFalpha requires site-specific ubiquitination of RIP1 and polyubiquitin binding by NEMO. *Mol Cell, 22*(2), 245-257. doi:10.1016/j.molcel.2006.03.026

Elmore, S. (2007). Apoptosis: a review of programmed cell death. *Toxicologic pathology, 35*(4), 495-516. doi:10.1080/01926230701320337

Epelman, S., Lavine, K. J., & Randolph, G. J. (2014). Origin and functions of tissue macrophages. *Immunity, 41*(1), 21-35. doi:10.1016/j.immuni.2014.06.013

Fearns, C., Pan, Q., Mathison, J. C., & Chuang, T. H. (2006). Triad3A regulates ubiquitination and proteasomal degradation of RIP1 following disruption of Hsp90 binding. *J Biol Chem, 281*(45), 34592-34600. doi:10.1074/jbc.M604019200

Fensterl, V., Wetzel, J. L., Ramachandran, S., Ogino, T., Stohlman, S. A., Bergmann, C. C., . . . Sen, G. C. (2012). Interferon-induced Ifit2/ISG54 protects mice from lethal VSV neuropathogenesis. *PLoS Pathog, 8*(5), e1002712. doi:10.1371/journal.ppat.1002712

Fiil, B. K., Damgaard, R. B., Wagner, S. A., Keusekotten, K., Fritsch, M., Bekker-Jensen, S., . . . Gyrd-Hansen, M. (2013). OTULIN restricts Met1-linked ubiquitination to control innate immune signaling. *Mol Cell, 50*(6), 818-830. doi:10.1016/j.molcel.2013.06.004

Fink, S. L., & Cookson, B. T. (2005). Apoptosis, pyroptosis, and necrosis: mechanistic description of dead and dying eukaryotic cells. *Infect Immun, 73*(4), 1907-1916. doi:10.1128/iai.73.4.1907-1916.2005

Fitzgerald, K. A., McWhirter, S. M., Faia, K. L., Rowe, D. C., Latz, E., Golenbock, D. T., . . . Maniatis, T. (2003). IKKepsilon and TBK1 are essential components of the IRF3 signaling pathway. *Nat Immunol, 4*(5), 491-496. doi:10.1038/ni921

Friedman, C. S., O'Donnell, M. A., Legarda-Addison, D., Ng, A., Cárdenas, W. B., Yount, J. S., . . . Ting, A. T. (2008). The tumour suppressor CYLD is a negative regulator of RIG-I-mediated antiviral response. *EMBO reports, 9*(9), 930-936. doi:10.1038/embor.2008.136

Fuchs, Y., & Steller, H. (2011). Programmed cell death in animal development and disease. *Cell, 147*(4), 742-758. doi:10.1016/j.cell.2011.10.033

Galluzzi, L., Vitale, I., Aaronson, S. A., Abrams, J. M., Adam, D., Agostinis, P., . . . Kroemer, G. (2018). Molecular mechanisms of cell death: recommendations of the Nomenclature Committee on Cell Death 2018. *Cell Death & Differentiation, 25*(3), 486-541. doi:10.1038/s41418-017-0012-4

Ginhoux, F., & Jung, S. (2014). Monocytes and macrophages: developmental pathways and tissue homeostasis. *Nat Rev Immunol, 14*(6), 392-404. doi:10.1038/nri3671

Goh, K. C., Haque, S. J., & Williams, B. R. (1999). p38 MAP kinase is required for STAT1 serine phosphorylation and transcriptional activation induced by interferons. *Embo j, 18*(20), 5601-5608. doi:10.1093/emboj/18.20.5601

Gomez-Diaz, C., & Ikeda, F. (2018). Roles of ubiquitin in autophagy and cell death. *Semin Cell Dev Biol*. doi:10.1016/j.semcdb.2018.09.004

Gonzalvez, F., & Ashkenazi, A. (2010). New insights into apoptosis signaling by Apo2L/TRAIL. *Oncogene, 29*(34), 4752-4765. doi:10.1038/onc.2010.221

Gorbunova, V., Hine, C., Tian, X., Ablaeva, J., Gudkov, A. V., Nevo, E., & Seluanov, A. (2012). Cancer resistance in the blind mole rat is mediated by concerted necrotic cell death mechanism. *Proc Natl Acad Sci U S A, 109*(47), 19392-19396. doi:10.1073/pnas.1217211109

Gordon, S., & Martinez-Pomares, L. (2017). Physiological roles of macrophages. *Pflugers Arch, 469*(3-4), 365-374. doi:10.1007/s00424-017-1945-7

Gordon, S., Pluddemann, A., & Martinez Estrada, F. (2014). Macrophage heterogeneity in tissues: phenotypic diversity and functions. *Immunol Rev, 262*(1), 36-55. doi:10.1111/imr.12223

Gough, D. J., Messina, N. L., Clarke, C. J. P., Johnstone, R. W., & Levy, D. E. (2012). Constitutive type I interferon modulates homeostatic balance through tonic signaling. *Immunity, 36*(2), 166-174. doi:10.1016/j.immuni.2012.01.011

Green, D. R. (2019). The Coming Decade of Cell Death Research: Five Riddles. *Cell, 177*(5), 1094-1107. doi:https://doi.org/10.1016/j.cell.2019.04.024

Green, D. R., Oberst, A., Dillon, C. P., Weinlich, R., & Salvesen, G. S. (2011). RIPK-dependent necrosis and its regulation by caspases: a mystery in five acts. *Mol Cell, 44*(1), 9-16. doi:10.1016/j.molcel.2011.09.003

Gurung, P., Man, S. M., & Kanneganti, T.-D. (2015). A20 is a regulator of necroptosis. *Nature Immunology, 16*, 596. doi:10.1038/ni.3174

Han, J., Lee, J. D., Tobias, P. S., & Ulevitch, R. J. (1993). Endotoxin induces rapid protein tyrosine phosphorylation in 70Z/3 cells expressing CD14. *J Biol Chem, 268*(33), 25009-25014.

Han, J., Zhong, C. Q., & Zhang, D. W. (2011). Programmed necrosis: backup to and competitor with apoptosis in the immune system. *Nat Immunol, 12*(12), 1143-1149. doi:10.1038/ni.2159

Harlin, H., Reffey, S. B., Duckett, C. S., Lindsten, T., & Thompson, C. B. (2001). Characterization of XIAP-deficient mice. *Mol Cell Biol, 21*(10), 3604-3608. doi:10.1128/mcb.21.10.3604-3608.2001

Heckmann, B. L., Tummers, B., & Green, D. R. (2019). Crashing the computer: apoptosis vs. necroptosis in neuroinflammation. *Cell Death Differ, 26*(1), 41-52. doi:10.1038/s41418-018-0195-3

Hershko, A., & Ciechanover, A. (1992). THE UBIQUITIN SYSTEM FOR PROTEIN DEGRADATION. *Annu Rev Biochem, 61*(1), 761-807. doi:10.1146/annurev.bi.61.070192.003553

Hershko, A., & Ciechanover, A. (1998). The ubiquitin system. *Annu Rev Biochem, 67*, 425-479. doi:10.1146/annurev.biochem.67.1.425

Hirayama, D., Iida, T., & Nakase, H. (2017). The Phagocytic Function of Macrophage-Enforcing Innate Immunity and Tissue Homeostasis. *International journal of molecular sciences, 19*(1). doi:10.3390/ijms19010092

Holler, N., Zaru, R., Micheau, O., Thome, M., Attinger, A., Valitutti, S., . . . Tschopp, J. (2000). Fas triggers an alternative, caspase-8-independent cell death pathway using the kinase RIP as effector molecule. *Nat Immunol, 1*(6), 489-495. doi:10.1038/82732

Honda, K., Takaoka, A., & Taniguchi, T. (2006). Type I Inteferon Gene Induction by the Interferon Regulatory Factor Family of Transcription Factors. *Immunity, 25*(3), 349-360. doi:https://doi.org/10.1016/j.immuni.2006.08.009

Honda, K., Yanai, H., Takaoka, A., & Taniguchi, T. (2005). Regulation of the type I IFN induction: a current view. *Int Immunol, 17*(11), 1367-1378. doi:10.1093/intimm/dxh318

Huang, D., Zheng, X., Wang, Z. A., Chen, X., He, W. T., Zhang, Y., . . . Han, J. (2017). The MLKL Channel in Necroptosis Is an Octamer Formed by Tetramers in a Dyadic Process. *Mol Cell Biol, 37*(5). doi:10.1128/mcb.00497-16

Huang, X., Xiao, F., Li, Y., Qian, W., Ding, W., & Ye, X. (2018). Bypassing drug resistance by triggering necroptosis: recent advances in mechanisms and its therapeutic exploitation in leukemia. *Journal of Experimental & Clinical Cancer Research, 37*(1), 310. doi:10.1186/s13046-018-0976-z

Hughes, M. A., Harper, N., Butterworth, M., Cain, K., Cohen, G. M., & MacFarlane, M. (2009). Reconstitution of the death-inducing signaling complex reveals a substrate switch that determines CD95-mediated death or survival. *Mol Cell, 35*(3), 265-279. doi:10.1016/j.molcel.2009.06.012

Ivashkiv, L. B., & Donlin, L. T. (2013). Regulation of type I interferon responses. *Nature Reviews Immunology, 14*, 36. doi:10.1038/nri3581

Jaco, I., Annibaldi, A., Lalaoui, N., Wilson, R., Tenev, T., Laurien, L., . . . Meier, P. (2017). MK2 Phosphorylates RIPK1 to Prevent TNF-Induced Cell Death. *Mol Cell, 66*(5), 698-710.e695. doi:10.1016/j.molcel.2017.05.003

Jeong, S.-I., Kim, J.-W., Ko, K.-P., Ryu, B.-K., Lee, M.-G., Kim, H.-J., & Chi, S.-G. (2018). XAF1 forms a positive feedback loop with IRF-1 to drive apoptotic stress response and suppress tumorigenesis. *Cell Death & Disease, 9*(8), 806. doi:10.1038/s41419-018-0867-4

Jin, J., Hu, H., Li, H. S., Yu, J., Xiao, Y., Brittain, G. C., . . . Sun, S. C. (2014). Noncanonical NF-kappaB pathway controls the production of type I interferons in antiviral innate immunity. *Immunity, 40*(3), 342-354. doi:10.1016/j.immuni.2014.02.006

Jin, Z., Li, Y., Pitti, R., Lawrence, D., Pham, V. C., Lill, J. R., & Ashkenazi, A. (2009). Cullin3-based polyubiquitination and p62-dependent aggregation of caspase-8 mediate extrinsic apoptosis signaling. *Cell, 137*(4), 721-735. doi:10.1016/j.cell.2009.03.015

Jouan-Lanhouet, S., Arshad, M. I., Piquet-Pellorce, C., Martin-Chouly, C., Le Moigne-Muller, G., Van Herreweghe, F., . . . Dimanche-Boitrel, M. T. (2012). TRAIL induces necroptosis involving RIPK1/RIPK3-dependent PARP-1 activation. *Cell Death Differ, 19*(12), 2003-2014. doi:10.1038/cdd.2012.90

Kaiser, W. J., Sridharan, H., Huang, C., Mandal, P., Upton, J. W., Gough, P. J., . . . Mocarski, E. S. (2013). Toll-like receptor 3-mediated necrosis via TRIF, RIP3, and MLKL. *J Biol Chem, 288*(43), 31268-31279. doi:10.1074/jbc.M113.462341

Kauppinen, A., Paterno, J. J., Blasiak, J., Salminen, A., & Kaarniranta, K. (2016). Inflammation and its role in age-related macular degeneration. *Cell Mol Life Sci, 73*(9), 1765-1786. doi:10.1007/s00018-016-2147-8

Kelliher, M. A., Grimm, S., Ishida, Y., Kuo, F., Stanger, B. Z., & Leder, P. (1998). The death domain kinase RIP mediates the TNF-induced NF-kappaB signal. *Immunity, 8*(3), 297-303.

Kemp, T. J., Kim, J. S., Crist, S. A., & Griffith, T. S. (2003). Induction of necrotic tumor cell death by TRAIL/Apo-2L. *Apoptosis, 8*(6), 587-599. doi:10.1023/a:1026286108366

Knuth, A.-K., Rösler, S., Schenk, B., Kowald, L., van Wijk, S. J. L., & Fulda, S. (2019). Interferons Transcriptionally Up-Regulate MLKL Expression in Cancer Cells. *Neoplasia, 21*(1), 74-81. doi:https://doi.org/10.1016/j.neo.2018.11.002

Koehler, H., Cotsmire, S., Langland, J., Kibler, K. V., Kalman, D., Upton, J. W., . . . Jacobs, B. L. (2017). Inhibition of DAI-dependent necroptosis by the Z-DNA binding domain of the vaccinia virus innate immune evasion protein, E3. *Proc Natl Acad Sci U S A, 114*(43), 11506-11511. doi:10.1073/pnas.1700999114

Kohyama, M., Ise, W., Edelson, B. T., Wilker, P. R., Hildner, K., Mejia, C., . . . Murphy, K. M. (2009). Role for Spi-C in the development of red pulp macrophages and splenic iron homeostasis. *Nature, 457*(7227), 318-321. doi:10.1038/nature07472

Kolb, J. P., Oguin, T. H., 3rd, Oberst, A., & Martinez, J. (2017). Programmed Cell Death and Inflammation: Winter Is Coming. *Trends Immunol, 38*(10), 705-718. doi:10.1016/j.it.2017.06.009

Kolumam, G. A., Thomas, S., Thompson, L. J., Sprent, J., & Murali-Krishna, K. (2005). Type I interferons act directly on CD8 T cells to allow clonal expansion and memory formation in response to viral infection. *J Exp Med, 202*(5), 637-650. doi:10.1084/jem.20050821

Kotlyarov, A., Neininger, A., Schubert, C., Eckert, R., Birchmeier, C., Volk, H. D., & Gaestel, M. (1999). MAPKAP kinase 2 is essential for LPS-induced TNF-alpha biosynthesis. *Nat Cell Biol, 1*(2), 94-97. doi:10.1038/10061

Kotwal, G. J. (1997). Microorganisms and their interaction with the immune system. *J Leukoc Biol, 62*(4), 415-429. doi:10.1002/jlb.62.4.415

Kovarik, P., Castiglia, V., Ivin, M., & Ebner, F. (2016). Type I Interferons in Bacterial Infections: A Balancing Act. *Frontiers in immunology, 7*, 652-652. doi:10.3389/fimmu.2016.00652

Lawrence, T. (2009). The nuclear factor NF-kappaB pathway in inflammation. *Cold Spring Harb Perspect Biol, 1*(6), a001651. doi:10.1101/cshperspect.a001651

Legarda, D., Justus, S. J., Ang, R. L., Rikhi, N., Li, W., Moran, T. M., . . . Ting, A. T. (2016). CYLD Proteolysis Protects Macrophages from TNF-Mediated Auto-necroptosis Induced by LPS and Licensed by Type I IFN. *Cell Rep, 15*(11), 2449-2461. doi:10.1016/j.celrep.2016.05.032

Li, J., McQuade, T., Siemer, A. B., Napetschnig, J., Moriwaki, K., Hsiao, Y. S., . . . Wu, H. (2012). The RIP1/RIP3 necrosome forms a functional amyloid signaling complex required for programmed necrosis. *Cell, 150*(2), 339-350. doi:10.1016/j.cell.2012.06.019

Li, W., Hofer, M. J., Songkhunawej, P., Jung, S. R., Hancock, D., Denyer, G., & Campbell, I. L. (2017). Type I interferon-regulated gene expression and signaling in murine mixed glial cells lacking signal transducers and activators of transcription 1 or 2 or interferon regulatory factor 9. *J Biol Chem, 292*(14), 5845-5859. doi:10.1074/jbc.M116.756510

Li, Y., Guo, X., Hu, C., Du, Y., Guo, C., Di, W., . . . Qi, X. (2018). Type I IFN operates pyroptosis and necroptosis during multidrug-resistant A. baumannii infection. *Cell Death & Differentiation, 25*(7), 1304-1318. doi:10.1038/s41418-017-0041-z

Li, Y., Sassano, A., Majchrzak, B., Deb, D. K., Levy, D. E., Gaestel, M., . . . Platanias, L. C. (2004). Role of p38alpha Map kinase in Type I interferon signaling. *J Biol Chem, 279*(2), 970-979. doi:10.1074/jbc.M309927200

Lin, F.-c., & Young, H. A. (2014). Interferons: Success in anti-viral immunotherapy. *Cytokine & growth factor reviews, 25*(4), 369-376. doi:10.1016/j.cytogfr.2014.07.015

Linkermann, A., Kunzendorf, U., & Krautwald, S. (2014). Phosphorylated MLKL causes plasma membrane rupture. *Molecular & cellular oncology, 1*(1), e29915-e29915. doi:10.4161/mco.29915

Liston, P., Fong, W. G., Kelly, N. L., Toji, S., Miyazaki, T., Conte, D., . . . Korneluk, R. G. (2001). Identification of XAF1 as an antagonist of XIAP anti-Caspase activity. *Nature Cell Biology, 3*(2), 128-133. doi:10.1038/35055027

Liu, T., Zhang, L., Joo, D., & Sun, S.-C. (2017). NF-κB signaling in inflammation. *Signal Transduction And Targeted Therapy, 2*, 17023. doi:10.1038/sigtrans.2017.23

Liu, X., Li, Y., Peng, S., Yu, X., Li, W., Shi, F., . . . Cao, Y. (2018). Epstein-Barr virus encoded latent membrane protein 1 suppresses necroptosis through targeting RIPK1/3 ubiquitination. *Cell Death Dis, 9*(2), 53. doi:10.1038/s41419-017-0081-9

Lockshin, R. A., & Zakeri, Z. (2007). Cell death in health and disease. *Journal of cellular and molecular medicine, 11*(6), 1214-1224. doi:10.1111/j.1582-4934.2007.00150.x

Lu, Z., & Xu, S. (2006). ERK1/2 MAP kinases in cell survival and apoptosis. *IUBMB Life, 58*(11), 621-631. doi:10.1080/15216540600957438

Mandal, P., Berger, S. B., Pillay, S., Moriwaki, K., Huang, C., Guo, H., . . . Kaiser, W. J. (2014). RIP3 induces apoptosis independent of pronecrotic kinase activity. *Mol Cell, 56*(4), 481-495. doi:10.1016/j.molcel.2014.10.021

Martin, S. J., & Henry, C. M. (2013). Distinguishing between apoptosis, necrosis, necroptosis and other cell death modalities. *Methods, 61*(2), 87-89. doi:https://doi.org/10.1016/j.ymeth.2013.06.001

McComb, S., Cessford, E., Alturki, N. A., Joseph, J., Shutinoski, B., Startek, J. B., . . . Sad, S. (2014). Type-I interferon signaling through ISGF3 complex is required for sustained Rip3 activation and necroptosis in macrophages. *Proc Natl Acad Sci U S A, 111*(31), E3206-3213. doi:10.1073/pnas.1407068111

McGuire, V. A., Rosner, D., Ananieva, O., Ross, E. A., Elcombe, S. E., Naqvi, S., . . . Arthur, J. S. C. (2017). Beta Interferon Production Is Regulated by p38 Mitogen-Activated Protein Kinase in Macrophages via both MSK1/2- and Tristetraprolin-Dependent Pathways. *Mol Cell Biol, 37*(1). doi:10.1128/mcb.00454-16

Mears, H. V., & Sweeney, T. R. (2018). Better together: the role of IFIT protein-protein interactions in the antiviral response. *J Gen Virol, 99*(11), 1463-1477. doi:10.1099/jgv.0.001149

Medzhitov, R. (2007). Recognition of microorganisms and activation of the immune response. *Nature, 449*(7164), 819-826. doi:10.1038/nature06246

Medzhitov, R. (2008). Origin and physiological roles of inflammation. *Nature, 454*(7203), 428-435. doi:10.1038/nature07201

Meier, P., & Vousden, K. H. (2007). Lucifer's labyrinth--ten years of path finding in cell death. *Mol Cell, 28*(5), 746-754. doi:10.1016/j.molcel.2007.11.016

Michalska, A., Blaszczyk, K., Wesoly, J., & Bluyssen, H. A. R. (2018). A Positive Feedback Amplifier Circuit That Regulates Interferon (IFN)-Stimulated Gene Expression and Controls Type I and Type II IFN Responses. *Frontiers in immunology, 9*, 1135. doi:10.3389/fimmu.2018.01135

Minegishi, Y., Saito, M., Morio, T., Watanabe, K., Agematsu, K., Tsuchiya, S., . . . Karasuyama, H. (2006). Human Tyrosine Kinase 2 Deficiency Reveals Its Requisite Roles in Multiple Cytokine Signals Involved in Innate and Acquired Immunity. *Immunity, 25*(5), 745-755. doi:https://doi.org/10.1016/j.immuni.2006.09.009

Mogensen, T. H. (2009). Pathogen recognition and inflammatory signaling in innate immune defenses. *Clinical microbiology reviews, 22*(2), 240-273. doi:10.1128/CMR.00046-08

Mompean, M., Li, W., Li, J., Laage, S., Siemer, A. B., Bozkurt, G., . . . McDermott, A. E. (2018). The Structure of the Necrosome RIPK1-RIPK3 Core, a Human Hetero-Amyloid Signaling Complex. *Cell, 173*(5), 1244-1253.e1210. doi:10.1016/j.cell.2018.03.032

Moquin, D. M., McQuade, T., & Chan, F. K. (2013). CYLD deubiquitinates RIP1 in the TNFalpha-induced necrosome to facilitate kinase activation and programmed necrosis. *PloS one, 8*(10), e76841. doi:10.1371/journal.pone.0076841

Moriwaki, K., & Chan, F. K. (2017). The Inflammatory Signal Adaptor RIPK3: Functions Beyond Necroptosis. *Int Rev Cell Mol Biol, 328*, 253-275. doi:10.1016/bs.ircmb.2016.08.007

Murphy, J. M., Czabotar, P. E., Hildebrand, J. M., Lucet, I. S., Zhang, J. G., Alvarez-Diaz, S., . . . Alexander, W. S. (2013). The pseudokinase MLKL mediates necroptosis via a molecular switch mechanism. *Immunity, 39*(3), 443-453. doi:10.1016/j.immuni.2013.06.018

Murphy, J. M., & Vince, J. E. (2015). Post-translational control of RIPK3 and MLKL mediated necroptotic cell death. *F1000Research, 4*, F1000 Faculty Rev-1297. doi:10.12688/f1000research.7046.1

Murphy, K. P., Murphy, K. M., Travers, P., Walport, M., Janeway, C., Mauri, C., & Ehrenstein, M. (2008). *Janeway's Immunobiology*: Garland Science.

Nailwal, H., & Chan, F. K.-M. (2019). Necroptosis in anti-viral inflammation. *Cell Death & Differentiation, 26*(1), 4-13. doi:10.1038/s41418-018-0172-x

Najafov, A., Chen, H., & Yuan, J. (2017). Necroptosis and Cancer. *Trends in cancer, 3*(4), 294-301. doi:10.1016/j.trecan.2017.03.002

Nakamura, N. (2018). Ubiquitin System. *International journal of molecular sciences, 19*(4), 1080. doi:10.3390/ijms19041080

Newton, K., Sun, X., & Dixit, V. M. (2004). Kinase RIP3 is dispensable for normal NF-kappa Bs, signaling by the B-cell and T-cell receptors, tumor necrosis factor receptor 1, and Toll-like receptors 2 and 4. *Mol Cell Biol, 24*(4), 1464-1469. doi:10.1128/mcb.24.4.1464-1469.2004

Nicholson, L. B. (2016). The immune system. *Essays in biochemistry, 60*(3), 275-301. doi:10.1042/EBC20160017

O'Connell, R. M., Saha, S. K., Vaidya, S. A., Bruhn, K. W., Miranda, G. A., Zarnegar, B., . . . Cheng, G. (2004). Type I interferon production enhances susceptibility to Listeria monocytogenes infection. *J Exp Med, 200*(4), 437-445. doi:10.1084/jem.20040712

O'Donnell, M. A., Legarda-Addison, D., Skountzos, P., Yeh, W. C., & Ting, A. T. (2007). Ubiquitination of RIP1 regulates an NF-kappaB-independent cell-death switch in TNF signaling. *Curr Biol, 17*(5), 418-424. doi:10.1016/j.cub.2007.01.027

O'Neill, L. A. J., & Bowie, A. G. (2007). The family of five: TIR-domain-containing adaptors in Toll-like receptor signalling. *Nature Reviews Immunology, 7*, 353. doi:10.1038/nri2079

Oeckinghaus, A., Hayden, M. S., & Ghosh, S. (2011). Crosstalk in NF-κB signaling pathways. *Nature Immunology, 12*, 695. doi:10.1038/ni.2065

Ofengeim, D., Ito, Y., Najafov, A., Zhang, Y., Shan, B., DeWitt, J. P., . . . Yuan, J. (2015). Activation of necroptosis in multiple sclerosis. *Cell Rep, 10*(11), 1836-1849. doi:10.1016/j.celrep.2015.02.051

Onizawa, M., Oshima, S., Schulze-Topphoff, U., Oses-Prieto, J. A., Lu, T., Tavares, R., . . . Ma, A. (2015). The ubiquitin-modifying enzyme A20 restricts ubiquitination of the kinase RIPK3 and protects cells from necroptosis. *Nat Immunol, 16*(6), 618-627. doi:10.1038/ni.3172

Pasparakis, M., & Vandenabeele, P. (2015). Necroptosis and its role in inflammation. *Nature, 517*(7534), 311-320. doi:10.1038/nature14191

Piehler, J., Thomas, C., Garcia, K. C., & Schreiber, G. (2012). Structural and dynamic determinants of type I interferon receptor assembly and their functional interpretation. *Immunol Rev, 250*(1), 317-334. doi:10.1111/imr.12001

Pires, B. R. B., Silva, R., Ferreira, G. M., & Abdelhay, E. (2018). NF-kappaB: Two Sides of the Same Coin. *Genes (Basel), 9*(1). doi:10.3390/genes9010024

Platanias, L. C. (2003). The p38 mitogen-activated protein kinase pathway and its role in interferon signaling. *Pharmacology & Therapeutics, 98*(2), 129-142. doi:https://doi.org/10.1016/S0163-7258(03)00016-0

Platanias, L. C. (2005). Mechanisms of type-I- and type-II-interferon-mediated signalling. *Nature Reviews Immunology, 5*(5), 375-386. doi:10.1038/nri1604

Prchal-Murphy, M., Semper, C., Lassnig, C., Wallner, B., Gausterer, C., Teppner-Klymiuk, I., . . . Muller, M. (2012). TYK2 kinase activity is required for functional type I interferon responses in vivo. *PloS one, 7*(6), e39141. doi:10.1371/journal.pone.0039141

Ragimbeau, J., Dondi, E., Alcover, A., Eid, P., Uzé, G., & Pellegrini, S. (2003). The tyrosine kinase Tyk2 controls IFNAR1 cell surface expression. *The EMBO journal, 22*(3), 537-547. doi:10.1093/emboj/cdg038

Ramsauer, K., Sadzak, I., Porras, A., Pilz, A., Nebreda, A. R., Decker, T., & Kovarik, P. (2002). p38 MAPK enhances STAT1-dependent transcription independently of Ser-727 phosphorylation. *Proc Natl Acad Sci U S A, 99*(20), 12859-12864. doi:10.1073/pnas.192264999

Ravichandran, K. S. (2011). Beginnings of a good apoptotic meal: the find-me and eat-me signaling pathways. *Immunity, 35*(4), 445-455. doi:10.1016/j.immuni.2011.09.004

Reiley, W., Zhang, M., Wu, X., Granger, E., & Sun, S.-C. (2005). Regulation of the deubiquitinating enzyme CYLD by IkappaB kinase gamma-dependent phosphorylation. *Mol Cell Biol, 25*(10), 3886-3895. doi:10.1128/MCB.25.10.3886-3895.2005

Reiley, W. W., Zhang, M., Jin, W., Losiewicz, M., Donohue, K. B., Norbury, C. C., & Sun, S. C. (2006). Regulation of T cell development by the deubiquitinating enzyme CYLD. *Nat Immunol, 7*(4), 411-417. doi:10.1038/ni1315

Robinson, N., McComb, S., Mulligan, R., Dudani, R., Krishnan, L., & Sad, S. (2012). Type I interferon induces necroptosis in macrophages during infection with Salmonella enterica serovar Typhimurium. *Nature Immunology, 13*(10), 954-962. doi:10.1038/ni.2397

Rock, K. L., Latz, E., Ontiveros, F., & Kono, H. (2010). The sterile inflammatory response. *Annu Rev Immunol, 28*, 321-342. doi:10.1146/annurev-immunol-030409-101311

Roderick, J. E., Hermance, N., Zelic, M., Simmons, M. J., Polykratis, A., Pasparakis, M., & Kelliher, M. A. (2014). Hematopoietic RIPK1 deficiency results in bone marrow failure caused by apoptosis and RIPK3-mediated necroptosis. *Proc Natl Acad Sci U S A, 111*(40), 14436-14441. doi:10.1073/pnas.1409389111

Rodriguez, D. A., Weinlich, R., Brown, S., Guy, C., Fitzgerald, P., Dillon, C. P., . . . Green, D. R. (2016). Characterization of RIPK3-mediated phosphorylation of the activation loop of MLKL during necroptosis. *Cell Death Differ, 23*(1), 76-88. doi:10.1038/cdd.2015.70

Ronchetti, S., Nocentini, G., Riccardi, C., & Pandolfi, P. P. (2002). Role of GITR in activation response of T lymphocytes. *Blood, 100*(1), 350-352. doi:10.1182/blood-2001-12-0276

Ronkina, N., Kotlyarov, A., Dittrich-Breiholz, O., Kracht, M., Hitti, E., Milarski, K., . . . Telliez, J. B. (2007). The mitogen-activated protein kinase (MAPK)-activated protein kinases MK2 and MK3 cooperate in stimulation of tumor necrosis factor biosynthesis and stabilization of p38 MAPK. *Mol Cell Biol, 27*(1), 170-181. doi:10.1128/mcb.01456-06

Sachet, M., Liang, Y. Y., & Oehler, R. (2017). The immune response to secondary necrotic cells. *Apoptosis, 22*(10), 1189-1204. doi:10.1007/s10495-017-1413-z

Saitoh, T., Yamamoto, M., Miyagishi, M., Taira, K., Nakanishi, M., Fujita, T., . . . Yamaoka, S. (2005). A20 is a negative regulator of IFN regulatory factor 3 signaling. *J Immunol, 174*(3), 1507-1512.

Saitoh, T., Yamamoto, M., Miyagishi, M., Taira, K., Nakanishi, M., Fujita, T., . . . Yamaoka, S. (2005). A20 Is a Negative Regulator of IFN Regulatory Factor 3 Signaling. *The Journal of Immunology, 174*(3), 1507. doi:10.4049/jimmunol.174.3.1507

Sarhan, J., Liu, B. C., Muendlein, H. I., Weindel, C. G., Smirnova, I., Tang, A. Y., . . . Poltorak, A. (2019). Constitutive interferon signaling maintains critical threshold of MLKL expression to license necroptosis. *Cell Death & Differentiation, 26*(2), 332-347. doi:10.1038/s41418-018-0122-7

Schenk, B., & Fulda, S. (2015). Reactive oxygen species regulate Smac mimetic/TNFalpha-induced necroptotic signaling and cell death. *Oncogene, 34*(47), 5796-5806. doi:10.1038/onc.2015.35

Schwabe, R. F., & Luedde, T. (2018). Apoptosis and necroptosis in the liver: a matter of life and death. *Nat Rev Gastroenterol Hepatol, 15*(12), 738-752. doi:10.1038/s41575-018-0065-y

Seo, J., Kim, M. W., Bae, K.-H., Lee, S. C., Song, J., & Lee, E.-W. (2019). The roles of ubiquitination in extrinsic cell death pathways and its implications for therapeutics. *Biochem Pharmacol, 162*, 21-40. doi:https://doi.org/10.1016/j.bcp.2018.11.012

Seo, J., Lee, E.-W., Sung, H., Seong, D., Dondelinger, Y., Shin, J., . . . Song, J. (2016). CHIP controls necroptosis through ubiquitylation- and lysosome-dependent degradation of RIPK3. *Nature Cell Biology, 18*, 291. doi:10.1038/ncb3314

https://www.nature.com/articles/ncb3314#supplementary-information

Shan, B., Pan, H., Najafov, A., & Yuan, J. (2018). Necroptosis in development and diseases. *Genes & development, 32*(5-6), 327-340. doi:10.1101/gad.312561.118

Shaul, Y. D., & Seger, R. (2007). The MEK/ERK cascade: from signaling specificity to diverse functions. *Biochimica et biophysica acta, 1773*(8), 1213-1226. doi:10.1016/j.bbamcr.2006.10.005

Shen, H., Kreisel, D., & Goldstein, D. R. (2013). Processes of sterile inflammation. *J Immunol, 191*(6), 2857-2863. doi:10.4049/jimmunol.1301539

Shih, V. F., Tsui, R., Caldwell, A., & Hoffmann, A. (2011). A single NFkappaB system for both canonical and non-canonical signaling. *Cell Res, 21*(1), 86-102. doi:10.1038/cr.2010.161

Silva, M. T. (2010). Secondary necrosis: the natural outcome of the complete apoptotic program. *FEBS Lett, 584*(22), 4491-4499. doi:10.1016/j.febslet.2010.10.046

Stawowczyk, M., Van Scoy, S., Kumar, K. P., & Reich, N. C. (2011). The interferon stimulated gene 54 promotes apoptosis. *J Biol Chem, 286*(9), 7257-7266. doi:10.1074/jbc.M110.207068

Strniskova, M., Barancik, M., & Ravingerova, T. (2002). Mitogen-activated protein kinases and their role in regulation of cellular processes. *Gen Physiol Biophys, 21*(3), 231-255.

Sugimoto, M. A., Sousa, L. P., Pinho, V., Perretti, M., & Teixeira, M. M. (2016). Resolution of Inflammation: What Controls Its Onset? *Frontiers in immunology, 7*, 160. doi:10.3389/fimmu.2016.00160

Sun, L., Wang, H., Wang, Z., He, S., Chen, S., Liao, D., . . . Wang, X. (2012). Mixed lineage kinase domain-like protein mediates necrosis signaling downstream of RIP3 kinase. *Cell, 148*(1-2), 213-227. doi:10.1016/j.cell.2011.11.031

Sun, S.-C. (2011). Non-canonical NF-κB signaling pathway. *Cell Research, 21*(1), 71-85. doi:10.1038/cr.2010.177

Sun, S. C. (2010). CYLD: a tumor suppressor deubiquitinase regulating NF-kappaB activation and diverse biological processes. *Cell Death Differ, 17*(1), 25-34. doi:10.1038/cdd.2009.43

Sun, S. C. (2017). The non-canonical NF-kappaB pathway in immunity and inflammation. *Nat Rev Immunol, 17*(9), 545-558. doi:10.1038/nri.2017.52

Suresh, R., & Mosser, D. M. (2013). Pattern recognition receptors in innate immunity, host defense, and immunopathology. *Advances in physiology education, 37*(4), 284-291. doi:10.1152/advan.00058.2013

Swatek, K. N., & Komander, D. (2016). Ubiquitin modifications. *Cell Research, 26*, 399. doi:10.1038/cr.2016.39

Takahashi, K., Yamamura, F., & Naito, M. (1989). Differentiation, maturation, and proliferation of macrophages in the mouse yolk sac: a light-microscopic, enzyme-cytochemical, immunohistochemical, and ultrastructural study. *J Leukoc Biol, 45*(2), 87-96. doi:10.1002/jlb.45.2.87

Takahashi, N., Duprez, L., Grootjans, S., Cauwels, A., Nerinckx, W., DuHadaway, J. B., . . . Vandenabeele, P. (2012). Necrostatin-1 analogues: critical issues on the specificity, activity and in vivo use in experimental disease models. *Cell Death &Amp; Disease, 3*, e437. doi:10.1038/cddis.2012.176

Takeuchi, O., & Akira, S. (2010). Pattern recognition receptors and inflammation. *Cell, 140*(6), 805-820. doi:10.1016/j.cell.2010.01.022

Tang, D., Kang, R., Coyne, C. B., Zeh, H. J., & Lotze, M. T. (2012). PAMPs and DAMPs: signal 0s that spur autophagy and immunity. *Immunol Rev, 249*(1), 158-175. doi:10.1111/j.1600-065X.2012.01146.x

tenOever, B. R., Ng, S.-L., Chua, M. A., McWhirter, S. M., García-Sastre, A., & Maniatis, T. (2007). Multiple Functions of the IKK-Related Kinase IKKε in Interferon-Mediated Antiviral Immunity. *Science, 315*(5816), 1274-1278. doi:10.1126/science.1136567

Tsuno, T., Mejido, J., Zhao, T., Schmeisser, H., Morrow, A., & Zoon, K. C. (2009). IRF9 is a key factor for eliciting the antiproliferative activity of IFN-alpha. *J Immunother, 32*(8), 803-816. doi:10.1097/CJI.0b013e3181ad4092

Uddin, S., Lekmine, F., Sharma, N., Majchrzak, B., Mayer, I., Young, P. R., . . . Platanias, L. C. (2000). The Rac1/p38 mitogen-activated protein kinase pathway is required for interferon alpha-dependent transcriptional activation but not serine phosphorylation of Stat proteins. *J Biol Chem, 275*(36), 27634-27640. doi:10.1074/jbc.M003170200

Uddin, S., Majchrzak, B., Woodson, J., Arunkumar, P., Alsayed, Y., Pine, R., . . . Platanias, L. C. (1999). Activation of the p38 mitogen-activated protein kinase by type I interferons. *J Biol Chem, 274*(42), 30127-30131. doi:10.1074/jbc.274.42.30127

Uribe-Querol, E., & Rosales, C. (2017). Control of Phagocytosis by Microbial Pathogens. *Frontiers in immunology, 8*, 1368. doi:10.3389/fimmu.2017.01368

Vanlangenakker, N., Vanden Berghe, T., & Vandenabeele, P. (2012). Many stimuli pull the necrotic trigger, an overview. *Cell Death Differ, 19*(1), 75-86. doi:10.1038/cdd.2011.164

Varol, C., Mildner, A., & Jung, S. (2015). Macrophages: Development and Tissue Specialization. *Annu Rev Immunol, 33*(1), 643-675. doi:10.1146/annurev-immunol-032414-112220

Venkatesh, D., Ernandez, T., Rosetti, F., Batal, I., Cullere, X., Luscinskas, F. W., . . . Mayadas, T. N. (2013). Endothelial TNF receptor 2 induces IRF1 transcription factor-dependent interferon-β autocrine signaling to promote monocyte recruitment. *Immunity, 38*(5), 1025-1037. doi:10.1016/j.immuni.2013.01.012

Vercammen, D., Beyaert, R., Denecker, G., Goossens, V., Van Loo, G., Declercq, W., . . . Vandenabeele, P. (1998). Inhibition of caspases increases the sensitivity of L929 cells to necrosis mediated by tumor necrosis factor. *J Exp Med, 187*(9), 1477-1485.

Verstrepen, L., Verhelst, K., van Loo, G., Carpentier, I., Ley, S. C., & Beyaert, R. (2010). Expression, biological activities and mechanisms of action of A20 (TNFAIP3). *Biochem Pharmacol, 80*(12), 2009-2020. doi:10.1016/j.bcp.2010.06.044

Voigt, S., Philipp, S., Davarnia, P., Winoto-Morbach, S., Röder, C., Arenz, C., . . . Adam, D. (2014). TRAIL-induced programmed necrosis as a novel approach to eliminate tumor cells. *BMC Cancer, 14*(1), 74. doi:10.1186/1471-2407-14-74

Wang, G., Gao, Y., Li, L., Jin, G., Cai, Z., Chao, J.-I., & Lin, H.-K. (2012). K63-linked ubiquitination in kinase activation and cancer. *Frontiers in oncology, 2*, 5-5. doi:10.3389/fonc.2012.00005

Wang, H., Meng, H., Li, X., Zhu, K., Dong, K., Mookhtiar, A. K., . . . Yuan, J. (2017). PELI1 functions as a dual modulator of necroptosis and apoptosis by regulating ubiquitination of RIPK1 and mRNA levels of c-FLIP. *Proc Natl Acad Sci U S A, 114*(45), 11944-11949. doi:10.1073/pnas.1715742114

Wang, H., Sun, L., Su, L., Rizo, J., Liu, L., Wang, L. F., . . . Wang, X. (2014). Mixed lineage kinase domain-like protein MLKL causes necrotic membrane disruption upon phosphorylation by RIP3. *Mol Cell, 54*(1), 133-146. doi:10.1016/j.molcel.2014.03.003

Wang, S., Zhang, C., Hu, L., & Yang, C. (2016). Necroptosis in acute kidney injury: a shedding light. *Cell Death & Disease, 7*(3), e2125-e2125. doi:10.1038/cddis.2016.37

Wang, W., Yin, Y., Xu, L., Su, J., Huang, F., Wang, Y., . . . Pan, Q. (2017). Unphosphorylated ISGF3 drives constitutive expression of interferon-stimulated genes to protect against viral infections. *Sci Signal, 10*(476). doi:10.1126/scisignal.aah4248

Wang, Y. Y., Li, L., Han, K. J., Zhai, Z., & Shu, H. B. (2004). A20 is a potent inhibitor of TLR3- and Sendai virus-induced activation of NF-kappaB and ISRE and IFN-beta promoter. *FEBS Lett, 576*(1-2), 86-90. doi:10.1016/j.febslet.2004.08.071

Wertz, I. E., O'Rourke, K. M., Zhou, H., Eby, M., Aravind, L., Seshagiri, S., . . . Dixit, V. M. (2004). De-ubiquitination and ubiquitin ligase domains of A20 downregulate NF-kappaB signalling. *Nature, 430*(7000), 694-699. doi:10.1038/nature02794

White, M. (1999). Mediators of inflammation and the inflammatory process. *J Allergy Clin Immunol, 103*(3 Pt 2), S378-381. doi:10.1016/s0091-6749(99)70215-0

Williams, J. W., Giannarelli, C., Rahman, A., Randolph, G. J., & Kovacic, J. C. (2018). Macrophage Biology, Classification, and Phenotype in Cardiovascular Disease: JACC Macrophage in CVD Series (Part 1). *J Am Coll Cardiol, 72*(18), 2166-2180. doi:10.1016/j.jacc.2018.08.2148

Wu, X. N., Yang, Z. H., Wang, X. K., Zhang, Y., Wan, H., Song, Y., . . . Han, J. (2014). Distinct roles of RIP1-RIP3 hetero- and RIP3-RIP3 homo-interaction in mediating necroptosis. *Cell Death Differ, 21*(11), 1709-1720. doi:10.1038/cdd.2014.77

Wyllie, A. H., Kerr, J. F., & Currie, A. R. (1980). Cell death: the significance of apoptosis. *Int Rev Cytol, 68*, 251-306.

Yarilina, A., Park-Min, K.-H., Antoniv, T., Hu, X., & Ivashkiv, L. B. (2008). TNF activates an IRF1-dependent autocrine loop leading to sustained expression of chemokines and STAT1-dependent type I interferon–response genes. *Nature Immunology, 9*, 378. doi:10.1038/ni1576

https://www.nature.com/articles/ni1576#supplementary-information

Zarubin, T., & Han, J. (2005). Activation and signaling of the p38 MAP kinase pathway. *Cell Research, 15*(1), 11-18. doi:10.1038/sj.cr.7290257

Zhan, Y., Carrington, E. M., Zhang, Y., Heinzel, S., & Lew, A. M. (2017). Life and Death of Activated T Cells: How Are They Different from Naïve T Cells? *Frontiers in immunology, 8*, 1809-1809. doi:10.3389/fimmu.2017.01809

Zhang, W., & Liu, H. T. (2002). MAPK signal pathways in the regulation of cell proliferation in mammalian cells. *Cell Research, 12*(1), 9-18. doi:10.1038/sj.cr.7290105

Zhang, X., & Mosser, D. M. (2008). Macrophage activation by endogenous danger signals. *J Pathol, 214*(2), 161-178. doi:10.1002/path.2284

Zhang, Y., Chen, X., Gueydan, C., & Han, J. (2017). Plasma membrane changes during programmed cell deaths. *Cell Research, 28*, 9. doi:10.1038/cr.2017.133

Zhao, J., Jitkaew, S., Cai, Z., Choksi, S., Li, Q., Luo, J., & Liu, Z. G. (2012). Mixed lineage kinase domain-like is a key receptor interacting protein 3 downstream component of TNF-induced necrosis. *Proc Natl Acad Sci U S A, 109*(14), 5322-5327. doi:10.1073/pnas.1200012109

Zhou, Q., Snipas, S., Orth, K., Muzio, M., Dixit, V. M., & Salvesen, G. S. (1997). Target protease specificity of the viral serpin CrmA. Analysis of five caspases. *J Biol Chem, 272*(12), 7797-7800. doi:10.1074/jbc.272.12.7797

CURRICULUM VITAE

NORAH ABDULLAH ALTURKI

EDUCATION

University of Ottawa Ottawa ON, Canada
PhD candidate in Microbiology and Immunology 2014 - present

- Project topic: Mechanistic Insights into Necroptosis of Macrophages
- Thesis title: "Signalling and Degradation of Necrosome in Murine Macrophages"
- Course: Advanced topic in cell death (A)
- Comprehensive exam (A-)

University of Ottawa Ottawa ON, Canada
M.Sc. in Microbiology and Immunology, completed 2009 - 2012

- Project topic: Engineering of single-domain antibodies
- Thesis title: "Expression of biotinylated multivalent peptide and protein antigens in bacteria for rapid and effective generation of recombinant antibodies from antibody display libraries"
- Courses: Host/Pathogen interaction and molecular immunology (A-), Immunochemistry (A)

University of Toronto
Academic English Language Program Toronto ON, Canada

- Excellent grade (A-) December 2008

King Saud University Riyadh, Saudi Arabia
B.Sc. in Clinical Laboratory Sciences 2001 - 2006

- Thesis study "DNA Microarray Technology, introduction, principle, and application"; Independent study

PUBLICATIONS

- Norah Alturki, Scott McComb, Dikchha Rijal, Robert G. Korneluk, Shao-Cong Sun, Emad Alnemri and Subash Sad. "Triad3a induces the degradation of early necrosome to limit RipK1-dependent cytokine production and necroptosis". Cell Death & Disease volume 9, Article number: 592 (2018)

- Alturki N, Henry KA, MacKenzie R, Arbabi-Ghahroudi M. "Isolation of camelid single-domain antibodies against native proteins using recombinant multivalent peptide ligands". Methods Mol Biol. 2015; 1348: 167–189. pmid:26424272.

• Scott McComb, Erin Cessford, Norah A. Alturki, Julie Joseph, Bojan Shutinoski, Justyna B. Startek, Ana M. Gamero, Karen L. Mossman, and Subash Sad. "Type-I interferon signalling through ISGF3 complex is required for sustained Rip3 activation and necroptosis in macrophages". PNAS 2014 111 (31) E3206-E3213; published ahead of print July 21, 2014, doi: 10.1073/pnas.140706811.

• Bojan Shutinoski, Norah A. Alturki, John Bertin, Peter J. Gough, Michael G. Schlossmacher and Subash Sad. "K45A mutation of RIPK1 results in poor necroptosis and cytokine signalling in macrophages which impacts inflammatory responses in vivo". Cell Death Differ. 2016; 23: 1628–1637.

• Rijal, D., Ariana, A., Wight, A., Kim, K., Alturki, N., Aamir, Z., Ametepe, E., Korneluk, R., Tiedje, C., Menon, M., Gaestel, M., McComb, S. and Sad, S. "Differentiated Macrophages Acquire a Pro-Inflammatory and Cell Death-Resistant Phenotype Due to Increasing XIAP and P38-mediated inhibition of RipK1". Biol. Chem. jbc.RA118.003614. doi:10.1074/jbc.RA118.003614. (2018).

• Ardeshir Ariana, Norah Alturki, Stephanie Hajjar, Gaestel Matthias, Perry J. Blackshear and Subash Sad. "Zfp-36 regulates TLR4-induced necrosome signalling in macrophages". Under revision

RESEARCH EXPERIENCE

National Research Council Canada — Ottawa, ON, Canada
2009 –2013

- Isolated and characterized single-domain antibody inhibitors against several cardiac disease markers.
- Isolated and characterized anti-IGFBP7 single-domain antibodies.

SKILLS AND EXPERTISE

• Molecular Biology

Four years' experience in PCR, RT-PCR, Western immunoblotting, ELISA, DNA sequence analysis, Phage display technology and HLA typing.

• Protein Expression and Purification

-Three years' experience in cloning, expression, purification of recombinant proteins and engineered proteins using E. coli, and mammalian expression systems.

- Three years' experience with protein expression using shaker flasks, and Corning flasks.

- Two years' experience with Thermo Scientific KingFisher and AKTA purification platforms using affinity resins (Nickel, Protein A/G resins), ion- exchange resins and size exclusion resins.

TEACHING EXPERIENCE

- Teaching Assistant at Clinical Laboratory Science department, College of Applied Medical Science, King Saud University.
- Supervised honors / summer student in molecular biology and protein engineering techniques.

AWARDS

- 2nd place poster winner, microbiology & immunology PhD Poster Day 2018.
- 3rd place poster winner, microbiology & immunology PhD Poster Day 2016.
- Two Rewards of excellence (2015) from Saudi Cultural Bureau, Ottawa, Canada
- Career Development Award, King Saud University Graduate Scholarship Program for Ph.D. in Immunology, 2013
- Career Development Award, King Abdullah Graduate Scholarship Program for M.Sc. in Immunology, 2009-2012
- Financial Rewards of Excellence, College of Applied Medical Sciences, King Saud University, 2003 and 2005

EMPLOYMENT

King Saud University, College of Applied Medical Sciences, Clinical Laboratory Science

- Teaching Assistant 2011 – 2015
- Lecturer 2016 - Present

TRAINING AND INTERNSHIP

- National Research Council of Canada Ottawa ON, Canada

M.Sc. Studentship September 2009-October 2012

- King Faisal Specialist Hospital and Research Center Riyadh, Saudi Arabia

Lab assistant at the molecular genetics' lab March-June 2008

- King Faisal Specialist Hospital and Research Center Riyadh, Saudi Arabia

Training in biochemical genetics lab April 2007 - May 2008

- King Abdulaziz Medical City Riyadh, Saudi Arabia

Internship in clinical labs September 2005-September 2006

Full-time internship in the diagnostic clinical laboratories of King Fahad National Guard Hospital. Completion with Excellence.

Trained in different medical laboratory technologies (rotating for one year), including Molecular Pathology & Genetics, Immunopathology (Serology, Histocompatibility, Flow cytometry), Histopathology, Medical Microbiology, Cytology, Hematology, and Clinical Biochemistry.

- King Faisal Specialist Hospital and Research Center Riyadh, Saudi Arabia

Summer trainee in biochemical genetics lab June-August 2004

CONFERENCES AND WORKSHOPS

- **Alturki Norah**, Triad3a induces the degradation of early necrosome to limit RipK1-dependent cytokine production and necroptosis, Canadian society of immunology (CSI) , London Ontario, 2018. (**Poster presentation**).

- **ALTurki N**., Arbabi M., Tanha J. Expression of biotinylated multivalent peptide and protein antigens in bacteria for rapid and effective generation of recombinant antibodies from antibody display libraries. University of Ottawa, BMI department seminar day, Ottawa ON, February 2011. (**Oral Presentation**)

- **ALTurki N.**, Arbabi M., Tanha J. Expression of biotinylated multivalent peptide and protein antigens in bacteria for rapid and effective generation of recombinant antibodies from antibody display libraries. University of Ottawa, BMI Department poster day, Ottawa ON, May 2010. (**Poster Presentation)**

- Protein and antibody engineering summit, April 2012, Boston, United States.